Investigating the pathogenic effects of antibodies against the VGKC-complex and N-methyl-D-aspartate receptor in CNS disorders

Philippa May Pettingill

A thesis submitted for the degree of Doctor of Philosophy

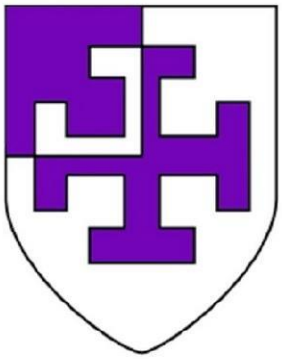

St Cross College

University of Oxford

Hilary Term 2013.

Abstract

Philippa May Pettingill, St Cross College, University of Oxford

A thesis submitted for the degree of Doctor of Philosophy, Hilary Term 2013.

Investigating the pathogenic effects of antibodies against the VGKC-complex and N-methyl-D-aspartate receptor (NMDAR) in CNS disorders

Over the last few years, antibody-mediated disorders of the central nervous system (CNS) have been a rapidly expanding field in neurology. The antibodies bind to extracellular domains of proteins expressed in the CNS and impair neuronal function. Patients with limbic encephalitis, Morvan's syndrome have antibodies that bind to the voltage gated potassium channel (VGKC)-complex proteins, LGI1 and CASPR2, while patients with antibodies to the NMDAR have more complex encephalopathies. Clinical evidence suggests that these antibodies are pathogenic as immunotherapy reduces antibody levels, which correlate closely with clinical improvement. Antibodies can be detected in patient sera using human embryonic kidney (HEK) cells transfected with CASPR2, LGI1 and NMDAR subunits, or by binding to rodent brain sections and primary neuronal cultures. *In vitro* NMDAR-antibodies have been shown to cross-link synaptic NMDARs and cause their subsequent internalisation from the cell membrane. It is not known if passive transfer of NMDAR-antibodies can recapitulate features of disease or if these pathogenic mechanisms occur with VGKC-complex antibodies.

The characteristics of LGI1 and CASPR2 antibodies were explored *in vitro.* IgG1 and IgG4 were identified as the predominant antibody subclasses, with all CASPR2 sera containing IgG1 antibodies and all LGI1 sera containing IgG4. On transfected cells both LGI1 and CASPR2 antibodies activated the classical pathway of the complement cascade. Furthermore CASPR2 antibody binding to transfected HEK cells showed a reduction in intensity over time which was most likely a result of internalisation of the CASPR2-antibody bound complex. Both CASPR2 and LGI1 antibodies bound strongly to the surface of live hippocampal neurons in culture, and this staining was reduced 24 hours after the removal of IgG, corresponding to a loss of antigen expressed at the cell surface.

Patients with NMDAR-encephalitis present with a psychotic disturbance, memory loss and seizures, usually progressing to a reduced level of consciousness and a marked movement disorder. A single injection of IgG, purified from patients with NMDAR-encephalitis was administered into the lateral ventricle of mice. Animals were observed for 40 days and showed significant behavioural changes, including a deficit in spontaneous alternation, dyskinetic hind-limb clasping and visual signs of spontaneous seizures, which are reminiscent to features of the disease. Behavioural changes were not observed in animals injected with IgG from healthy individuals. These behavioural alterations appeared to be reversible and were no longer present at day 40, which was supported by protein analysis showing equivalent levels of the NMDAR expressed in the hippocampus in animals receiving patient and control IgG.

In summary, these findings provide further evidence that supports a direct role of autoantibodies in NMDAR-encephalitis, limbic encephalitis and Morvan's syndrome.

Acknowledgments

First and foremost I would like to express my gratitude to my supervisors, Professor Angela Vincent and Dr Camilla Buckley for their expertise, guidance and generosity. This project was partially funded by the Medical Research Council with additional financial support from Professor Vincent.

It's been a great pleasure to work in the Oxford Neuroimmunology group. Special thanks go to Dr Bethan Lang and Dr Patrick Waters for providing invaluable scientific discussions, their mentoring in the lab and for always being available when the going got tough. Dr Sarosh Irani collected the serum samples and clinical data and charitably proof-read this thesis. I would like to thank Dr Leslie Jacobsen for kindly running my sera on the diagnostic NMDAR-antibody assay and Mrs Linda Clover for sharing her wisdom of immunohistochemical staining techniques. I would like to thank "the weekenders"- Luigi, Kasia, Rosie and Anjan who have shared the early mornings, the late nights and the long weekends, your company was a blessing.

I would like to thank all members of Professor David Bannerman's mouse behavioural unit who welcomed me into the group. I am particularly grateful to Dr Robert Deacon, Mrs Amy Taylor and Dr Christopher Barkus for their expertise and patience; and for always being more than a pair of accompanying hands during surgery. I would like thank David Bannerman for extending his open-door policy to me and for reminding me of the positives within the data.

Last but not least, I would like to thank my parents, my sister and Dave, without whose unconditional love, encouragement and provision of food, I would not have finished this thesis.

List of figures

List of tables

Abbreviations

3,4DAP	3,4 diaminopyridine
4-AP	4-diaminopyridine
Abs	Antibodies
AChR	Acetylcholine receptor
ADAM	A disintergrin and metalloproteinase
ADLTE	Autosomal dominant lateral temporal lobe epilepsy
AMPAR	Amino-3-hydroxy-5-methyl-4-isoxazolepproprionic acid receptor
AQP-4	Aquaporin-4
BBB	Blood brain barrier
BSA	Bovine serum albumin
CASPR2	Contactin-associated
CBA	Cell based assay
CC	Corpus collosum
CDFE	Cortical dysplasia focal epilepsy
CHO cells	Chinese hamster ovary cells
CNS	Central nervous system
CSF	Cerebrospinal fluid
D-AP5	D-(-)-2-Amino-5-phosphonopentanoic acid
DAPI	4',6'-diamidino-2-phenylindole
DG	Dentate gyrus
Div	Days *in vitro*
DMEM	Dulbecco's Modified Eagle Medium
DRG	Dorsal root ganglia
EAE	Experimental autoimmune encephalomyelitis
EAMG	Experimental autoimmune myasthenia gravis
EAR	Epilepsy associated repeat
EGFP	Enhanced green fluorescent protein
ELISA	Enzyme linked immunosorbent assay
EMG	Electromyography
Fab	Fragment antibody region
FBDS	Faciobrachial dystonic seizures
FCS	Fetal calf serum
FIPA	Fluorescent immunoprecipitation assay
GABAR	Gamma-aminobutryric acid receptor B
GFP	Green fluorescent protein
GFU	Green fluorescent units
GLT-1	Glutamate transporter-1
GlyR	Glycine receptor
HBSS	Hank's balanced salt solution
HC	Healthy control
HEK cells	Human embryonic kidney cells
HRP	Horse-radish peroxidase
Htt	Huntintin
ICV	Intracerebroventricular injection
IgG	Immunoglobulin G

iGluR	ionotrophic glutamate receptor
IHC	Immunohistochemistry
LE	Limbic encephalitis
LEMS	Lamber Eaton Myasthenic Syndrome
LGI1	Leucine glioma inactivated protein
LPS	Lipopolysaccharide
LRR	Leucine rich repeat
LTP	Long term potentiaton
LV	Lateral ventricle
MAC	Membrane attack complex
MAP-2	Microtuble-associated protein-2
MEM	Minimum Essential Medium
MG	Myasthenia gravis
mGluR	metabotrophic glutamate receptor
MoS	Morvan's sydnrome
mRS	Modified Rankin Score
MuSK	Muscle specific kinase
MWt	Molecular weight
NB^+ media	Neurobasal media
NB-1 cells	Neuroblastoma-1 cells
NgR1	Nogo receptor 1
NGS	Normal goat serum
NMDAR	N-methyl-d-asparate receptor
NMJ	Neuromuscular junction
NMT	Neuromyotonia
NP-SLE	Neuropsychiatric systemic lupus erythematosus
PBS-T	Phosphate buffer containing tween-20
PCP	Phenycylcidine
PEI	Polyethylimine
PIC	Protease inhibitor cocktail
PLL	Poly-l-lysine
PNH	Peripheral nerve hyperexcitability
PSA	Penicillin/streptomycin/amphotericin
PSD	Post synaptic density
PTX	Phosphate buffer containing triton-X
RIA	Radio-immuno assay
SCLC	Small cell lung carcinoma
SD	Standard deviation
SEM	Standard error of the mean
SLE	Systemic lupus erythematosus
SPS	Stiff person's syndrome
Tag-1	Transient axonal glycoprotein-1
VGCC	Voltage gated calcium channel
VGKC	Voltage gated potassium channel
α-DTX	alpha-dendrotoxin

CHAPTER 1: General Introduction

Over the past 11 years antibodies directed against extracellular epitopes of cell-surface proteins expressed in the central nervous system (CNS), have been identified in a number of neurological disorders, including encephalitis and epilepsy (reviewed by (Vincent, 2011; Dalmau, 2012)). The discovery of the antigenic targets of antibodies in patient sera and CSF has altered the disease prognosis, as many of these patients have a favourable response to immunomodulatory intervention. Despite the increasing number of antigenic targets identified, the cellular and synaptic mechanisms of antibody pathogenicity have not been definitively demonstrated.

This thesis aims to investigate the targets of such autoantibodies and some of the underlying pathogenic mechanisms of antibody-mediated autoimmunity. It has been divided in to two sections; section one focuses firstly on the measurement and characterisation of voltage gated potassium channel antibodies (VGKC-Abs) in patients with limbic encephalitis and Morvan's syndrome and the subsequent investigation of their pathogenic effector mechanisms *in vitro*.

An important proof of antibody pathogenicity is the ability to model the disease *in vivo*, which can be achieved by transferring patient antibodies to mice and examining the reproducibility of the clinical and neuropathological disease features. A successful animal model would allow the pathogenic mechanism of disease and potential novel therapies to be further explored. Section two of this thesis concentrates on modelling the pathogenic effects of antibodies against the NMDA receptor *in vivo* after injection of antibodies directly in to the cerebrospinal fluid compartment.

Section 1: Investigating the pathogenic effects of VGKC-complex antibodies *in vitro*

CHAPTER 2: Introduction

This introduction will briefly discuss the structure of immunoglobulin (Ig) molecules and give an overview of Ig subclasses in the blood. The identification and subsequent modelling of pathogenic antibodies in Myasthenia Gravis, a disorder affecting the peripheral nervous system will be discussed as being the paradigm for all antibody-mediated disorders. The latter half of this introduction will focus on disorders associated with VGKC-antibodies including; the evidence supporting the pathogenic role of these antibodies in disease and the current model for the molecular arrangements of VGKC's and their associating proteins.

2.1. General Immunology

The immune system is a complex defence barrier that allows the body to respond to external insults and is composed of the innate and the adaptive immune responses. The adaptive immune response consists of T and B-lymphocytes that determine the specificity of an immune response. The immune system is dependent on its ability to distinguish `self' from `non-self 'or` foreign' molecules and self-tolerance mechanisms exist to protect against inappropriate immune responses thus eliminating self-reactive T and B-lymphocytes. Autoimmune disorders occur when there is a defect in the regulation of the adaptive immune response resulting in a sustained immune response against the body's own tissue. The underlying dysfunction of the immune system is likely to involve a combination of both genetic susceptibility and environmental factors.

2.1.1 Antibody biology

Antibodies are produced by B-cells and plasma blasts. In humans there are five antibody isotypes; IgA, IgD, IgE, IgG and IgM, which differ in their serum concentration, structure and functional ability

to interact with different effector molecules. IgG and IgA molecules are further subdivided in to IgG(γ)1, IgG2, IgG3 and IgG4 and IgA1 or IgA2 subclasses. Developing B cells initially express IgM molecules and later express IgD molecules on their cell surface. IgM antibodies have relatively low affinity, but form pentamers containing ten antigenic binding sites, conferring an overall higher avidity of the molecule. Upon B cell activation class switching occurs in the heavy chain of the antibody enabling the production of monomeric IgA, IgE and IgG antibodies without affecting the specificity for the antigen. IgG molecules are the predominant isotype secreted in to the blood and will be the focus of this thesis.

2.1.2 Structure of the immunoglobulin

The basic structure of an antibody molecule is a Y-shaped molecule consisting of four polypeptide chains, two identical light chains and two identical heavy chains (α, δ, ε, γ and μ respectively). These are connected by disulphide bonds in the hinge region of the molecule and additional non-covalent bonds throughout the molecule, as shown in Figure 2-1 . The antigenic binding site is formed by hypervariable regions in the arms of the molecule and variability in this region determines the antibody specificity. In one antibody molecule, two identical antigen binding sites exist which are collectively known as the fragment antibody region (Fab). The Fc-domain is composed of the carboxyl-terminal constant regions of the two heavy chains and is responsible for some functional properties of the molecules, including antibody-dependent cell mediated cytotoxicity and activation of the complement cascade (see below). A proline to serine switch in the hinge region of IgG4 molecules only, results in an exchange of the Fab-arms between two IgG4 molecules under reducing conditions. This has been reported to result in the formation of bi-specific monovalent antibodies (Aalberse, 1999; Petersen, 1974).

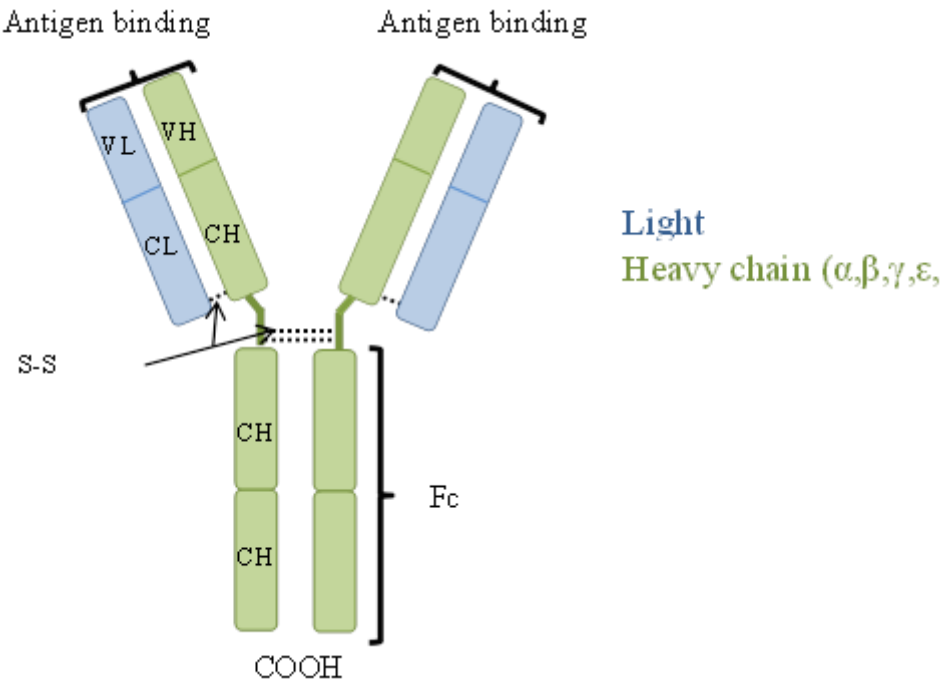

Figure 2-1 Schematic overview of an immunoglobulin G molecule.

IgG molecules consist of two heavy (green) and two light chains (blue) connected to one another inter-disulphide bonds. Each molecule has two antigen binding sites at the amino terminal of the protein. The carboxyl terminal is known as the Fc-domain and mediates many effects of the molecule.

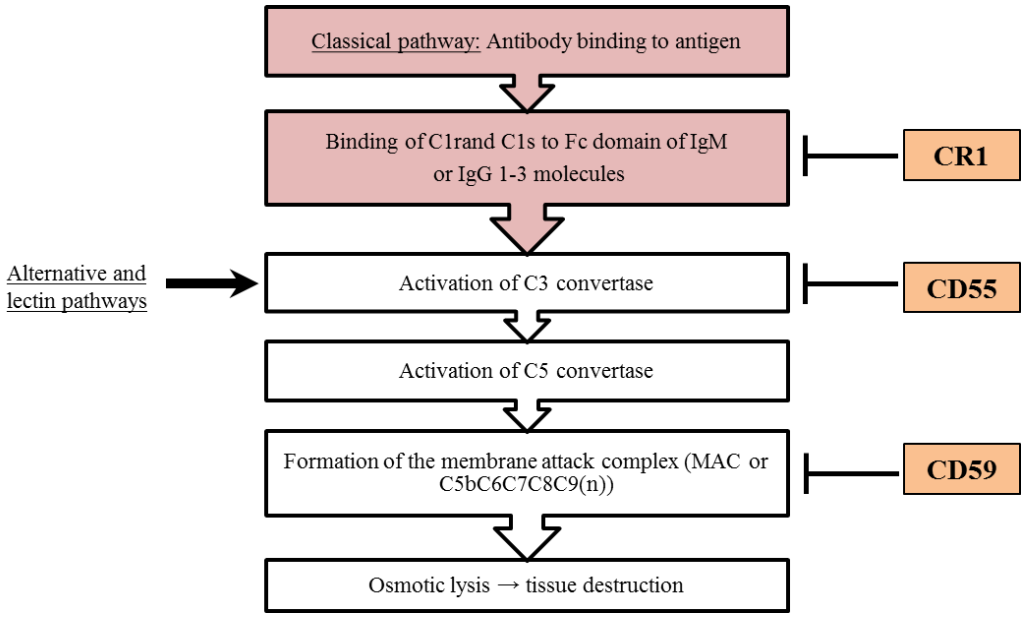

Figure 2-2 Overview of the complement cascade.

The complement cascade can be activated by the classical, alternative or lectin pathways, all of which converge at the activation of C3 convertase. The cascade is regulated at various stages by numerous molecules including CR1, CD55 and CD59.

2.1.3 Complement-mediated damage

The complement system is a component of the innate immune system and consists of series of proteins found synthesised in the liver and transported in to the serum. The complement system is normally inactive, but upon activation results in an amplifying proteolytic cascade. A summary of the cascade is shown in Figure 2-2. The complement cascade can be activated by three distinct pathways; the classical, alternative or lectin pathways. Antibody mediated activation of the complement cascade occurs through the classical pathway and requires the initial interaction of antibody (IgM or IgG) and antigen, resulting in the binding of complement proteins, C1q, via the Fc-domain of the Ig molecule. Binding of C1q leads to the subsequent activation of serine protease C1r and C1s, propagating the cascade. The IgG isotypes have differing ability to activate the complement cascade; IgG1 and IgG3 are both potent activators. IgG4 molecules are the only IgG isotype which cannot activate the complement cascade, as a proline to serine substitution at position 331 of the CH_2 domain, renders the molecule unable to bind to C1q (Tao, 1993).

Antibody-independent pathways exist and are known as the alternative and lectin pathways. All three pathways converge at the assembly of C3 convertase, a proteolytic enzyme that cleaves C3 in to C3a and C3b molecules. The terminal stage of the complement cascade is the formation and insertion of the membrane attack complex (MAC) in to the cell surface, which disrupts the integrity of the cell membrane, resulting in osmotic lysis and destruction of the targeted cell (Morgan, 1989) . In addition, cleaved peptide fragments C3a, C4a and C5a are anaphylatoxins and promote inflammation, and C3b fragments bind to the surface of antibody bound cells, and act to mark the cell for phagocytosis.

The complement system is tightly regulated to prevent unwanted destruction of the host tissue and a large numbers of regulators exist at multiple stages of the cascade in both the serum and on the membrane of host cells. Three examples of complement regulation are the C1 inhibitor, which prevents the proteolytic activity of C1r and C1s molecules at the beginning of the classical pathway, CD55 that disrupts the assembly of the C3-convertase and speeds up its disassembly. The final regulator in the cascade, CD59 attenuates MAC assembly by preventing the incorporation of C9 molecules in to the membrane (for a comprehensive review see Zipfel, 2009). In the CNS,

complement molecules may be synthesised locally by activated glial cells (Lévi-Strauss, 1987), however the expression of complement regulators on a given cell is likely to influence its susceptibility to complement-mediated damage. In the presence of normal human serum (with complement proteins present), cultured foetal neurons spontaneously activate the complement cascade resulting in cell lysis, which was not observed in glial cells (Singhrao, 2000) . This is thought to be due to complement-mediated lysis as glial cells express significantly lower levels of complement regulators, including CD55 and CD59 (Gasque, 2000).

2.2. Antibody-mediated autoimmune disorders

In the 20th century, Paul Ehlrich proposed that autoimmunity did not exist, and this thought transcended the immunological field for many decades. Despite this finding, only four years later, anti-P antibodies, which bound to the surface of red blood cells at low temperatures, were reported in post-infectious haemolytic anaemia in children (reviewed in Weens, 1974). Antibodies have since been described in a variety of disorders and can be classified as being systemic or organ-specific. In systemic autoimmune disorders, such as systemic lupus erythematous (SLE), the immune response affects multiple organs, whereas in organ-specific autoimmune disorders, such as Grave's disease and Hashimoto's thyroiditis, only the organ expressing the auto-antigen is affected.

2.2.1 Koch's postulates

In the 19th century, Robert Koch postulated a causal relationship between microbes and disease which was extended in 1957 by Witebsky as an attempt to establish whether a human disease had an autoimmune aetiology (Witebsky, 1957) . These criteria were subsequently revised (Rose & Bona, 1993) and are summarised in Table 2-1 and 2-2.

1. Presence of an autoimmune response mediated by autoantibodies or self-reactive T-cells
2. Identification of antibodies or T-cells in the target organ
3. Transfer of disease by injection of antibody into an animal
4. Transfer of disease by T-cell into an immunocompromised animal
5. Induction of disease by active immunisation against with the antigenic target and transfer of antibody/T-cell into naïve animal

Table 2-1 Modified of Koch's postulates for all autoimmune disorders

1. Antibodies directed against extracellular epitopes of functionally important proteins
2. Immunotherapy intervention (plasma exchange/immunosuppression) correlates with clinical improvement
3. Transfer of human disease by injection of patient antibodies into animals
4. Demonstration of functional effects of patient antibodies using appropriate *in vitro* techniques

Table 2-2 Postulates of antibody-mediated autoimmune disorders
*(modified from **Vincent, Neuroimmunology 2004**)*

The mere presence of a circulating antibody in a given disease does not necessarily infer that the antibody is directly causing disease. Antibodies can be divided broadly into two categories based on whether the antigen is located. Antibodies against intracellular antigens (nuclear or cytoplasmic) such as the neuronal antigens Hu, Yo, CRMP5 and Ma2, have been described in limbic encephalitis (LE) and are commonly associated with an underlying distant malignancy and therefore, are referred to as paraneoplastic neurological disorders. These disorders are not considered to be antibody-mediated and are instead thought to be caused by aberrant T-cell immune responses, and have been reviewed in detail by Dalmau & Rosenfeld, 2008 . The evidence against a pathogenic antibody in these disorders originates firstly that intracellular antigens are inaccessible to circulating antibodies. Secondly, attempts to transfer human disease by passive transfer of patient IgG or active immunisation of the specific antigen have failed to reproduce neurological features reminiscent of disease *in vivo*, despite inducing antibody responses (Graus, 1991; Greenlee, 1995). Furthermore, patients generally do not improve clinically with immunotherapies aimed to reduce antibody levels and neuropathological findings show extensive cytotoxic T-cell infiltrates and neuronal death in patient post mortem brain tissue (Dalmau, 1991; Giometto, 1997). These antibodies are likely to be bystanders of T-cell immune response; however their detection is important for the identification of an underlying malignancy. This evidence highlights that antibodies against intracellular antigenic targets in LE are not pathogenic and do not fulfil the criteria of an antibody-mediated autoimmune disorder outlined in Table 2-2.

The second group of antibodies are directed against extracellular epitopes of cell surface proteins and will be the focus of this work. Antibodies against components of the peripheral nervous system, including the acetylcholine receptor (AChR), the voltage gated calcium channel (VGCC) and the voltage gated potassium channel (VGKC) have been identified in myasthenia gravis (MG), Lambert Eaton myasthenic syndrome (LEMS) and acquired neuromyotonia (NMT), respectively (Lindstrom, 1976; Lennon, 1989; Shillito, 1995). The evidence for antibody involvement in myasthenia gravis will be reviewed below.

2.2.2 Myasthenia gravis as the paradigm for an antibody-mediated disorder

Myasthenia gravis is a disorder affecting neuromuscular transmission in the peripheral nervous system and is characterised by the subacute onset of muscle weakness and fatigability, commonly associated with an underlying thymoma or thymic hyperplasia. An autoimmune basis for myasthenia was first postulated based upon lymphocyte infiltrates present in muscle neuromuscular junction (NMJ) and thymus tissue from patients, and the cytolytic effect of patient sera *in vitro* (Weigert, 1901, Natsuk, 1960). In 1973, rabbits immunised with purified acetylcholine receptor (AChR) from the electric organ of the electric ray, developed flaccid paralysis and demonstrated abnormal electromyographs which were characteristic of MG (Patrick, 1973). These similarities led to the model being described as experimental autoimmune MG (EAMG) and the subsequent identification of AChR antibodies in 80% of autoimmune myasthenic sera, which were detected using a iodinated (^{125}I-α-bungratoxin) radioimmunoprecipitation assay (Lindstrom, 1976). EAMG has subsequently been demonstrated in multiple species including primates, guinea pigs and rodents, but requires native AChR to be pathogenic (Goyco, 1986; Lennon , 1976; Lennon, 1991; Lennon et al. 1975). The induction of EAMG is highly dependent on the strain of rodent used, which has been shown to be at least partially a result of genetic variation in the major histocompatibility complex (Fuchs, 1976). Characterisation of antibody subclass showed AChR antibodies were predominantly IgG1 and IgG3, and therefore capable of fixing complement (Newsom-Davis, 1982).

The pathogenic effects of AChR antibodies have been extensively studied *in vitro* and *in vivo*. Firstly, transfer of patient antibodies replicated the histological findings seen in myasthenia, including the loss of AChR's, IgG and complement deposition at the NMJ (Fambrough, 1973; Engel, 1977). Secondly, mice displayed weakness and had reduced miniature endplate potentials, reminiscent of myasthenia. Both features were enhanced by administration of the complement component C3 (Toyka, 1975; Toyka, 1977). The mechanism of receptor loss was shown to be caused by antibody mediated receptor cross-linking, which resulted in the internalisation and increased degradation of the AchR's. Antibody internalisation was shown to be dependent on antibody divalency, as cleavage of antibodies into monovalent Fab fragments did not cause receptor internalisation (Drachman, 1978). Some

AChR-antibodies directly blocked the AChR, through binding to the agonist binding site on the foetal form (γ-subunit) of the receptor, reducing the inward flux of sodium ions (Rimersa, 1996). This mechanism, although rare in typical MG, is thought to underlie arthrogryposis which is a condition characterised by the development of multiple joint contractures leading to foetal paralysis whilst in utero. Patients with AChR antibodies show a significant clinical improvement with immunotherapy, including plasma exchange, which removes circulating antibodies from the body (Pinching, 1976; Newsom-Davis, 1978). Taken together, the clinical and experimental evidence fulfil Witebsky's criteria and have led to myasthenia gravis being considered the paradigm for all antibody-mediated disorders. The effector mechanisms of AChR antibodies are illustrated in Figure 2-3. Antibodies against muscle specific receptor tyrosine kinase (MuSK) have been detected in 50% of myasthenia patients without AChR antibodies (Hoch, 2001). MuSK is involved in agrin-induced clustering of the AChR's at the NMJ and retrospective experimental evidence demonstrated that these antibodies were pathogenic when transferred to mice (Burges, 1994). Unlike typical MG, loss of AChR expression at the neuromuscular junction end-plate and complement deposition are not observed in MuSK-Ab positive patients (Shiraishi, 2005). Indeed, analysis of antibody subclass found that MuSK antibodies are predominantly of the IgG4 subclasses which are unable to fix complement, indicating distinct molecular mechanisms from AChR antibodies. As IgG4 antibodies do not activate complement and have been reported to be functionally monovalent, MUSK-antibodies are typically thought to interfere with MUSK signalling to mediate MG (McConville, 2004).

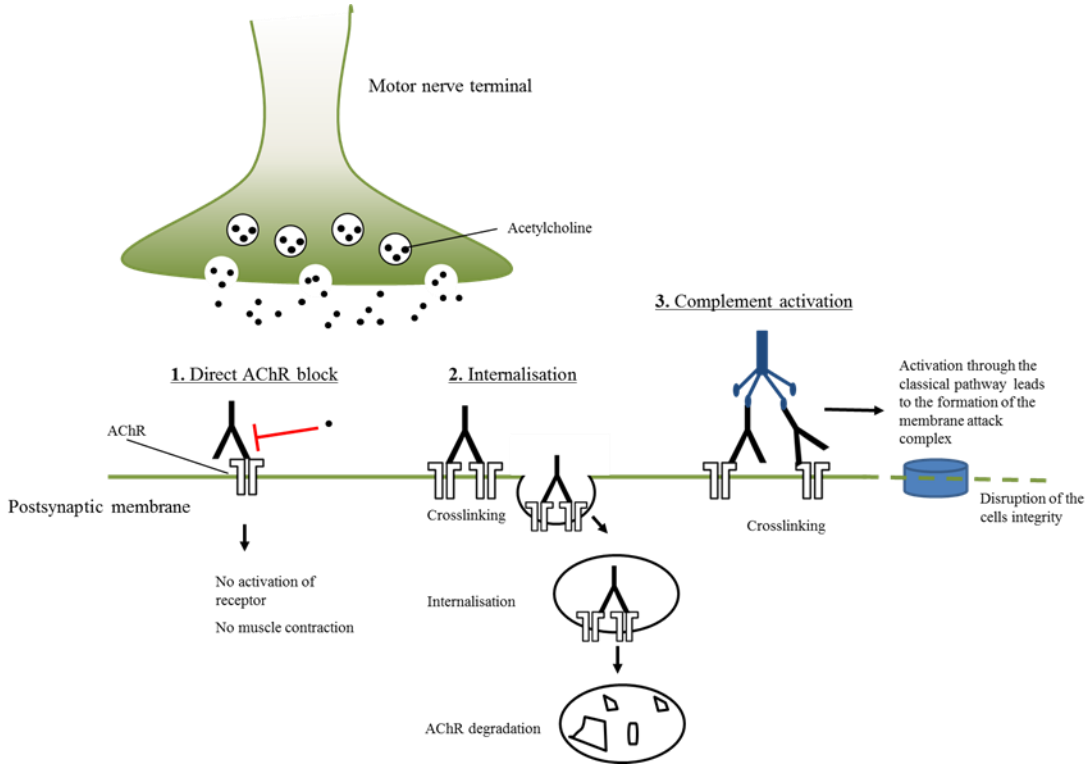

Figure 2-3 Pathogenic effector mechanisms of AChR antibodies in myasthenia gravis.

1) Antibody binding to acetylcholine site of the AChR causes a direct block of the AChR by preventing acetylcholine binding and subsequent receptor activation 2) Divalent antibodies crosslink AchR's on the postsynaptic membrane and become internalised in endocytic vesicles where they are degraded, resulting in reduced AChR expression at the neuromuscular junction. 3) Antibody binding to the AChR activates the complement cascade via the classical pathway leading to the formation of the membrane attack complex in the postsynaptic membrane and ultimately results in the destruction of the folds of the postsynaptic membrane

2.3. Spectrum of disorders associated with antibodies to the VGKC- antibodies

2.3.1.Neuromyotonia

Neuromyotonia (NMT), also known as Isaacs' syndrome, is a rare disorder characterised by spontaneous and continuous muscle activity at rest, which manifests clinically as visible muscle twitching (90%), cramps (70%), myopathy, stiffness and impaired muscle relaxation (reviewed in Maddison, 2006). NMT is characterised on electromyographs (EMG) by doublet, triplet or multiplet-firing of the motor unit with a high 30-300Hz intra-burst frequency which has been demonstrated to originate from the peripheral nerve (Isaacs, 1961). The association of NMT with other autoimmune disorders including myasthenia gravis, elevated AChR-antibodies, rheumatoid arthritis and thymoma suggested a possible autoimmune aetiology in some patients. Direct evidence for an autoimmune aetiology came from the demonstration that plasma exchange significantly reduced the number of neuromyotonic discharges (Sinha, 1991; Newsom-Davis, 1993).

2.3.2 Pathogenic mechanisms of Neuromyotonia IgG *in vivo*

The first evidence for the role of antibodies in NMT came from early passive transfer studies. Mice receiving intraperitoneal injections of NMT-plasma (1ml) or purified IgG (17 mg/ml) for 12-21 days did not display clinical signs of NMT but showed an increased resistance to d-tubocurarine compared to controls in *ex vivo* nerve-diaphragm preparations (Sinha, 1991). Subsequent passive transfer experiments reported an increase in the amplitude of the end plate potential and a 21% increase in quantal content release in similar nerve-muscle preparations from mice receiving NMT-IgG which were mimicked by the application of 1-100 μM of the VGKC blocker, 4-diaminopyridine (4-AP), (Shillito, 1995). Superficial peroneal nerve preparations showed prolonged duration of the compound action current which were mimicked by the VGKC-blocker 3,4 diaminopyridine (3,4 DAP). Lastly, the authors show that incubation of dorsal root ganglion cells (DRG) with NMT-IgG or VGKC-blockers (500 μM 3,4 DAP) induced spontaneous repetitive firing *in vitro*. Spontaneous movements and electrophysiological changes resembling NMT were observed in Drosophila carrying a mutation

in the Kv1 subunit (Butler, 1989), leading to the hypothesis that patient serum contained antibodies that were directed against the VGKC channels .

2.3.3 VGKC-antibodies in Neuromyotonia sera

Shillito *et al* developed a radioimmunoprecipitation assay (RIA) using mammalian brain extract as a concentrated source of VGKC's. VGKC's were labelled with iodinated alpha-dendrotoxin (^{125}I-αDTX), a neurotoxin derived from the venom of the Dendroaspis angusticeps (Green mamba snake) which binds specifically to the Kv1.1, 1.2 and 1.6 subtypes of the Shaker channel family (Scott, 2002). The authors found three of six patients studied, precipitated ^{125}I-αDTX counts that were significantly higher than controls levels (>100 pM) (Shillito, 1995).

2.3.4 VGKC: structure and function

VGKC channels (Kv1-12) represent the largest family of genes expressed in the CNS. The Shaker potassium channels (Kv1 family), of which VGKC-complex antibodies are directed against are composed of four alpha subunits, each subunit containing six transmembrane spanning domains and cytosolic N and C-termini, which assemble to form hetero-tetramers alongside four cytosolic auxiliary beta subunits. Kv1 expression in the brain is predominantly neuronal and is localised to the axon, in particular the juxtaparanode and nerve terminals (Wang 1993, Trimmer 2004). In the juxtaparanode, the clustered Kv1.1/Kv1.2 channels regulate neuronal excitability by stabilising conduction and contributing to the intermodal resting potential (Rasband 1998), whereas pre-synaptically they are proposed to modulate neurotransmitter release and help return the cell to its resting state. The overall distribution of Kv1's is vast, but particular attention has been emphasised in particular to the the cerebellum and the hippocampus in the CNS, as rare human mutations in the Kv1.1 and Kv1.2 have been reported in disorders with disrupted neuronal excitability, including cerebellar ataxia and epilepsy, highlighting the importance of Kv1 channels in controlling normal neuronal function (Browne 1993, Zuberi 1999).

2.3.5 Pathogenic mechanisms of NMT-IgG *in vitro*

Once VGKC-antibodies had been identified in NMT patients, the functional effects *in vitro* were demonstrated in multiple studies using neuronal cell lines to examine the direct effect on potassium channel currents. A summary of the individual studies can be seen in Table 2-3. Incubation of NMT-IgG induced spontaneous repetitive firing of dorsal root ganglion (DRG) cells and suppressed potassium channel currents in PC-12 and neuroblastoma cells (NB-1) without affecting channel kinetics (Shillito, 1995; Sonoda, 1996; Nagado, 1999). These effects were only observed with chronic (days) but not acute (10 minutes- 2 hour) application of IgG. In a more recent study, NMT-IgG and F(ab')2 fragments suppressed potassium currents in NB-1 cells, but VGKC channel suppression was no longer observed when IgG molecules were cleaved into monovalent Fab or Fc fragments (Tomimitsu, 2004). These findings are similar to those reported by Drachman *et al* in myasthenia and are suggestive of antibody-mediated internalisation. Tomimitsu *et al* were the only authors to investigate the role of complement; the authors showed incubation with NMT-IgG for three days suppressed potassium channel currents independently of added complement. When the effects of NMT-IgG were studied in Chinese hamster ovary (CH0) or human embryonic kidney (HEK) cells transfected with the Kv1.1 or Kv1.6 subunits, conflicting results were reported. One study reported chronic incubation of NMT-IgG suppressed Kv1.1 and Kv1.6 currents in transfected Chinese hamster ovary (CHO) cells (Nagado, 1999), however these findings were not reproduced in transfected HEK cells (Irani, 2010).

While available evidence is limited the precise mechanisms of how VGKC antibodies may be causing NMT is not clear. However, the time-dependent effects observed *in vitro* suggest that the antibodies do not directly block channel function. The suppression of potassium channel currents *in vitro* by divalent but not monovalent patient IgG indicated that antibody-mediated cross-linking of the VGKC's and their subsequent internalisation may be one mechanism contributing to hyperexcitability of the peripheral nerve.

Method used to measure VGKC-antibodies	Experiment (n = number of different patients studied)	Cell type	Electrophysiological effects	Other observations	Reference
Not done	Passive transfer of NMT plasma / purified IgG for 12-21 days to mice n=1	Dissected phrenic nerve-diaphragm preparation	NMT-IgG mice showed increased resistance to d-tubocurarine at the NMJ No spontaneous muscle activity	NMT mice appeared less active (not quantified)	Sinha 1991
VGKC RIA range 161-890pM	Passive transfer of NMT plasma /purified IgG for 10-30 days n= 6	Dissected peripheral nerve: Dissected superficial peroneal nerve	NMT-IgG mice showed an increased end plate potential amplitude (+2 to 50mV above control) which was a result of increased quantal content release (mean +21%) No spontaneous action potentials Aαβ action currents prolonged (+1.5-2.9msec from NMT mice), mimicking the effects of 100μM 4,DAP	Mice did not developed clinical features of NMT	Shillito 1995
VGKC RIA 247pM	Incubated for 2 hours or 24 hours with NMT IgG n=1	Dorsal root ganglion culture	Repetitive firing of action potentials after 24 hour (seen in 10% of control cells, and up to 70% in cells with NMT IgG). No effect seen at 2 hours	Mimics the effects of 500μM 4,DAP	Shillito 1995
Not mentioned. Previously measured by Western blot of PC-12 cell extract	Incubation for 1 or 3 days with NMT IgG n=4	NB-1 cells	6 days incubation caused a decrease in net K^+ current (control 27.6±7.8pA/pF; NMT 6.8±5.5pA/pF) NMT IgG suppressed K^+ currents		Sonoda 1999
VGKC RIA >100pM	Incubation for 1 or 3 days with NMT IgG n= 4 patients	NB-1 cells	Patch clamp recording showed suppressed K^+ channel currents with patient IgG	Effects were independent of complement and dependent on antibody divalency	Tomimitsu 2004
Not mentioned	Incubation for 1 or 3 days with NMT IgG n=4 patients	NB-1 cells Transfected CHO cells with either Kv1.1 or Kv1.6	Patch clamp recordings showed reduced K^+ channel currents with NMT sera at 3 days (peak current density; control 48.1pA/pF; NMT IgG 6.03pA/pF). No effect was seen at 1 day . No difference in activation kinetics The potassium channel currents suppressed in CHO cells transfected with either Kv1.1 or Kv1.6, without affecting channel kinetics	Suppression of K^+ channel currents in patients with idiopathic generalised myokymia without pseudomyotonia	Nagado 1999
VGKC RIA	Incubation for 1 or 3 days with NMT sera n=7	Transfected HEK cells with Kv1.1 or Kv1.6	Patch clamp recordings showed no effect on K^+ channel currents . Acute application of α-DTX suppressed K^+ channel currents .	Patient serum did not bind to the extracellular domains Kv1.1 or Kv1.6 transfected cells.	Irani 2010 and personal communication

Table 2-3 Studies investigating the pathogenic effects of VGKC-complex antibodies in neuromyotonia. 6/7 of the studies did not show binding of patient IgG to the relevant tissue used in the experiments.

2.3.6 Spectrum of peripheral nerve hyperexcitability

Hart *et al* compared the clinical and autoimmune features of 60 patients presenting with acquired peripheral nerve hyperexcitability (PNH), segregated by the presence or absence of EMG myokymic discharges characteristic of neuromyotonia (Hart, 2002). The authors observed no significant difference in the presenting clinical features, the association with thymoma and other autoimmune disorders. In thymoma patients, 80% had detectable VGKC antibodies. However the presence of an antibody was not dependent on EMG-status, suggesting a common autoimmune mechanism in patients with PNH. Unfortunately the authors did not compare the treatment response between those with and without a serum antibody. Notably some of the patients in this study had CNS symptoms including personality changes, anxiety and insomnia, which becomes particularly relevant with reference to Morvan's syndrome.

2.3.7 Morvan's Syndrome

In 1890 a French clinician, Augustin Morvan described 'la chorée fibrillaire' in a male patient presenting with peripheral nerve hyperexcitability, hyperhidrosis, insomnia and delirium. This disorder was subsequently termed Morvan's syndrome (MoS) and involves a triad of neuromyotonia, dysautonomia and CNS dysfunction. Morvan's is a rare disorder and its association with malignancy and other autoimmune disorders, including MG, indicated an underlying autoimmune aetiology (Lee, 1998). The observation that neuromyotonia is the most consistent clinical feature of Morvan's (and in some patients neuromyotonia is associated with VGKC antibodies), strengthened the immune-mediated hypothesis. Furthermore patients showed a favourable response to plasma exchange (Madrid, 1996). Based on these accumulating pieces of evidence, VGKC antibodies were subsequently identified by radioimmoprecipitation in Morvan's syndrome and their reduction correlated with the observed clinical improvement (Lee, 1998; Barber, 2000). In 2012, Abou-Zeid reviewed 28 cases of Morvan's reported in the English literature (1986-2009) and reported the most commonly presenting CNS disturbances were insomnia and sleep disturbance (86%), encephalopathy, neuropsychiatric changes including hallucinations and delusions (64%). Peripheral nerve hyperactivity, including myokymia and neuromyotonia was observed in all patients and hyperhidrosis

(93%) was the most common symptom of autonomic dysfunction. Cardiovascular instability, impotence, constipation and incontinence were also reported in some patients. Thymoma was the most common malignancy identified in 14/15 patients, 10 patients had AChR antibodies, seven of which had clinical signs of myasthenia gravis and an overall male preponderance of 13:1 was found. Similarly to patients with neuromyotonia, where serum positivity on the RIA is approximately 40%, only 13 of 18 (72%) patients tested had detectable VGKC antibodies in their serum (Abou-Zeid, 2012).

One study investigated the immunoreactivity of one Morvan's patient with high serum VGKC-antibodies (3,000 pM) but undetectable antibodies in their CSF. The authors observed that patient IgG bound to neurons in the hippocampus, thalamus, striatum and cerebellum which reportedly showed similarities to commercial Kv1.2 antibody immunoreactivity (Liguori, 2001; Rhodes, 1997). Post-mortem analysis of the same patient showed IgG deposition on neurons in the thalamus and striatum where non-specific leakage of IgG was observed, however IgG leakage was not as noticeable in the cortex. As this patient had only serum VGKC-antibodies detected, this finding suggests that the CNS symptoms observed in patients with Morvan's syndrome, but not seen in neuromyotonia, may be a result of blood-brain barrier breakdown.

The pathogenic mechanisms of VGKC antibodies in MoS have not been studied. One study investigated the electrophysiological effects of the serum and CSF from a patient without detectable VGKC-complex antibodies, with a suspected autoimmune aetiology based upon the presence of oligoclonal bands in the CSF (Löscher, 2004). Acute application of patient serum or CSF for 45 minutes with rat nerve preparations did not affect peripheral nerve excitability. The authors acknowledged the pathogenic effects of NMT-IgG *in vitro* were only observed after chronic incubation, and a longer incubation would be necessary to determine an immune aetiology in this patient. The authors did not study the effect of patient IgG on potassium channel function, despite this being the most consistent reported effect of VGKC antibodies in NMT. Interestingly the patient did not improve with intravenous Ig (IvIg), did not have a thymoma or MGs, and improved clinically with carbamazepine, arguing against an antibody-mediated aetiology.

2.3.8 Limbic encephalitis and epilepsy

The recognition of an autoimmune aetiology in Morvan's syndrome soon led to the identification of patients with a purely central nervous system disorder associated with VGKC antibodies and often hyponatremia (Buckley, 2001; Vincent, 2004). This disorder, known as limbic encephalitis (LE) is characterised by a sub-acute onset of symptoms including amnesia, confusion, seizures and psychiatric features (Vincent, 2004). The association of LE with malignancy is typically significantly lower than reported in NMT and MoS (Thieben, 2004). Like NMT and MoS, patients responded well to immunotherapy and in most cases there was a close correlation with a fall in serum VGKC-antibodies (Vincent, 2004). However a few reports of spontaneous improvement along with a fall in antibody levels exist (Buckley, 2001; Thieben, 2004). As reported for Morvan's sera, incubation of patient sera was assessed on rat brain sections and intense IgG staining to the hippocampus was reported in a pattern similar to commercial Kv1.2 antibodies (Buckley, 2001). The similar IgG immunoreactivity observed, along with the detection of VGKC-antibodies, may suggest that LE and MoS serum both contain a common antibody.

Oligoclonal bands are thought to represent antibody production in the CNS and have been described in a few cases of LE associated with VGKC antibodies (Vincent, 2004; Tan, 2008). However two studies (n=17 and n=6 respectively) reported normal intrathecal IgG synthesis in all CSFs tested (Thieben, 2004; Jarius, 2008). VGKC antibodies are not routinely measured in the CSF, but are generally considered to be much lower than serum values, typically 1-10 % of serum values from patients with the highest serum titers (Pozo-Rosich 2003, Vincent 2004, Thieben 2004). One study found that only 46% of paired CSF samples from patients with VGKC-antibodies with CNS involvement (n=24), were positive on the RIA, and had a median CSF antibody titer 6% of the serum value. Interestingly only one patient had CSF antibodies which were 1.3 times higher than the serum titer (Tan, 2008). This evidence highlights a lack of VGKC-antibodies detected in the CSF, and suggests that the primary immune response is generated in the periphery.

Given that the clinical data suggests that VGKC-antibodies are pathogenic and are capable of binding neuronal tissue, it is considered an enigma how an immune response generated in the periphery can

affect the brain, especially without clear consistent evidence of antibodies in the CSF. The idea of a blood-brain barrier (BBB) was first suggested in the 1885 when Paul Ehlrich observed that intravenous injection of trypan blue dye stained all organs of the body except the brain and spinal cord (Ehlrich, 1885). Antibodies are large macromolecular proteins that are generally considered too large to permeate the blood-brain barrier (Pardridge, 1998). A route of entry for antibodies could be via the fenestrated epithelial cells of circumventricular organs which lie outside of the blood-brain barrier or upon entry of B-cells in to the brain which could secrete antibodies locally. In VGKC-Ab encephalitis, the few available post-mortem reports show perivascular lymphocytic infiltrates, which were predominantly B cells ($CD20^{+}$), however only sparse B cells were detected in the brain parenchyma (Khan, 2009; Park, 2007; Dunstan & Winer, 2006). Despite this, one report observed intense IgG binding to neurons in the hippocampus on autopsy, indicating that IgG is indeed present (Bien, 2012). Reports of a preceding infection in some patients suggest that a transient disruption of the blood brain barrier may allow antibodies access in to the CNS parenchyma (Vincent, 2003). Indeed one study showed that 35 % of limbic encephalitis patients had a disruption of the blood-CSF barrier integrity (CSF/serum albumin quotient) (Jarius, 2008), however the authors did not report whether this finding was associated with a preceding infection in these patients.

Finally, Faciobrachial dystonic seizures (FBDS), have recently been described as a distinctive seizures semiology which commonly precedes the onset of VGKC-complex limbic encephalitis (77%) (Irani, 2011). Seizures are frequent (median 50/day) and are triggered by stimuli in 28% of cases (auditory or emotion) predominantly affecting the arm (100%), ipsilateral face (76%), leg (36%) and trunk (28%).

2.4 How can multiple distinctive syndromes be explained VGKC-complex antibodies?

VGKC antibodies have been identified in neuromyotonia, Morvan's syndrome, limbic encephalitis and epilepsy (particularly FBDS). Furthermore, VGKC antibodies have also been described in CNS disorders associated with only one of the features observed in LE, such as epilepsy, psychosis or

dementia (McKnight, 2005; Zandi, 2011; Flanagan, 2010). It was previously unclear how such diverse clinical presentations could be associated with the same antibody, although some early evidence suggested that VGKC-antibodies targeted different potassium channel subunits, depending on the neurological disorder (Hart, 1997; Kleopa, 2006). In fact the potassium channels are not the target of most "VGKC" antibodies as patient antibodies did not bind to the surface of HEK cells transfected with Kv1.1, 1.2 or 1.6 subunits (Irani, 2010). Antibody binding in the VGKC RIA was sensitive to increasing amounts of detergent, despite commercial antibody binding to Kv1.1 and Kv1.2 being unaffected, indicating that associating proteins of the VGKC complex were the targets of the VGKC-antibodies. A candidate approach identified leucine-rich glioma-inactivated protein 1 (LGI1), contactin-associated protein-like 2 (CASPR2) and Contactin-2 as possible antigenic targets, and (Vincent, 2009; Irani, 2010a; Lai, 2010). Therefore, these antibodies were subsequently termed VGKC-complex antibodies. Cell based assays (CBA's) using HEK cells transfected with cDNA encoding CASPR2, LGI1 or Contactin-2 were used to determine the specific antibody specificities in a cohort of patients with VGKC-complex antibodies. Patient IgG was applied to the surface of live unpermeablised cells and any specific IgG binding was measured. Antibodies against LGI1 and CASPR2 were independently confirmed in patient sera by a mass-spectrometry proteomic approach (Lai, 2010; Lancaster, 2011a).

The Oxford Neuroimmunology investigated the antibody specificities in 96 patients with VGKC-complex antibodies and the authors found that the antigenic targets correlated well, but not perfectly, with the clinical phenotype, which will be discussed in further detail below. The neuronal localisation of contactin-2, CASPR2 and LGI1 is shown in Figure 2-4 and Figure 2-5.

2.4.1 LGI1 antibodies

Fifty-five of 96 patients studied had LGI1 antibodies, of these 49 (89%) had limbic encephalitis. The predominant clinical features were amnesia (8 %), seizures (89%) and neuropsychiatric disturbance (75%). Thirty-four patients had hyponatremia (62%) and brain magnetic resonance imaging showed high medial temporal lobe signal in 31 patients (56%). LGI1 antibodies were also found in 2/5 of

patients with MoS, 1/11 with NMT, 1/4 with epilepsy and 2/12 with other disorders (Irani, 2010a). All of the FBDS cases when tested acutely had LGI1 antibodies (Irani, 2010).

In an independent study, LE sera were screened on permeabilised HEK cells co-transfected with LGI1 and its receptors ADAM22 or ADAM23 and confirmed LGI1 antibodies in 57/57 (100%) (Lai, 2010).

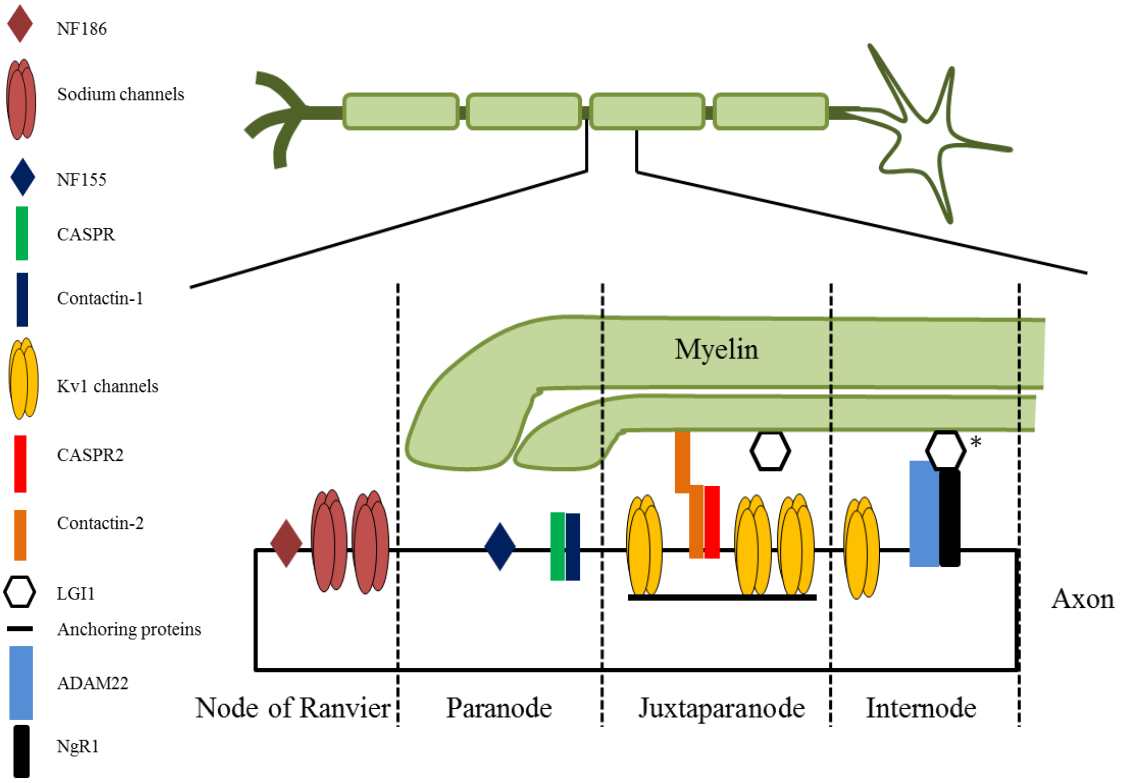

Figure 2-4 The neuronal localisation of CASPR2, LGI1 and Contactin-2

CASPR2 is located at the juxtaparanode underneath the myelin sheath where it interacts directly with Contactin-2 and indirectly with VGKC channels. Contactin-2 interacts in cis or in trans with itself forming the VGKC-complex. LGI1 is expressed in oligodendrocytes and Schwann cells and is weakly expressed at the juxtaparanode of the sciatic nerves and most likely in the CNS also. Expression of ADAM22 and NogoR1, interactors of LGI1, at the internode, suggests that LGI1 (*) may also be present in the same compartments, although the interact with the VGKC subunits has not been depicted in this diagram.

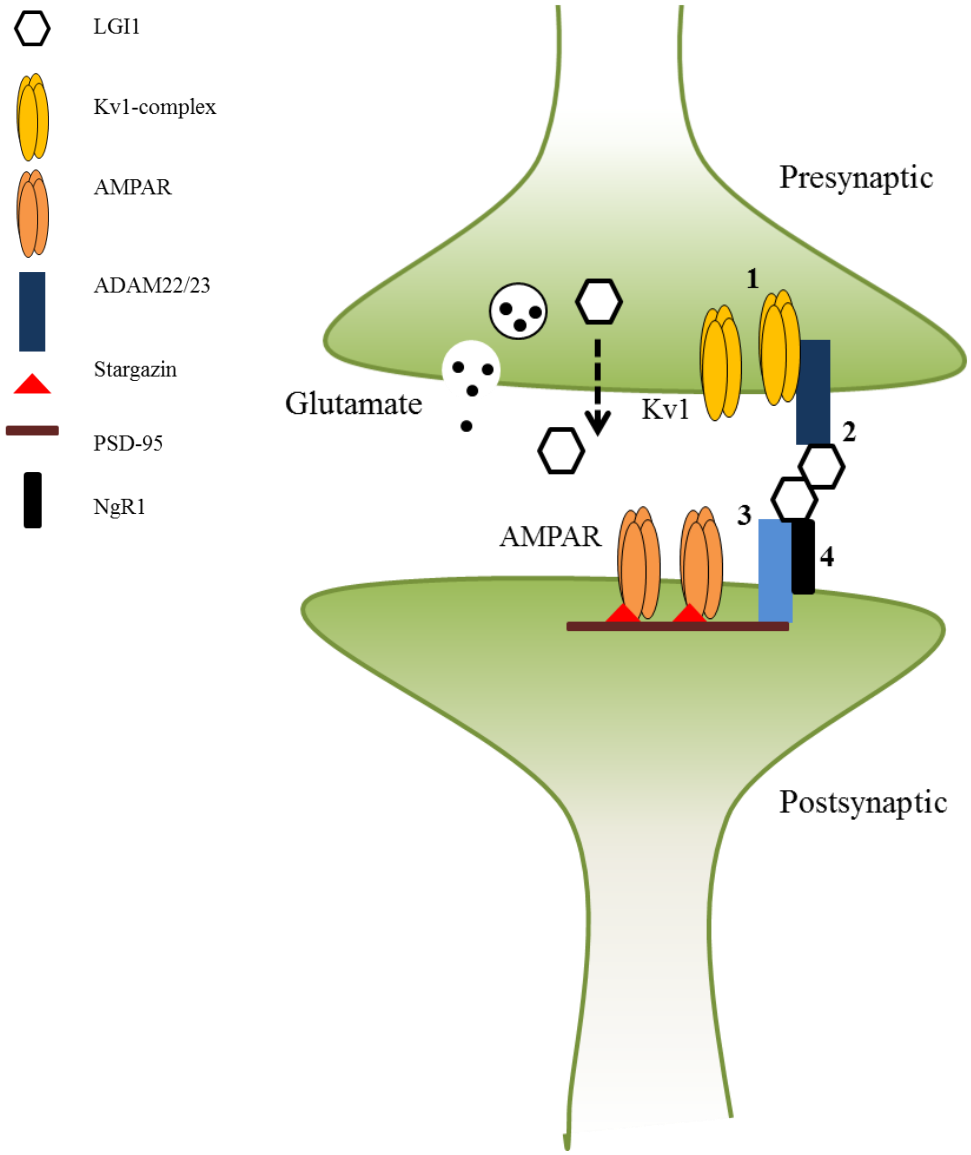

Figure 2-5 LGI1-protein interactions at the synapse

LGI1 is secreted at glutamatergic synapses and is proposed to form a trans-synaptic complex linking presynaptic ADAM23 to postsynaptic ADAM22 molecules. 1) Secreted LGI1 associates with VGKC-complexes indirectly via ADAM23 and regulates neurotransmitter release by antagonism of Kvβ1-mediated inactivation of the Kv1 channel. 2) In vitro LGI1 stimulates neurite outgrowth through its interaction with ADAM23 and 3) binds to ADAM22 enhancing surface expression of AMPAR and AMPAR-mediated neurotransmission in hippocampal slices. 4) LGI1 is a ligand for NgR1 and facilitates neurite extension in vitro. Expression of NgR1 enhances LGI1's interaction with ADAM22.

2.4.2 CASPR2 antibodies

Nineteen out of 96 (20%) patients tested had CASPR2 antibodies in their serum, of which seven out of eleven patients had a diagnosis of NMT (64%). CASPR2 antibodies were also present in some patients with CNS symptoms; 3/5 patients with MoS, 7/64 patients with LE and 2/4 patients with epilepsy (Irani, 2010). Overall, seizures (53%), hyponatremia (11%) and MRI changes (26%) were present but significantly less common than in patients with LGI1 antibodies. Neuromyotonia (53%), neuropathic pain (37%), weight loss (32%), insomnia (32%) and thymoma (32%) were significantly more common than in LGI1 antibody patients. Malignancies were only found in patients with CASPR2 antibodies (Irani, 2010a).

Another group reported CASPR2 antibodies in eight patients, however unlike in the Oxford study, antibodies were only observed in 1/18 (5.5%) patients with PNH. The remaining patients had a diagnosis of MoS (n=4) and LE (n=2) (Lancaster, 2011a). In contrast to a third of the Oxford cohort, none of the CASPR2-antibody positive patients had an underlying malignancy. One patient did not have detectable antibodies by VGKC-radioimmunoprecipaton, suggesting that detection of antibodies by cell based assay may be more sensitive.

The authors confirmed the specificity for LGI1 and CASPR2 antibodies by immunostaining of LGI1 or CASPR2 null mice and immunoadsorption of serum against HEK expressing cells the specific antigen which abrogated the precipitation of ^{125}I-αDTX-VGKC-complexes from brain extract. An overview of the clinical findings are summarised in Table 2-4

2.4.3 Contactin-2 antibodies

Five out of 96 patients (5%) had antibodies against Contactin-2, four of which had additional antibodies against CASPR2, LGI1 or Kv1 (Irani, 2010a).

2.5 Molecular and biochemical targets of VGKC-complex antibodies

The cellular and molecular characteristics of LGI1, CASPR2 and contactin-2 will be discussed below.

2.5.1 LGI1

The LGI1 gene encodes a neuronal secreted glycoprotein of 557 amino acids with a predicted molecular weight of approximately 64 kDa (Furlan, 2006; Senechal, 2005; Sirerol-Piquer, 2006). Three paralogues of LGI1 have been identified and are named LGI2, LGI3 and LGI4 respectively (Gu, 2002). LGI proteins have an amino-terminal signal sequence and two structural domains, the N-terminus contains three leucine rich repeats (LRR) which are flanked on either sides by conserved cysteine residues, The C-terminus comprised of seven 40-43 amino acid repeats that forms a beta-propellor structure which is known as the epilepsy-associated region (EAR 1-7) (Staub, 2002). Both the LRR and EAR motifs are thought to mediate protein-protein interactions (Bella, 2008; Paoli, 2001). Supporting the association of LGI1 antibodies in LE, expression of the LGI1 transcript is predominantly observed in the brain, although intermediate-low levels have also been reported in the peripheral nerve (Chernova, 1998). Within the brain, LGI1 is highly expressed in the hippocampus including the outer and middle molecular layer of the dentate gyrus, the mossy fibres and CA1&3 pyramidal cells and granule cells of the dentate gyrus (Senechal, 2005; Furlan, 2006; Schulte, 2006). Many studies have reported limited expression of LGI1 in glia cells and recent reports have confirmed LGI1 expression in oligodendrocytes and Schwann cells (Ogawa, 2010; Silva, 2010).

	LGI1-antibodies		CASPR2-antibodies		Antigen negative	
	Irani	Lai	Irani	Lai	Irani	Lai/Lancaster
LE	51*	57	7	2	8	0
NMT	1	0	7	1	3	17
Mos	2	0	3	4	0	2
Epilepsy	1	-	2	-	0	-
Other	2	0	0	1	10	-
FBDS (n=26)**	23	-	2	1	3	-

Table 2-4 Summary of antibody specificities in syndromes associated with VGKC-complex antibodies.

Data from Irani 2010a, Lai 2010, Lancaster 2011a, Irani 2011.

** 9/51 patients were positive on an optimised version of the LGI1 assay, (see chapter 4), **= a seizure semiology associated with limbic encephalitis.*

2.5.1.1 LGI1 in potassium channel complexes

The precise biological function of LGI1 remains uncertain, however LGI1 can be immunoprecipitated from rat brain extract using a commercial Kv1.1 antibody (Schulte, 2006). In agreement, commercially available LGI1-antibodies precipitated 60% of the total number of ^{125}I-αDTX binding sites in the diagnostic VGKC- radioimmunoprecipitation assay (Irani, 2010a). Immunohistochemistry showed that LGI1 has a presynaptic localisation with an overlapping expression pattern with Kv1.1, Kv1.4 and Kvβ1 complexes in the hippocampal-circuitry. The only study investigating the direct interaction between LGI1 and Kv1-complexes was performed in Xenopus oocytes transfected with Kv1.1, 1.4, β1 and LGI1. Electrophysiological recording of Kv1.1 and Kvβ1 showed rapid inactivation of the channel by Kvβ1. LGI1 expression inhibited Kvβ1-mediated inactivation which was hypothesised to result in prolonged membrane repolarisation and thus reduce the probability of neurotransmitter release at LGI1 containing synapses (Schulte, 2006).

2.5.1.2 LGI1 in synaptic protein complexes

Immunoprecipitation studies also identified LGI1's in a post synaptic complex with the excitatory scaffolding protein post-synaptic density-95 (PSD-95) and a disintergrin and metalloproteinase (ADAM) family protein member, ADAM22 (Fukata, 2006). Computational models proposed that LGI1 interacts with ADAM22 via its EAR domain (Leonardi, 2011), however this interaction is not exclusive as LGI1 also binds with varying affinity to the extracellular domains of ADAM11 and presynaptic ADAM23 (ADAM23>ADAM22>ADAM11 (Sagane, 2008). It has been reported *in vitro* that LGI1's interaction with ADAM22 is weak but can be facilitated by co-expression with Nogo receptor 1 (NgR1), which directly interacts with ADAM22 *in vitro* (Thomas, 2010). Despite this Fukata *et al* showed that LGI1 can be precipitated in abundance from wild-type mice using a commercial antibody against ADAM22. LGI1 knockout models demonstrated that LGI1 is a trans-synaptic ligand that bridges presynaptic ADAM23 and post-synaptic ADAM22 molecules (Fukata, 2010) and a schematic overview of LGI1 and its interactors is shown in Figure 2-5. *In vitro*, LGI1 stimulated neurite outgrowth in dorsal root ganglia and hippocampal cultures via its interaction with ADAM23 (Owuor, 2009) and enhanced glutamatergic neurotransmission through an increase in the

number of AMPA receptors in rat hippocampal slices via is interaction ADAM22 and PSD-95 (Fukata, 2006).

2.5.1.3 LGI1 mutations in autosomal dominant epilepsy

LGI-proteins share homology of their EAR domain with VLGP1 proteins, and a mutation in this region of the MASS1 gene fragment results in audiogenic epilepsy in the Frings mouse (Scheel, 2002). Mutations in the LGI1 gene have been described in approximately 50% of patients with autosomal dominant lateral temporal lobe epilepsy (ADLTE), which is characterised by auditory auras and focal seizures that present in late adolescence (Gu, 2002; Kalachikov, 2002; Morante-Redolat, 2002). To date 36 mutations including missense, truncations and microsatellite repeats have been identified in the LGI1 gene and tend to cluster in the LRR domain, but can also found in the EAR domain. Despite the wide variety of mutations, the phenotype is relatively homogenous (Ho, 2012). Analysis of all but one ADLTE mutation in transfected cells (1219C>T, (Striano, 2011)) prevented the secretion of LGI1 into the cell medium (reviewed in (Nobile, 2009)) and failed to antagonise Kvβ1 inactivation of Kv1 channels (Schulte, 2006). Rodents expressing one mutant LGI1 allele, $LGI1^{+/+/835delC}$ or $LGI1^{+/L385R}$ do not develop spontaneous seizures but are more susceptible to seizure induction with acoustic stimulation or GABAergic antagonism with 50 μM picrotoxin, than wild-type litter mates (Zhou, 2009; Baulac, 2012). This finding infers the subtle pathology of ADLTE, as patients infrequently experience tonic-clonic seizures (one/year).

One study looking at the development of glutamatergic synapses in mice expressing a transgene encoding truncated LGI1 (835delC) reported a reduction in dendritic development as a result of decreased dendritic pruning which resulted in an increase in glutamatergic but not gabaergic neurotransmission (Zhou, 2009). As most patients with VGKC-complex antibodies already have a developed nervous system, the role of glutamatergic synaptic maturation in the context of LGI1-antibody disease is not clear.

2.5.1.4 LGI1 knockout mice

LGI1 knockout mice developed characteristic myoclonic, dystonic and generalised seizures two week after birth which results in death around postnatal day 15 but showed no histological abnormalities (Chabrol, 2010; Fukata, 2010; Yu, 2010). Similar lethal seizure phenotypes were observed for knockout mice for many proteins interacting with LGI1 including ADAM22, ADAM23 and Kv1.1 and Kv1.2 subunits (Smart, 1998; Sagane, 2005; Owuor, 2009; Brew, 2007). In LGI1 null mice the seizure phenotype can be rescued by the neuronal expression of the LGI1, but not the LGI3 transgene (Fukata, 2010). In one study, electrophysiological evidence suggested that this phenotype is due to an excess release of presynaptic glutamate, as determined by an increased frequency but not size of miniature excitatory postsynaptic potentials (mEPSPs) in CA1 pyramidal neurons (Yu, 2010). In contrast, Fukata *et al* showed that LGI1 null mice had decreased AMPAR-mediated currents in the hippocampus and hypothesised that a reduction of glutamatergic transmission in inhibitory interneurons would contribute to hyperexcitability of the hippocampus (Fukata, 2010) . Furthermore the authors showed a biochemical reduction in the amount of Kv1.1, Kv1.2, ADAM22 and ADAM23 expression in the brain, which may further propagate the seizure phenotype in the model.

The phenotype in these mice is not only related to the CNS as one study that examined mouse behaviour before seizure onset showed reduced locomotor activity and muscle strength due to hypomyelination of the peripheral nerve (Silva, 2010). This may explain the phenotype of NMT in one patient with LGI1 antibodies (Irani, 2010a).

2.5.1.5 Pathogenic mechanisms of LGI1 antibodies

Only one study has examined the pathogenicity of LGI1 antibodies. Rat hippocampal slices were incubated for two hours with IgG from a healthy control or a patient with limbic encephalitis with LGI1 antibodies (VGKC-RIA 5,084 ρM). LGI1-IgG, but not control IgG evoked epileptiform activity in the CA3 region of the hippocampus, which was a result of enhanced firing activity of CA3 pyramidal cells (Lalic, 2011). Interestingly, α-DTX, a selective Kv1 antagonist mimicked the effects of the LGI1-Ab IgG suggesting that the antibodies may be directly affecting the function of the potassium channels. As the experiments were performed for only 2 hours at 34˚C, effects of

Kv1/LGI1 internalisation may not have been detected. Unfortunately, VGKC and LGI1 expression levels were not addressed in this study.

In summary, LGI1 is a secreted protein that interacts with a variety or presynaptic and postsynaptic. It is predominantly expressed in the CNS and its precise function remains unclear. LGI1 has been implicated in postnatal maturation of glutamatergic circuits, neurite outgrowth, and potentiation of postsynaptic glutamatergic neurotransmission and inhibition of presynaptic neuronal function. Disruption of LGI1 secretion results in an epilepsy syndrome in mice and humans, which is a core feature of LGI1-antibody associated LE. Unlike ADLTE and LGI1 null mice, LE occurs in adult life after normal development of glutamatergic synapses is complete. The precise effector mechanisms of LGI1-antibodies and how they cause LE may be due to enhanced glutamatergic neuronal excitability.

2.5.2 CASPR2

The CNTNAP2 gene encodes the CASPR2 protein, a member of the neurexin superfamily. CASPR proteins mediate neuronal-glia interactions in the peripheral and central nervous system. In total there are five CASPR homologues, CASPR1-5, however only CASPR2 associates with Kv1 channels. The CNTNAP2 gene encodes a glycosylated transmembrane protein with 1331 amino acids with a predicted molecular weight of 180kDa. CASPR2 spans the membrane once and consists of a large extracellular amino terminal (αα 28-1373) which contains an amino terminal signal peptide, an F5/8 type discoidin domain, two epidermal growth factor repeats and four laminin-G like domains (Poliak, 1999). The cytoplasmic domain of CASPR2 contains a PDZ binding domain and an additional binding site for protein 4.1. CASPR2 is located predominantly in the juxtaparandoes of large myelinated axons in the PNS and CNS (Poliak, 2003). Immunohistochemical analysis in the mouse brain shows CASPR2 expression in the cell bodies and dendrites in the stratum radiatum of the hippocampus, the dentate gyrus, striatum, amygdala, thalamus, cerebellum and cortex. In addition, CASPR2 has been detected in the ventricular proliferative zones and the ganglionic eminences suggesting CASPR2 has additional roles in neuronal migration and neurodevelopment (Peñagarikano,

2011). Immunoprecipitation experiments have shown that CASPR2 co-precipitates with Kv1 subunits via its cytoplasmic domain (1317-1331αα), and commercial CASPR2 antibodies can precipitate 20% of the total number of ^{125}I-αDTX binding sites in the diagnostic VGKC-radioimmunoprecipitation assay, illustrating that less than 50 % of Kv1 sites contain CASPR2 (Poliak, 1999; Irani, 2010a). In brain immunoprecipitation studies, CASPR2 was detected in Kv1.1 (Schulte, 2006) and Contactin-2 immune precipitates (Traka, 2003). Transfection experiments with CASPR2 with VGKC subunits demonstrated that this interaction was not direct, however the C-terminal domain of CASPR2 alone (αα 1373-1384) could immobilise Kv1.2 subunits from rat brain homogenate, illustrating that CASPR2's PDZ domain is important for the interaction with VGKC's (Poliak, 1999). CASPR2's interacts with Contactin-2 directly through an in cis interaction and is important in maintaining axo-glial interactions (Traka, 2003). CASPR2 molecules are required for the correct organisation of VGKC's at the juxtaparandoes, in CASPR2 null mice the correct nodal architecture is no longer maintained and both VGKC's and Contactin-2 are re-located in to the paranodal compartment (Poliak, 2003).

2.5.2.1 CASPR2 associations with neurological disorders

Mutations in CNTNAP2 were first identified in Amish children with cortical dysplasia focal epilepsy (CDFE) (Straus, 2006). CDFE is characterised by macrocephaly, diminished deep tendon reflexes and focal epilepsy and after seizure onset, mental retardation, and social and language deficits emerge. Similarly, in patients with CASPR2 antibodies, seizures were observed in thirteen of 28 patients studied (Irani, 2010a; Lancaster, 2011a). MRI identified gross structural malformations in 3/9 CDFE patients and histological investigation identified abnormal neuronal organisation in the neocortex, ectopic neurons and reactive astrocytosis. Most interestingly, CDFE biopsy tissue showed a reduction in CASPR2 expression in the temporal lobe and Kv1.1 was reported to be mislocalised from the axon into the soma, supporting biochemical data that CASPR2 is important for determining Kv1 localisation at the juxtaparanode (Poliak, 2003). Since then subsequent studies have associated mutations and polymorphisms in the CNTNAP2 gene with schizophrenia, psychosis, mental

retardation, seizures, epilepsy and increased susceptibility to autism (Friedman, 2007; Zweier, 2009; Arking, 2008).

2.5.2.2 CASPR2 knockout mice

CASPR2 null mice were born without apparent gross defects but were reported to be initially smaller than their heterozygous or wild-type litter mates (Poliak, 2003). Myelination, axon calibre and nodal architecture, including Na^+ channels, CASPR and NF155 localisation was unaffected. As reported above, Kv1 channel clustering and Contactin-2 expression was no longer seen in the juxtaparanode but was dispersed along the paranode and internode respectively in both CNS and PNS neurons, although protein expression in nerve lysates showed no effect on Kv1.2 expression. Mutant mice displayed normal electrophysiological recordings of nerve conduction and had no alterations in conduction velocity, refractory period or spontaneous activity that would be indicative of the spontaneous discharges observed in NMT. Detailed behavioural analyses of the same mice later showed stress-induced seizures after six months of age which were characterised as generalized interictal spike discharges during slow-wave sleep (Peñagarikano, 2011). Comprehensive behavioural testing in mice studied prior to seizure onset focused on autism-spectrum behaviours. Mice were hyperactive, displayed stereotypical behaviours, had enhanced nociceptive responses to thermal stimuli, behavioural inflexibility and had communication and social deficits, yet were not anxious and showed normal learning on the Morris water maze. Risperidone, a dopamine antagonist, reversed all deficits except those in social interaction and sensory hypersensitivity, suggesting that multiple brain circuits may be affected in this model. Histological analysis before the onset of seizures (postnatal day 14) revealed neuronal migration abnormalities in cortical neurons and a reduced number of GABAergic interneurons in the cortex and hippocampus. More detailed findings revealed asynchronous neuronal firing in layers II/III of the somatosensory cortex, with a reduced paired neuron firing time that was independent of firing rate and amplitude. This finding was suggested to be indicative of an overall network dysfunction and hypothesised to underlying the complex behavioural phenotypes, in particular, the cognitive deficit displayed in the CASPR2 knockout mouse.

2.5.3 Contactin-2/ Tag-1

Tag-1 (transient axonal glycoprotein-1) is the rodent homologue of Contactin-2. Contactin-2 is a large, 110kDa GPI-anchored cell adhesion molecule comprised of immunoglobulin domains and four fibronectin repeats. TAG-1 interacts with numerous cell adhesion molecules and has been implicated in development of the nervous system, and facilitation and guidance of neurite outgrowth (Furley, 1990). Like CASPR2, Contactin-2 is expressed in the nerves and glia of myelinated axons in the PNS and CNS where it is located at the juxtaparanode and interacts directly with CASPR2. Contactin-2 also interacts in trans with itself between the nerve and glia cells Mice deficient in TAG-1 have disrupted organisation of the juxtaparanode identical to CASPR2 knockout mice and display no gross abnormalities or changes in nerve conductance (Traka, 2003). Savvaki *et al* quantified protein expression in the brain of TAG1 knockout mice and found a significant reduction CASPR2 and Kv1.1 in the cerebellum, hippocampus and olfactory bulb, but not in the entorhinal cortex. Null mice showed some cognitive deficits on the Morris water maze and object recognitions tests, reduced motor activity, abnormal gait and increased response to noxious stimuli (Savvaki, 2008). Few null mice were reported to develop spontaneous seizures but further studies showed mice had an increased susceptibility to convulsant stimuli compared to wild type mice (Fukamauchi, 2001) .

2.6 Cell surface antibodies to other CNS proteins

Antibodies to aquaporin-4 (AQP4), the N-methyl-D-aspartate receptor (NMDAR), the amino-3-hydroxy-5-methyl-4-isoxazolepproprionic acid receptor (AMPAR), the γ-aminobutryric acid receptor B ($GABA_B$ receptor), the glycine receptor (GlyR) and the metabotrophic glutamate receptor mGluR5, have all recently been identified in patients with CNS disease (Lennon, 2005; Dalmau, 2007; Lai, 2009; Lancaster, 2010b; Hutchinson, 2008; Lancaster, 2011c). In the majority of cases, antibodies were first recognised by their distinct immunoreactive binding patterns to rodent brain sections. Routinely, these surface antibodies are detected in CBA's, as described for LGI1 and CASPR2 detection, where HEK cells have been transfected with the relevant target.

Whilst the clinical presentation associated with the different antibodies can range from focal limbic encephalitis to a more diffuse encephalopathy, depending on the anatomical distribution of the

antigenic target, the syndromes can often mimic genetic or pharmacological disruption of the affected protein. For CNS disorders, where the periphery appears to produce the antibody and the antigenic target is located behind the blood-brain barrier, it is not known whether disruption of the blood-brain barrier permits the diffusion of serum antibodies into the brain or whether intrathecal synthesis of the specific autoantibodies in the CSF or infiltrating plasma cells are required to initiate disease. Accumulating pieces of experimental evidence suggest mechanisms for the action of these antibodies include the cross-linkage and subsequent internalisation of receptors, which has been demonstrated for both NMDAR and AMPAR antibodies (Dalmau, 2008; Lai, 2009), a direct effect on channel function, which has been reported for GABA antibodies (Lancaster, 2010b) or complement-dependent cell lysis as reported in *in vitro* and *in vivo* models of AQP-4 antibody mediated disease (Hinson, 2007; Saadoun, 2010).

2.7 Conclusion and Summary

VGKC-complex antibodies have been described in disorders affecting the PNS, the CNS, or both. Recent studies have shown these antibodies are directed against proteins associated with the VGKC-complex; CASPR2, LGI1 and contactin-2. Genetic models in humans and animals suggest that disruption of these proteins result in neurological impairment which share features reminiscent of LGI1 and CASPR2 autoimmune disease. The distribution of the antigens appears to explain the majority of the clinical syndrome localisation. For example, in limbic encephalitis, VGKC-complex antibodies are predominantly against LGI1 which is predominantly expressed in the CNS. The antibody specificities have been described in only a small number of patients with Morvan's syndrome, (total n=9, CASPR2 n= 7, LGI1 n=2).

These disorders fulfil two of the revised criteria for an antibody-mediated disorder; firstly antibodies present in patient sera bind to extracellular epitopes of a functionally important protein, and secondly patients show a significant improvement with immunotherapies including plasma exchange and IvIg, which correlate with a fall in the serum antibody-titer.

Previous experiments have shown that IgG from patients with NMT (now known to be against CASPR2) suppress potassium channel currents and increase the excitability of the peripheral nerve,

whereas IgG from a patient with LE (LGI1-Ab) enhances excitatory neurotransmission in hippocampal brain slices. However the precise pathogenic mechanisms by which these antibodies mediate their effects are not known.

2.8 Aims

The overall aim of this thesis was to investigate the pathogenic mechanisms underlying antibody-mediated disorders. The first results chapter introduces the cell based assays used to determine the specificities of VGKC-complex antibodies and describes the development of the LGI1 cell based assay. Furthermore the chapter focuses on the antibody specificities in a cohort of patients with MoS, as this has only received limited attention in established studies. In the second results chapter of section one the structural and biological properties of CASPR2 and LGI1 antibodies were characterised in patients with limbic encephalitis or Morvan's syndrome *in vitro*. Finally, section two of this thesis will focus on modelling the pathogenic effects of NMDAR antibodies *in vivo*. These chapters aimed to better understand the serological characteristics of patient antibodies and their pathogenic mechanisms underlying disease.

Chapter 3: Materials and methods

3.1 Antibodies and plasmid constructs

Antibodies used in this thesis are listed below and grouped according to the techniques they were used.

Immunocytochemistry	Dilution	Alexa Fluor secondary antibody
Rabbit anti CASPR2 ab104525 (Abcam) Mouse anti CASPR2 K67/25 (Neuromab)	1:100 1:100	A-11011, 1:750 A11029, 1:750
Goat anti LGI1, sc-9581 (Santa-Cruz) Goat anti LGI1, sc-9583 (Santa-Cruz)	1:100 1:100	A-11057, 1:750
Rabbit anti contactin-2, gift from Dr E. Peles	1:100	A-11011, 1:750
Mouse anti human IgG1, 2, 3, 4 MC003, 005, 006, 011 (The Binding Site)	1:50	A11029, 1:750
Rabbit anti C3b, A0062 (Dako)	1:200	A-11011, 1:750
Mouse anti MAP-2, M3696 (Sigma)	1:1000	A11029, 1:1000
Western blot	Dilution	Anti-HRP conjugated secondary antibody (Dako)
Rabbit anti GFP, ab6556 (Abcam)	1:1000	P0448, 1:2000
Rabbit anti CASPR2, ab33394 (Abcam)	1:1000	P0448, 1:2000
Rabbit anti actin, A2066 (Sigma)	1:5000	P0448, 1:2000
Mouse anti NR1, mab363 (Millipore)	1:200	P0161, 1:5000

Table 3-1 Antibodies used in this thesis

All cDNA constructs encode the full length humans sequences for CASPR2 (pEGFP-N1), wild type LGI (pcDNA3.1+), contactin-2 (a kind gift from Dr Karagogeos, Cyprus), the NMDAR subunits NR1 and NR2B (pcDNA3.1) and AQP4 (pEGFP-C2). All constructs have been described previously (Leite et al. 2008; Irani et al. 2010a) and a schematic of the plasmid vectors can be found in the appendix, figure 1 and 2.

All molecular biology described in this thesis was performed by Dr Patrick Waters. As part of this thesis, LGI1 which is a secreted protein was tethered to the cell membrane by fusion on to the transmembrane domain and C-terminus of CASPR2 (residues 1248-13331). The wild type LGI1 construct was digested with restriction enzymes XhoI/PmeI and amplified by polymerase chain reaction with primers 1 and 2 (below). The stop codon was removed from the LGI1 sequence by site directed mutagenesis using the primers 3 and 4 below to give a final product of LGI1 in pcDNA3.1+. This construct is referred to as membrane or tethered LGI1 and is no longer secreted from the cell.

Primer 1: GATCCTCGAGGGACAAGGCCAAGCTATAAGAAATG

Primer 2: ATCGTTTAAACTCAAATGAGCCATTCCTTTTTGC

Primer 3: GTTGACTTAAGCGCAGGACTCGAGGGACAAGG

Primer 4: CCTTGTCCCTCGAGTCCTGCGCTTAAGTCAAC

3.2 VGKC-complex radioimmunoprecipitation assay (RIA)

This assay was performed as described previously (Vincent, 2004) - and is referred throughout the thesis as the "diagnostic assay". VGKC-complexes were extracted from rabbit whole brain membranes and solubilised in 2% digitonin (Calbiochem, USA) in DTX buffer (100mM NaCl, 20 mM Tris, 5 mM KCl adjusted to pH 7.12) in a 37˚C water bath for 30 minutes. The membranes were centrifuged at 13,000 rpm for 10 minutes; the supernatant collected and subsequently diluted 2:1 in PTX (0.02 M phosphate buffer, 0.1% Triton X100, pH 7.2). The extracted VGKC-complexes were labelled with ^{125}I-α DTX at one million counts per minute (cpm) per ml of extract. For each reaction, 50 µl of labelled extract was incubated with serum, either 1µl and 5µl, made up to a total volume of 50 µl with PTX, and incubated overnight at 4˚C. The following morning 50 µl of goat anti-human IgG

(Binding Site, UK) was added to each reaction. After 90 minutes, 500 µl of PTX was added to each reaction and the antibody-antigen complex was immunoprecipitated by centrifugation at 13,000rpm for 5 minutes. The supernatant was discarded and the pellet washed twice in 500 µl of PTX. The pellets were finally counted on a Cobra 2 gamma counter (Perkin Elmer).

3.3 Cell culture

3.3.1 Human Embryonic Kidney 293 cells

All tissue culture techniques were performed under sterile conditions in a class II tissue culture hood. Human embryonic kidney 293 (HEK) cells were cultured in Dulbecco's Modified Eagle medium (DMEM) supplemented with 10% fetal calf serum (FCS) and 1% penicillin/streptomycin/amphotericin (PSA), maintained in T175cm^2 flasks and grown in a humidified 37˚C, 5% CO_2 incubator. Cells were split every 3-4 days when they reached 90% confluency. The medium was aspirated off of the cells and 1% trypsin in phosphate buffer solution (PBS) was added to each flask. With gentle agitation, cells detached from the flask and were neutralised in FCS/DMEM. Cells were re-suspended in fresh DMEM, counted and re-seeded into new culture flasks.

3.3.2 Transfection of HEK293 cells

For cell based assays, 13mm glass coverslips were transferred in to 6-well culture plates and submerged in poly-L-lysine (PLL) for 15 minutes. PLL was aspirated and the plate's air dried. HEK cells were counted using a haemocytometer and 4x10^5 cells were seeded per well in 2 ml of medium. The following day, cells were transfected. Each well was transfected with a DNA transfection mix containing 3 µg of DNA with 1.25 µl of 20% sterile glucose and 1.5 µl of polyethylimine (PEI) per well in 2 mls of medium. After 16 hours, the transfection medium was removed from the well and replaced with fresh media. Coverslips were used for detecting patient antibody binding 24-36 hours after transfection.

3.3.3 Primary hippocampal neuronal cultures

Wistar rat pups, postnatal day 0 (P0) were sacrificed by decapitation and stored on ice. Using fine scissors the skin was cut along the midline on the head and the skull removed and the brain placed into a petri dish containing ice cold Hank's balanced salt solution (HBSS). With fine-tip forceps, hippocampi were dissected out of the brain and the meninges carefully removed. Dissected hippocampi were placed into fresh HBSS on ice until all hippocampi from the litter had been processed. Hippocampi were washed in HBSS and dissociated in 1% trypsin-HBSS solution for 20 minutes at 37˚C. All steps from here onwards were performed in a sterile laminar flow hood. The trypsin was aspirated and replaced with complete Minimal Essential Medium (MEM, 450 ml, supplemented with 10% FCS and 1% PSA) and cells gently triturated twenty times with a p1000 and then a p200 pipette tip until no visible clumps of tissue remained. The cell suspension was gently centrifuged at 1,000 rpm for 5 minutes, the supernatant aspirated and the cell pellet resuspended in complete MEM medium. Cells were counted and $2x10^5$ cells per well were plated on to PLL-glass coverslips of a 6-well plate in and placed in a humidified 37˚C, 5% CO_2 incubator. After two hours the media was aspirated and replaced with 3 mls of Neurobasal medium (supplemented with 1% B-27 serum free supplement, 200mM L-glutamine and 1% PSA (referred to as NB^+ media)). Half the culture medium was replaced every 3 days with fresh NB^+ media. Neurons were grown for a fortnight before staining on days *in vitro* (DIV) 14-18.

3.4 Immunofluorescence detection of VGKC-complex antibodies

3.4.1 Transfected HEK293 cells

Thirty-six hours after transfection coverslips were transferred to individual wells of a 24-well culture plate containing sera diluted 1:20 - 1:100 in wash buffer (500 ml DMEM, 200 mM HEPES) supplemented with 1% bovine serum albumin (BSA, Sigma) for one hour and incubated at room temperature. Positive and negative controls were included in each assay. The cells were washed three times in wash buffer, fixed for 15 minutes in 250 µl of 3% formaldehyde in PBS and then washed three times. To detect IgG binding the cell surface expressed antigen, coverslips were incubated with

goat-anti human IgG Alexa Fluor 568-conjugated secondary antibody (A-21090) diluted 1:750 for 45 minutes. The coverslips were washed three times in wash buffer, followed by twice in PBS and the coverslips mounted on glass slides with mounting medium (DakoCytomation, Cambridge, UK) containing 4',6'-diamidino-2-phenylindole (DAPI, 1:1000) to label the cell's nuclei. Coverslips were visualised using a on a fluorescent microscope with a MacProbe v4.3 digital imaging system.

3.4.2 Scoring of IgG binding on the CBA

Surface binding of patient IgG was assessed in a semi-quantitative manner. Cover slips that showed no detectable binding of IgG were given a score of zero whereas cover slips that showed detectable binding of IgG were scored on a scale 1-4. Intense IgG co-localisation with a 100% of transfected cells was given a score of maximum score of 4, with decreasing intensity of IgG binding given a score an intermediary score (2 or 3). Typically, samples given scores of 1 or 2 bound to fewer than 50% of transfected cells. All samples deemed positive were repeated and counter scored by an independent observer.

3.4.3 Determining CASPR2 and LGI1 subclasses by CBA

Antibody IgG subclasses were determined on the CBA for patients with available sera. After cells had been incubated with patient sera washed and fixed and washed, (as described in 2.4.1), cells were incubated with subclass specific anti-human IgG1, IgG2, IgG3 or IgG4 primary antibodies (The Binding Site, UK) diluted 1:50 in DMEM/HEPES/1% BSA for 45 minutes. The cells were washed three times and specific binding visualised with Alexa Fluor IgG goat anti mouse IgG 568 (A11029) diluted 1:750 for 1 hour. The cell were washed three times in wash buffer, twice in PBS and subsequently mounted as described previously.

3.4.4 Complement activation of CASPR2 and LGI1-antibodies by CBA

Serum from a single healthy control donor was used as a source of complement proteins. After blood withdrawal, blood is collected in to a glass container and centrifuged at 5,000 g for 15 minutes separating the blood cells from the serum. The serum was collected, aliquoted and stored at -80˚C immediately to preserve complement activity.

For detection of deposited complement on transfected cells, patient sera was heat inactivated (30 minutes at 56˚C) prior to incubation on live transfected HEK cells. Live cells were washed three times and incubated for 30 minutes at 37˚C with fresh human sera diluted 1:100 in DMEM-HEPES-1% BSA. To prevent cells from further lysis, cells were immediately placed on ice washed, fixed and incubated with rabbit anti-C3b commercial antibody diluted 1:200 and specific binding detected using Alexa Fluor goat anti rabbit IgG 568 (A-11011). For all patients that deposited complement on transfected cells, the assay was repeated in both the presence of the fresh serum and heat inactivated serum.

3.4.5 Detection of antibodies against the surface of live primary neuronal cultures

Coverslips were transferred to individual wells of a 24-well culture plate containing patient serum diluted 1:100 in NB^+ medium supplemented with 1% bovine serum albumin (NB^+/BSA) and incubated at room temperature for one hour. Coverslips were washed three times in NB^+ medium , fixed for 15 minutes in 3% formaldehyde in PBS and then re-washed three times before incubating with Alexa Fluor goat-anti human IgG 488 (A-11013) diluted 1:1000 for 45 minutes. Cells were washed three times in NB^+ media before being permeabilised with 0.25% Triton-X-100 in PBS (PBS-TX100) for 15 minutes. Coverslips were incubated with mouse monoclonal anti-MAP2 antibody, diluted 1:1000 in NB^+/BSA, to identify the neuronal cells in the preparation. After one hour coverslips were washed three times and incubated with the appropriate secondary antibody for 45 minutes, washed 3 times in NB^+/BSA, twice in PBS and mounted as described previously.

3.4.6 Preadsorption of specific antibodies

For adsorption of CASPR2 or LGI1-antibodies, cells were transfected with expression vectors encoding CASPR2, LGI1 or AQP-4. After 36 hours cells were trypsinised, re-suspended in DMEM-1% HEPES and counted. Limiting quantities of sera (determined from end-point titration experiments), were adsorbed 3 times sequentially against $4x10^7$ live HEK cells in solution. Briefly, serum diluted 1:10 was incubated against cell pellets for one hour at room temperature on a rotator.

The adsorbed samples were re-tested on the cell based assay (1:20 – 1:100) to confirm complete absorption.

3.5 Preparation of purified IgG

The IgG fraction of plasma or serum can be purified using protein G Sepharose beads (Sigma, UK). At a neutral pH, protein G binds to the Fc domain of mammalian IgG molecules, including all human IgG subclasses. The protein G beads are supplied as slurry in 20% ethanol. Before use the beads were washed 3 times in Hartmann's solution before being loaded in to a chromatography column. Patient serum or plasma was heat inactivated (56˚C for 30 minutes), diluted 1:4 in Hartmann's solution and applied to the column. The solution was passed through the column slowly with an approximate flow rate of 0.2 ml/minute allowing the IgG to become immobilised on the beads whilst other serum proteins pass through the column. The column was washed with Hartmann's solution using 10x the volume of serum loaded to remove non-specifically bound proteins. Using a Coomassie stain the final wash fraction was confirmed to be absent of protein. Serial fractions of 2mls were eluted as quickly as possible from the column using 0.1M Glycine (pH 2.3) and eluted fractions quickly neutralised in 100 µl of 1M Tris (pH 8.0). IgG fractions were kept on ice and an aliquot of each sample was used to determine the protein content with Coomassie dye. All fractions containing protein were pooled, placed in Snakeskin dialysis tubing (10,000kDa cut off (ThermoScientific, UK)) and dialysed five times in 1L of Hartmann's solution for 2 hours at room temperature. IgG was subsequently concentrated using Amicon ultra-4 10kDa filter units, filter sterilised and the IgG concentration determined using an IgG radial-immuno diffusion kit (Bindarid IgG, The Binding Site). IgG was aliquoted and stored at 4˚C.

3.6 Antibody Internalisation studies

For internalisation experiments assessing surface human IgG binding over time on transfected HEK cells and hippocampal cultures, coverslips were stained initially as described in the respective methods, see section 0 and 3.4.5, but using purified IgG instead of serum (at equivalent concentrations). After incubation of coverslips for one hour at room temperature in purified IgG,

coverslips were washed and either stained immediately (time 0 hours) for surface anti-human IgG binding before fixing in 3% formaldehyde or placed back in to the incubator for 2, 4, 8, 12 or 24 hours. These coverslips were also stained for surface human IgG binding prior to fixation. HEK cells were subsequently washed, fixed and mounted and hippocampal neuronal coverslips were washed, fixed, permeabilised and stained for MAP-2.

3.6.1 Transfected HEK293 cells

To study the effect of CASPR2-antibodies on CASPR2 surface expression cells were transfected with CASPR2 cDNA in either 6-well plates or T175cm^2 flasks. For T175 cm^2 flasks, the transfection mix consisted of 60 μg of the appropriate DNA, 25 μl glucose and 30 μl PEI per flask. Sixteen hours later the transfection mix was aspirated and replaced with fresh media or media supplemented with 0.3 mg/well or 6 mg/T175flask of human IgG. Two healthy control IgG, two LGI1-IgG and three CASPR2-IgG preparations were used.

In six well plates, 24 hours after the addition of IgG, coverslips were washed, and live unfixed cells stained with rabbit anti CASPR2 commercial antibody (ab104525, Abcam). Coverslips were subsequently washed, fixed and antibody binding visualised with rabbit anti mouse IgG Alexa Fluor 568 (A-11061) diluted 1:750. Surface IgG binding and surface CASPR2 expression was scored by two independent observers. Representative photographs were taken at 100x magnification (9 fields) and the number of surface CASPR2 positive (red), CASPR2-EGFP positive (green) and DAPI positive cells (blue) were manually counted using Image J Cell Counter software.

After 24 hours T175cm^2 flasks were washed thoroughly and the intracellular and extracellular protein fractions collected using the Cell Surface Protein Isolation Kit (89881, Thermo Scientific). Briefly, live cells were incubated with EZ-Link® Sulfo-NHS-SS-Biotin, labelling surface proteins in the cell membrane. After 30 minutes the reaction was quenched, harvested and lysed and the labelled proteins isolated on a NeurtrAvidin Agarose column. Unbound proteins were collected in the flow through; this was considered the intracellular fraction (500 μl). The column was washed and membrane proteins eluted in 100 μl of SDS-PAGE buffer (Invitrogen UK) containing 50 mM DTT. The protein

content of the intracellular fraction was determined using a bicinchoninic acid (BCA) BCA assay kit (23227, Pierce UK). Equal concentrations of membrane and intracellular cell extract fractions were analysed by SDS-PAGE and western blot, and their CASPR2 and actin content examined.

3.6.2 Primary hippocampal cultures

Methods for staining primary neuronal cultures with patient IgG has been described in section 3.4.5. For internalisation studies coverslips were tested for anti-human IgG binding immediately, 0 hours or 24 hours after removal of patient IgG prior to fixing and permeabilisation of the neurons. The viability of hippocampal neurons on coverslips placed back in to the incubator for 24 hours was compared using fresh NB^+ medium or conditioned NB^+ medium that had been collected from neurons of a similar age (Div 14-18) in culture. In the final experiments all neurons were incubated, washed and replaced in conditioned NB^+ medium

3.6.3 Quantification of surface IgG binding

For all quantification analysis, fluorescent images were collected using a confocal microscope (Bio Rad MRC 1024-UV). To avoid sampling bias 16-21 images from 10 coverslips were collected from regions of interest by observing the DAPI counter stain. All images were taken at 400x magnifications, with equal exposure times and subsequently analysed using Metamorph (Molecular Devices, version 6.1). All images were set to equal thresholds and their integrated fluorescent intensities calculated. For data with significant differences in their MAP2 intensities, a ratio of IgG intensity/MAP2 intensity was calculated. The number of IgG puncta was calculated with Image J software.

3.7 Protein extraction

For CASPR2-EGFP and LGI1-EGFP protein extraction experiments the quantity of cells was scaled up. $1.2x10^7$ HEK cells were seeded in to T175cm^2 culture flasks and transfected the following day with 60µg of the appropriate DNA, 25 µl glucose and 30 µl PEI per flask and the culture medium replaced the following morning. 48 hours after transfection all culture media was aspirated from the

cells and the cells were extracted in 3ml of extraction buffer (10 mM Tris pH 8.0, 100 mM NaCl, 1 mM EDTA) containing 1% digitionin and immediately before use supplemented with protease inhibitor cocktail (PIC,1:1000). After gentle agitation the supernatant was collected, rotated at 4˚C for 2 hours before being centrifuged at 13,000 g for 10 minutes. Extracted proteins in the supernatant were collected and the EGFP content was assessed from a 100 µl of extract on a fluorescent plate reader (Victor^3, Perkin Elmer). EGFP was quantified as green fluorescent units (gfu). Protein extract was stored at -20˚C until required.

3.7.1 Fluorescent immunoprecipitation assay (FIPA)

HEK cells transfected with CASPR2 or membrane LGI1 tagged with EGFP were extracted and diluted to 25,000 gfu/ 100µl. 5 µl of patient (LGI1-Ab n=10, CASPR2-Ab n=10) or healthy control serum were incubated with 100µl of CASPR2-EGFP or LGI1-EGFP cell extract overnight at 4˚C. Immunocomplexes were precipitated using 50 µl of Protein-G Sepharose beads (Sigma, P3296), washed three times in PTX, resuspended and counted. The cut off for the assay represents the mean of healthy control samples (n=10) plus 3 standard deviations.

3.8 Gel electrophoresis

3.8.1 Sample preparation and gel electrophoresis

Protein content in cell extracts were determined using the BCA assay and diluted appropriately in 4x SDS loading buffer (Invitrogen, UK) supplemented with 10x reducing agent (Invitrogen, UK). Samples were boiled for 10 minutes at 95˚C, centrifuged at 13,000 g for 5 minutes and the supernatant collected. Tris-Acetate 3-8% gels (NuPage, Invitrogen) were loaded into a gel electrophoresis tank (XCell Sure Lock gel tank, Invitrogen) containing 1x Tris Acetate buffer (NuPage, Invitrogen). Appropriate concentrations of protein extract were loaded in to the lanes on the gel. 6 µl of a HiMark™ protein standard (Invitrogen, UK) was used to determine transfer efficiency and to identify proteins of different molecular weights. The gels were run at 150V for 90 minutes. After electrophoresis, gels were removed and assembled in to an X Cell II Blotting Module (Invitrogen, UK) according to the manufactures instructions. Gels were transferred at 30V for 90 minutes in a 10%

methanol transfer buffer (NuPage, Invitrogen) and the proteins transferred from the gel to the nitrocellulose membranes.

3.8.2 Western blotting

Membranes are washed three times in PBS-T (PBS, 0.1% Tween, pH 7.4) and then blocked in 5% milk powder in PBS-T for 2 hours. Membranes are exposed to primary antibody in 1% milk in PBS-T overnight at 4˚C. Membranes are washed in PBS-T three times five minutes and then incubated in the appropriate horse radish peroxidase (HRP)-conjugated secondary antibody (1:200) for one hour at room temperature. Membranes were washed three times for five minutes in PBS-T, and incubated with ECL (32106, Pierce) for one minute. The membranes are exposed to photographic film and the signal visualised.

3.9 Statistical analysis

The normality of the data was tested with the Shapiro-Wilko test before selecting parametric versus non parametric data analyses. For parametric data unpaired t-tests were used and for data which violated the assumptions of normality, Mann Whitney-U tests were used. For experiments involving three or more data sets, data was analysed with a one way ANOVA test followed by Dunn's post-test to compare all pairs of groups. $p<0.05$ was considered statistically significant.

Chapter 4: Characterisation of voltage gated potassium channel-complex antibodies *in vitro*

4.1 Clinical cohorts

VGKC-complex antibodies are routinely detected using the diagnostic RIA. It has recently been shown in patients with LE and NMT that many of these antibodies are against extracellular epitopes of proteins associated with the VGKC-complex; CASPR2, LGI1 and Contactin-2 (Irani 2010a; Lai, 2010). However there are still approximately 30% of patients with VGKC-complex antibodies without a defined antigenic target. Circulating antibodies that recognise extracellular epitopes are theoretically able to access and bind the antigenic target and be pathogenic.

The aim of this chapter is to introduce the CBA's used to detect antibodies to associated proteins of the VGKC-complex and describe the optimisation of the LGI1 assay to increase the detection rate of LGI1 antibodies in patients with a diagnosis of LE. The second aim of this chapter was to investigate the VGKC-complex antibody specificities in a cohort of patients with Morvan's syndrome, as this has only received limited attention in established studies. Several techniques were used to detect antibody binding to extracellular proteins in the chapter, including a solubilised immunoprecipitation assay, primary neuronal cultures and immunohistochemistry, and their sensitivity and specificities explored.

4.1.1 VGKC-complex antibody cohort (Irani 2010)

All VGKC-complex antibody positive sera used in this chapter are shown in Table 4-1 and 4-2 Sera in table 4-2 (n=96) are organised according to their known antigenic status with information about their VGKC-complex antibody titer and clinical diagnosis (courtesy of Dr Sarosh Irani) and had been previously screened on CBAs for CASPR2, LGI1 and Contactin-2 antibodies. Forty-six were found to have LGI1-Abs, 19 CASPR2-Abs and Contactin-2-Abs were observed in 5 sera (4 of 5 had additional antibody immunoreactivities). Twenty-six patients did not have antibodies to CASPR2, LGI1 or Contactin-2, and sufficient sera were still available for 18 of these patients. Serum was also available for all LGI1-Ab sera (n=46), and 18/19 CASPR2-Ab samples. All patients in Table 4-2 were referred

to Oxford as having a probable diagnosis of Morvan's syndrome and will be discussed in more detail in section 4.3

4.1.2 Control cohort

Fifteen serum samples from healthy controls were screened on all assays. They were provided anonymously with information about age and sex unavailable. Twenty sera from autoimmune disease control patients were used including thirteen patients with a diagnosis of neuromyelitis optica (NMO) with aquaporin-4 (AQP4) antibodies, and seven patients with NMDAR-antibody encephalitis.

4.2 Detection of VGKC-complex antibodies

4.2.1 Detection of surface expression of CASPR2, LGI1 and Contactin-2 in transfected HEK cells

To confirm the surface expression of VGKC-complex proteins, live HEK cells expressing CASPR2, LGI1 or Contactin-2, were probed with commercial antibodies directed against extracellular epitopes of the respective proteins. Commercial antibodies bound specifically to HEK cells transfected with the appropriate cDNA only (Figures 4-1,4-2 and 4-3), demonstrating specificity of the assays.

Antigenic target	VGKC- antibody titre (pM)	Clinical diagnosis
LGI1	637-8840 (median 2154)	42 LE, 2 NMT, 1 Seizure, 1 MoS
CASPR2	154-3746 (median 1198)	7 LE, 10 NMT, 1 Seizure
Unknown	435-7606 (median 843.5)	10 LE, 2 NMT, 1 MoS, 1 FBDS, 1 Startle, 3 Encephalopathy

Table 4-1 Clinical information of VGKC-antibody patients and their antibody specificities (n=86) ***from Irani et al 2010****.*

LE = limbic encephalitis, NMT = neuromyotonia, MoS = Morvan's syndrome, FBDS = Faciobrachial dystonic seizures

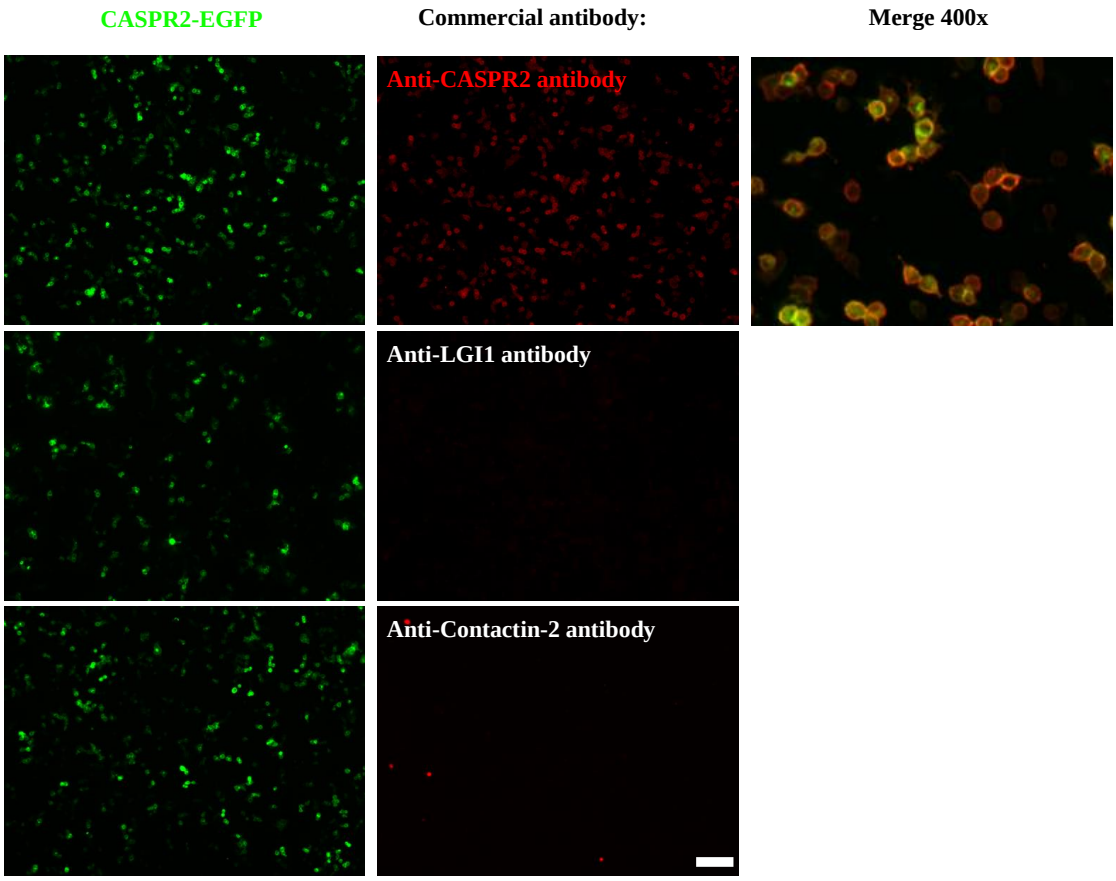

Figure 4-1 Staining of surface epitopes with CASPR2 commercial antibody.

The EGFP tag attached to the CASPR2 protein allows the visualisation of CASPR2 expression (left column, green). Surface binding of a CASPR2-commercial antibody is visualised with a secondary antibody (middle column, red). The commercial antibody co-localises on the surface of transfected cells (right column). Commercial antibodies against LGI1 and Contactin-2 do not bind to CASPR2-transfected cells. Magnification x100 and x400 (merge). Scale bar represents 200µm.

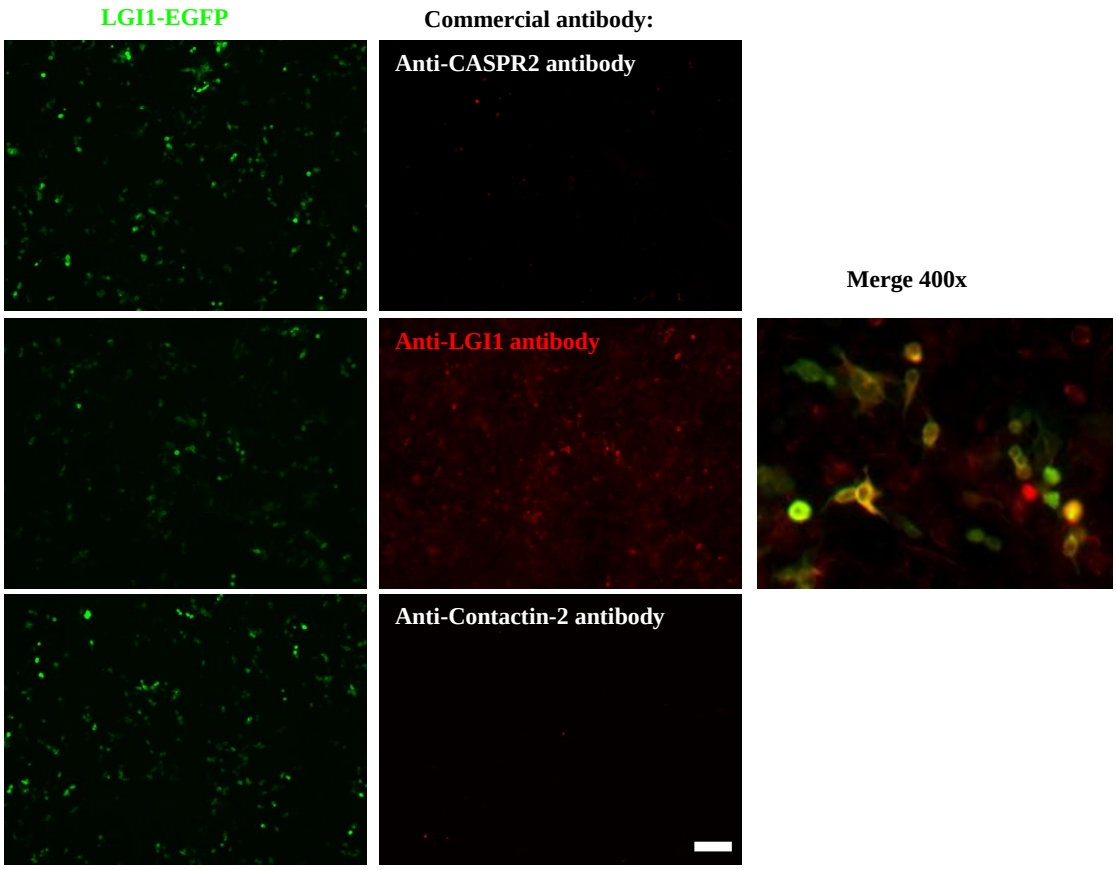

Figure 4-2 Staining of surface epitopes with LGI1 commercial antibody.

The EGFP tag attached to the LGI1 protein allows the visualisation of LGI1 expression (left column, green). Surface binding of a LGI1-commercial antibody is visualised with a secondary antibody (middle column, red). The commercial antibody co-localises on the surface of transfected cells (right column). Commercial antibodies against CASPR2 and Contactin-2 do not bind to LGI1-transfected cells. Magnification x100 and x400 (merge). Scale bar represents 200µm.

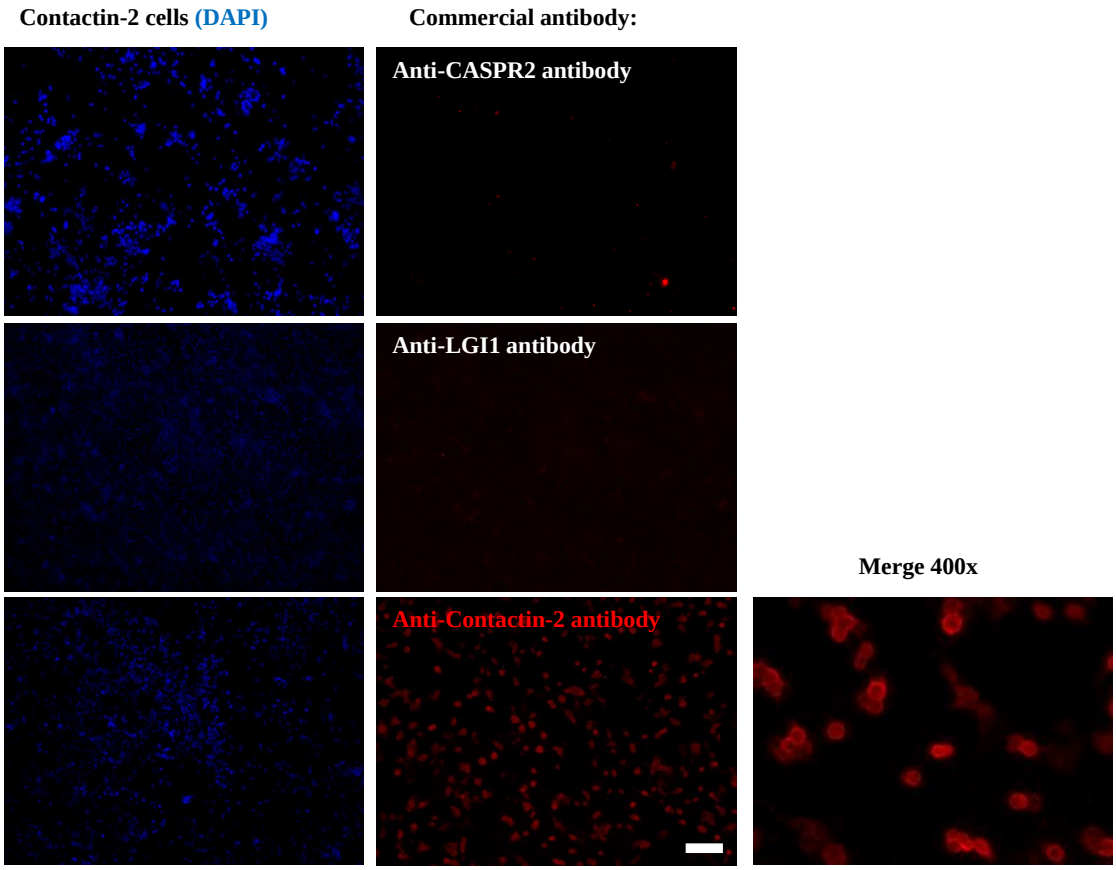

Figure 4-3 Staining of surface Contactin-2 commercial antibody.

All cells on the coverslip are stained with DAPI (left column, blue) as the Contactin-2 construct did not contain an EGFP tag. Surface binding of a Contactin-2 commercial antibody is visualised with a secondary antibody (middle column, red). Commercial antibodies against CASPR2 and LGI1 do not bind to Contactin-2-transfected cells. Magnification x100 and x400 (merge). Scale bar represents 200µm.

4.2.2 CBA scoring system

Similarly, live HEK 293 cells transfected with CASPR2, LGI1 or Contactin-2 were incubated in patient sera (1:20-1:100) for one hour, washed, fixed and specific binding detected using an anti-human IgG secondary antibody. Surface binding of patient IgG was assessed in a semi-quantitative manner. Cover slips that showed no detectable binding of IgG were given a score of zero whereas cover slips that showed detectable binding of IgG were scored on a scale 1-4. Representative sera for the CASPR2 CBA scoring can be seen in Figure 4-4. All serum samples that scored 1 or more were deemed positive and were repeated for confirmation.

4.2.3 Optimisation of LGI1-antibody detection by cell based assay

LGI1 antibodies were initially detected in VGKC-complex Ab sera by screening sera on live HEK cells transfected with cDNA encoding wild type LGI1 (Irani, 2010). LGI1 contains no transmembrane domain and has been shown to be secreted into the cell culture medium (Senechal, 2005). LGI1-Ab sera bound indistinguishably to all cells on the coverslip, including those that were not transfected, as reported in Irani *et al*, 2010. This occasionally resulted in a low intensity of IgG positivity, with inconsistencies in observer scoring (data not shown). Methods used for detecting the specific antibody target should be sensitive enough to pick up all positive samples without detecting false positives in control samples. To investigate the sensitivity of the LGI1 assay, the LGI1 construct was modified to incorporate the C-terminal transmembrane domain and 13 extracellular amino acids of CASPR2, resulting in a membrane-tethered LGI1 protein.

To compare the sensitivities of the two LGI1 constructs, 46 sera with LGI1-Abs by the secreted assay were screened on the modified construct. All 46 LGI1-Ab sera bound to both the secreted and the tethered LGI1 assay, indicating 100% assay sensitivity. As shown in Figure 4-5, patient LGI1-Ab binding on the secreted version showed diffuse positivity to all cells on the coverslip, whereas in HEK cells expressing the membrane-tethered LGI1, the

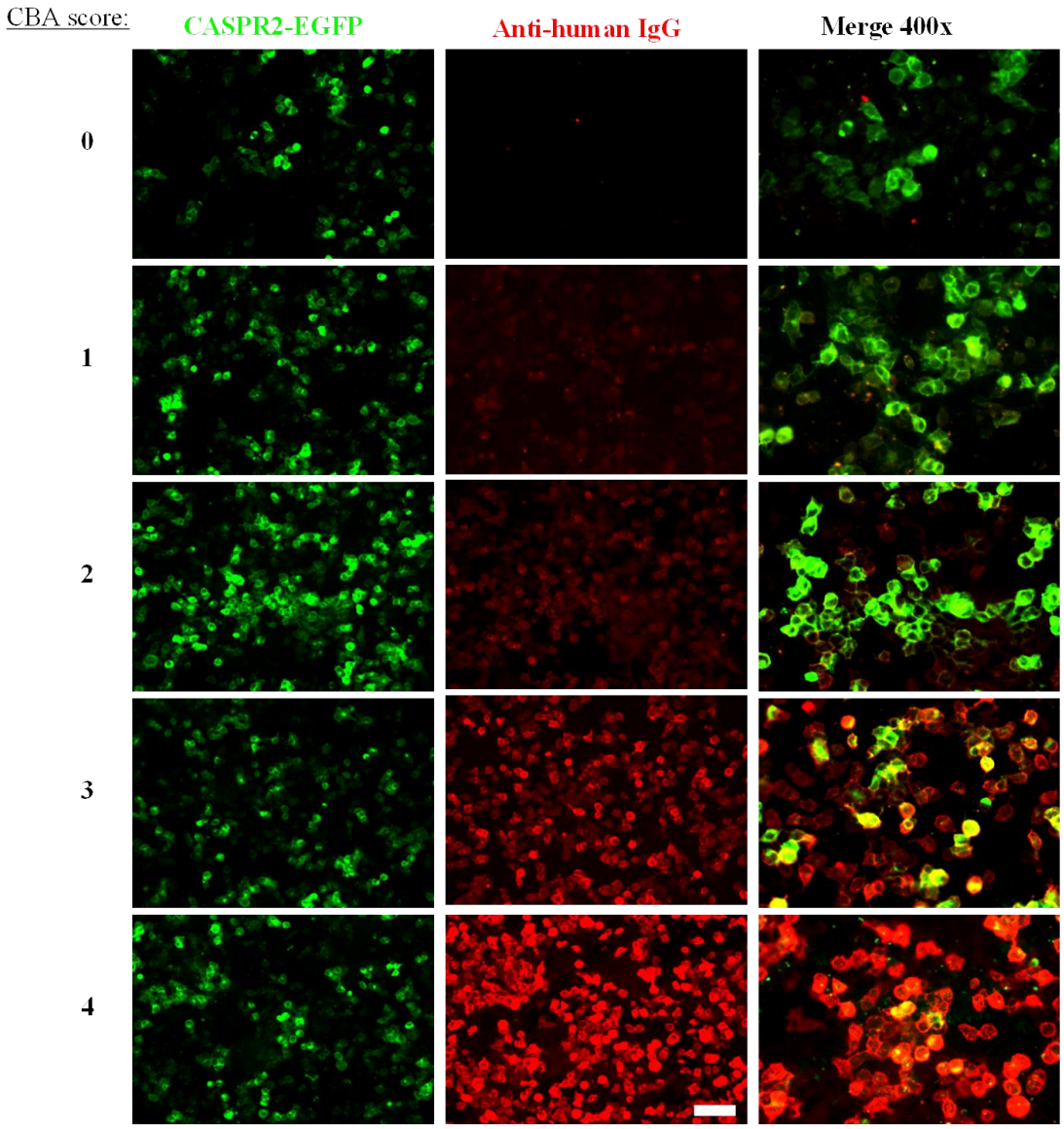

Figure 4-4 CBA scoring system: CASPR2-transfected HEK cells.

An example of the semi-quantitative scoring system used for the CBA assays described in this thesis. Scores range from zero (negative) to four (strong binding of IgG to the cell surface) as detailed in Leite 2008. CASPR2-EGFP expression is shown on the left (green), Alexa Fluor anti-human IgG 568 is shown in the middle panel (x100). Merged image showing the co-localisation of CASPR2-EGFP and patient sera is shown on the right (x400). CBA score is based on the intensity and also the number of positive cells bound by the patient serum. Scale bar represents 75µm.

same patient IgG bound to only the transfected cells, indicated by an EGFP tag. This finding indicates that the LGI1 protein was no longer secreted from the cell.

Eighteen VGKC-complex antibody sera that were previously “antigen negative” on the CASPR2 and LGI1 CBA’s were re-screened for LGI1-Abs using the modified construct. Nine of these sera now bound to the cells expressing the membrane-tethered LGI1 and nine patients did not bind to the surface of cells using either LGI1 construct, resulting in a sixteen percent increase in the sensitivity of detecting LGI1 antibodies in this cohort. 55 of a total of 82 patients studied had LGI1-Abs, of these 51/55 (92.7%) had a diagnosis of LE. Healthy (n=15) and disease control sera (AQP4-Ab or NMDAR-Ab (n=20)) did not bind to either LGI1 construct, Figure 4-a. A comparison of the VGKC-complex antibody titers measured using the diagnostic brain RIA for LGI1 serum samples positive only using the modified assay, did not show a significant difference when compared to the serum samples detected using the modified construct (p=0.9546, Mann-Whitney, Figure 4-6b).

4.2.4 Investigating the specificity of the optimised LGI1 cell based assay

Methods used for detecting the specific antibody target should be sensitive enough to pick up all positive samples without detecting false positives in control samples. The CASPR2 molecule consists of a large extracellular domain (1234 amino acids) and there was the potential that the 13 extracellular amino acids of CASPR2 present in the membrane-tethered LGI1 construct might be sufficient to pick up a false-positive result in sera with CASPR2-Abs. To investigate the specificity of the modified assay, 18 patients with high CASPR2-Abs were screened on the membrane-tethered construct. None of the 18 patients bound to the surface of HEK cells expressing the tethered LGI1 construct, indicating that the specificity of the optimised assay was 100%, whilst showing a significant improvement in sensitivity. All future experiments described in this thesis will use the membrane-tethered construct.

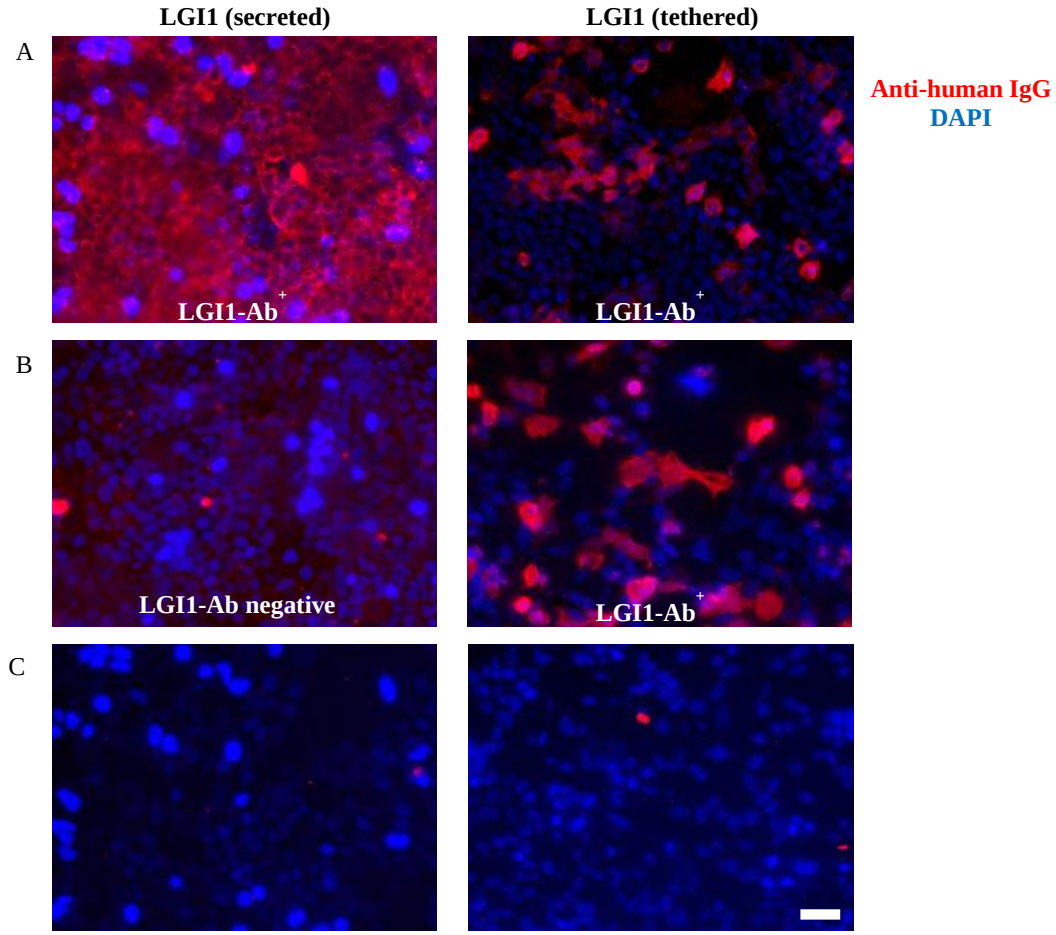

Figure 4-5 Expression of LGI1 in HEK cells.

HEK293 cells transfected with cDNA for secreted LGI1 (left) or tethered LGI1 (right). A) VGKC-complex antibody positive sera bound to the surface of transfected HEK cells expressing both the secreted wild type and membrane tethered LGI1 (top row). B) VGKC-antibody sera bound only to the surface of the membrane tethered LGI1 (middle row). C) Healthy control serum did not bind to cell transfected with either construct (bottom row). Images x200, scale bar represent 50µm

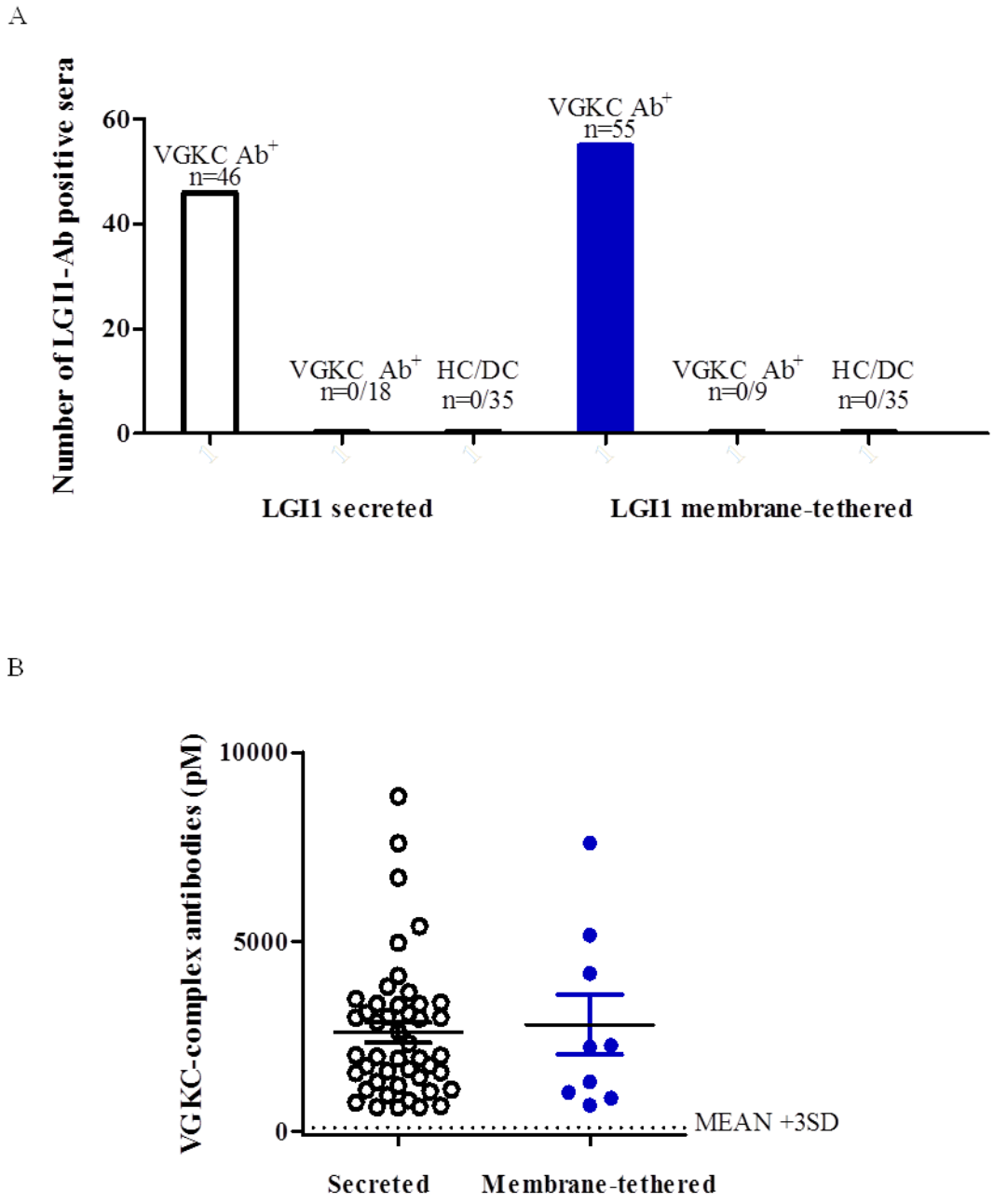

Figure 4-6 Membrane tethered LGI1 increases the sensitivity of LGI1-antibody detection.

A) An additional 9 patients had LGI1 antibodies detectable in their serum with the membrane tethered LGI1 construct. No LGI1 antibodies were found in healthy control sera (n=15), or autoimmune disease control sera (n=20). B) Comparison of VGKC-complex antibody titre of LGI1-antibody positive sera did not differ significantly from those identified by the original secreted construct (white circles) versus the nine sera detected on the modified assay (blue circles, p= 0.9546, Mann-Whitney).

4.3 Investigating VGKC-complex antibodies in Morvan's Syndrome

As outlined in chapter 2, LGI1-Abs are most commonly found in patients with LE (92.7%), whereas patients with NMT commonly have antibodies against CASPR2 (64%). To date the specificity of VGKC-complex antibodies in MoS, a disorder characterised by both peripheral and central features, has received only limited attention (Irani, 2010a; Lancaster, 2011a).

4.3.1 Clinical characteristics of Morvan's sera

Serums from 29 patients with a diagnosis of MoS were available and are described n Table 4-2, with information regarding their sex, age, tumour status and VGKC-complex antibody titer.

4.3.2 Detection of VGKC-complex antibodies in Morvan's sera

Using the diagnostic RIA, twenty-three (79.3%) patients had detectable antibody levels in their serum, ranging between 154 - 3670pM (cut off >100pM). Twenty-seven patients had sufficient serum available for further investigations of their antibody status. All sera were tested for antibodies on the CASPR2, LGI1 and Contactin-2 CBAs. Twenty four patients had detectable antibodies in their sera by CBA; six patients had CASPR2-Abs (22.2%) and three (11.1%) patients had LGI1-Abs. Furthermore 15 patients (55.6%) had antibodies to two or more proteins within the VGKC-complex; 12 to LGI1 and CASPR2 and 3 patients had antibodies to all three antigens tested. No patients had antibodies against AQP-4, excluding potential non-specific binding. Two patients, one with LGI1 antibodies and one with both LGI1 and CASPR2 antibodies determined by CBA had undetectable VGKC-complex antibody levels measured by RIA, indicating that the RIA is less sensitive than transfected HEK cells. Only three patients did not have VGKC-complex antibodies by either method. There was no statistically significant difference in VGKC-complex antibody titers when patients were grouped by their antibody specificities ($p=0.0693$, one-way ANOVA, Figure 4-7).

	Sex	Age (years)	Tumour	VGKC-antibodies by RIA (pM)
MoS1	M	64	N	2016
MoS2	M	58	N	444.5
MoS3	M	35	Y (thymoma)	1013
MoS4	M	50	N	618
MoS5	M	57	Y (thymoma)	1148
MoS6	F	50	Y (thymoma)	1462
MoS7	M	60	N	610
MoS8	M	66	N	3670
MoS9*	M	34	N	94
MoS10	M	35	N	470
MoS11	M	57	N	0
MoS12	M	62	N	0
MoS13	M	76	Y (SCLC)	3000
MoS14	M	67	N	2063
MoS15*	M	69	N	1552
MoS16	F	51	Y (thymoma)	591.5
MoS17	M	70	N	385
MoS18	M	73	Y (thymoma)	376
MoS19	M	19	N	218
MoS20	M	80	N	0
MoS21	M	31	Y (thymoma)	0
MoS22	M	51	Y (thymoma)	158
MoS23	M	75	N	154
MoS24	M	50	Y (thymoma)	329
MoS25	M	38	Y (thymoma)	493
MoS26	M	55	N	274
MoS27	M	29	Y (thymoma)	1609.5
MoS28	M	60	Y (thymoma)	765
MoS29	M	36	N	0

Table 4-2 Overview of Morvan's cohort (n=29).

M = male, F = female, N = no, Y= Yes, SCLC = small cell lung carcinoma
** Samples with no serum available for subsequent testing (n=2)*

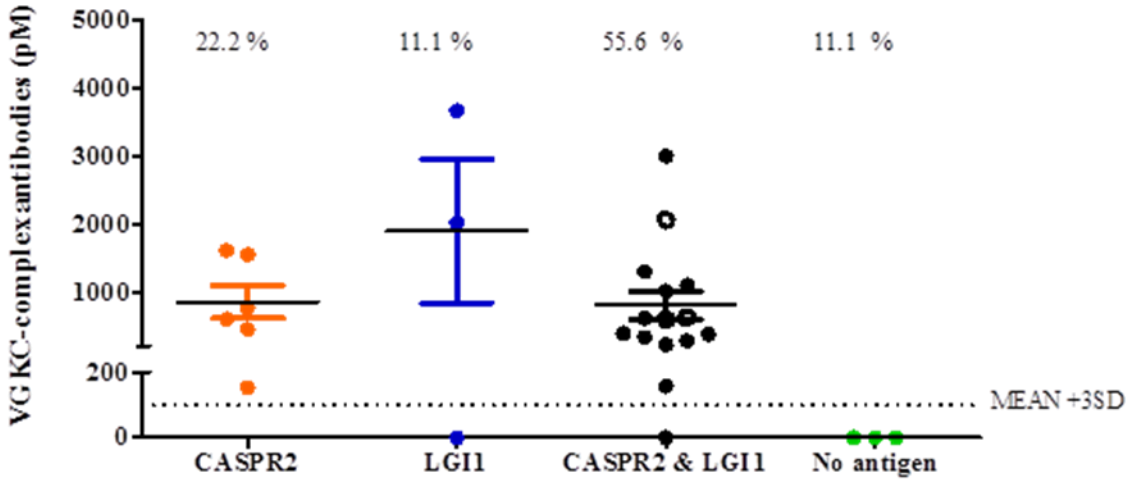

Figure 4-7 Relationship between VGKC-complex antibody titer and antibody specificities in Morvan's syndrome (n=27).

Patients were grouped according to their antibody specificities; CASPR2, LGI1, CASPR2 and LGI1 (and Contactin-2) or antigen unknown. Cut off of the VGKC-RIA (dotted line) represents the mean plus 3 standard deviations (100pM). There was no statistically significant difference in VGKC-complex antibody titres when patients were grouped by their antibody specificities (one-way ANOVA p=0.0693), Pettingill et al, 201.2

4.3.3 Investigation of multiple specificities in Morvan's sera

As 15 patients had multiple antibody specificities in their serum, it was possible that these antibodies might bind an epitope common to these three proteins. To exclude the possibility of a common epitope, serum from LE is patients with monospecific antibodies against LGI1 (n=3) or CASPR2 (n=3) were adsorbed against cells transfected with LGI1, CASPR2 or AQP-4, and then re-tested on the relevant CBA. As expected, CBA reactivity was abolished only when serum was adsorbed against its target antigen. Four Morvan's sera that contained both LGI1 and CASPR2 antibodies (MoS # 3, 4, 5 and 6) were then preadsorbed as above. After adsorption against cells expressing LGI1, IgG binding to the CASPR2 CBA was unaffected. Likewise, after adsorption against cells expressing CASPR2, reactivity to the LGI1 CBA was unaffected. Preadsorption against both CASPR2 and LGI1 transfected cells abolished immunoreactivity on both assays. This demonstrates the presence of multiple antibody specificities in these sera. Representative staining from preadsorption experiments are shown in Figure 4-8).

Six MoS sera (#1, 2, 3, 4, 5 and 6) and commercial antibodies against CASPR2 and LGI1 were sent to a collaborator in Cyprus (Professor Kleopa) for immunohistochemical analysis of binding to rodent brain sections. LGI1-commercial antibodies bound predominantly to neurons with some axonal staining and CASPR2 commercial antibodies showed binding to the neuropil, in both cases consistent with the previous literature (Senechal, 2005; Schulte, 2006). Monospecific sera (MoS1 and LE1 (LGI1-Ab) and MoS2 and LE2 (CASPR2-Ab) bound to tissue that reflected their CBA-determined specificities. Monospecific LE1 immunoreactivity was unaffected when tested on CASPR2$^{-/-}$ brain sections. In contrast, LE2 bound predominantly to the neuropil of wild-type sections and the immunoreactivity was abolished on CASPR2$^{-/-}$ brain sections. After adsorption of LE # 1 & 2 sera against their respective antigens the samples no longer bound to brain sections, confirming the presence of a single antibody in these sera (data not shown, see appendix; Pettingill *et al*, 2012).

Sera with multiple antibody specificities (MoS 3, 4, 5 and 6) bound to the tissue showing mixed immunoreactivities, consistent with both commercial antibody staining for CASPR2 and LGI1. To investigate further the multiple specificities in some MoS sera, MoS 5 & 6, which had both LGI1 and

CASPR2 reactivities, were investigated on brain sections. Both sera showed immunoreactivity with the neuropil and neuronal cell bodies as predicted. As expected, neuropil immunoreactivity was abolished when tested on CASPR2$^{-/-}$ tissue, but neuronal binding, indicating the binding of LGI1-antibodies, remained. After adsorption of sera against both LGI1 and CASPR2-transfected cells some immunoreactivity to brain sections remained, particularly towards neuronal cell bodies in the thalamus and brainstem. This finding is suggestive of a third antibody present in these sera, shown in Figure 4-9. A summary of the immunohistochemistry results from the preadsorption experiments can be seen in Table 4-3.

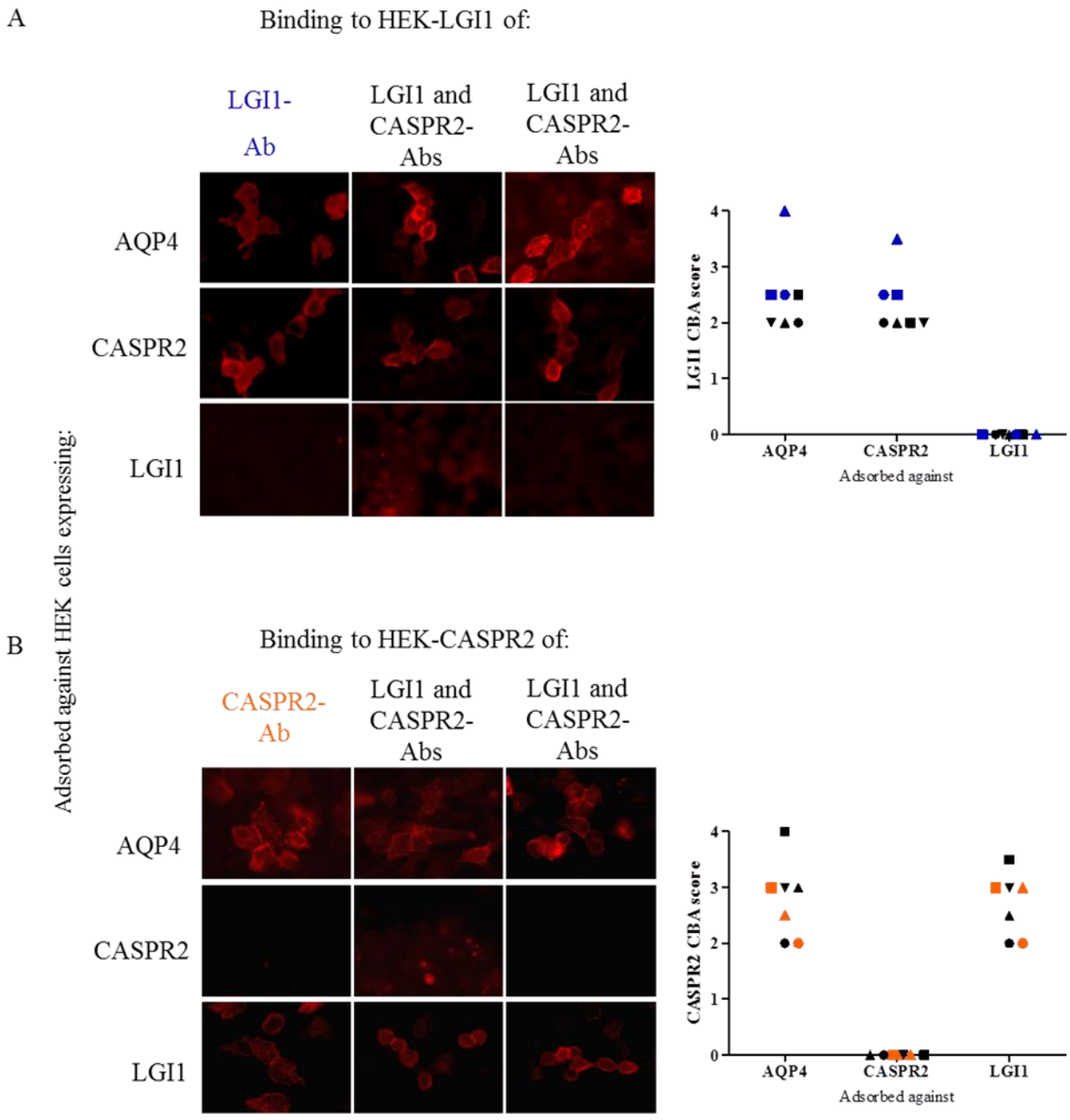

Figure 4-8 Representative images from preadsorption experiments of CASPR2 and LGI1-antibodies.

A) Binding of monospecific LGI1-Ab sera (n=3) were not affected by preadsorption with AQP-4 or CASPR2 transfected cells, but was abolished after adsorption against LGI1-expressing cells (left column). B) Similarly binding of monospecific CASPR2-Ab sera (n=3) was only abolished after preadsorption with CASPR2-transfected cells (left column). Preadsorption of Morvan's sera (CASPR2&LGI1-Ab, n=4) with AQP-4 cells did not affect binding to either assay. After adsorption against cells expressing LGI1, binding to the CASPR2 CBA was unaffected. Likewise, after adsorption against cells expressing CASPR2, reactivity to the LGI1 CBA was unaffected. Pettingill et al, 2012.

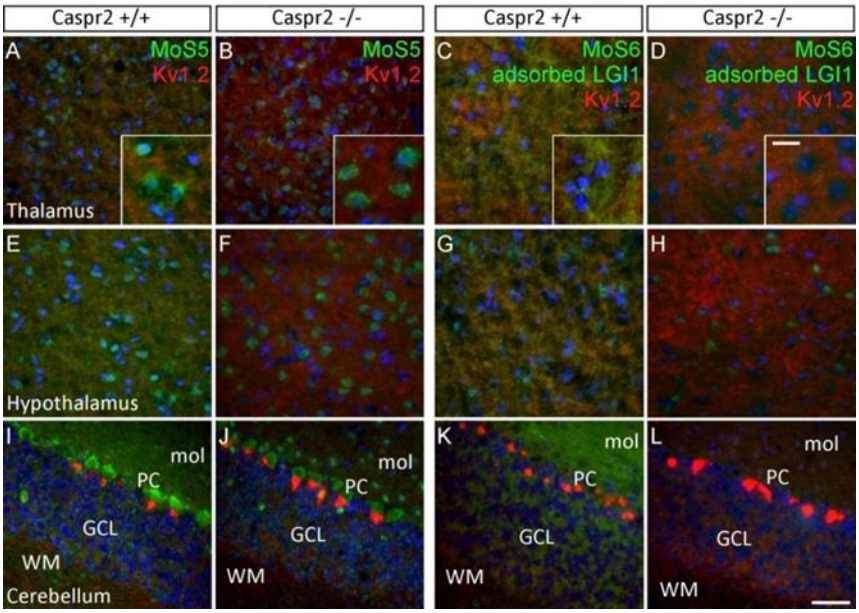

Figure 4-9 Immunohistochemical analysis of Morvan's sera binding to the thalamus, hypothalamus and cerebellum in wild type (CASPR2$^{+/+}$) and CASPR2 null (CASPR2$^{-/-}$) brain.

Sera S5 and S6 have CASPR2 and LGI1-antibodies. S5 bind to both the neuropil and neurons in multiple areas of the brain (green) (panels A, E, I). CASPR2 reactivity to the neuropil is abolished on CASPR2$^{-/-}$ tissue however LGI1 immunoreactivity to the neurons remains (panels B, F, J). After adsorption of MoS 6 against LGI1, CASPR2 immunoreactivity is still present in wild-type tissue (panels C,G,K), but neuropil binding is absent in CASPR2$^{-/-}$ tissue (panels D,H,L). Some residual binding is seen in S6 CASPR2$^{-/-}$ tissue after preadsorption of LGI1-antibodies suggest of additional immunoreactivities in these sera. Scale bar=30µm. ***Immunohistochemistry performed by Professor Kleopa.*** *Pettingill et al, 2012*

Patient serum	CBA antigen specificity	Wild-type IHC	CASPR2$^{-/-}$ IHC	LGI1 preadsorbed sera	CASPR2 preadsorbed sera	CASPR2 & LGI1 preadsorbed sera	Conclusion
LE 1	LGI1 (1/4860)	Neuronal	Neuronal	Negative	-	-	LGI1
LE 2	CASPR2 (1/14580)	Neuropil	Negative	-	Negative	-	CASPR2
MoS 1	LGI1 (1/540)	Neuronal	-	-	-	-	LGI1
MoS 2	CASPR2 (1/14580)	Neuropil	-	-	-	-	CASPR2
MoS 3	CASPR2 & LGI1 (1/1620, 1/540)	Neuropil & neuronal	-	-	-	-	CASPR2 & LGI1
MoS 4	CASPR2 & LGI1 (1/1620, 1/180)	Neuropil & neuronal	-	-	-	-	CASPR2 & LGI1
MoS 5	CASPR2 & LGI1 (1/4860, 1/180)	Neuropil & neuronal	Neuronal	Neuropil & neuronal	Neuronal	Neuronal	CASPR2 & LGI1 & another antigen
MoS 6	CASPR2 & LGI1 (1/48740, 1/540)	Neuropil & neuronal	Neuronal	Neuropil & neuronal	Neuronal	Neuronal	CASPR2 & LGI1 & another antigen

Table 4-3 Summary of monospecific and bi-specific sera binding to wild-type rodent brain tissue and CASPR2 knockout tissue before and after preadsorption.

4.3.4 CASPR2 antibody titers are higher than LGI1 in sera with multiple specificities

As 15 patients with Morvan's syndrome showed multiple antibody immunoreactivities it was important to directly compare the titers of CASPR2 antibodies to those of LGI1 in these samples.

As the majority of CASPR2 and LGI1-Absera in this thesis bound strongly in the CBAs, sera were serially titrated (LE sera; CASPR2-Ab sera n=6, LGI1-Ab sera n=11, MoS sera; CASPR2-Ab sera n=20, LGI1-Ab sera n=14)). The last dilution that the serum remained positive on the CBA (CBA score of 1) was used as a more quantitative assessment of the specific antibody titer. End titration points for CASPR2-Abs were significantly higher, approximately 8-10 fold, of LGI1-Abs in both LE and MoS cohorts (LE p=0.046, MoS p=0.0088, Mann-Whitney, Figure 4-10). However a fair comparison of antibody titers assumes that the two antigens are expressed at comparable levels. This result led us to ask whether there were difference in protein expression of CASPR2 and LGI1 levels in our diagnostic CBAs.

4.3.5 Comparison of protein expression in CASPR2 and LGI1 transfected cells

Gross visualisation of HEK cells transfected with CASPR2-EGFP showed more EGFP positive cells which individually appear brighter than those transfected with LGI1-EGFP, Figure 4-11a.

4.3.6 CASPR2 and LGI1 total protein expression

To quantify the visual difference in CASPR2 and LGI1 expression, proteins were extracted from cells transfected with equal amounts of CASPR2 or LGI1 and the amount of antigen-EGFP measured on a fluorescent plate reader. Equal quantities of detergent-extracted CASPR2-EGFP and LGI1-EGFP, or untransfected HEK cells, had their amount of EGFP fluorescence measured. CASPR2 cells expressed significantly higher quantities of EGFP than LGI1 transfected HEK cells, (p=0.003, unpaired t-test, Figure 4-11b). The quantified CASPR2-EGFP levels were approximately 10-fold greater than LGI1. The total EGFP content in cell extracts were further analysed by western blot. Equal quantities of LGI1 or CASPR2 cell extract, were serially diluted (1:1) and both extracts probed using a GFP antibody. Bands sizes of ~210kDa and ~90kDa were observed in the CASPR2 and LGI1 extract respectively, Figure 4-11c. Both bands are approximately 30kDa more than the expected molecular

weights of CASPR2 and LGI1; this extra weight represents the attached EGFP molecule. The band intensity for CASPR2 cell extract is significantly greater than LGI1. Comparable band intensity were seen for 20 μg of LGI1 extract (lane 1) versus 0.625 μg of CASPR2 extract (lane 6), approximately a 30-fold difference in expression. These experiments combined demonstrate that CASPR2 is expressed ten to thirty times more than LGI1 in the cell lysate of transfected HEK cells.

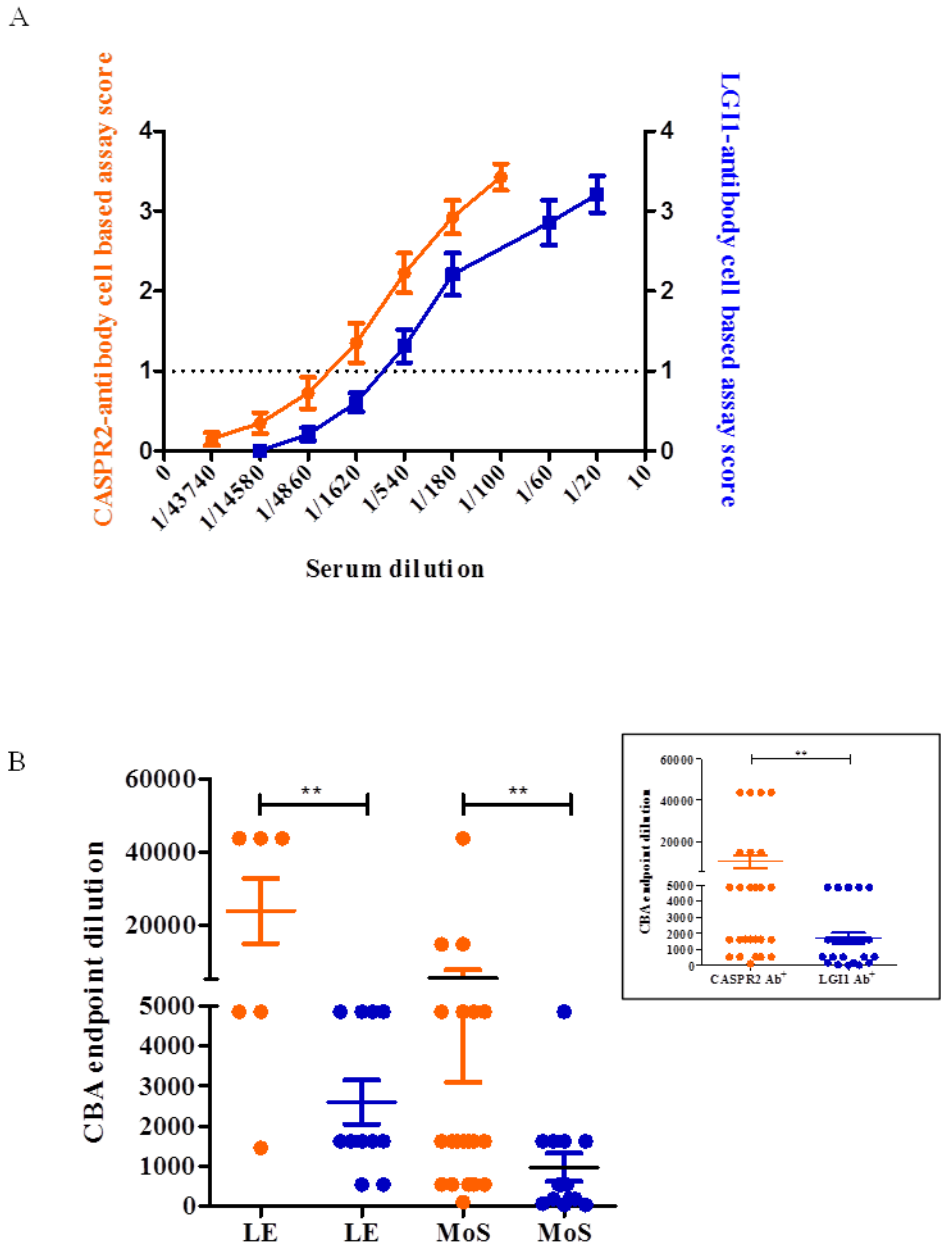

Figure 4-10 CASPR2 and LGI1-antibody end dilution point on CBA.

Samples were serially diluted three-fold to determine the endpoint serum positivity of available CASPR2 (n=26) and LGI1 (n=25) sera. A) The CBA scores for each dilution point (mean + SEM) are shown. B) CASPR2 antibody endpoint dilutions were higher than LGI1-antibodies in limbic encephalitis (LE) and Morvan's (MoS) sera (LE; p=0.046, MoS; p=0.0088, pooled LE & MoS (insert) p= 0.0075, Mann-Whitney).

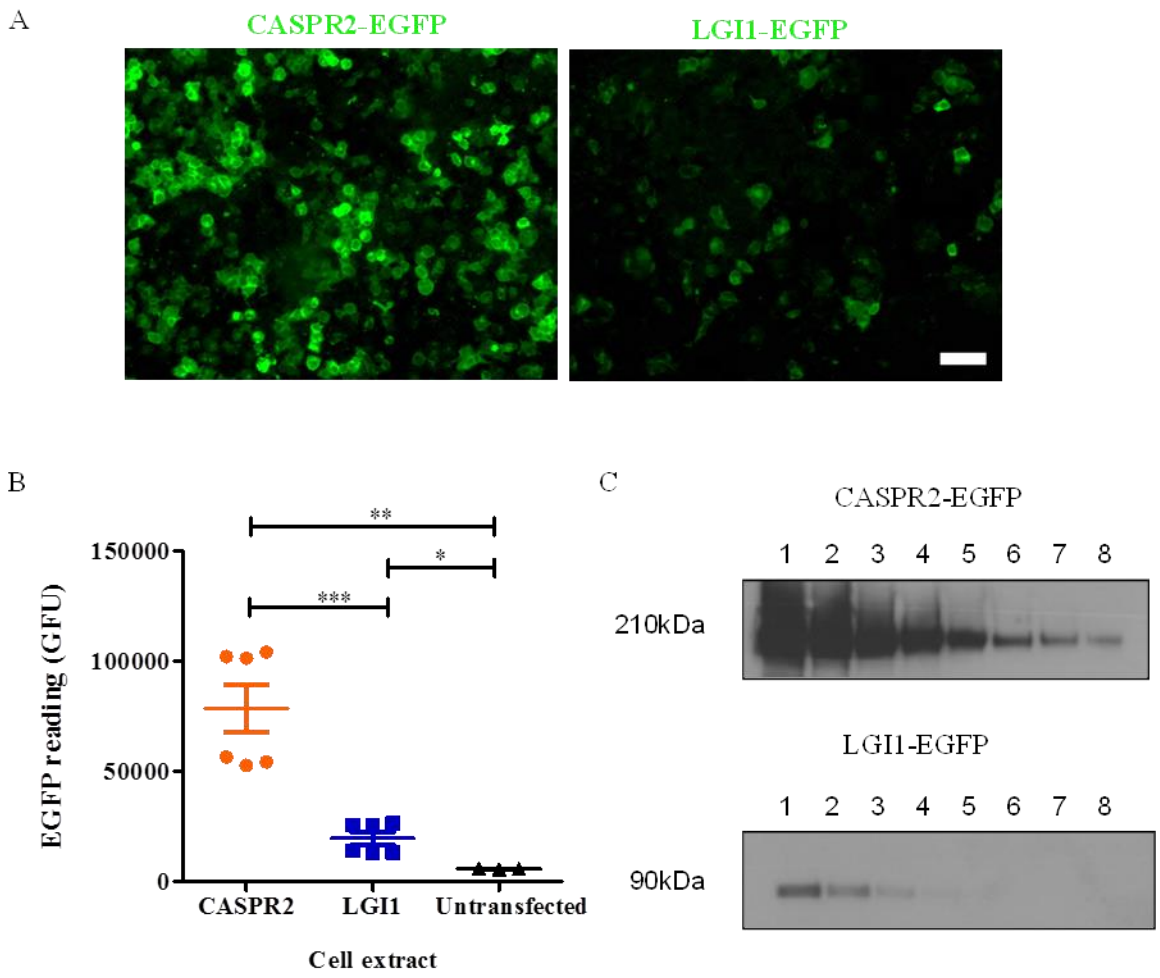

Figure 4-11 CASPR2-EGFP expression is higher than LGI1-EGFP expression in transfected HEK cells.

A) EGFP attached directly to the CASPR2 and LGI1 proteins enables us to visualise protein expression (green). Images for both CBA were taken at a capture exposure of 100ms. CASPR2-transfeted cells (left) appear more green than LGI1-transfected cells (right). B) Quantification of CASPR2-EGFP levels are ~8x higher LGI1 cells (p=0.0033, unpaired t test). C) Cells extracts using rabbit anti-GFP commercial antibody were used to probe wells loaded with CASPR2 or LGI1 cell extracts (extract loaded 20 μg (lane 1) and subsequently serially diluted 1:1 (lanes 2-8). Intense bands can be seen in cells expressing CASPR2 (~210kDa), and less intense bands for the comparable loading of LGI1 (~90kDa) extract.

4.3.7 Normalising of CASPR2 antibody titers

As expression levels of CASPR2 in the CBA is ten to thirty times higher than that of LGI1, the end titration value of CASPR2 antibodies was conservatively divided by ten to control for equal antigen expression in the assay. After normalisation for CASPR2 expression there was now no longer a significant difference observed between CASPR2 and LGI1 antibody titres in patients with LE (p=0.3382, two tailed Mann Whitney). Instead, there was a trend towards higher LGI1 antibody titres in the MoS cohort, although this was not statistically significant (p=0.0595, Mann-Whitney, Figure 4-12). However when the LE and MoS cohorts were combined, LGI1 antibodies were now found to be significantly higher than CASPR2 antibodies (p=0.0063, two-tailed Mann Whitney). Dissecting out the available MoS sera with multiple antibody specificities only (n=10), showed no significant difference between the antibody titers in these patients (p=0.4702, Mann-Whitney, Figure 4-13). However two patients, MoS #13 and 14, had one antibody specificity that was noticeably higher than the other. MoS #13 had elevated CASPR2-Abs (1/1458) versus LGI1-Abs (1/20) and MoS #14 had high LGI1-Abs (1/4860) and lower CASPR2 Abs (1/54).

4.3.8 Fluorescent immunoprecipitation assay (FIPA) for the detection of CASPR2 or LGI1-antibodies

An alternative way to quantify CASPR2 and LGI1 antibody titers between patients is to perform an antibody binding assay in solution, known as a FIPA, and quantify the amount of antigen-EGFP precipitated. FIPA's have been used previously to quantify the titers of antibodies against AQP-4 during disease relapse and remission in neuromyelitis optica (Waters, 2008). To directly compare the CASPR2 and LGI1 assays, equal amounts of solubilised antigen-EGFP (25,000 gfu) cell extract was incubated with 5 µl of patient sera. IgG-antigen immune complexes were captured using protein G Sepharose beads and the amount of antigen precipitated (antigen-EGFP fluorescence) measured. A positive cut off for the each assay was calculated as the mean of the healthy controls plus 3 standard deviations (mean+ 3SD) for each antigen.

In the CASPR2 FIPA, a statistically significant difference in the amount of CASPR2-EGFP precipitated was observed across all sera tested (one-way ANOVA p=0.0003 (mean gfu: CASPR2-Ab

sera 2869, LGI1-Ab sera 384, control sera 479)). A Dunn's post hoc analysis showed CASPR2-Absera precipitated significantly more antigen than healthy controls and LGI1-Ab sera but there was no difference in the amount precipitated by control and LGI1-Ab sera, Figure 4-14a). Likewise for the LGI1 FIPA, there was an effect of group on the amount of LGI1-EGFP precipitated (one way ANOVA p=0.0004 (mean gfu; LGI1-Ab sera 1152, CASPR2-Absera 427, control sera 429)) and post-hoc analysis showed that LGI1-Ab sera precipitated significantly more LGI1-EGFP than healthy control and CASPR2-Ab, but there was no difference in the amount of LGI1-EGFP precipitation between control and CASPR2-Ab sera, Figure 4-14b). When comparing CBA-antibody positive sera on their respective FIPAs shows a trend for higher antigen-EGFP precipitation for CASPR2-Ab sera versus LGI1-Ab sera, although this was not statistically significant (p=0.0626, Mann-Whitney). Whereas comparison of the amount of antigen-EGFP precipitated by healthy control sera was not significant between the two antigens (p=0.6850, Mann-Whitney).

Patient scores on the FIPA and the CBA plotted against one another to investigate the correlation of the two assays. A strong positive correlation was observed for the detection of CASPR2 antibodies by CBA and FIPA (r=0.6989, p=0.0013, Spearman's rank correlation, Figure 4-15a). For LGI1 antibodies a lower correlation between the amount of LGI1-EGFP precipitated in the FIPA compared to CBA score (r=0.4255, p=0.0483, Spearman's rank correlation, Figure 4-15b).

On both FIPA's, no healthy or respective antibody-controls were greater than the allocated cut off indicating that the specificity of the solubilised assay was one hundred percent. Of the 18 antibody positive sera screened on the CASPR2 FIPA and 22 sera on the LGI1 FIPA, 7 (39%) and 12 (55%) of the samples respectively did not did not precipitate antigen-EGFP at levels higher than the mean plus three standard deviations of healthy control sera and were thus deemed negative by this method of screening.

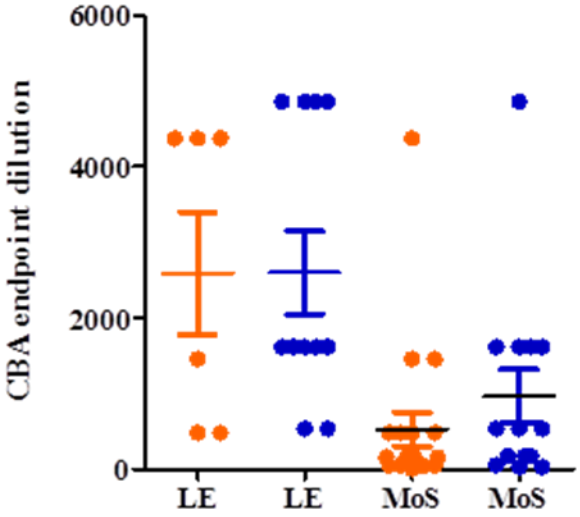

Figure 4-12 Normalised CASPR2 and LGI1-antibody end dilution points for LE and MoS sera.

End dilution points are equivalent after normalising for 10-fold higher CASPR2 expression in the CBA (LE; p=0. 3382, MoS; p=0.0595 Mann-Whitney).

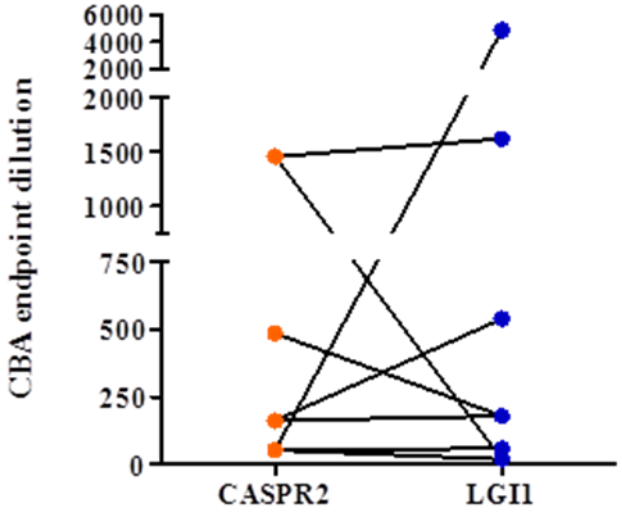

Figure 4-13 Normalised CASPR2 and LGI1-antibody end dilution points for MoS with multiple antibody specificities (n=10).

End dilution points are equivalent after normalising for 10-fold higher CASPR2 expression in the CBA (p=0. 4702, Mann-Whitney).

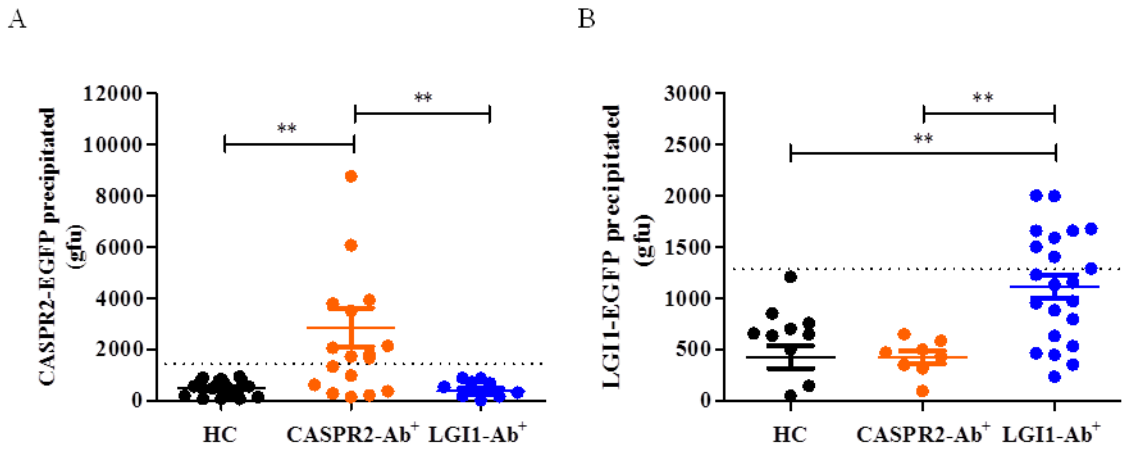

Figure 4-14 Fluorescent immunoprecipitation of patient sera with CASPR2 or LGI1-EGFP extract (25,000gfu).

A) 80% of CASPR2-Ab sera and B) LGI-Ab sera precipitated antigen-EGFP levels higher than the mean plus three standard deviations of ten healthy controls (dotted line). (CASPR2-FIPA; one way-ANOVA p=0.0003, LGI1-FIPA; one-way ANOVA p=0.0004).

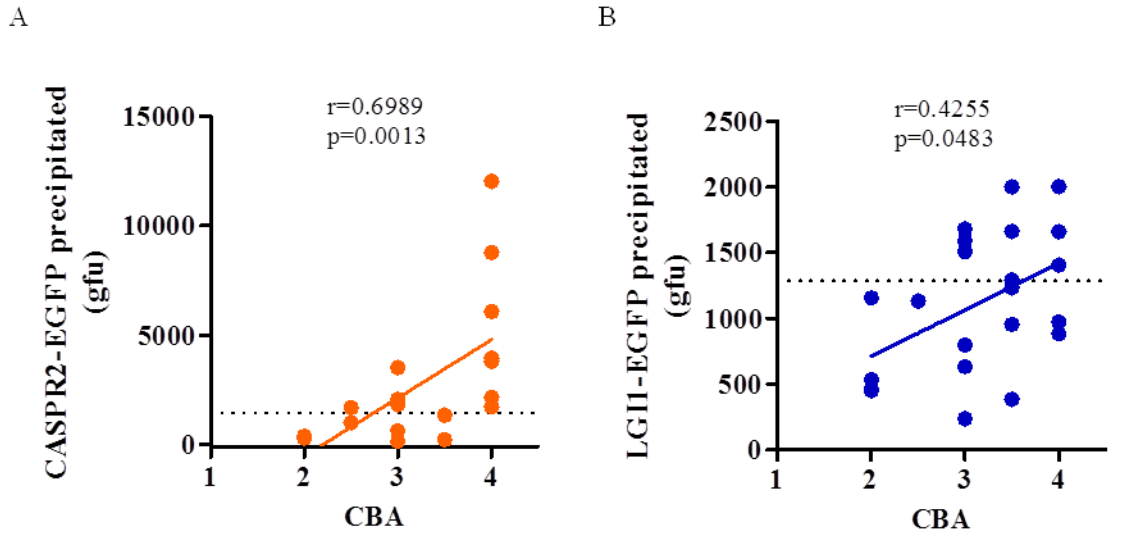

Figure 4-15 Correlation of FIPA and CBA scores for CASPR2 and LGI1 assays.

Ten patients with either CASPR2 or LGI1-Abs were used to compare the FIPA to the CBA. Overall a positive correlation was observed for both assays.

4.4 Appearance of a second antibody specificity in one Morvan's patient

For only two MoS patients were sequential serum samples available. One patient, MoS #15, presented in late 2006 with NMT including burning in his feet and weight loss, with high serum VGKC-complex antibodies (1552 pM). No detectable tumour was found and CSF showed a raised protein only (0.79g/L). CBA's showed his antibodies were only against CASPR2 and despite being treated with IvIg and prednisolone his antibodies remained high. Six months later, the patient developed insomnia, reduced mood and memory problems, which persisted until 2009. His presenting symptoms improved somewhat during this period but still troubled him. His clinical syndrome was quantified using the modified rankin scale (mRS), which is a scale quantifying disability, and is scored from zero to six; zero being no symptoms and six representing death (van Swieten, 1988). His mRS score went from 4 to 1, however in the last 2 years things have regressed with a return in the burning pain (2011). His VGKC-complex antibody levels were monitored throughout and remained high; with high CASPR2 antibodies (end titration point 1/4860) in all samples. Surprisingly, low levels of LGI1 antibodies were also detected in all three of his follow up samples, (Figure 4-16). In contrast, MoS #1 had multiple serum samples taken over a two year period, all of which showed high LGI1-antibodies (end titration point 1/4860) with no appearance of CASPR2-antibodies (data not shown).

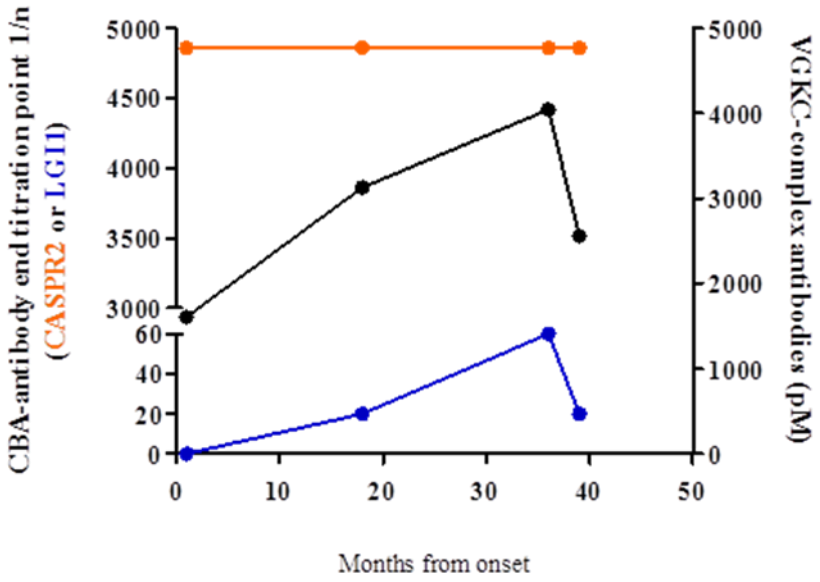

Figure 4-16 Appearance of second antibody specificity in one patient with Morvan's syndrome: CBA and VGKC-antibody titers.

High VGKC-complex and CASPR2-Abs (1/4860) were detected in patient sera at all-time points measured. Low LGI1-Abs appeared twenty months (1/20) after the initial presentation, and in all subsequent samples. Dotted line represents LGI1 cut off.

4.5 Morvan's syndrome: Clinical features

Clinical data were collated by Dr Sarosh Irani and have been summarised in Table 4-4, according to antibody specificities. The classical features of MoS were seen in the majority of patients. Twenty-seven patients were male (93.1%), NMT was present in all cases and dysautonomia, neuropsychiatric features and insomnia were seen in 93.1%, 96.6% and 89.7% of patients respectively. Interestingly, some of the clinical features dichotomised with antigen specificity; tumours, MG and weight loss were only present in patients with CASPR2-Abs, whereas serum hyponatremia was seen only in patients with LGI1-Abs. The three patients with antibodies to LGI1, CASPR2 and Contactin-2 all developed tachycardia and alterations in blood pressure, although these autonomic features were also present in a third of the patients in the cohort. Clinical outcomes were measured using the mRS and showed that the presence of a tumour, and probably consequentially an association with CASPR2-Abs, correlated with a poor prognosis. Fifty percent of patients with a tumour died compared to 17.6% of non-tumour patients ($p=0.0016$, Mann-Whitney, Figure 4-17.

	All MoS serum (n=27)	LGI1 & CASPR2-Abs (N=15)	CASPR2-Abs (N=6)	LGI1-Abs (N=3)
Tumour	12 (41.1%)	8 (53.3%)	3 (50.0%)	0
Myasthenia gravis (9 AChR-Abs)	10 (34.5%)	6 (40.0%)	3 (50.0%)	0
Weight loss	13 (48.2%)	5 (33.3%)	5 (83.3%)	0
Delusions	7 (25.9%)	3 (20.0%)	0	2 (66.7%)
FBDS/Myoclonus	3 (11.1%)	2 (13.3%)	0	1 (33.3%)
Change in mood	4 (14.8%)	1 (6.7%)	1 (16.7%)	2 (66.7%)
Serum hyponatraemia	7 (25.9%)	5 (33.3%)	0	2 (66.7%)
Hallucinations	14 (51.9%)	8 (53.3%)	2 (33.3%)	3 (100.0%)
Anxiety	3 (11.1%)	3 (20.0%)	0	0
Agitation	10 (34.5%)	7 (46.7%)	1 (16.7%)	1 (33.3%)
Confusion/disorientation	19 (65.5%)	7 (46.7%)	5 (83.3%)	3 (100.0%)
Amnesia	15 (55.6%)	5 (33.3%)	4 (66.7%)	3 (100.0%)
Seizures	10 (34.5%)	4 (26.7%)	2 (33.3%)	2 (66.7%)
Peripheral neuropathy	15 (51.7%)	7 (46.7%)	3 (50.0%)	3 (100.0%)
Pain	18 (62.1%)	10 (66.7%)	5 (83.3%)	3 (100.0%)
Death	9 (33.3%)	4 (26.7%)	4 (66.7%)	1 (33.3%)

Table 4-4 Clinical investigations of Morvan's Syndrome grouped by their antibody specificities.

Neuromyotonia, sleep disturbances and dysautonomia are common features in Morvan's syndrome and have been excluded from this analysis, alongside two Morvan's patients with insufficient serum to determine their antibody reactivities. Patients with CASPR2, LGI1 and Contactin-2 antibody reactivities have been grouped with patients with dual antibody specificities. Pettingill et al, 2012.

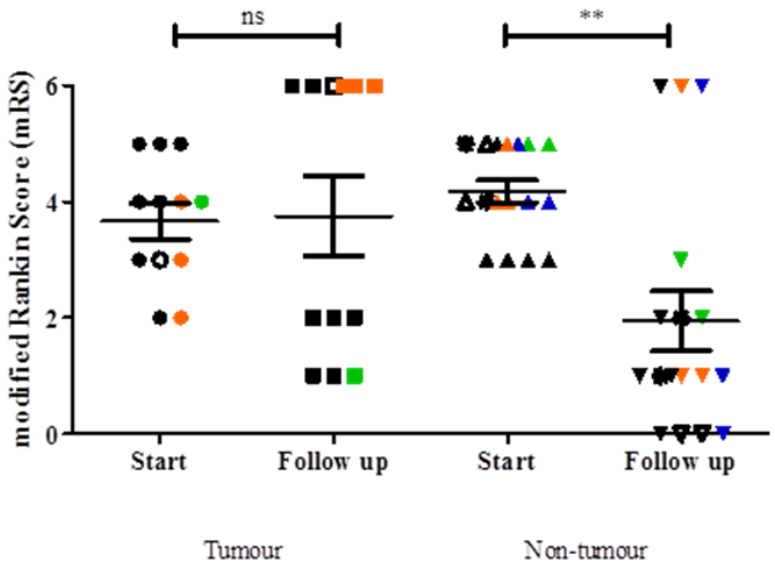

Figure 4-17 Clinical outcomes of 29 patients with Morvan's syndrome.

Patients without a detectable tumour had the best prognosis than patients with a tumour (tumour p=0.8845, non-tumour p=0.0016, Mann-Whitney). Orange = monospecific CASPR2-Abs, blue = monospecific LGI1-Abs, black = CASPR2&LGI1-Abs, green = CASPR2&LGI1&Contactin-2-Abs. Pettingill et al, 2012.

4.6 Immunodetection of surface autoantibodies to live primary hippocampal neuronal cultures

All of the above experiments were performed using transfected heterologous cells. To investigate the binding of patient sera to a native cell line, primary hippocampal neuronal cultures were studied. Primary hippocampal neurons were prepared from P0 rats and plated out on to coverslips. After 14 days *in vitro*, live, unpermeablised cultures were incubated with serum from healthy control or VGKC-complex antibody patients. Available sera from 15 patients with monospecific CASPR2 (LE=7, NMT= 3, MoS n=6) or 13 LGI1 (LE n=10, MoS n=3) antibodies were used. A further 11 Morvan's sera with multiple antibody specificities were also tested. All 40 serum samples (100%) bound to the surface of hippocampal neurons. Representative staining of two monospecific sera containing either CASPR2 or LGI1-antibodies can be seen in Figure 4-18. Sera from healthy control samples did not bind to the surface of neurons.

For an antibody to be pathogenic, it must bind to an extracellular determinant of a cell surface protein. As the hippocampal neurons were 100% sensitive for detecting surface antibodies against LGI1 and CASPR2, identified by both the cell based assay and RIA; the immunoreactivity of sera from nine patients with VGKC-complex antibodies whose antibody specificity remained unknown (LE n=2, NMT n=2, encephalopathy n=3, FBDS n=2, startle syndrome n=1) was investigated. Four of these sera (44% (LE = 2/2 and encephalopathy 2/3)) bound to the surface of hippocampal neurons, Figure 4-19a. Binding to hippocampal was not dependent on VGKC-complex antibody titer, as no significant difference was observed in RIA results between sera that did and sera that did not stain surface epitopes (p=0.2857, Mann-Whitney, Figure 4-19b

To investigate the presence of a novel pathogenic antibody in the three patients with a diagnosis of Morvan's syndrome without VGKC-complex antibodies, the immunoreactivity of these sera to the neuronal surface were assessed. In contrast, none of the three sera bound to the surface of primary neuronal cultures, Figure 4-20. This result may be interpreted as a non-antibody mediated disease in these three cases; however screening of patient sera against primary cultures prepared from alternative

regions of the brain affected in Morvan's syndrome may be more suitable. In particular IgG binding to neurons in the thalamus, hypothalamus and brainstem may help to explain the prominent features of insomnia and dysautonomia observed in the majority of these patients, but not commonly seen in limbic encephalitis associated with VGKC-complex antibodies.

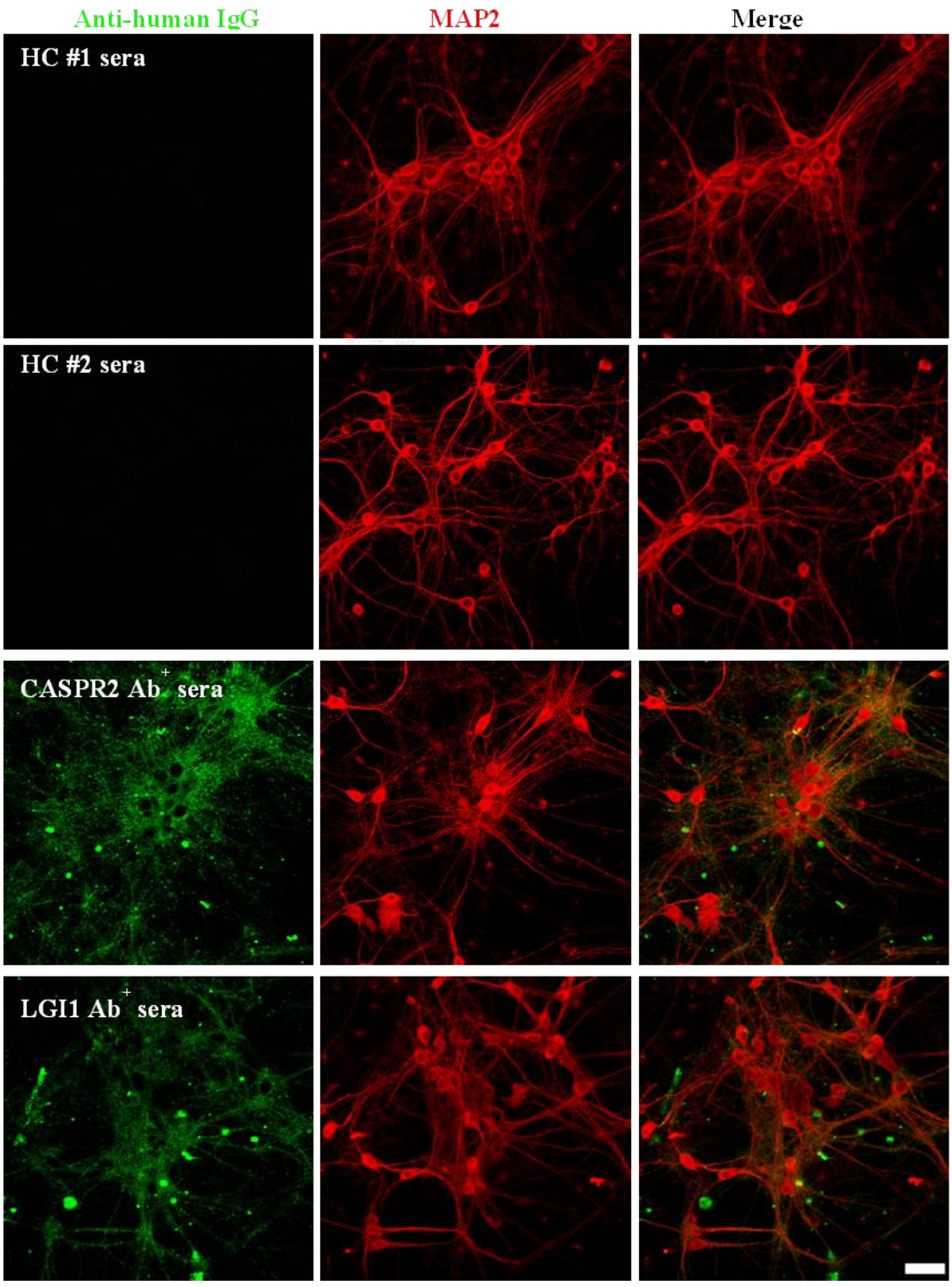

Figure 4-18 CASPR2 and LGI1 antibodies binds to the surface of hippocampal neurons

Hippocampal neurons were incubated with healthy control, CASPR2 Ab or LGI1-Abs. IgG binding was visualised with anti-human IgG (green). Healthy control sera (top rows) showed no binding to the surface of neurons. CASPR2 and LGI1-antibody positive sera bound strongly to the surface of neurons (row three and four, left column). Neurons were subsequently fixed, permeabilised and stained for MAP2 (red, middle panel). Images x200, scale bar represents 100µm.

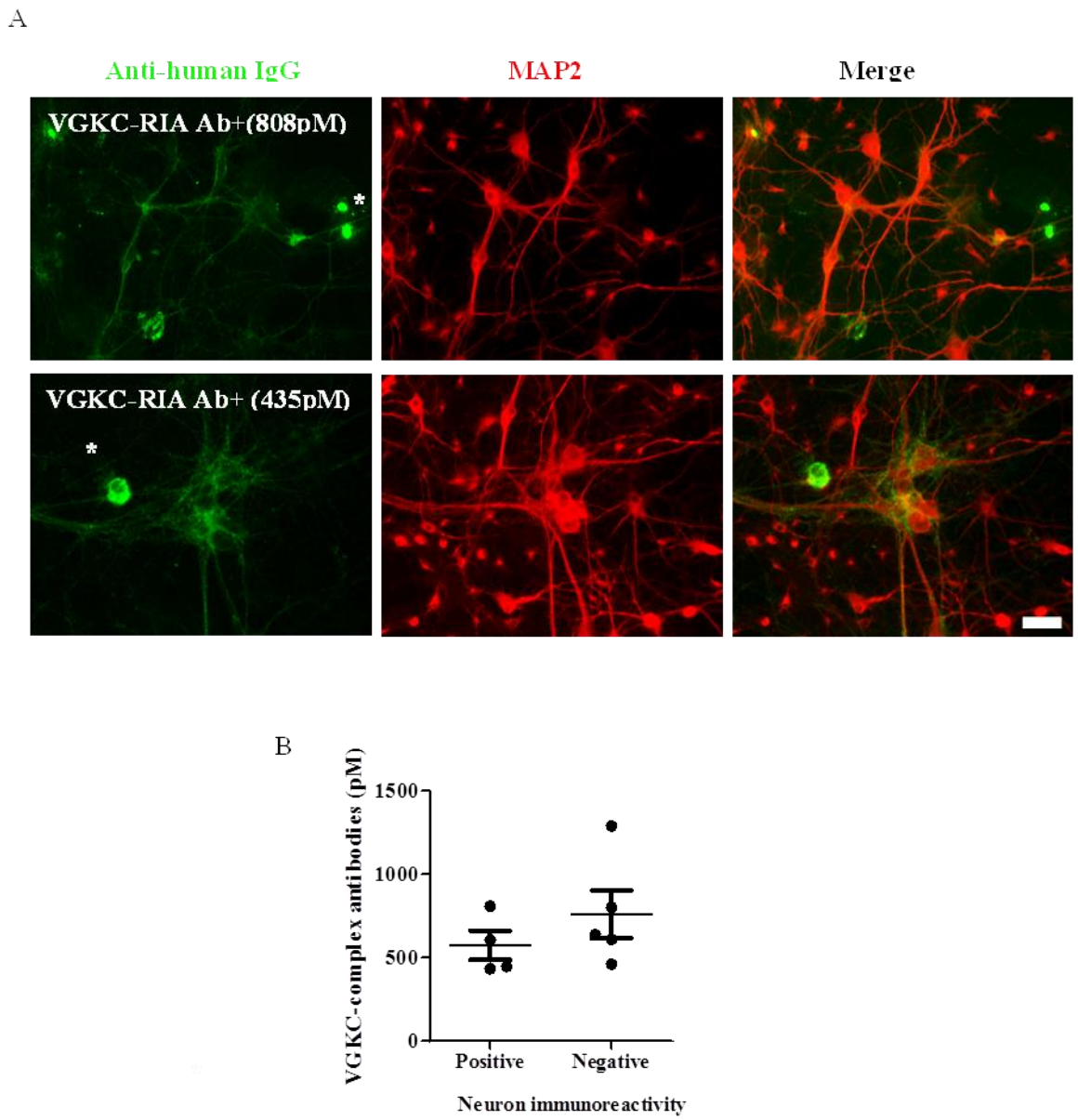

Figure 4-19 Seronegative VGKC—RIA positive sera bind to the surface of hippocampal neurons.

Representative staining of two patients IgG's (green) that bound to the surface of neurons (MAP2, middle panel). Non-specific binding can be seen in all sera to glial cells (*) Magnification 200x, scale bar = 100µm. B) No significant difference in the VGKC-complex antibody titres was observed in samples that bound to the surface of neuronal cultures (p=0.2857, Mann-Whitney).

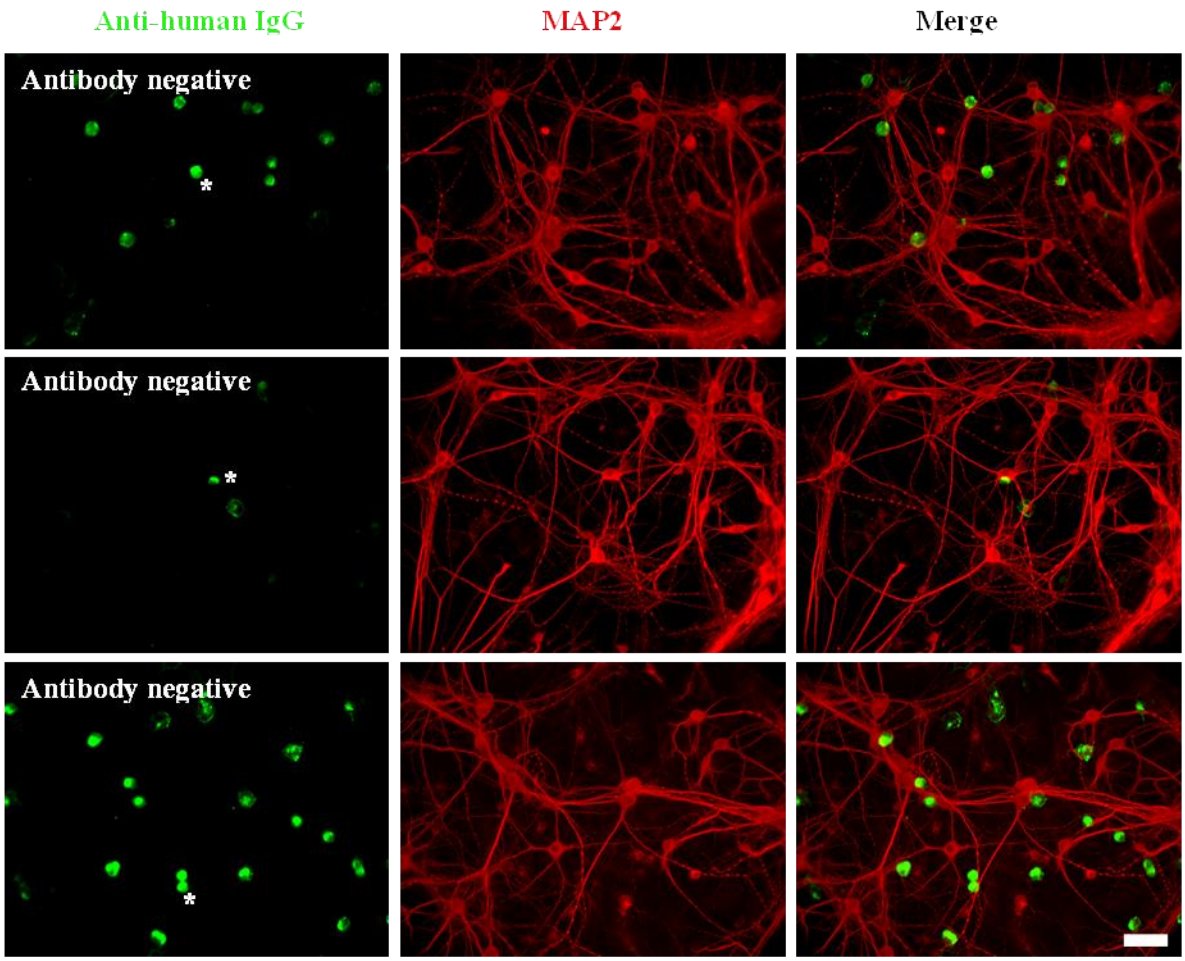

Figure 4-20 Morvan's sera without VGKC-antibodies do not bind to the surface of primary hippocampal neurons.

The three VGKC-antibody negative Morvan's sera did not bind to the surface of neurons (left column). Neurons were subsequently fixed, permeabilised and stained for MAP2 (red, middle panel). Non-specific binding can be seen in all sera to glial cells (*). Magnification 200x, scale bar = 100µm.

4.7 Discussion

4.7.1 Improvement of LGI1 assay sensitivity

Irani *et al* initially reported the detection of LGI1 antibodies by transfection of LGI1 in to HEK cells where it binds to receptors inherently present on HEK cells and confirmed that LGI1 is secreted from the cell in to the culture medium (Irani, 2010; Senechal, 2005). Some serum immunoreactivity was often weak and some patients with LE did not appear to have antibodies detected in their sera, yet appeared to have an identical syndrome to the LGI1-Ab cases. The initial aim of this chapter was to improve the sensitivity of detecting LGI1-Abs, by expressing LGI1 at the cell surface using the transmembrane domain of CASPR2 as an anchor. Expressing LGI1 in a membrane-tethered format identified LGI1-Abs in fifty percent of the antigen-negative samples, without affecting the assay specificity. The nine previously seronegative sera did not have significantly lower VGKC-complex antibody titers than those samples originally identified as having LGI1-Abs in their serum. One explanation for this may be that many of the serum samples used in this thesis are old and subsequently antibodies could have degraded over repeated freeze-thaw cycles, although this was not re-checked on the RIA. Alternatively, some patients with MG have low affinity antibodies to the acetylcholine receptor, that require the antigen to be clustered by rapsyn, concentrating it the cell surface (Leite, 2008). It may be that these nine patients had low-affinity LGI-Abs. As the modified LGI1 assay was significantly more sensitive at detecting serum antibodies, it was used in all future diagnostic assays.

Overall, 55 patients in this study had a single antibody specificity directed against LGI1, of these 51 (92.7%) had LE (1 had NMT, 2 had MoS and 1 presented with seizures only). One study found LGI1 antibodies in 100% of patients with VGKC-antibody associated LE using HEK cells co-transfected with LGI1 and its receptors ADAM22/23 (Lai, 2010); that study did not find LGI1 antibodies in patients with NMT. Whether the interaction of the LGI1 with its receptors ADAM22/23 is a more sensitive assay for detection of LGI1-antibodies has not been examined. Two of our nine patients negative for both CASPR2 and LGI1-Abs had LE and it may be possible that the interaction of LGI1's EAR domain with ADAM22/23 produces a conformational epitope for some VGKC-antibody

positive sera. However one cannot exclude the possibility that these antibodies may be directed against other unidentified proteins associated with the VGKC-complex, including ADAM22 or ADAM23.

4.7.2 Clinico-serological specificities

Whilst LGI1-Abs have been associated with LE and CASPR2 antibodies with nNMT the antibody specificities in MoS had not been previously explored. Morvan's syndrome is a multifocal disease affecting both the peripheral and various locations within the central nervous system and fittingly both CASPR2 and LGI1-Abs were observed in the majority of patient sera studied (56%). Monospecific antibodies to CASPR2 and LGI1 were also observed in 22% and 11% of patients respectively. Interestingly there has been only three VGKC-complex antibody patients reported to have both CASPR2 and LGI1-Abs in the literature to date, and these patients were reported as having LE or FBDS preceding LE (Lai, 2010; Irani, 2011). The high frequency of multiple reactivities in our MoS cohort was surprising so rigorous preadsorption studies against either CASPR2 or LGI1-transfected cells were performed, and multiple immunoreactivities were confirmed in all four sera studied. In data collected outside of this thesis, 111 VGKC-complex antibody positive patients, with unknown clinical presentations were collected over a three month period and their antibody specificities determined. CASPR2 or LGI1 monospecific antibodies were identified in 49.5% of patient sera, however only two patients had both CASPR2 and LGI1-Abs(1.8%) (Pettingill and Vincent, unpublished observations) which is in keeping with the estimate of MoS in a prospective cohort of patients with VGKC-complex antibodies (Tan, 2008).

Overall this indicates that the detection of multiple VGKC-complex antibody specificities could be a strong indicator of Morvan's syndrome and is intuitive to the phenotype of a disorder of both peripheral and central involvement.

The multiple immunoreactivities in the majority of Morvan's sera may help to explain the multifocal presentation. Neuropsychiatric features were more common in patients with LGI1-Abs, consistent with findings in LE and patient prognosis was worse in thymoma patients, most of whom had CASPR2-Abs. Sleep dysfunction, in particular insomnia, is a principal feature in MoS, yet patients

with NMT with CASPR2-Abs do not suffer from sleep disturbance. Liguori *et al* reported IgG deposition in the thalamus of a patient with MoS, implicating it as a possible site of origin for the sleep disturbances (Liguori, 2001). In neuromyotonia, CASPR2-Abs may not penetrate the brain, thus explaining the lack of CNS symptoms in these patients. To date there have been no human mutations in CASPR2, LGI1 or Contactin-2 associated with sleep disorders, however a reduction in sleeping time has been reported in Drosophila with a mutation in their *Shaker* gene encoding the Kv1 subunits and similarly in Kv1.2 knockout mice (Cirelli, 2005; Douglas, 2007). Therefore VGKC-complex antibodies may indirectly affect the function of the potassium channels, resulting in disruption of the normal sleep circuitry.

4.7.3 Multiple antibody specificities

It is possible that multiple antibody specificities occur simultaneously or dual specificities arise in Morvan's syndrome as a result of epitope spreading. In a rat model of EAMG, immunisation with a peptide against the α-subunit of the AChR resulted in the production of additional antibodies against other subunits of the AChR complex (β and γ), which did not cross-react with the original immunising peptide sequence (Agius, 1998). As CASPR2 and LGI1 are members of the VGKC-complex and thus closely associated, it is feasible that epitope spreading could occur in a similar manner. NMDAR antibodies are predominantly against the NR1 receptor subunit but approximately ten percent of patients with NMDAR antibodies have been reported to have additional antibodies against the NR2 subunits (Dalmau, 2008). The same authors have described antibodies against both the AMPA 1 and AMPAR2 subunits in one patient with LE, however for both antibodies the authors did not discuss whether this was attributed to multiple antibody specificities or a cross-reactive epitope (Dalmau, 2008; Lai, 2009). The uncertainties that have arisen from these studies could have been addressed by incubating patient sera on live unfixed and unpermeablised cells in conjunction with the thorough preadsorption experiments described in this thesis.

To understand whether MoS presents initially with multiple specificities in the majority of patient sera or whether there is development of the immune response needs to be addressed. Early recognition of

the disorder in a prospective study and frequent follow up samples would allow monitoring of the antibody specificities over time.

4.7.4 Detection of VGKC-complex antibodies: Assay sensitivity and specificity

The majority of patients in this thesis were included based on the detection of VGKC-complex antibodies in their serum. However, approximately one quarter of MoS patients recorded in the literature do not have a VGKC-complex antibody detected by RIA (Abou-Zeid, 2012), so this requirement did not apply when considering patients with Morvan's syndrome. Consistent with these findings, five of 27 (18.5 %) MoS patients in this chapter did not have antibodies detected in the sera by RIA. Interingestly, two of the five sera were later positive by CBA techniques; which is likely to be due to the concentrated expression of the antigenic target in the CBA, making it a more sensitive method of detection. CASPR2-Abs were recently described in nine patients with cerebellar ataxia, eight of whom did not have VGKC-complex antibodies measure by RIA (Becker, 2012). Furthermore, convalescent serum samples from VGKC-complex antibody patients following treatment can be negative on the RIA but still positive by CBA (Pettingill and Vincent unpublished observations). Whether these findings reflect residual low antibody levels after disease or could be an early predictor of disease relapse is yet to be established. However where a diagnosis of Morvan's is made, accompanied with a negative RIA result, the sera should be screened by CBA's for CASPR2, LGI1 and Contactin-2 antibodies. The diagnostic value of confirming the precise antigenic target of patient VGKC-complex antibodies is of great biological interest but also clinically important as CASPR2-Abs are often associated with an underlying active thymoma and a worse prognosis (Irani, 2011).

4.7.5 Comparisons of antibody assays

When measured using the RIA, VGKC-complex antibody titers were reported to be significantly higher in patients with LGI1-Abs, which was attributed to a higher proportion of LGI1 than CASPR2 molecules being associated with the VGKC complex (Irani, 2010). In contrast, endpoint titrations on the CBA's were found to be significantly higher for CASPR2-Ab sera. The results quantifying EGFP

expression showed a thirty fold higher expression with the CASPR2 constructs. This could be a direct result of the two constructs being in different expression vectors (pEGFP-N1 and pcDNA3.1 respectively). As differences in antigen expression may affect the end titration point, the data was normalised, and CASPR2 end titrations divide by ten. These results now suggested that CASPR2 antibodies were no longer higher than LGI1 antibodies. Given that the CASPR2 titers were normalised only 10-fold, when in fact CASPR2 expression was between 10-30 times higher, LGI1 antibodies levels may be much higher than reflected in this study.

The FIPA was used as an alternative method to directly compare the amount of antigen-EGFP precipitated and despite equal amounts of antigen-EGFP being used, samples in the two FIPA's did not precipitate significantly higher levels than the other, although CASPR2 sera showed a trend towards higher antibody titers. One assumption of the FIPA is that that equal amounts of antigen have assembled in to the correct native conformation, which is recognisable by serum antibodies. The non-significant trend towards higher CASPR2 antibodies on the FIPA may like the CBA be skewed. For future development of the LGI1 CBA and FIPA, it is worth considering expressing LGI1 in the pCDNA3.1 vector, to see if this aids its expression to levels comparable to those seen in CASPR2 transfections.

Despite these findings, around half of all positive serum samples were negative on their respective FIPA's. These findings are in accordance with the sensitivity of detecting AQP-4 Abs by FIPA in NMO being only 53% sensitive compared to the CBA (Waters, 2008). This result illustrates that the CBA is a more sensitive method for the detection of autoantibodies than the FIPA.

4.7.6 Antigen negative sera

In total 12 patients discussed in this chapter did not have antibodies against CASPR2, LGI1 or Contactin-2. All CASPR2 and LGI1 patient sera tested on hippocampal neurons showed surface IgG binding. Four of nine antigen-negative patients with a positive RIA result also bound to the surface of hippocampal neuronal cultures. The finding is important as these antibodies are likely to be pathogenic and warrant further investigation to identify the target. Obvious antigenic targets for these remaining sera are proteins associated with the VGKC-complex, including ADAM22 and ADAM23

which interact directly with LGI1 (Fukata, 2006; Ogawa, 2010) and NogoR1 which are part of the post-synaptic complex alongside ADAM22 and AMPARs. Immunoprecipitation of the patient antibody-antigen complexes followed by a mass spectrometry analysis has successfully identified AMPA and $GABA_{(B)}$ receptors as the novel antibody targets in LE, and a similar approach could be used to identify the antibody target in these four sera (Lai, 2009; Lancaster, 2010b).

The three patients with MoS with a negative RIA presented with a sub-acute onset and responded well to immunotherapy (mRS at presentation was 4.67±0.57 and dropped to 1±2 (mean± SD) at last follow up), which is suggestive of an immune aetiology. Despite this, neither patient bound to the surface of hippocampal neurons. Instead, these patients may have antibodies in their sera against non-hippocampal surface proteins. Further screening of these sera on brain sections, or focusing on neuronal cultures from different brain regions affected in MoSe, including the thalamus where IgG deposition has been observed, may allow the detection of an antibody in these patients (Liguori, 2001). Unfortunately, limiting amounts of sera for these samples prevented further follow up experiments.

In conclusion data in this chapter has confirmed that antibodies to the VGKC-complex are against CASPR2, LGI1 and Contactin-2 and that membrane tethering of LGI1 increased the sensitivity of detecting LGI1-Abs. Multiple antibody specificities are a common occurrence in patients with MoS. The cell based assay was the most sensitive method of detecting patient antibodies, even detecting patient antibodies in sera without a positive RIA result. However some patients with VGKC-complex antibodies but no defined antigenic target bound to the surface of hippocampal neurons, indicating the presence of a cell surface pathogenic antibody. The next step of this thesis was to investigate the pathogenic effects of CASPR2 and LGI1-Abs *in vitro*.

Chapter 5: Characterisation of the structural and pathogenic effects of VGKC-complex antibodies *in vitro*

4.8 Introduction

Many patients with VGKC-complex antibodies often have a beneficial response to immunomodulatory therapies, which correlates with a fall in their antibody titer (Shillito, 1995; Buckley, 2001; Vincent, 2003). These findings strongly support a pathogenic role for VGKC-complex antibodies. As the targets for VGKC-complex antibodies have been only recently described, very little is known about the effects of these antibodies on their target proteins. VGKC-complex antibodies now known to be against CASPR2 have previously been investigated in the PNS but no direct effect on CASPR2 function or expression has been studied (see Table 2-3). VGKC-complex antibodies have been shown to bind to rodent brain sections including the hippocampus, cerebellum, hypothalamus and thalamus; and deposits of IgG have been shown in the brains of patients with serum VGKC-complex antibodies (Liguori, 2001, Buckley, 2004, Bien, 2012). As previously discussed, in myasthenia gravis there are three effector mechanisms of AChR antibodies: 1) internalisation and increased degradation of AChR, 2) antibody-mediated complement damage on the postsynaptic membrane and 3) direct binding and blocking of the AChR function.

The aim of the work in this chapter is to similarly characterise the pathological mechanisms that may underlie VGKC-complex antibody CNS disease *in vitro*. Firstly IgG subclasses were determined before examining the role of complement in CASPR2 and LGI1-mediated disease. Secondly, internalisation experiments examining the effect of patient IgG on CASPR2 surface expression in transfected HEK cells were studied to observe an example of internalisation. Finally as IgG deposits are found in the hippocampus of rodent brain, hippocampal high signal is frequently seen in LE cases and VGKC-complex antibodies bind to live primary hippocampal neurons, the effect of patient IgG binding on antigen expression was assessed in cultured hippocampal neurons.

4.9 Results

4.9.1 CASPR2 and LGI1-antibodies are predominantly IgG1 and IgG4

Of the four main subclasses of IgGs, IgG1 and IgG3 are the main subclasses that can activate the complement cascade. To determine which subclasses were present in patients with VGKC-complex antibodies, sera were tested on the CBAs and antibody binding detected using specific secondary antibodies against the individual subclasses.

Individual IgG subclasses were studied in 32 patients with VGKC-complex Abs. 13 had CASPR2-Abs (LE n=5, MoS n=8) and 19 had LGI1-Abs (LE n= 13, MoS n=6). Both IgG1 and IgG4 were present in the majority of CASPR2-Ab sera (69.2%), with high IgG1 antibodies present in every serum tested. Eight sera also had IgG2 CASPR2-Abs, often at high levels, whilst five of these sera had appreciable levels of all four subclasses. For LGI1-Ab sera, IgG4 antibodies were present in all sera tested (100%) and 16 sera (84.2%) had additional subclasses (IgG1, IgG2 or both). No LGI1-Ab sera contained IgG3 antibodies. Analysis of subclasses showed a significant difference between group for both CASPR2 and LGI-1 antibodies ($p=0.0001$ and $p<0.0001$, Kruskal-Wallis respectively, Figure 5-1). For CASPR2-Abs, IgG1 antibodies were found at significantly higher concentrations than IgG2 ($p<0.05$) and IgG3 ($p<0.001$). For LGI1-Ab sera, IgG4 antibodies were significantly higher than all other IgG subclasses (all $p<0.001$) and IgG1 antibodies were higher than IgG3 ($p<0.05$). No clear differences were seen when comparing those with LE or MoS, Figure 5-2.

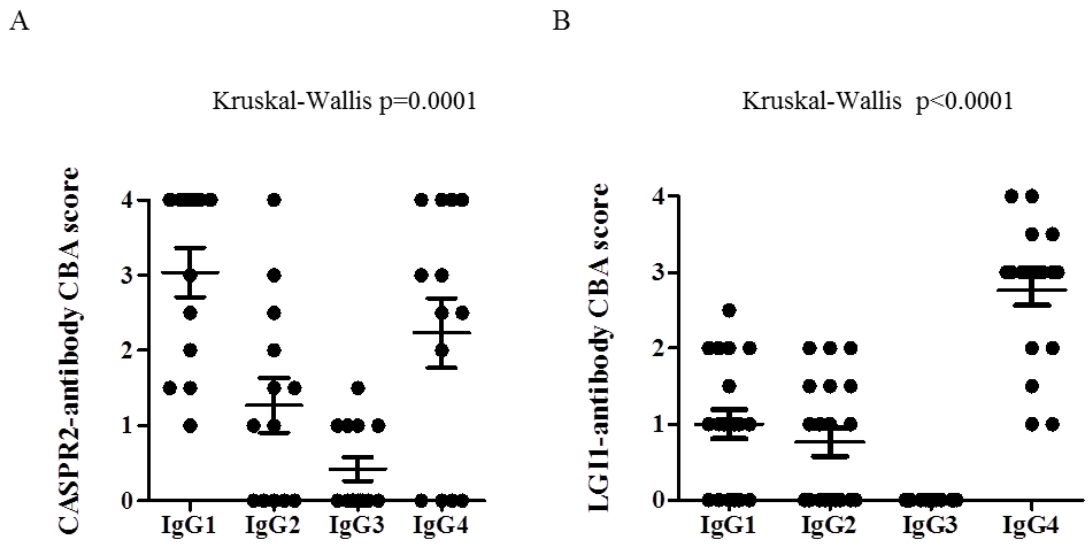

Figure 5-1 CASPR2 and LGI1 antibody subclasses are predominantly IgG1 and IgG4.

IgG subclasses determined by CBA. Data analysed using a one-way ANOVA. A) IgG1 and IgG4 antibodies were the predominant subclasses in CASPR2-Ab sera (n=13, IgG1>IgG2 & 3 & 4 ($p<0.05$, $p<0.001$ and $p<0.05$)). B) LGI1-Ab sera were predominantly of the IgG4 subclass (n=19, IgG4>IgG1 & 2 & 3 ($p<0.001$, $p<0.001 p<0.001$), and IgG1>IgG3 ($p<0.05$)). Positive ≥1.

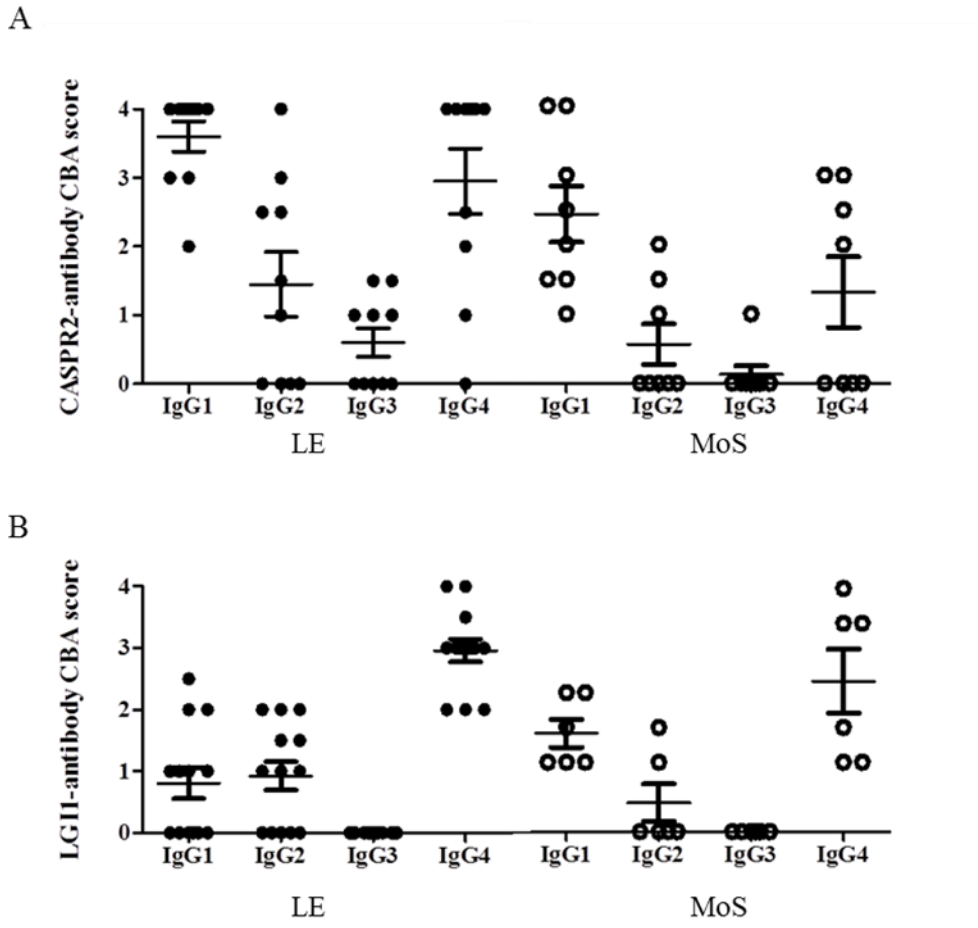

Figure 5-2 Antibody subclasses for patients with limbic encephalitis and Morvan's syndrome are predominantly IgG1 and IgG4.

Similar distribution of IgG subclasses were seen in patients with limbic encephalitis (LE) and Morvan's syndrome (MoS). A) CASPR2 antibodies were predominantly IgG1 and IgG4. B) LGI1-antibodies were predominantly IgG4.

4.9.2 CASPR2 and LGI1-antibodies fix complement

As IgG1 and IgG3 antibodies are known to activate the complement cascade we looked to see if CASPR2-Ab or LGI1-Ab sera, which were heat inactivated, could fix a fresh source of human complement on the surface of transfected-HEK cells at 37˚C. The cells were subsequently washed, fixed, and stained with a specific anti-C3b antibody. Complement activation was determined by visualisation of anti-C3b binding to transfected cells. Binding of C3b was visualised in 7/11 CASPR2-Ab (63.6%) patients, Figure 5-3a. Of these 4 patients had LE and 3 patients had MoS (non-complement fixers: 3 MoS, 1 LE). Seven of seventeen LGI1-Ab sera (41.2%) fixed C3b on transfected HEK cells, Figure 5-3b. Six patients had LE and one patient had MoS (non-complement fixers: 2 MoS, 8 LE). As expected C3b deposition was not observed in any of the nine healthy control sera. No deposition of C3b was seen on the surface of transfected-HEK cells in any sera in the absence of active complement. Representative staining of complement activation can be seen in Figure 5-3c.

Despite 63% of CASPR2 and 41% of LGI1-Ab IgG binding C3b, a large number did not. All 14 sera that fixed complement had IgG1 specific-antibodies present in their sera. Of those which did not fix complement, all CASPR2 sera had IgG1 antibodies. To explore why there was no observed complement deposition, despite the presence of IgG1, we explored concentration differences between the IgGs. C3b deposition was plotted against the VGKC-complex antibody titer (determined by RIA). CASPR2 sera that fixed complement had significantly higher VGKC-complex antibody titers than those that did not ($p=0.0190$, Mann-Whitney, Figure 5-4a).

All LGI1 antibodies studied are predominantly IgG4. All seven sera which fixed complement had IgG1 antibodies and of the ten sera that did not, seven also had low levels of IgG1. LGI1-Ab sera that deposited C3b *in vitro* showed a non-statistically significant trend to elevated VGKC-complex antibody titers compared to sera that did not ($p= 0.0787$, Mann-Whitney, Figure 5-4b). The three patients with LGI1 antibodies which were only of the IgG4 subclass, did not fix complement, which is consistent with the non-complement fixing properties of IgG4 molecules (Tao, 1993).

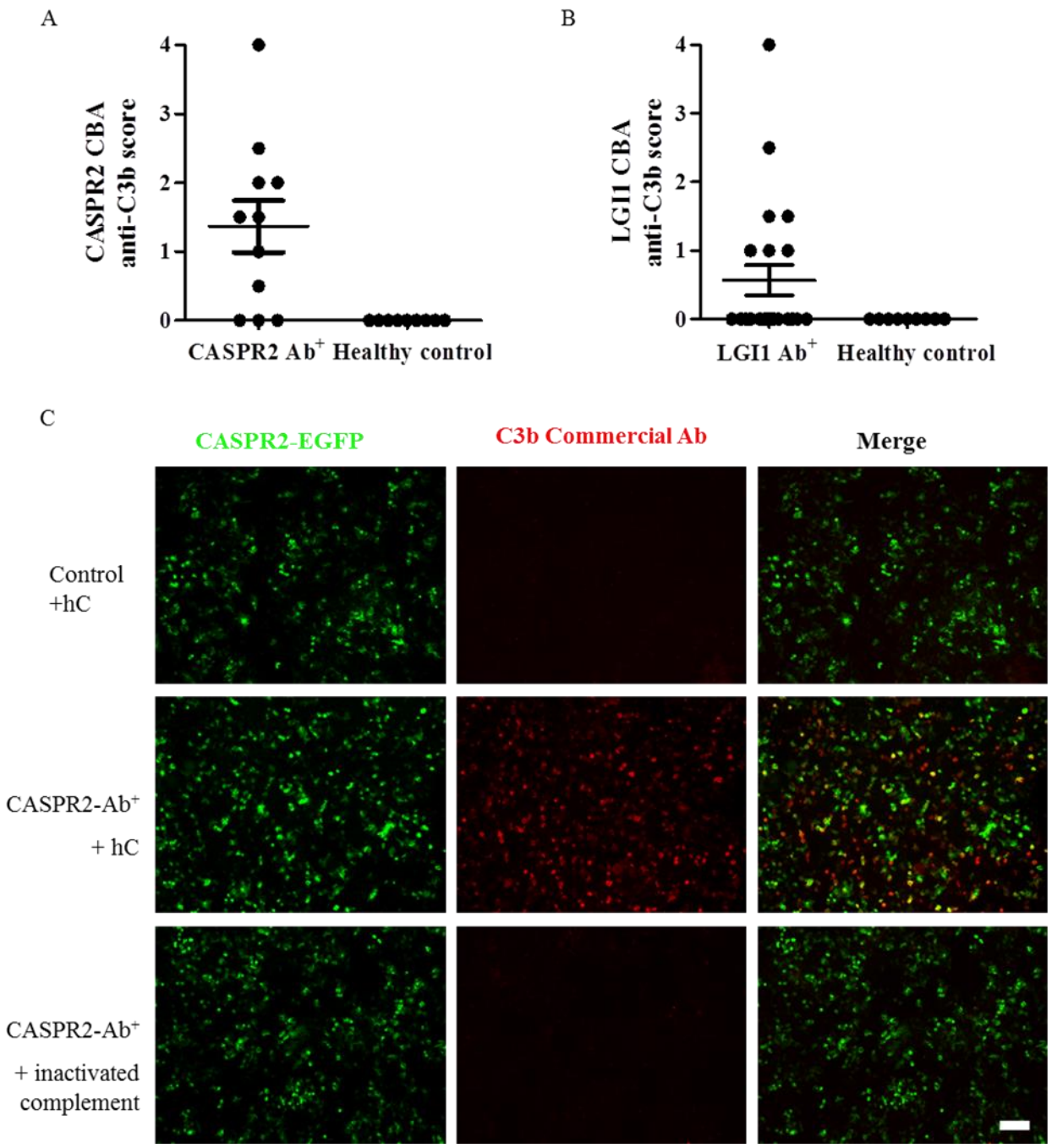

Figure 5-3 CASPR2 and LGI1-antibodies activate complement on transfected HEK cells.

The activation of the complement system detected using a commercial antibody against complement component C3b. A) 7/11 CASPR2-antibody positive serum activated the complement cascade. B) 7/17 patients with LGI1-antibodies fixed complement. Healthy control sera did not show deposition of C3b in either assay. (c) Representative staining of control and CASPR2-patient serum can be seen (C3b:red middle panel). Inactivating the fresh source of complement eliminated C3b in all CASPR2-patients. Image magnification 100x, scale bar = 200µm

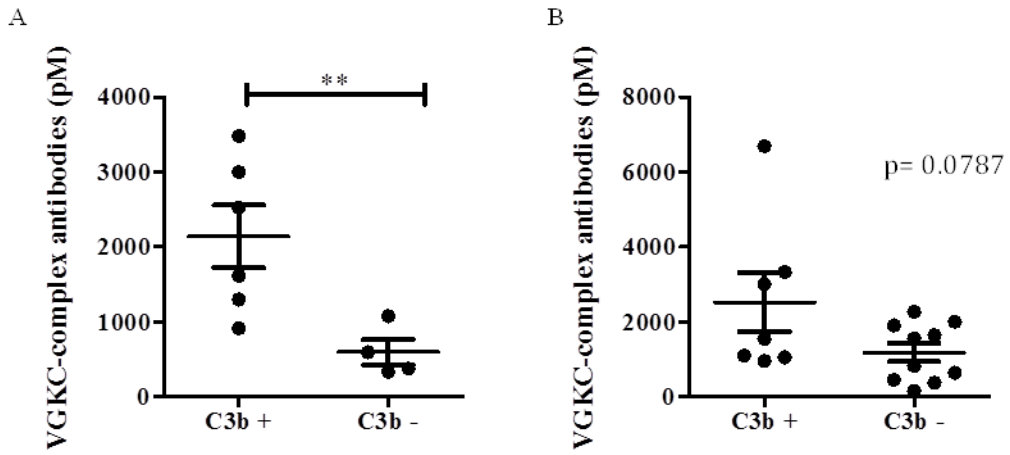

Figure 5-4 Sera with high VGKC-complex antibody titers fix complement component C3b.

Complement was plotted in relation to the VGKC-complex antibody titre measured by RIA. A) CASPR2 sera with statistically significant higher VGKC-complex antibody titres activate the complement cascade (p=0.0190, Mann-Whitney). B) LGI1 sera shows a non-significant trend for complement deposition in samples with higher VGKC-complex antibody titres (p=0.0787, unpaired t-test).

4.9.3 Internalisation of CASPR2- in transfected HEK cells

The above findings explored one pathogenic mechanism of CASPR2 antibodies. To understand whether CASPR2 antibodies could cause internalisation, CASPR2 transfected cells were incubated with IgG from two patients ((#50 and #52) for one hour, the cells washed and placed back into the incubator for 0, 2, 4, 8, 12, or 24 hours and the amount of IgG bound to the surface of the transfected cells measured.

After incubation with CASPR2-Ab IgG, bound IgG was immediately observed as previously shown. After the unbound sera was removed from the cells, IgG surface binding to CASPR2-transfected cells was significantly reduced in patient 1 ($p=0.0033$, two-way ANOVA) and patient 2 ($p=0.0401$ two way ANOVA over the 24 hour period, shown in Figure 5-5. This result could represent either the internalisation of the IgG-CASPR2 complex into the cell, or reflect the dissociation of the IgG molecule from CASPR2.

To study whether CASPR2-IgG was internalised, CASPR2-HEK cells were incubated for 24 hours with IgG from healthy control, LGI1 or CASPR2-antibody patients, and the cells were subsequently stained for surface CASPR2 expression using a commercial antibody against an extracellular epitope of CASPR2. Surface binding of the CASPR2 commercial antibody was quantified using the CBA scoring system. Two LGI1-Ab (#18 and #65, both with LE), and 3 CASPR2-Ab patients (#50, #52 had LE and #64 with epilepsy) IgGs were used in these experiments.

Initial experiments were performed to show that CASPR2-Ab does not prevent the commercial antibody binding to CASPR2 cells, coverslips were incubated with CASPR2-Ab patient IgG for one hour and then immediately stained with the commercial CASPR2 antibody. The CASPR2 commercial antibody showed no gross difference to control coverslips (data not shown). An effect of treatment was seen on extracellular CASPR2 immunoreactivity after 24 hours incubated with control or patient IgG (Kruskal-Wallis $p<0.0001$) CASPR2-transfected cells incubated with CASPR2-Ab IgG showed a significant reduction in the surface binding of the commercial CASPR2 antibody compared to cells incubated with LGI1-Ab, healthy control or to cells incubated with media alone (Dunn's multiple comparisons, all $p<0.001$). Representative images from these experiments can be seen in Figure 5-6.

In cells treated with CASPR2-IgG, CASPR2-EGFP cells appear more clumped. To analyse the effect of CASPR2-Ab^{+} sera quantitatively, low magnification images were taken of coverslips and the number of total cells (DAPI positive), CASPR2-transfected cells (EGFP positive) and CASPR2-surface expressing cells (CASPR2 commercial antibody counted. All data was normally distributed and analysed using a one-way ANOVA. There was no effect of serum specificity on the number of total cells counted (Kruskal-Wallis, $p=0.1472$). However, CASPR2-IgG specifically reduced the number of EGFP positive cells (Kruskal-Wallis, $p=0.0035$) and CASPR2 positive cells (Kruskal-Wallis, $p=0.0002$) when compared to control-IgG, LGI1-IgG or no IgG (EGFP cells; no IgG $p<0.01$, healthy control or LGI1 IgG $p<0.05$, CASPR2^{+} cells; all $p<0.001$). No significant difference was observed between cells treated with healthy control-IgG, LGI1-IgG or medium. Surface IgG semi-quantitative binding (CBA score), number of DAPI^{+}, EGFP^{+} and number of CASPR^{+} cells can be seen in Figure 5-7.

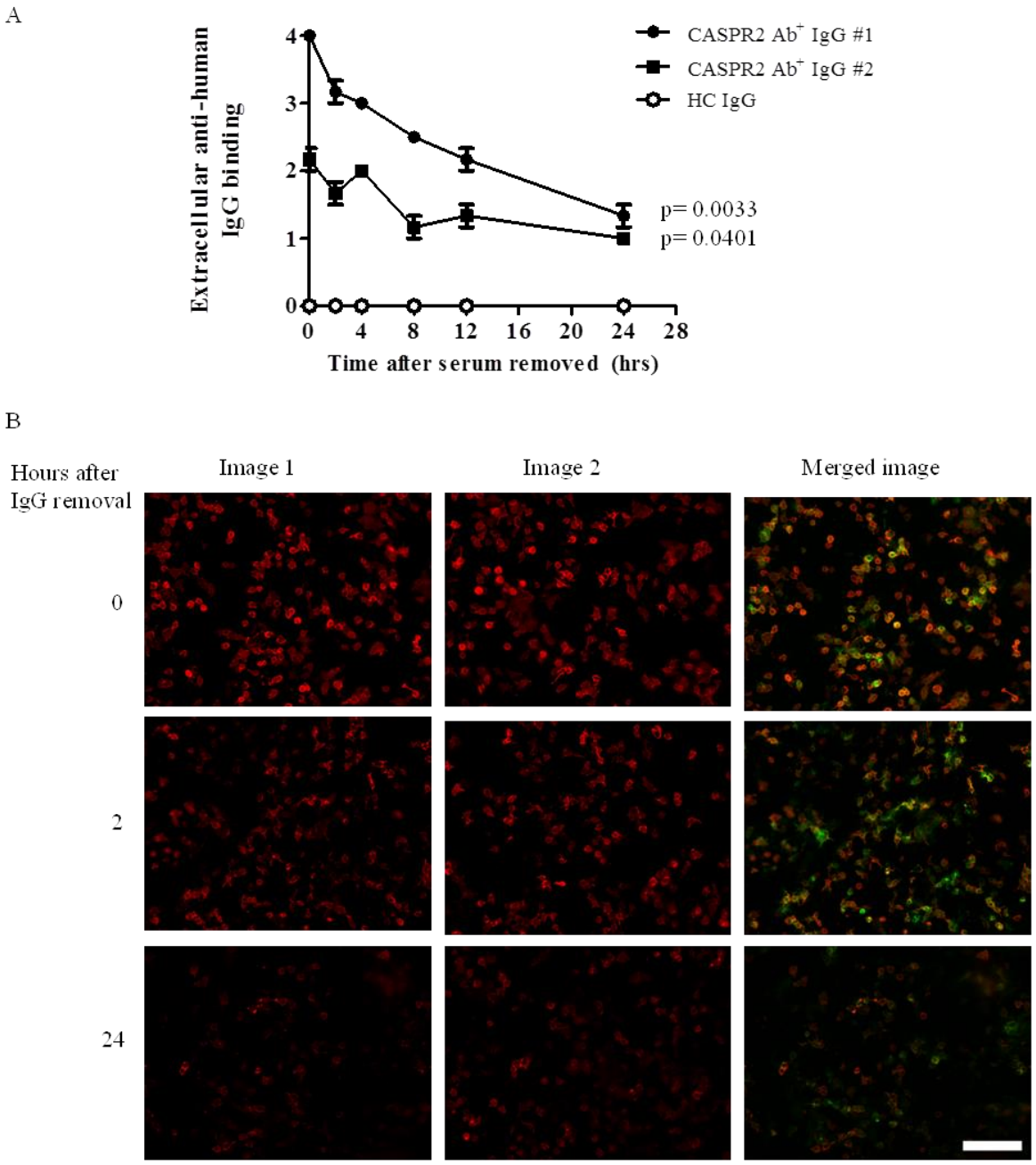

Figure 5-5 Reduction in CASPR2-IgG binding on the surface of CASPR2-transfected cells.

CASPR2 transfected cells were stained with CASPR2-Ab IgG from two patients. IgG was removed and cells incubated in media for as shown. A) An effect of time was seen in surface IgG binding for both patients (p=0.0033 and p=0.0401), healthy control IgG did not bind to transfected cells (blue). B) Representative images of surface IgG binding from patient #1 at 0, 2 and 24 hours (red) and the merge with CASPR2-EGFP (far column). Image magnification 200x, scale bar = 200µm.

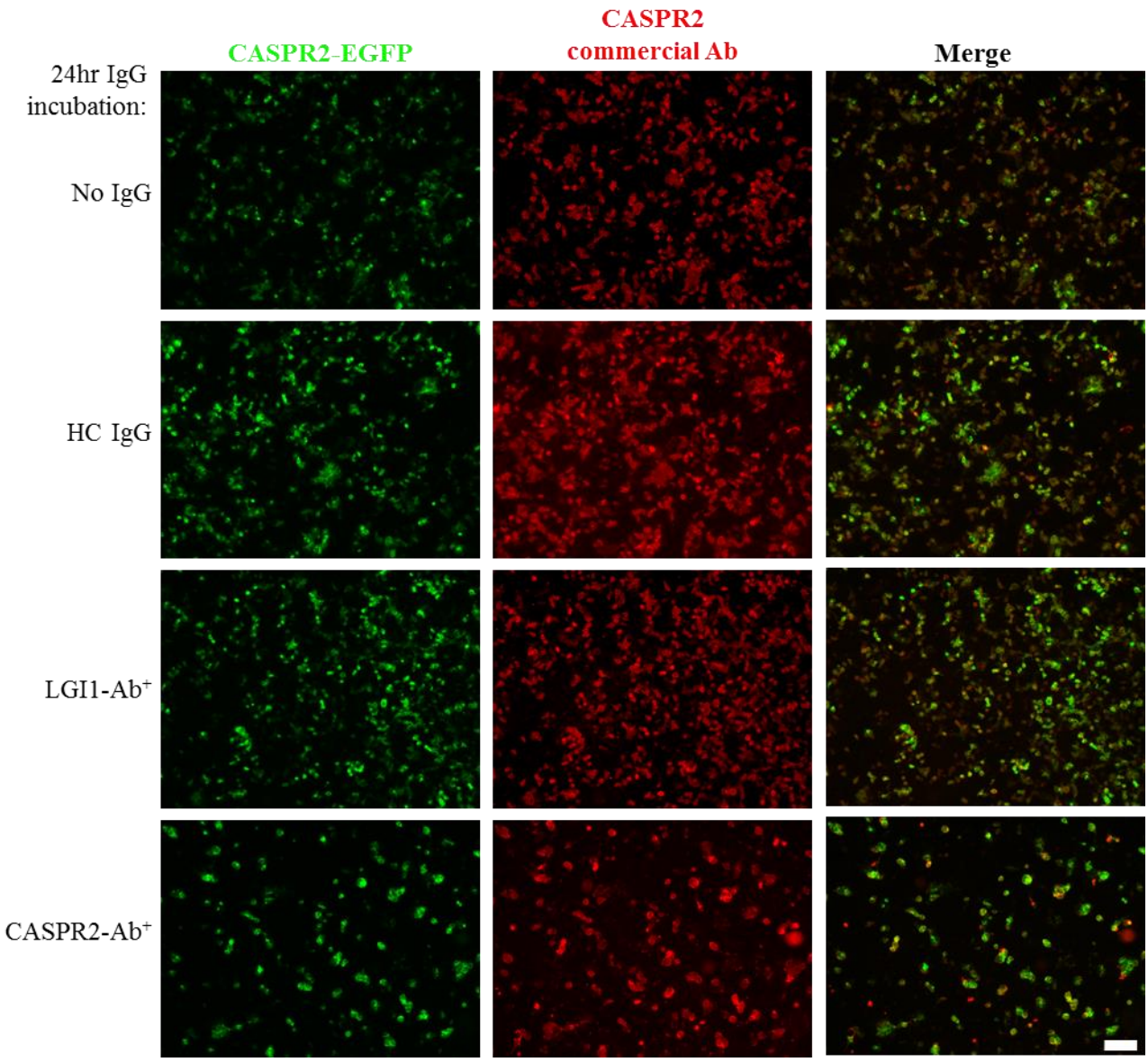

Figure 5-6 CASPR2-IgG reduces surface expression of CASPR2.

CASPR2 transfected cells were incubated for 24 hours with healthy control IgG (HC), LGI1-IgG (n=2) CASPR2-IgG (n=3) (100µl) and compared to cells incubated in media alone. CASPR2 surface expression was visualised with an anti-CASPR2 commercial antibody and detected with a specific antibody (red). A reduction in CASPR2 stained cells can be seen in coverslips incubated with CASPR2-IgG (middle panel, bottom row). No gross affects were seen in cells incubated with media, HC or LGI1-IgG. Image magnification 200x, scale bar = 100µm.

To investigate whether this change could be monitored biochemically, cells were incubated in T-175cm^2 flasks incubated with culture medium (n=1), or medium supplemented with 0.6mg of total purified IgG from a healthy control (n=1), LGI1-IgG (n=2) or CASPR2-IgG patients (n=2) for 24 hours. Cells were subsequently washed, surface proteins biotinylated, and then solubilised with 1% digitonin. Membrane and intracellular fractions were collected and the CASPR2 and actin content analysed by western blot. Mouse brain extract was included as a positive control for the commercial antibodies.

In the brain extract, CASPR2 has a molecular weight at ~180kDa; however CASPR2 from transfected HEK cells has a molecular weight of ~210kDa due to the addition EGFP attached to its C-terminus, Figure 5-8). Probing with a CASPR2 commercial antibody showed a less intense band in the membrane fractions from cells incubated with CASPR2-IgGs (lanes 5 and 6). A similar profile was seen in the intracellular fraction for one of the CASPR2-IgG samples, but was more evident in the second IgG sample. The CASPR2 band for cells incubated with healthy control and LGI1-IgG did not show a visible difference from untreated cells. Membranes were probed with an actin antibody to control for differential loading. Immunodetection of actin was weak in the membrane preparations indicating that there is little intracellular contamination in the preparation. Whilst the actin bands in the intracellular fraction were easily visualised. The concentration of CASPR2-Abs in patient #2 was higher than patient #1 (1:43740 versus 1:4860 end dilution point), which is likely to explain the bigger decrease in CASPR2 band intensity in both the intra and extracellular fractions.

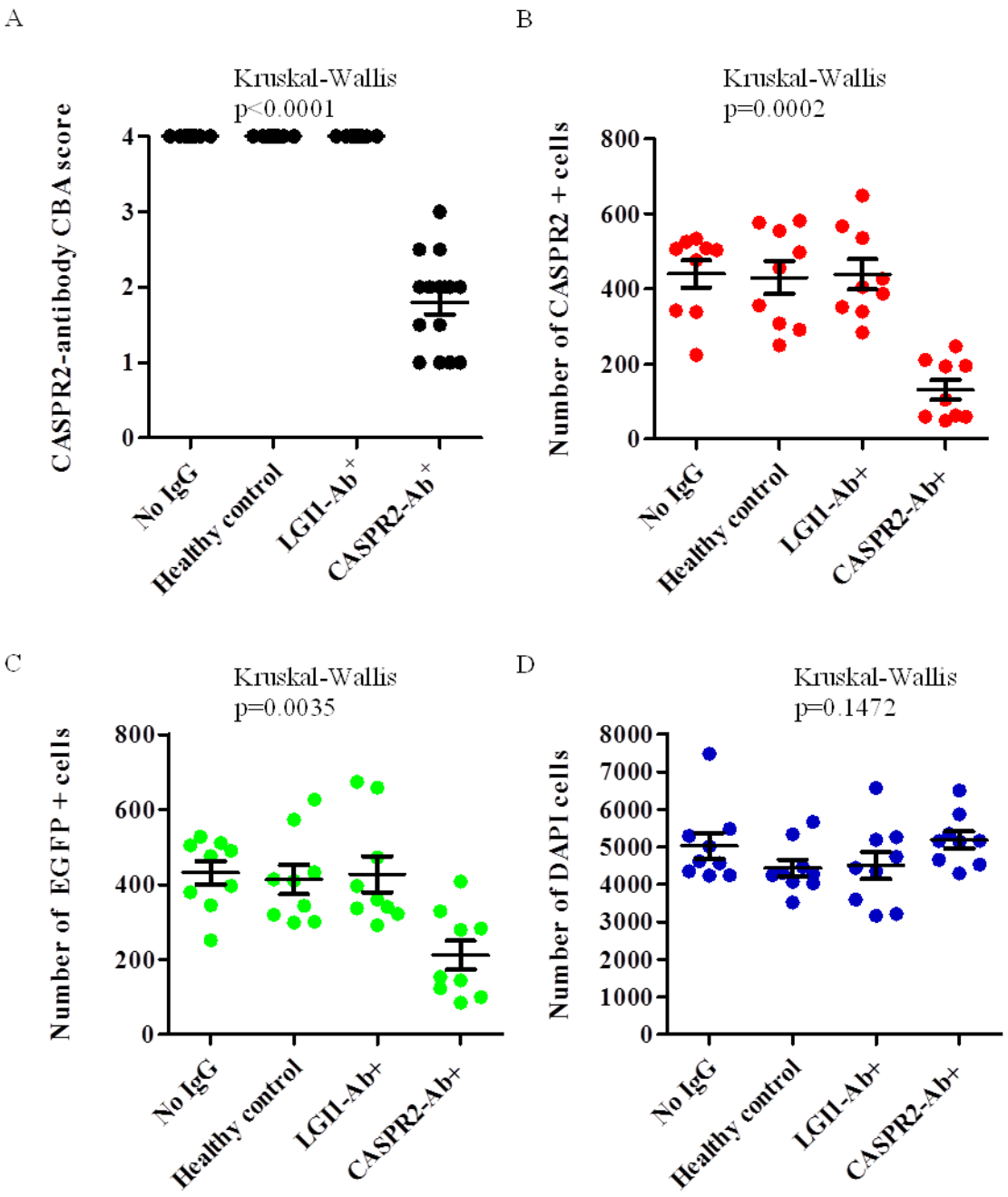

Figure 5-7 CASPR2-IgG reduces the number of CASPR2 positive cells.

24 hour incubation of CASPR2-transfected cells incubated with medium (no IgG), healthy control IgG, LGI1- IgG or CASPR2- IgG. Cells were subsequently stained for surface expression of CASPR2 using a commercial antibody. A) The number of CASPR2-positive cells was reduced by semi-quantitative CBA score B) the number of CASPR2-positive cells detected with commercial CASPR2 antibody and C) the number of CASPR-EGFP positive cells. D) The number of total DAPI-positive cells was unaffected.

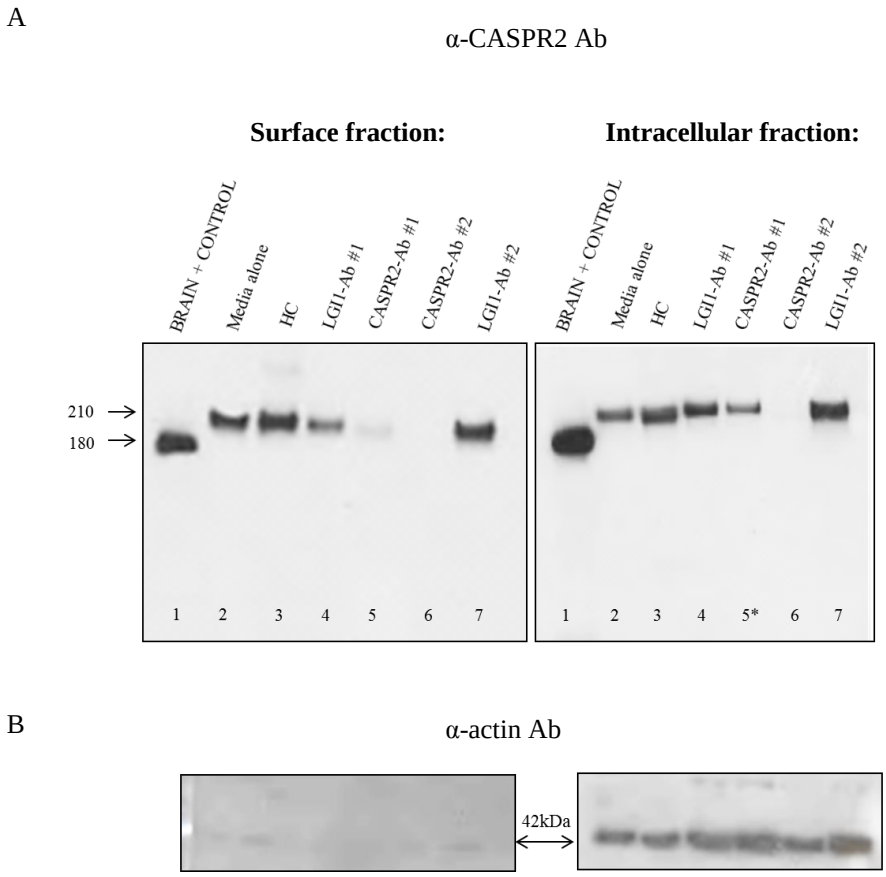

Figure 5-8 CASPR2-IgG reduces the expression of CASPR2.

Equal quantities of protein from the surface or intracellular fraction were loaded of CASPR2 cells incubated with media, control, LGI1 or CASPR2- IgG. A) Mouse brain (lane 1) was loaded for a positive control, and CASPR2 is detected at ~180kDa. CASPR2-EGFP from transfected cells has a molecular weight of ~210kDa. Cells incubated with CASPR2- IgG (lanes 5 and 6) show much lower levels of surface CASPR2 expression. CASPR2-IgG (lane 6) significantly reduced intracellular CASPR2 levels, whilst lane 5 was only slightly reduced. B) Probing the surface fraction with an actin antibody showed faint bands in all samples, actin bands were more prominent in the intracellular loading fraction.

4.9.4 Internalisation of CASPR2 and LGI1 in primary neuronal cultures

These results indicated that CASPR2 antibodies are able to internalise CASPR2 from the surface of transfected cells as has been shown *in vitro* for antibodies against AQP-4 (Hinson, 2007) . To study these effects in a model representing a native neuronal population, internalisation of surface antigen by CASPR2 and LGI1 patient antibodies was studied using live primary hippocampal neuronal cultures.

Optimisation experiments showed that the application of healthy control and patient sera affected the morphology and survival of the neurons but use of purified IgG from the serum samples helped to minimise these effects (data not shown). After removal of the IgG it was essential to wash the coverslips and then incubate them in 'conditioned' media that had been collected and stored from neurons of a similar age (DIV 14). Incubating hippocampal neurons with fresh cultured media (no IgG present) affected the viability of the neurons, which showed fewer networks of neurons with shortened dendrites, Figure 5-9.

IgG purified from patients with CASPR2-Abs (n=3) and LGI1-Abs (n=2) were applied to hippocampal cultures at DIV 14 for one hour at 37˚C (1:100), before washing in conditioned media. IgG binding to the surface of live neurons was assessed immediately or 24 hours after the application of IgG. Cells were subsequently fixed and stained for MAP2. Immunostaining was quantitated using Metamorph imaging software, the integrated intensity of IgG and MAP2 were calculated separately. The number of IgG puncta was calculated with Image J software.

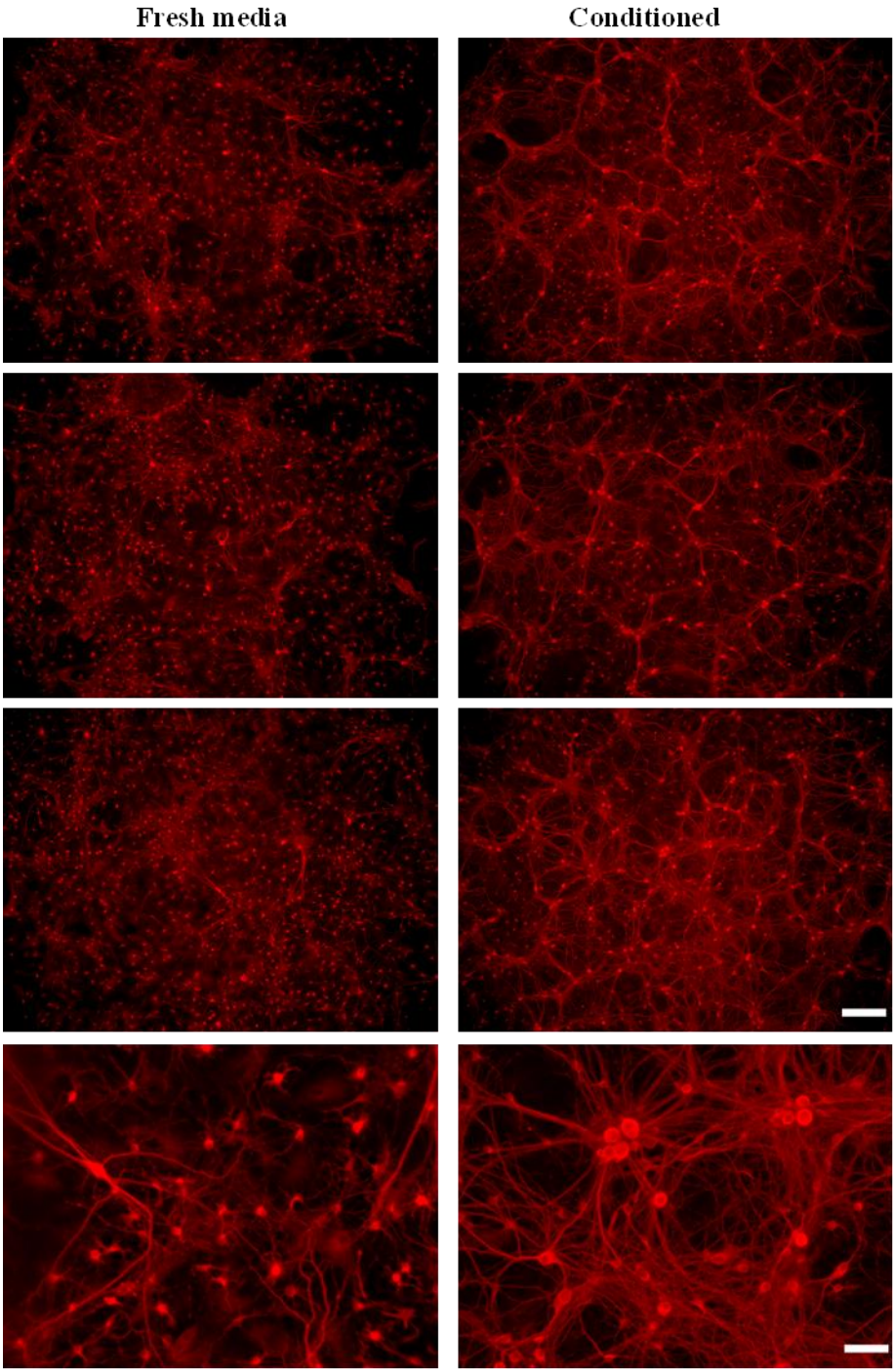

Figure 5-9 Conditional neurobasal media maintains the integrity of the hippocampal neurons.

Primary hippocampal neurons (Div 14) were incubated in fresh neurobasal media or conditioned neurobasal media overnight before being immunostained for MAP-2, a neuronal marker (red). Neurons replaced with fresh media (left) show decreased dendritic branching compared to cells incubated with conditioned media (right). Magnification 100x and 400x (bottom), scale bar 100µm.

CASPR2-antibodies

CASPR2-Abs bound strongly to the surface of hippocampal neurons at 0 hours, which was visibly reduced 24 hours later, Figure 5-10. Analysis of the integrated intensity for surface IgG binding was significantly reduced in all three patient sera studied at 24 hours (patient 1, 2 and 3, all $p < 0.001$, unpaired t-test). The integrated intensity for MAP2 was significantly reduced at 24 hours for two of three sera (patient 1 $p=0.02$, patient 2 $p=0.0696$ patient 3 $p=0.0003$, unpaired t-test, Figure 5-11a). To determine whether the decrease in surface IgG binding at 24 hours was due to fewer neurons on the coverslips, the fraction of IgG to MAP2 was calculated at both 0 and 24 hours, Figure 5-11b). There was a significant reduction in the IgG/MAP2 ratio for patient 1 ($p= 0.0001$, unpaired t-test) and patient 2 ($p < 0.0001$, unpaired t-test), but not for patient three ($p=0.0990$, unpaired t-test). To further quantify these effects, the number of IgG puncta observed per field was quantified using Image J analysis. The numbers of puncta were divided by the area of MAP2-positivity in the given field and showed a significant reduction in the number of IgG puncta at 24 hours compared for each of the patient sera examined ($p<0.0001$, unpaired t-test all samples), Figure 5-11c.

LGI1-antibodies

The above experiments were also performed with LGI1-IgG preparations. LGI1-Abs bound strongly to the surface of hippocampal neurons at 0 hours, and a reduced IgG signal was observed 24 hours later, Figure 5-12. Analysis of IgG binding showed a significant reduction in the IgG integrated intensity at 24 hours compared to 0 hours with both patient IgGs (both $p<0.0001$)) as well as the number of IgG puncta counted (both $p<0.0001$), Figure 5-13a. As there was no difference seen in MAP2 integrated intensity at 0 and 24 hours (patient 1 $p=0.4625$, patient 2 $p= 0.8426$), the IgG/MAP2 percentage was not calculated. The number of IgG puncta that were counted was significantly lower in both patients ($p<0.0001$), Figure 5-13b.

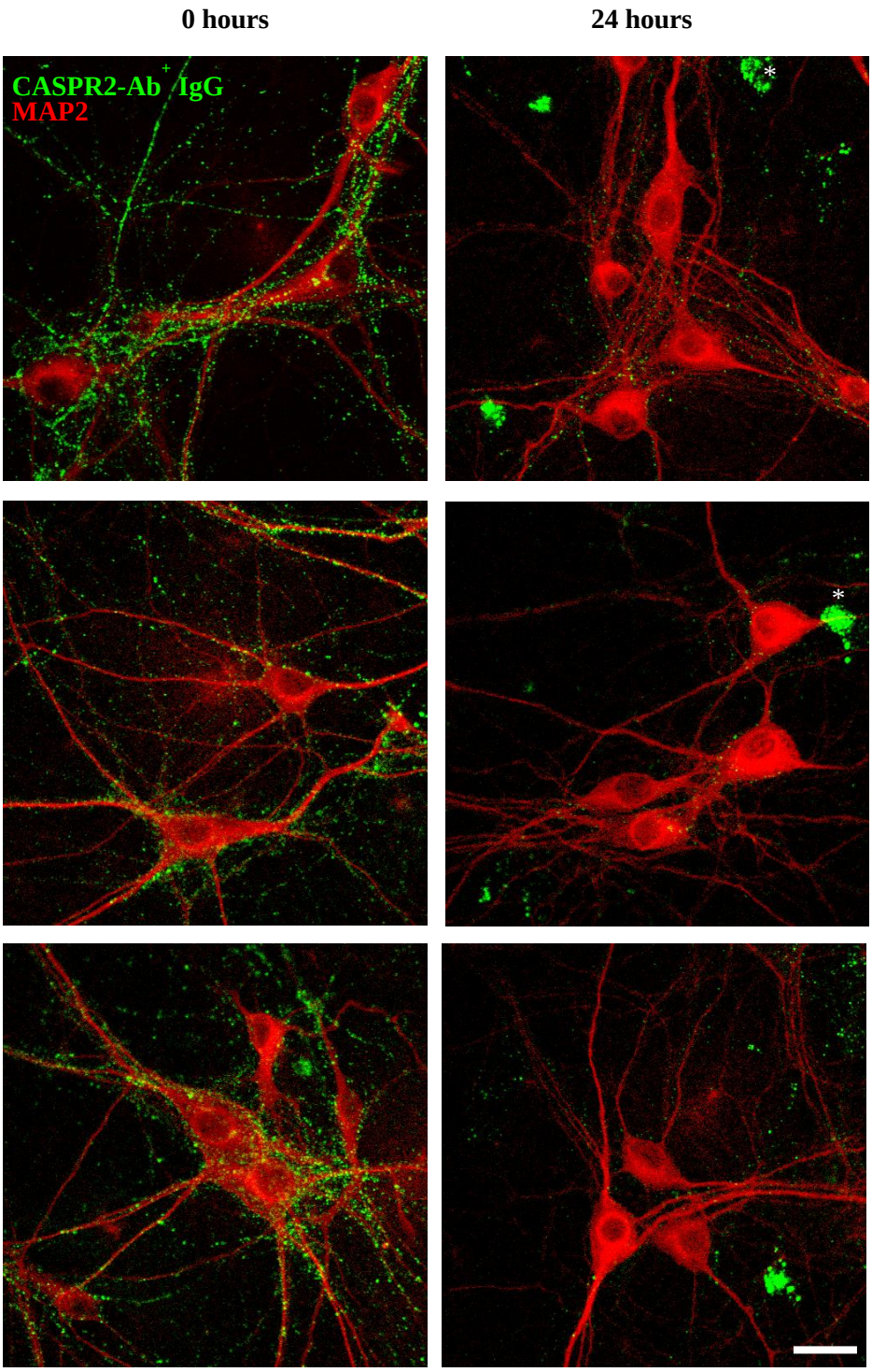

Figure 5-10 Surface IgG binding to hippocampal neurons at 0 and 24 hours after the application of CASPR2- IgG.

*Hippocampal neurons (Div 14) were incubated with CASPR2-IgG and specific binding was visualised using an anti-human antibody (green). Cells were subsequently fixed, permeabilised and stained for neuronal marker, MAP2 (red). Patient IgG strongly binds to the surface of neurons at 0 hours (left column), binding of IgG is reduced 24 hours later (right column). *Non specific stain. Magnification 400x, scale bar = 75 μm.*

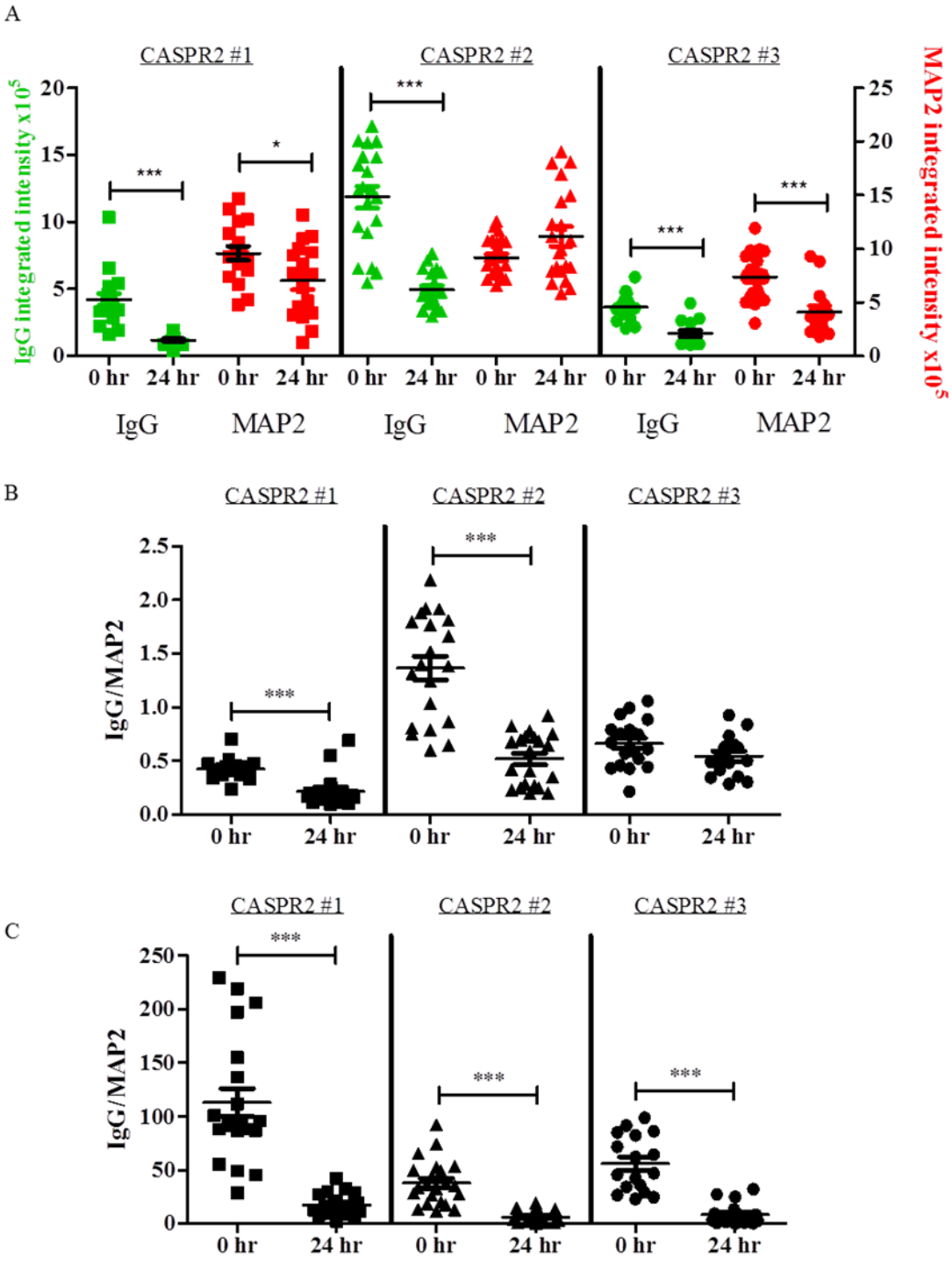

Figure 5-11 IgG surface binding and MAP-2 is reduced 24 hours after incubation of hippocampal neurons with CAPR2-IgG.

The amount of patient IgG binding and amount of MAP-2 quantified using Metamorph imaging software. Where both values were affected, they were expressed as a ratio. Total number of IgG puncta was counted. A) IgG surface binding and the number of neurons (MAP-2) were reduced after 24 hours in all patients tested. B) The IgG/MAP2 ratio showed a significant reduction in patients 1 & 2 but no overall effect was seen in patient 3 (p=0.0990, unpaired t-test). C) The number of IgG puncta when compared to MAP2 were reduced in all three patients analysed.

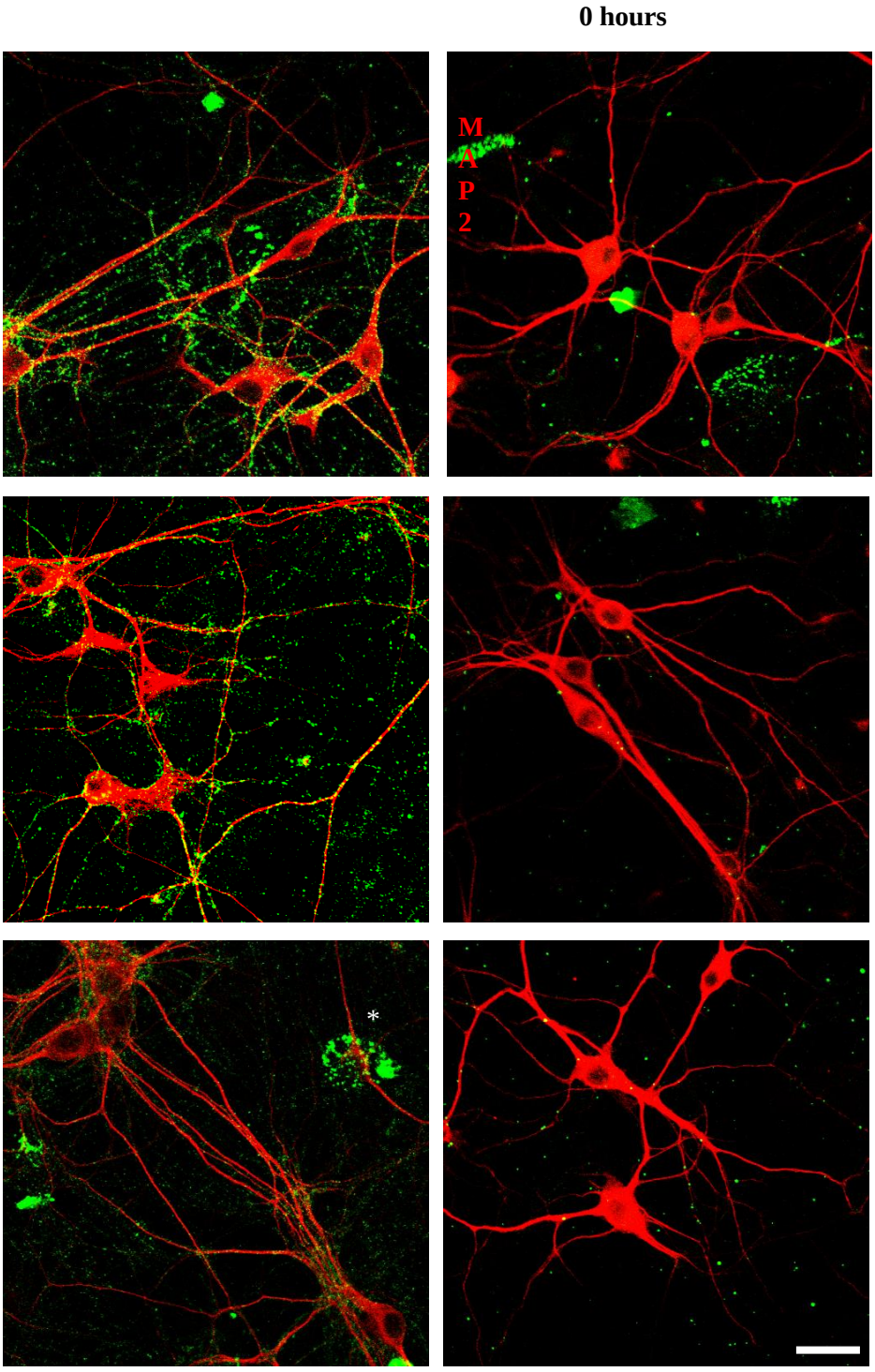

Figure 5-12 Surface IgG binding to hippocampal neurons at 0 and 24 hours after the application of LGI1- IgG.

*Hippocampal neurons (Div 14) were incubated with LGI1 IgG, specific binding was visualised using an anti-human antibody (green). Cells were subsequently fixed, permeabilised and stained for neuronal marker, MAP2 (red). Patient IgG strongly binds to the surface of neurons at 0 hours (left column), binding of IgG is reduced 24 hours later (right column). *Non specific stain*
Magnification 400x, scale bar = 75µm.

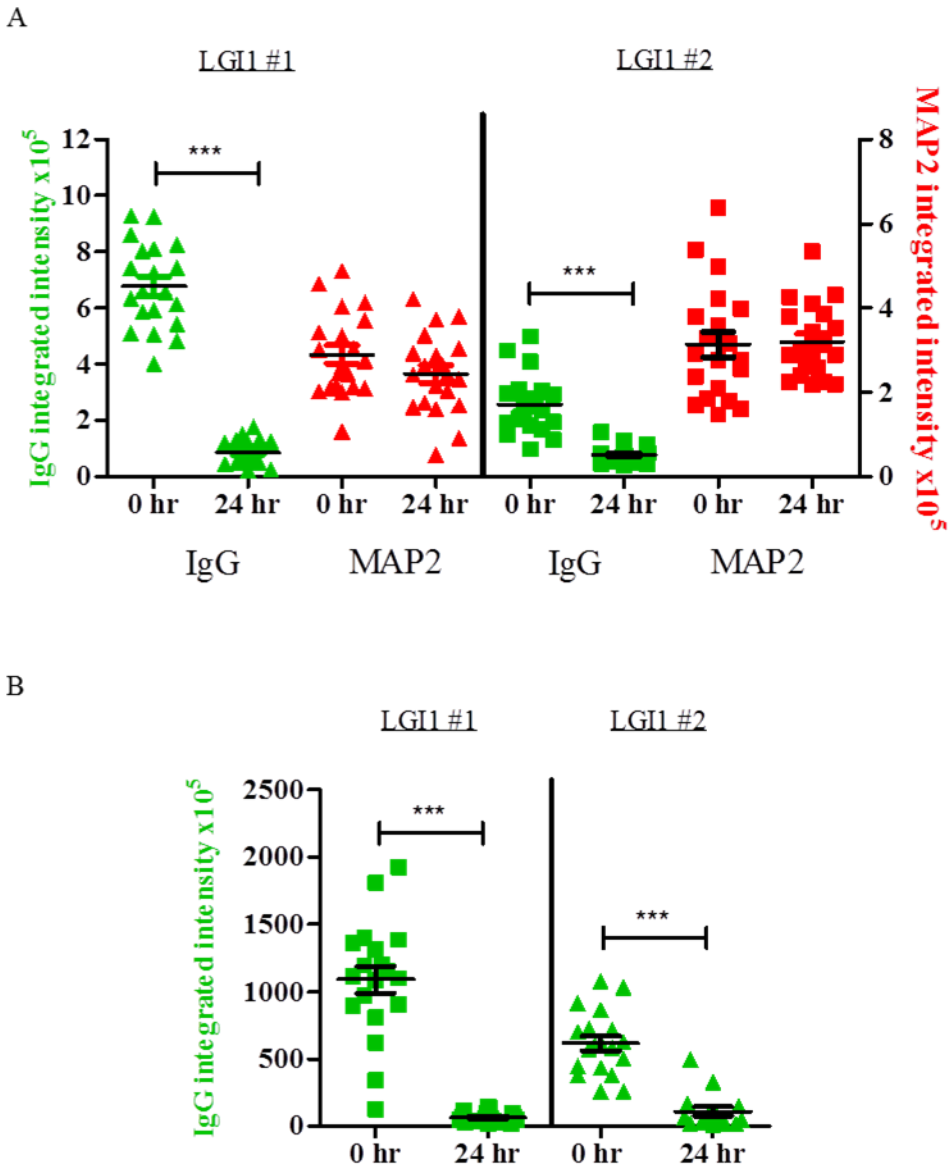

Figure 5-13 IgG surface binding and MAP-2 is reduced 24 hours after incubation of hippocampal neurons with LGI1-IgG.

The amount of patient IgG binding and amount of MAP-2 quantified using intensity analysis. Total number of IgG was counted. A) IgG surface binding was reduced at 24 hours compared to 0 hours in both patients ($p<0.0001$ for both, unpaired t-test), with no effect on MAP-2 intensity ($p=0.4625$ and $p=0.8472$, unpaired t-test). B) The number of IgG puncta were reduced at 24 hours for patient #1 and patient #2 ($p<0.0001$, unpaired t-test both).

4.10 Discussion

4.10.1 VGKC-complex antibodies are predominantly IgG1 and IgG4

VGKC-complex antibodies in CNS disorders were found to be predominantly IgG1 and IgG4. In some CASPR2 sera, IgG2 and IgG3 subclasses were also observed. IgG4 antibodies were found in all patients with LGI1-Abs. Fourteen patients (56%) with IgG1 antibodies deposited early components of the complement cascade on the surface of transfected HEK cells. This finding was independent of clinical phenotype but was dependent on antibody titer, illustrating a possible lack of sensitivity in this assay compared with conventional immunofluorescence techniques. Sensitivity for the detection of complement is difficult due to the short half-life of C3b in plasma being in the millisecond range (Pangburn, 2000). Complement detection sensitivity could be improved by increasing the incubation time with the source of human complement, increasing the concentration of the fresh complement or alternatively by blocking complement regulators that are endogenously expressed in HEK cells. In myasthenia gravis, low-affinity AChR antibodies only activated the complement cascade in the presence of blocking antibodies to complement regulators CD55 and CD59 (Jacob, 2012; Leite, 2008) and this manoeuvre may allow the detection of complement deposition in the remaining 11 VGKC-complex antibody patients tested with lower IgG1 antibodies.

4.10.2 VGKC-complex antibodies: Complement activation

The only previous work investigating the role of complement in VGKC-complex antibody positive disease *in vitro* was studied in patients with neuromyotonia. The authors found that incubation of NB-1 cells with patient IgG for three days suppressed potassium currents by antigen crosslinking which was independent of added complement (Tomimitsu, 2004). Two of five patients with neuromyotonia and CASPR2-antibodies also deposited C3b on HEK cells expressing CASPR2 (data not shown), which is consistent with complement deposition found in 50 % of sera with a CNS disorder tested in this thesis.

In a paper published this year, Bien *et al* were the first people to look at complement deposition in brain biopsy and autopsy material from patients with VGKC-complex antibodies. They showed IgG

and complement (MAC) deposition on the surface of hippocampal and cortical neurons in three of four patients studied (Bien, 2012). All patients had a diagnosis of LE however due to serum availability the antigenic target was only identified in one patient, as LGI1. In the only autopsy case (VGKC antibody titer 958pM, antigen status not determined), neuronal loss was observed in the CA4 region and dentate gyrus of the hippocampus confirming previous histological findings in these patients (Dunstan & Winer 2006; Khan, 2009; Park, 2007). Long term residual cognitive deficits associated with hippocampal atrophy have been reported in some patients, which might be a result of complement activation in these patients (Bien, 2012; Vincent, 2004). However the reversibility of the disease in the majority of cases suggests that in fact, complement mediated tissue destruction may not play a significant role in the pathophysiology of these patients, despite complement activation observed *in vitro*. The importance of complement in the pathogenesis of neuromyelitis optica has been demonstrated *in vivo*. In mice, the addition of human complement alongside AQP-4 IgG is required to reproduce the characteristic NMO lesion with complement deposition, neuroinflammation and loss of AQP4 and GFAP immunoreactivity (Saadoun, 2010; Lucchinetti, 2002). In contrast, NMDAR antibodies have been shown to fix complement in transfected HEK cells and on hippocampal neurons, yet this has not been observed in patient brains at autopsy (Irani, 2010b; Martinez-Hernandez, 2011). Future studies, investigating the effect of VGKC-complex antibodies *in vivo*, both in the presence and absence of complement are required.

4.10.3 VGKC-complex antibodies: Internalisation

Another pathogenic mechanism associated with autoimmune diseases is crosslinking of the antigen and subsequent internalisation of the antigen-antibody complex. There have been no publications in the literature reporting the effects of internalisation by VGKC-complex antibodies in CNS disorders, although this has been shown for patients with VGKC-antibodies and neuromyotonia (Tomimitsu, 2004). In this thesis, surface binding of patient IgG to CASPR2-transfected cells showed a reduction in IgG signal over time. This loss of IgG was not due to dissociation of the IgG from the CASPR2 molecule as chronic incubation with patient IgG reduced the amount of CASPR2 expressed at the cell surface as well as in the intracellular fraction. This is likely to represent intracellular degradation of

the CASPR2-IgG complex, which has previously been shown *in vitro* for AQP-4 antibodies and could be examined further with co-staining of IgG with lysosomal or early endosomal markers (Ratelade, 2011, Hinson, 2007) .

Internalisation of CASPR2 and LGI1-antibodies was also studied in primary neuronal cultures as a more native and physiological model. Dalmau *et al* previously showed that NMDAR-antibodies in patient CSF co-localised with the majority of surface NR1. Neurons incubated with NMDAR-IgG for three to seven days had reduced NR1 surface expression defined as the co-localisation of patient IgG with commercial antibody staining (Dalmau, 2008). As commercial antibodies for CASPR2 and LGI1, did not bind to the surface of neuronal cultures despite binding to transfected HEK cells, similar co-localisation studies were not possible (data not shown). The lack of binding of commercial antibodies to neuronal cultures may be explained by the lower endogenous expression of these proteins compared to transiently transfect HEK cells. Antibody cross-reaction with rat tissue is claimed by the manufacturer but was not investigated within these experiments. Instead, patient antibody binding was used as a measure of surface protein expression. Using this measure, a reduction of IgG bound to the surface of neurons after 24 hours of incubation with patient IgGs was observed for CASPR2 and LGI1 antibodies and is likely to reflect antigen internalisation. An alternative explanation may be that patient antibodies dissociate from the antigenic target resulting in reduced IgG binding over time, although this seems unlikely as chronic incubation with CASPR2-IgG reduces surface expression in HEK cells.

In summary, these experiments support internalisation as a potential pathogenic mechanism of disease. Future experiments, confirming the loss of CASPR2 and LGI1 in membrane fractions prepared from neuronal cultures will strengthen the hypothesis of antibody mediated internalisation. The final proof of principle for antibody internalisation by antigen-crosslinking was demonstrated in myasthenia, and requires IgG or divalent $F(ab')_2$ fragments, but not monovalent Fabs (Drachman, 1978).Ultimately, confirmation of a specific loss of CASPR2 or LGI1 in the patient brains from autopsy and findings mimicking this scenario *in vivo* are required to satisfy protein internalisation as a pathogenic mechanism in disease pathology.

4.10.4 VGKC-complex IgG4-antibodies are monovalent

CASPR2 and LGI1 antibodies have a large IgG4-representation. Structurally, IgG4 molecules lack inter-heavy chain disulphide bonds and have been reported to switch one heavy and one light chain, generating a monovalent molecule. This mechanism is reported to result in the formation of recombinant, asymmetric IgG4 molecules comprising of two different antigen binding specificities, which has been reported to be unable to cross-link and thus immuno-precipitate antigen (Zee & Swieten 1986). In contrast, VGKC-complex antibodies, including 3/3 patients with only LGI1-IgG4 antibodies described in this thesis, did precipitate antigen in the VGKC-RIA. Further evidence from work in section 4.3.3, showed preadsorption of four Morvan's sera with multiple antibody specificities (CASPR2 and LGI1) against LGI1 transfected cells abolished immunoreactivity to the LGI1 assay but did not affect antibody binding to the CASPR2 assay, and vice versa, strongly indicating that these antibodies are not bi-specific and are thus capable of cross-linking antigen.

4.10.5 Pathogenic mechanisms of the CASPR2 and LGI1 antibodies

How might the internalisation of CASPR2 and LGI1 mediate the clinical phenotype? CASPR2 antibodies have been reported in 64% of patients with NMT (64 %) and 78% of patients MoS, in which NMT features. As peripheral nerve conduction is unaffected in CASPR2 knockout mice (Poliak, 2003), it is unlikely that internalisation of CASPR2 alone is sufficient to cause the peripheral nerve hyperexcitability. It is possible that CASPR2 co-internalises with associating proteins of the VGKC-complex, or indeed the juxtaparanodal potassium channels themselves. CASPR2 is expressed abundantly in large myelinated axons of the peripheral and central nervous system and is 0.5-10% of CASPR2 is reported to associate with potassium channels, although immunoprecipitation of CASPR2 from rabbit brain extract suggest this finding may be higher, around 40% (Poliak, 1999; Irani, 2010). Knowledge of the precise proportion of CASPR2 or LGI1 co-expressed with Kv1 channels in the PNS and CNS will be important for understanding the contribution of Kv1 dysfunction in antibody-mediated disease. Interingestly, point mutations in the Kv1.1 subunit are known to produce neuromyotonia in humans ((Browne et al. 1994; Kinali, 2004), therefore the effect of antibodies may be via co-internalisation of the associated Kv1 molecules. Co-internalisation of proteins has been

previously described in NMO. Hinson *et al* showed that AQP-4 and the excitatory amino acid transporter, EAAT2, exist as a macromolecular complex in astrocyte and incubation of astrocyte cultures with AQP4-IgG reduced the surface expression of both molecules, localising them to cytoplasmic endosomal vesicles (Hinson, 2008).

Seizures and memory dysfunction are prominent features of VGKC-limbic encephalitis and the majority of these patients have antibodies against the LGI1 protein. LGI1-Abs are also found in 67 % of MoS sera, albeit with lower titers, where seizures and amnesia are less common (34.5% and 55.6% respectively; Pettingill, 2012). LGI1 knockout mice develop a lethal seizure phenotype and die postnatally around three weeks of age. Furthermore, mutations in the LGI1 gene have been reported in 50% of patients with ADLTE and prevent the secretion of LGI1, demonstrating that LGI1 is important for normal neuronal function (Ottman et al. 2008). These findings suggest that cross-linking and subsequent internalisation of LGI1 alone may be sufficient to cause the neurological dysfunction observed in these patients.

LGI1 proteins are thought to mediate protein-protein interactions through both their LRR and EAR domains (Leonardi, 2011. Although not explored in this thesis, LGI1-Abs may bind to LGI1 as it is secreted in to the synaptic cleft, preventing the interaction with presynaptic and postsynaptic interacting proteins. Alternatively antibody binding may weaken LGI1's interactions with its associated proteins, including ADAM22, ADAM23 and the Kv1 subunits. As for CASPR2, LGI1 is closely associated with Kv1 subunits in brain extract (Schulte, 2006; Irani, 2010), and it is possible that LGI1 antibodies interfere with potassium channel function, either by co-internalisation or indirectly. Indeed incubation of LGI1-IgG with rat brain slices induced epileptiform activity in the hippocampus after two hours, mimicking the effects of potassium channel blocker, α-DTX (Lalic, 2010) and reduced Kv1.1 and Kv1.2 expression was reported in LGI1 knockout mice, further implicating disruption of the potassium channels in disease pathophysiology.

In summary, preliminary investigations for the pathogenic mechanisms of VGKC-complex antibodies have shown that CASPR2 and LGI1 antibodies are predominantly IgG1 and IgG4. CASPR2 and LGI1

antibodies can deposit C3b on the surface of transfected HEK cells *in vitro* as well as decrease surface IgG binding and the expression of their target antigen, which may be indicative of antibody cross-linking. Further studies of human post mortem tissue and the effects of antibodies *in vivo* are required to validate these findings.

Section 2: Investigating the pathogenic effects of NMDAR-antibodies *in vivo*

Chapter 6: NMDAR antibody encephalitis

6.1 Introduction

Antibodies against the NMDAR were first described in 2007 in the serum and CSF of twelve women with paraneoplastic encephalitis presenting with psychiatric disturbances, memory loss, seizures, dyskinesias, dysautonomia and hypoventilation (Dalmau, 2007). Since then, *in vitro* and *in vivo* evidence suggests their pathogenicity (Hughes, 2010). This section aims to further the known pathogenic effects of NMDAR antibodies and to explore the effects of patient antibodies on mouse behaviour after injection directly in to the cerebrospinal fluid compartment.

6.1.1 The NMDA receptor

Glutamate is the predominant excitatory neurotransmitter in the CNS. It can bind and activate both ionotropic cation channels (iGluR) and metabotropic receptors (mGluR). There are three types of ionotropic glutamate receptors, classified according to their selective pharmacological agonists; α-amino-3-hydroxyl-5-methyl-4-isoxazole-propionate (AMPA), kainate and N-methyl-D-aspartate (NMDA).

Three different NMDAR subunits exist; the NR1, NR2 and NR3 subunits, now known as GluN1, GluN1 and GluN3 (Collingridge, 2009)., but for the purpose of this thesis, the old nomenclature is favoured. Each subunit consists of four discrete domains, including a large extracellular N-terminal domain (380 amino acids), which is involved in ligand-binding, a membrane domain consisting of three transmembrane domains (M1, M3, and M4), a re-entrant loop (M2) that lies between M1-3 forming the receptor pore, and an intracellular C-terminal domain. The NMDAR is a heteromeric protein complex, comprised of two NR1 subunits containing the glycine binding site and two NR2 or NR3 subunits, which confer functional heterogeneity of the receptor through alterations in channel

activation kinetics (Masu,1991; Monyer, 1992; Ulbrich, 2008). The NR1 subunit is obligatory in NMDAR complexes and facilitates the expression of NR2 or NR3 subunits to the cell surface (McIlhinney, 1996; Pérez-Otaño, 2001). The NR2 subunit expression patterns differs both temporally and regionally in the brain. In the early postnatal brain NR2B is predominantly expressed, whereas NR2A is the most abundant subunit in the adult CNS and NR2C is strongly expressed in the granule cells of the cerebellum (Y, 1992; Monyer, 1994)

6.2 NMDAR-encephalitis

In 2007, NMDAR-antibodies were reported in 12 patients with treatment responsive paraneoplastic encephalitis whose sera and CSF bound to predominantly, but not exclusively, the hippocampal neuropil in rat brain sections (Dalmau, 2007) . In 2008, the authors published a cohort of 100 patients identifying and characterising patient antibodies (Dalmau, 2008). NMDAR-antibodies were detected by binding to HEK cells that were transfected with NR1 and NR2A/B subunits of the NMDAR after the cells were fixed and permeabilised. The authors demonstrated that the antibodies were predominantly against the extracellular N-terminus, as deletion of residues 25-380 from the NR1 construct abolished antibody binding in 92/100 sera. In the supplementary data of this paper, the authors report that eight sera had immunoreactivity to cells expressing the NR2A (n=6), NR2B (n=8) or NR2C (n=4) subunits. As these studies were performed on permeabilised cells, it is not known if these antibodies bind to intracellular or extracellular epitopes of the NR2 subunits. If the antibodies bind to intracellular epitopes that are inaccessible to circulating antibodies, then they are unlikely to be pathogenic, and may instead be markers of cell damage. Subsequent studies from the Oxford Neuroscience laboratory confirmed that sera from 44 patients bound to the surface of live, unpermeablised HEK cells transfected with NR1 and NR2B subunits, and to NR1 subunits expressed on their own (Irani, 2010b).

6.2.1 Clinical characteristics of NMDAR-antibody encephalitis

Patients presented initially with neuropsychiatric disturbance (including anxiety, agitation, hallucinations, memory loss, dysphasia, delusions, paranoia, disinhibiton, hyperphagia, and social

withdrawal), and seizures, which progress to a reduction in consciousness, the development of a mood movement disorder (dyskinesias, choreoathetoid and abnormal posturing) and autonomic dysfunction (Dalmau, 2008; Irani, 2010b). Irani *et al* identified that the time lag of approximately 10-20 days between the onset of early features (cognitive, psychiatric, seizure syndromes) coincides with CSF lymphocytic pleocytosis, and the later features (movement disorder, fall in consciousness, dysautonomia) correlated broadly with the development of oligoclonal bands (Irani, 2010b). A high proportion of patients have a prodromal episode including headaches and fever before the onset of features; however no common causative infectious factor has been identified. These findings may suggest that the immune response is initiated in the periphery and subsequently developed in the CNS. Patients with NMDAR-antibodies were initially reported as being predominantly young women, frequently associated with an ovarian teratoma, however the disorder is becoming increasingly recognised in men, women and children, with and without the presence of a tumour (Florance, 2009; Irani, 2010b). Since the early reports, NMDAR antibodies have been described in a spectrum of neurological disorders under the umbrella of the presenting symptoms including 5/19 unexplained new-onset epilepsy patients (Niehusman, 2009), 10/20 patients with encephalitis lethargica (Dale, 2009) and in 3/46 patients with first episode schizophrenia (Zandi et al. 2011).

6.2.2 Serum antibodies and response to immunotherapy

Multiple reports have highlighted the favourable prognosis with early immunomodulatory intervention and early removal of the tumour, where relevant. In the majority of patients who show clinical improvement, NMDAR-antibody titers in the serum become low or absent, which correlates with a fall in mRS (Dalmau, 2008). The majority of patients show intrathecal synthesis of NMDAR antibodies, determined by antibody presence in the CSF, although the absolute serum levels are almost always higher in the serum (Dalmau, 2008; Irani, 2010b). Due to the invasive procedure of collecting CSF, follow up CSF samples are normally not obtained. Dalmau *et al* showed that serum and CSF antibodies remain high in four patients who did not show clinical improvement with immunotherapy. Furthermore one patient with a protracted clinical presentation had detectable

NMDAR-antibodies only in the CSF and not the serum (Dalmau, 2011), but this has been only very rarely in seen the experience of the Oxford diagnostic assay laboratory.

6.2.3 Neuropathology of NMDAR-antibody encephalitis

Neuropathological investigations found mature ovarian teratomas, associated with young (>18 years old) female patients of non-Caucasian origin. Twenty-five teratomas studied (100%) contained neuronal tissue expressing the NMDAR (NR1/NR2A/NR2B) subunits (Dalmau, 2008). However pathological studies in NMDAR-antibody mediated disease are limited. Tüzun *et al* reported two patients that died 3 and 4 months after symptom presentation, at autopsy mature teratomas were found and in both cases IgG deposition, reactive gliosis and microglial activation were observed in the hippocampus, forebrain, basal ganglia and the spinal cord(Tüzün, 2009; Dalmau, 2007). One of the patients had significant atrophy of the hippocampus and temporal lobes, and specifically a loss of pyramidal neurons was observed in the hippocampus. The second patient showed no significant atrophy but mild neuronal loss was observed in the basal ganglia. Inflammatory infiltrates were uncommon but antibody secreting plasma cells were seen in the perivascular spaces. Patient antibodies are predominantly IgG1 and fix complement *in vitro* (Tüzün, 2009; Irani, 2010b), however complement deposition was not observed in the frontal or temporal lobes of three patients on post mortem and three frontal lobe biopsies (Martinez-Hernandez, 2011; Camdessanché, 2011; Bien, 2012). A reduction of NR1 expression was observed in the hippocampus of two patients studied, by quantifying the intensity of commercial NR1-antibody binding by immunohistochemistry (Hughes, 2010) .

6.3 Evidence for pathogenicity of NMDAR-antibodies

6.3.1 Effects of NMDAR antibodies *in vitro*

Dalmau *et al* were the first to study the effects of patient antibodies on hippocampal primary cultures. They showed that application of patient CSF (20 μl of CSF/day (1:15)) for 1, 3 or 7 days reduced the expression of surface NMDARs, and this effect was titer dependent. Furthermore this effect was reversed four days after the removal of patient CSF (Dalmau, 2007). In another study by Mikasova *et a*l,

incubation of patient CSF (1:300) with hippocampal neurons transfected with NR2A-SEP and NR2B-SEP, SEP being a pH-sensitive eGFP molecule at its N-terminus, reduced the fluorescent signal after both 2 and 20 hours (19 and 50% reduction, respectively), indicating that the whole heterotetameric receptor is affected by NMDAR antibodies (Mikasova, 2012). As originally demonstrated for AChR-antibodies in myasthenia gravis, internalisation of the NMDAR was mediated by cross-linking of IgG molecules and divalent Fab-fragments which was not observed after NMDAR-antibodies were cleaved into monovalent Fab fragments (Hughes, 2010). Furthermore whole cell-patch clamp recordings with hippocampal pyramidal cells showed a decrease in NMDAR-mediated currents after incubation with patient CSF for 24 hours, which is in accordance with the reduced NMDAR levels observed after internalisation. Patient IgG did not alter the morphology of the synapse, $GABA_A\alpha1R$, $GABA_A\alpha2R$ and AMPAR (GluR2/3) expression or AMPAR-mediated currents. In contrast, NMDAR-IgA antibodies have recently been described in patients with cognitive decline. IgA antibodies reduced NMDAR expression and currents, but also reduced synaptic markers, synaptophysin and synapsin, illustrating potentially that the immunoglobulin isotypes may have subtle differences in their pathogenic mechanisms (Prüss et al. 2012).

Four studies have investigated the short term effects of NMDAR-IgG *in vitro*, but none examined the effect on effects of NMDAR expression. The first three studies showed a reduction in NMDAR function. Firstly, a one hour incubation of cerebellar granule cell neurons with CSF (1:10) from a patient with isolated hemidystonia suppressed NMDAR-dependent calcium influx (Rubio-Agustí, 2011). A second study, incubating mice brain slices with CSF (up to 1:30) from three patients suppressed long term potentiation (LTP), a form of neuroplasticity, in Schaffer collateral CA1 synapses of mouse hippocampal slices after five minutes. This effect was significantly reduced after preadsorption of NMDAR-antibodies out of the CSF, and was not seen with CSF from patients with herpes simplex virus or non-encephalitis controls (Zhang, 2012). Finally, Thouin *et al* reported that acute incubation of patient IgG (n=3, dilution and duration not reported) reduced NMDAR-synaptic function in rat brain slices and reduced γ-oscillations in the entorhinal cortex, with no effect seen in the CA3 region of the hippocampus (Thouin, 2012). In contrast, acute incubation of NR1/NR2B transfected HEK cells with three patient CSF IgGs (1:100) and agonist (2 mM glutamate, 1 μM glycine) for seven minutes, prolonged the opening duration

of the channel (Gleichman, 2012). As none of these studies investigated the effect on NMDAR surface expression, the mechanism of this antibody action is not certain. It is possible given the speed of the effects, that these may represent a direct effect of antibody on channel function.

6.3.2 Effects of NMDAR-antibodies *in vivo*

The effects on NMDAR-antibodies *in vivo* have been described in four studies, which are summarised in Table 6-1. The seminal study by Hughes *et al* investigated the effects of patient CSF (n=5) chronically infused (at a rate of 0.5 µl/hour) into the hippocampus of Wistar rats for 14 days. Western blot and immunohistochemical analysis of the infused hippocampi showed a titer-dependent reduction in NR1 expression, confirming the reduced hippocampal NR1 expression in two autopsy samples. Consistent with the neuropathology findings, no significant cell death was observed and NR1 expression was unaffected in the contralateral, uninjected hippocampus (Hughes, 2010). Intense immunolabelling of patient IgG was observed in the infused hippocampi and IgG deposits were reported in areas of reduced NMDAR clusters. These findings were confirmed in a second study by Mikasova *et al*, who injected patient IgG (n=1, 0.4 µl) in to the CA1 region of the hippocampus of FVB mice, and showed approximately 20% reduction five to seven hours later (Mikasova, 2012).

In another study, 5 µl CSF from patients with NMDAR-antibodies (n=5) was infused (1 µl/min) in to the prefrontal area (rFr2) of rats and the effect on afferent facilitation of corticomotor responses in the forelimbs and hind limbs were assessed. The authors showed patient CSF increased the excitability of the motor cortex, and a similar effect was also observed with purified patient IgG (Manto, 2011). The authors hypothesised that this mechanism may explain some of the clinical presentations of the disease including agitation, anxiety and seizures. The same authors also injected NMDAR-antibodies into the CA1 of the hippocampus and demonstrated infusion of patient CSF (5 µl) caused a dose-dependent increase in extracellular glutamate levels which led to glutamate dysregulation. These effects were measured 30-75 minutes after intracerebral delivery of NMDAR-antibodies and the authors did not confirm whether these effects were mediated by receptor internalisation or mediated by an antagonistic effect of the antibodies (Manto, 2010).

Reference	Species (strain)	Weight (g)	Patient CSF/ IgG	Injection location	Total volume (µl)	Dosing	Time to sacrifice	Effect on NMDAR expression	Functional effects
Hughes 2010	Rat (Lewis)	126-150*	CSF	Hippocampus	168	0.5µl/hour for 2 weeks	Immediate	Reduced in the hippocampus	Not studied
Manto 2010	Rat (Wistar)	240-430	CSF/IgG	Prefrontal area/ hippocampus	5	Single (1 µ/min)	Nd	Not studied	Increased extracellular glutamate Imbalance of NMDA/AMPA Increase NO
Manto 2011	Rat (Wistar)	240-430	CSF/IgG	Prefrontal area	5	Single (1 µ/min)	Nd	Not studied	Increased excitability of motor cortex
Mikasova 2012	Mouse (FVB)	20	CSF/IgG	Hippocampus	0.4	Single	5-7 hours	Reduced in the hippocampus. No change in striatum	Disrupt of NMDAR's interaction with Ephrin-B2 receptor

Table 6-1 Overview of in vivo experiments using NMDAR-autoantibodies

6.4 NMDA receptor hypofunction

6.4.1 Pharmacological manipulation of the NMDAR

NMDA receptors have been implicated in both neurological and psychiatric disorders, including chronic pain, Huntington's disease, Alzheimer's disease and schizophrenia (for a review see (Waxman & Lynch 2005)). The hypothesis of NMDAR hypofunction in schizophrenia is based upon studies with NMDAR antagonists, ketamine and phencyclidine (PCP), which induced the positive (e.g delusions, hallucinations), negative (e.g deficits in social interaction and reduced mood) and cognitive deficits of schizophrenia in healthy individuals (Krystal, 1994; Luby, 1959; DC & Zukin, 1991). In rats, PCP (7 mg/kg) induced hyperactivity and stereotypy, whereas anaesthetic doses of ketamine (100 mg/kg) induced oral-tongue dyskinesias (Haggerty, 1984; Aides, 1988). As many of the clinical features of NMDAR-antibody encephalitis have been compared to those of NMDAR antagonism and schizophrenia (Dalmau, 2011), the behavioural outcomes of mice with reduced NMDAR expression generated as a model of schizophrenia will be discussed in further detail.

6.4.2 Genetic manipulation of the NMDAR

Complete ablation of functional NMDAR's in mice resulted in early death, 8-15 hours after birth due to respiratory failure (Forrest, 1994). However, Mohn *et al* produced a mouse that expressed 5-10% of the normal NR1 protein, termed NR1-hypomorph mice, with normal life spans (Mohn, 1999). These mice were hyperactive, displayed stereotypical behaviours and showed deficits in social interaction that were comparable to wild type mice treated with NMDAR antagonists, 3 mg/kg PCP or 0.2 mg/kg MK-801 (Duncan , 2004; Duncan, 2006; Fradley, 2005). Mice also showed deficits in sensorimotor gating on the pre-pulse inhibition acoustic startle test which is comparable to deficits seen in schizophrenia. Cognitive deficits were observed on the spontaneous alternation T-maze task (see Tests of cognition), the spatial Y-maze as well as displaying an increased seizure susceptibility to kainic acid compared to litter mate controls (Barkus, 2012; Duncan, 2010).

One current hypothesis underlying the pathogenesis of NMDAR-Ab encephalitis is a reversible glutamate hypofunction, predominantly effecting NMDA receptors on GABAergic inhibitory interneurons (Moscato, 2010), although no experiments have specifically dissected out the neuronal populations that patient antibodies bind to nor studied the direct effects on inhibitory neurons. However the restricted deletion of NMDAR subunits in 50% of cortical GABAergic interneurons alone is sufficient to reproduces the schizophrenia endophenotypes seen in NR1 hypomorph mice (Belforte, 2009).

6.5 Glutamate receptor antibodies in other neurological disorders

6.5.1 Rasmussen's encephalitis

Other antibodies against glutamate receptors have also been reported in neurological disorders. Antibodies against the GluR3 subunit of the AMPAR were first reported in Rasmussen's encephalitis (RE) (Rogers, 1994) and later focal epilepsy (Wiendl, 2001), although later studies did not confirm these findings (Watson, 2004). Rabbits immunised with GluR3 peptides developed seizures and histopathological changes reminiscent of Rasmussen's, however the pathogenic potential of GluR3 antibodies is patient sera is controversial. One study demonstrated that patient sera evoked kainite-responsive GluR3-mediated currents in mouse cortical neurons that were inhibited by CNQX, suggestive of a direct effect on channel function (Twyman, 1995; Levite, 1999), however subsequent studies could not replicate these findings in cultured neurons or oocyte transfected with the GLuR3 subunit (Frassoni, 2001, Watson, 2004).

6.5.2 Limbic encephalitis, Ophelia's syndrome and cerebellar ataxia

Antibodies to GluR1 and GluR2 subunits of the AMPA receptor have recently been described in a form of limbic encephalitis commonly associated with tumours of the breast, lung and thymus (Lai, 2009). Like NMDAR-antibodies, tumours in these patients also express the antigenic targets, in this case GluR1/2 subunits. Patients respond well to immunotherapy, but have a propensity to relapse (Graus, 2010). Antibodies have also been infrequently found against the metabotropic glutamate receptors, mGluR1 and mGluR5 in cerebellar ataxia and Ophelia's syndrome respectively (Smitt,

2000; Marignier, 2010; Lancaster 2011c). These antibodies also bound extracellular epitopes of proteins measured by binding to cell based assays and primary neuronal cultures. The pathogenicity of all these antibodies is suggested by the specificity of antibodies for the disease, a favourable response to immunotherapy and the antibody binding to extracellular determinants. Only for mGluR1 is there *in vivo* evidence of pathogenicity.

In addition, there are accumulating data of *in vitro* pathogenicity. For example, incubation of live hippocampal primary cultures for six days with AMPAR antibodies (20 μl/day (1:15)) produced a reversible reduction in the number of synaptic GluR2-containing AMPAR clusters, which is likely to be a result of receptor internalisation (Lai, 2009). Application of mGluR1 antibodies (1:1000) to mGluR1 transfected CHO cells for one hour blocked glutamate-stimulated mGluR1 formation of inositol phosphatases in a dose-dependent manner and disrupted long-term depression in cerebellar slices (Smitt, 2000). Furthermore, injection of patient purified IgG (20 μl (range IgG 10-400μg), or specific-mGluR1 antibodies only (3 μg) into the cisterna magna caused severe ataxia within 30 minutes of injection. These effects peaked between 2-4 hours and had disappeared within 24 hours. A second passive transfer model infused mGluR1 antibodies over seven days using an osmotic mini-pump (0.5 μl/ hour, 5-10 mg/ml) directly placed into the flocculus of the cerebellum (a region involved in ocular motor control) caused deficits in compensatory eye movements, which was reversed within five days of removal of the osmotic pump (Coesmans, 2003). This evidence demonstrates mGluR1 antibodies fulfil the criteria of an antibody-mediated disorder outlined in Table 2-2.

Whether all glutamate receptor antibodies have multiple effector functions, such as the receptor internalisation, complement activation and direct modulation of the receptor has not yet been determined.

6.5.3 Glutamate antibodies and antibody access to the CNS

In SLE with neuropsychiatric manifestations (NP-SLE), studies have shown anti-double stranded DNA (dsDNA) antibodies in patient sera and CSF that cross-react with a pentapeptide DWEYS, present in the extracellular domain of the NR2A and NR2B subunits (DeGiorgio, 2001). These

antibodies are detected by ELISA and Western blots techniques and are not found in patients with NMDAR-encephalitis (Dalmau, 2007). Whether ds-DNA antibodies are able to bind to conformational NR2 structures is contentious. Regardless of the antigenic target, in a more clear-cut set of experiments, peripheral injection of SLE IgG alone into mice was not pathogenic. Disruption of the blood brain barrier with lipopolysaccharide (LPS) or direct injection of patient IgG into the CNS parenchyma was required to cause excitotoxicity, neuronal death and cognitive dysfunction reminiscent of disease (DeGiorgio, 2001; Kowal, 2006; Kowal, 2004).

Other models of non-glutamate antibody mediated CNS disorders also require disruption of the blood-brain barrier to allow antibody access to the brain. Mice with experimental autoimmune encephalomyelitis (EAE) have a leaky blood brain barrier and have been passively transferred with amphiphysin-antibodies from a patient with stiff person syndrome (SPS) and AQP4-antibodies in neuromyelitis optica leading to behavioural and neuropathological changes reminiscent of diseases (Sommer, 2005; Kinoshita, 2009). Alternatively, Saadoun *et al* circumvented the blood brain barrier by direct intracerebral injection of purified NMO-IgG inducing characteristic NMO-like lesions in the brain parenchyma when co-injected with a source of human complement. Furthermore, the authors found destruction and loss of AQP-4 in the ependyma cells lining the ventricles after intraventricular injection of patient IgG and complement (Saadoun, 2010). These findings demonstrate that complement is an essential component of NMO-pathogenesis but also, that injection of NMO-IgG in to the ventricles shows binding to CNS tissue.

6.6 Aims

Since the identification of NMDAR-antibodies in 2007 there is accumulating evidence that these antibodies are pathogenic. This comes from observations showing a reduction in NMDAR-antibody titers which correlate with neurological improvement, and experimental studies in which patient antibodies reduce the expression of NMDARs both *in vitro* and *in vivo models*, an observation that has also been confirmed in human autopsy material. Consistent with an antibody-mediated reduction in NMDAR expression, NMDAR antagonists produce symptoms similar to patients with NMDAR-antibodies including psychosis and cognitive disturbances in humans, and isomorphic behaviours in rodents.

At the beginning of this DPhil in 2009, the only known pathogenic mechanism of NMDAR-antibodies was their effect on NMDAR internalisation in hippocampal neuronal cultures (Dalmau 2007). There had been no report of NMDAR-antibody passive transfer experiments modelling the clinical manifestations seen in patients. The aim was to identify patients with high NMDAR-antibody titers and investigate whether NMDAR-antibodies fulfilled Koch's postulates of an autoantibody mediated disease by passively transferring patient antibodies into mice to try to reproduce clinical features seen in the human disease.

Chapter 7: Methods

7.1 Detection of patient antibodies

All sera positive for NMDAR-antibodies described in this chapter were identified by the routine laboratory screening of referred sera or CSFs and their features characterised by Dr Sarosh Irani. Biological samples were aliquoted and kept long-term at -20˚C. Due to limiting volumes of available sera sent in for detection of NMDAR antibodies, plasma exchange material from seven patients with NMDAR-antibody mediated encephalitis was used as the main source of NMDAR-antibodies. Two healthy control samples were used in this thesis. Both healthy controls were tested on the NMDAR diagnostic assay and were found to be negative for NMDAR-antibodies.

7.1.1 Cell based assay

In brief, $5x10^5$ HEK293 cells were grown on coverslips of in a 6 well plate, and after 24 hours cells were transfected with PEI and glucose, with a total of 3µg of untagged NR1 and NR2B cDNA (3:1) per well. An eGFP expression vector (0.15µg) was co-transfected to visualise transfection. The following morning the media was aspirated and replaced with fresh medium, supplemented with 500µM ketamine to prevent cytotoxicity. CBA staining was performed as described previously in section 0.

7.1.2 Primary hippocampal culture

Primary hippocampal cultures were prepared and stained as described previously, see section 3.4.5.

7.1.3 Immunohistochemistry (IHC)

C57BL/6 wild type mice were anaesthetised with pentobarbitone and transcardially perfused with PBS. Brains were removed, bisected and snap-frozen in isopentane chilled on dry ice. On a cryostat 10µm sagittal sections were prepared and collected on to slides and allowed to air dry overnight before storing at -20˚C. For staining, sagittal sections were thawed for one hour at room temperature and blocked in PBS with 10% normal goat serum (NGS, made in PBS)) for one hour at room temperature. Sections were subsequently incubated with either healthy control plasma (n=2) or

NMDAR-antibody plasmas (n=7 (NMDAR-Ab # 1-7)) diluted 1:200 or NMDAR-antibody positive CSF diluted 1:10 (n=1 (NMDAR-Ab CSF# 1) for 2 hours at room temperature. Sections were washed three times in 300ml of PBS and specific IgG binding was detected using Alexa Fluor goat anti-human IgG secondary antibody (1:2000) for 1 hour at room temperature. Slides were washed 3 times in PBS, air dried and mounted with DAKO fluorescent mounting medium containing DAPI. All IHC staining of patient plasma samples were performed on two brain sections.

To quantitate immunoreactivity of patient sera to the hippocampus, the cumulative probability of pixel intensity in the hippocampal molecular layer was analysed as described previously by Hughes *et al*, 2010. Images were taken using the same intensity parameters at the same magnification from comparable regions of the brain. Each image was converted to greyscale and a cumulative histogram was measured using a macro supplied by Image J online, (http://rsbweb.nih.gov/ij/macros/examples/CumulativeHistogram.txt):

```
//Cumulative histogram
getRawStatistics(area, mean, min, max, std, h);
 for (i=1; i< h.length; i++)  h[i] = h[i-1]+h[i];
 Plot.create("Cumulative Histogram of "+getTitle, "Value", "Sum of pixel count", h);
Plot .show ();
//end
```

Using a nonlinear curve of regression, $\log_{EC50}$ values were generated for the mean of each sample.

7.2 Preparation of purified IgG

IgG was purified and concentrated to 25 mg/ml as described in section 3.5 for three NMDAR-antibody positive plasmas (#3, 4, 7) and two healthy controls.

7.2.1 Preadsorption of NMDAR-antibodies

For adsorption of the NMDAR-antibodies from patient IgG samples, cells were transfected with NR1 and NR2B in T175 cm^2 flasks. As described previously in section 3.4.6, limiting quantities

(determined by end-point titrations) of IgG from three patients were used for adsorption studies. The adsorbed samples were re-tested on the diagnostic NMDAR assay to confirm complete absorption of the specific NMDAR-antibodies and subsequently re-screened on hippocampal neurons.

7.3 Passive transfer experiments

All *in vivo* experiments documented in this thesis were performed in accordance with the United Kingdom Home Office Animals in Scientific Procedures Act (1986), in accordance with institutional guidelines, under the following licences:

PIL-7447 (Miss Philippa Pettingill)

PLL 30-2398 (Professor Angela Vincent)

7.3.1 Animals

Three cohorts of female wild type C57BL/6 mice (Harlan, United Kingdom) were used. Mice were housed in holding rooms on a 12/12hr light/dark cycle (lights off at 19:00-07:00 hours). Mice were housed in groups of 6-9 with *ad libitum* food and water, and were approximately ten weeks of age at the time of surgery. Forty eight hours before surgery, mice were marked for identification with commercial hair-dye (Jerome Russell Blonde Highlighting kit). All behavioural testing was performed during the light phase unless stated otherwise.

One day before surgery, mouse performance on the burrowing task, a species-specific test which is sensitive to subtle changes in mouse behaviour (see 7.4.1), was assessed and mice subsequently matched and allocated into IgG treatment groups.

7.3.2 Stereotaxic injection of IgG into the lateral ventricle

Mice were placed into an induction chamber filled with 3% isoflurane at a flow rate of 2.0 l/min O_2. Mice were injected subcutaneously with 0.1 ml of meloxican (5 mg/ml, Metacam, Boehringer Ingelheim) to provide pain relief during surgery, the scalp shaved and cleaned with Hibiscrub (4% w/v chlorhexidine gluconate, Regent Medical Ltd) before placement into the stereotaxic frame (Kopf Instruments, model 940). Anaesthesia was maintained throughout surgery using isoflurane at a

concentration of 2% at a flow rate of approximately 1.0 l/min O_2. A rectal probe and a homeothermic heat pad (Haravrd Apparatus) were used to monitor and regulate body temperature. A small incision was made into the scalp to expose the skull and 4% lidocaine hydrochloride (Xylocaine, AstraZeneca UK Ltd) was applied to the exposed tissue to provide local anaesthetic. Measurements of bregma were recorded, and the stereotaxic needle moved into position. Stereotaxic coordinates were calculated from bregma and the coordinates used for surgery were; anterior -0.34 mm, lateral +1.0 mm, and ventral -2.3 mm. A small hole was drilled into the skull above the injection site using a dental drill (Technoboz 810, BienAir) and the area cleared of debris with a sterile cotton bud before lowering a modified 34 gauge stainless steel needle 1mm ventrally into the tissue. The needle was raised and washed with 30% ethanol twice, sterile PBS 3 times, before loading with IgG. Each mouse recieved a single 10 µl injection (1 µl/min) of purified IgG (healthy control or NMDAR-antibody). After infusion, the needle was raised 1 mm and left for two minutes before being removed. The scalp was sutured closed and a thin layer of super glue was applied to the secure the suture knot. Mice were placed in a heated recovery chamber (30˚C) and given 30% sucrose solution instead of water on the day of surgery. The syringe was washed as described abover between each injection.

One mouse died in the sterotaxic frame prior to injection of IgG. Instead, 10 µl of Evan's blue was injected into the lateral ventricle to confirm the stereotaxic coordinates.

In total four mice receiving healthy control IgG were sacrificed either one hour (n=2) or 24 hours (n=2) after injection for direct analysis of IgG presence in the brain. Mice were euthanised, transcardially perfused with PBS, and subsequently perfused in 4 % paraformaldehyde (in PBS), and the brain dissected and placed into 4% PFA for 24 hours at 4˚C. Brains were subsequently washed in PBS and transferred into ascending concentrations of sucrose (5%, 10%, 25%, for one day each) for cryoprotection at 4˚C. Brains were snap-frozen in isopentane chilled on dry ice.

7.3.3 Experimental cohorts

Three behavioural cohorts are described; Cohort one (n= 12), cohort two (n =14) and cohort 3 (n=24). The same patient and control samples was used in both cohorts one and two (healthy control IgG #1,

NMDAR IgG # 7). Cohort three used the IgGs from cohort one, and two additional NMDAR-antibody positive patients (NMDAR IgG #3 NMDAR IgG #4). One additional healthy control IgG (#2) was also used. Six mice in cohort one and 8 mice in cohort two received either healthy control IgG or NMDAR Ab- IgG. In cohort three, 15 mice received one of three NMDAR-IgG preparations and 9 mice received control IgG. This is illustrated in Table 7-1.

Initial experiments with cohort one were performed with treatment group known to the experimenter. Subsequently cohorts two and three were performed coded.

	Mice receiving:	
	Healthy control IgG	**NMDAR-Ab$^+$ IgG**
Cohort 1	6 (Control #1)	6 (Patient #7)
Cohort 2	7 (Control #1)	7 (Patient #7)
Cohort 3	9 (Control #1, 2)	15 (Patient #3, 4, 7)

Table 7-1 Overview of mice in experimental cohorts 1, 2 and 3

7.4 Behavioural testing

7.4.1 General monitoring and species typical behaviour

Postoperative checks were performed daily for each mouse for seven to fourteen days after surgery. Mice were weighed, observed and scored for any signs of malaise or ill health.

Burrowing

Burrowing is a species-typical behaviour that is seen in almost all rodents. Burrowing levels can be measured to assess the disruption of normal mouse behaviour. Cylinders, raised 3 cm (dimensions; length 20 cm, diameter 6.8 cm) with one end closed and the other end open were filled with 200 grams (g) of food pellets and placed into a clean cage lined with bedding. Mice were placed into the cage three hours prior to the dark cycle. The amount of pellets displaced (g) from the burrows was measured twice during the task; two hours into the task and again the following morning. Due to time constraints, burrowing on days one and two were only assessed the following morning. Burrowing was assessed the day before surgery (day 0) and after surgery on days 1, 2, 5 and 15.

7.4.2 Tests of locomotor activity

Open field

A grey Perspex arena (dimensions height x width, 50 x 30cm), divided into 10 cm squares was used to assess locomotor activity. Mice were placed into the open field and manually observed for three minutes. The time taken to rear, the number of rears and the number of squares entered were counted. Mice were assessed on days 1-5 after surgery.

Overnight locomotor activity

The Threshold system (Version 3, Med Associates) was used to measure locomotor activity over a fifteen hour period. The apparatus converts the pressure generated from a mouse's movement in a home cage cell (dimensions 22.5 x 12.5 x 13cm) into voltage. In these experiments, the detection threshold was set to record at a lower detectable threshold of 20 mV and an upper threshold value of 50 mV. Mice were placed into the apparatus two hours before the dark-cycle (17:00 hours) and provided with *ad libitum* food and water throughout the fifteen hour recording period. Mice were

removed from the cages the following morning. The time spent above the threshold limits, represents the locomotor activity of an individual mouse. Data were collected in one hour time bins. Mice were assessed on days 4 and 14 post surgery.

Rotarod

Motor performance was assessed using an accelerating rotarod. Mice were placed on to a moving rotarod (start speed 4rpm). After ten seconds, the accelerator was activated and the speed at which the mouse falls off was recorded. The maximum speed of the rotarod was 40rpm. Mouse performance was assessed on days 13 and 18 post surgery.

7.4.3 Tests of anxiety

Tests of anxiety used in this thesis are based upon observations that rodent's innate behaviour is to explore a novel environment. Rodents prefer enclosed dark areas and avoid open, brightly illuminated or elevated areas (Crawley & Goodwin, 1980).

Light/Dark box

The light/dark box is a test of anxiety and consists of an enclosed dark compartment with a removable lid (15 x 20 x 20cm), and an open white aversive compartment (30 x 20 x 20cm). A small entrance hole (3 x 3cm) links the two compartments. The anxiogenic nature of the white compartment is intensified by additional illumination using a 60W lamp placed 45cm above the centre of the compartment. Mice were placed into the middle of the dark compartment, facing away from the entrance hole, and the lid closed. The latency to cross from one compartment to another, the time spent in each compartment and the numbers of transitions between compartments were measured. Behaviour was measured on day 4 post surgery.

Successive alleys

The successive alley is a test for anxiety and consists of four joined alleys with progressively increasing anxiogenic nature (Contet, 2001). Each alley is 25cm long and fixed 0.5 meters above the floor, adding an extra anxiogenic aspect to the task. Alley one is painted black and is the widest alley with high walls (width x height 8.5 cm x 25 cm), alley two (8.5 cm x 1.3 cm), three (3.5 cm x 0.8 cm) and four (1.2 cm x 0.2 cm) get progressively thinner, and lighter. Mice were placed into the middle of

the first alley, facing the wall and behaviour in in the task assessed over five minutes. The latency to cross from alley one to alley two (defined by all four feet entering the compartment), the time spent in each alley and the number of transitions between compartments measured. Behaviour was measured on day 8 post surgery.

7.4.4 Tests of cognition

Spontaneous alternation

The spontaneous alternation test involved a T-shaped maze and is often used, particularly in the pharmaceutical industry to assess memory function. The apparatus used in this experiment has been described in detail previously (Deacon, 2006). A T-shaped maze (30 x 10 x 29 cm) with a central partition extending 7 cm into the start maze at the choice end of the maze was placed in the centre of the testing room. Dirty bedding from same sex mice lined the bottom of the maze. Each trial is composed of two runs, carried out in close succession. Mice are placed at the stem of the maze and allowed a free choice of entry to either arm. Upon choosing an arm, a timer is started and the mouse is confined to the choice arm by use of a guillotine door. After thirty seconds, the mouse is removed from the maze and the partition removed and all doors re-set. The mouse is placed back into the start arm of the maze and allowed a further choice of arms. If a mouse enters the alternate arm on the second run it is said to have "alternated" correctly, which is thought to be indicative of intact working memory in the rodent (Lalonde, 2002).

Cohort one was assessed on days 1-9, 14, 17, 21-30 and 41-44 and cohorts two and three assessed each day from days 1-40. Mice were tested in 3 trials per day. The percentage of correct alternations was grouped and analysed into four day blocks for cohorts two and three.

7.5 Histological processing

All mice from cohorts 1 and 2 were sacrificed on day 46. Ten mice from cohort three were sacrificed on day and 22 and the remaining mice sacrificed on day 46. Briefly animals were overdosed with 0.3 ml Euthatal (200 mg/ml pentobarbital sodium, Merial Animal Health Ltd) and transcardially perfused with 50 ml of sterile PBS. Their brains were removed, bisected before being snap frozen in isopentane

that had been pre-chilled on dry ice. Specimens were cut in 10 µm sagittal sections, collected on slides and dried overnight at room temperature. Slides were stored at -20˚C until required.

7.5.1 Immunohistochemical staining for human IgG and mouse IgG

Sagittal brain sections from mice injected with healthy control IgG and culled 1 hour (n=2) and 24 (n=2) hours after injection or a non-immunised mice (n=1) were blocked for 1 hour in 10% NGS/PBS. Sections were incubated with Alexa Fluor goat anti-human IgG or Alexa Fluor goat anti mouse IgG secondary antibodies (1:2000, Invitrogen) for 2 hours at room temperature. Slides were washed 3 times in PBS, air dried and mounted with fluorescent mounting medium containing DAPI. Six sections per mouse brain were analysed.

7.5.2 Immunohistochemical staining for astrocytes and microglia

Sagittal sections (n=3) from nine mice injected with healthy control IgG (n=3), or NMDAR-IgG (n=3 culled on day 22 and n=3 on day 46 after ICV injection) were blocked for 1 hour in 10%-PBS-NGS. Sections were incubated with commercial antibodies against astrocytes (rabbit anti GFAP, diluted 1:500, DAKO Z0334) or microglial cells (mouse anti CD68, diluted 1:100, DAKO MO718) for 2 hours at room temperature. Sections were washed three times in 300 ml of PBS and specific IgG binding was detected using Alexa Fluor goat anti-rabbit IgG or goat anti mouse IgG secondary antibody (1:2000). Slides were washed, air dried and mounted with DAKO fluorescent mounting medium containing DAPI. Sections were observed for gross morphological differences between control and patient IgG injected mice.

7.5.3 Quantitation of NMDA receptors

Brain hemispheres were thawed from thirty ICV injected brains (healthy control IgG n=10, NMDAR-antibody IgG n=20) from days 22 and days 46 post injection and two control brains (n=1 uninjected wild type and n=1 un-injected NR1 hypomorph, courtesy of Glaxo SmithKline) and the hippocampus dissected. Proteins were extracted in 200µl of extraction buffer (10 mM Tris, 100 mM NaCl, 1 mM 0.5 M EDTA pH 8.0, 1% digitionin), supplemented with PIC (1:1000). Extracts were centrifuged at 13,000 rpm for 10 minutes and the supernatant collected. The protein concentration for each sample

was determined using the BCA kit (Pierce). Standards ranging from 0-2mg/ml were prepared according to the manufactures instructions.

10 µg of protein extract was loading on to a 4-12% Bis-Tris Acetate gel (Invitrogen) and after electrophoretic transfer to nitrocellulose membranes the immunoblots were blocked in PBS-0.1% Tween (PBS-T) with 10% milk powder for 2 hours. Immunoblots were probed with a mouse anti NR1 antibody (1:200 in 5% milk powder w/v PBS-T) overnight at 4˚C. Blots were washed three times in PBS-T, stained with anti-mouse IgG HRP secondary antibody for 1 hour before washing in distilled water. Blots were developed with ECL, and the intensity of the NR1 band quantified using Image J software.

7.6 Statistical analyses

Repeated measure ANOVAs were used to assess mouse weight, mouse performance on burrowing, open field, the threshold activity system, rotarod and spontaneous alternation. Homogeneity of variance was verified using Mauchly's test of sphericity and where data violated the assumptions of normality or equal variation, the p-values were adjusted via Greenhouse Geisser transformations and the original degrees of freedom reported. The effect of time was included as a within-subjects factor and the effect of treatment and cohort were included as between-subject factors. Where no effect of cohort was found ($p>0.05$), cohort was excluded as a between-subjects factor. When a significant interaction between treatment and time were observed, simple main effects were performed using Bonferroni comparisons. T-tests were performed where appropriate; however as clasping behaviour data was binomial, data was analysed using a Fischer's test, with the data collapsed across the testing period. $p<0.05$ was considered statistically significant and all statistics were performed with PASW Statistical Data Editor.

8 Results

8.1 Detection of NMDAR-antibodies

A summary of the seven patients used in the study are shown in Table 8-1.

Seven patients who had undergone plasma exchange during their disease course had NMDAR-Abs detected at high levels (CBA score of 4) in their serum and plasma. An example of NMDAR-Ab binding in a cell based assay can be seen in Figure 8-1.

	Sex	Age	Tumour	Clinical features	Death
NMDAR #1	F	12	N	Dysk, ans	N
NMDAR #2	F	25	N	Cog, seiz, dysk, ans	N
NMDAR #3*	M	17	N	Psy, cog, seiz, dysk, ans	N
NMDAR #4*	F	17	N	Seiz, ans	N
NMDAR #5	F	20	Y (OT)	Cog, seiz, dysk, ans	N
NMDAR #6	M	Not known	Not known	Not known	Not known
NMDAR #7*	F	25	Y (OT)	Cog, seiz, dysk, ans	Y
NMDAR CSF (pooled n=10)	Not known	Not known	Not known	Not known	Not known

Table 8-1 NMDAR-antibody patient samples used in this thesis.

*Summary of patient plasma samples used with clinical information including sex, age, tumour status (OT=ovarian teratoma), and core clinical features if present (psy=psychiatric, cog =cognitive, seiz= seizures, dysk=dyskinesia, ans=autonomic symptoms), and death., * Asterisks represents patients used in passive transfer experiments.*

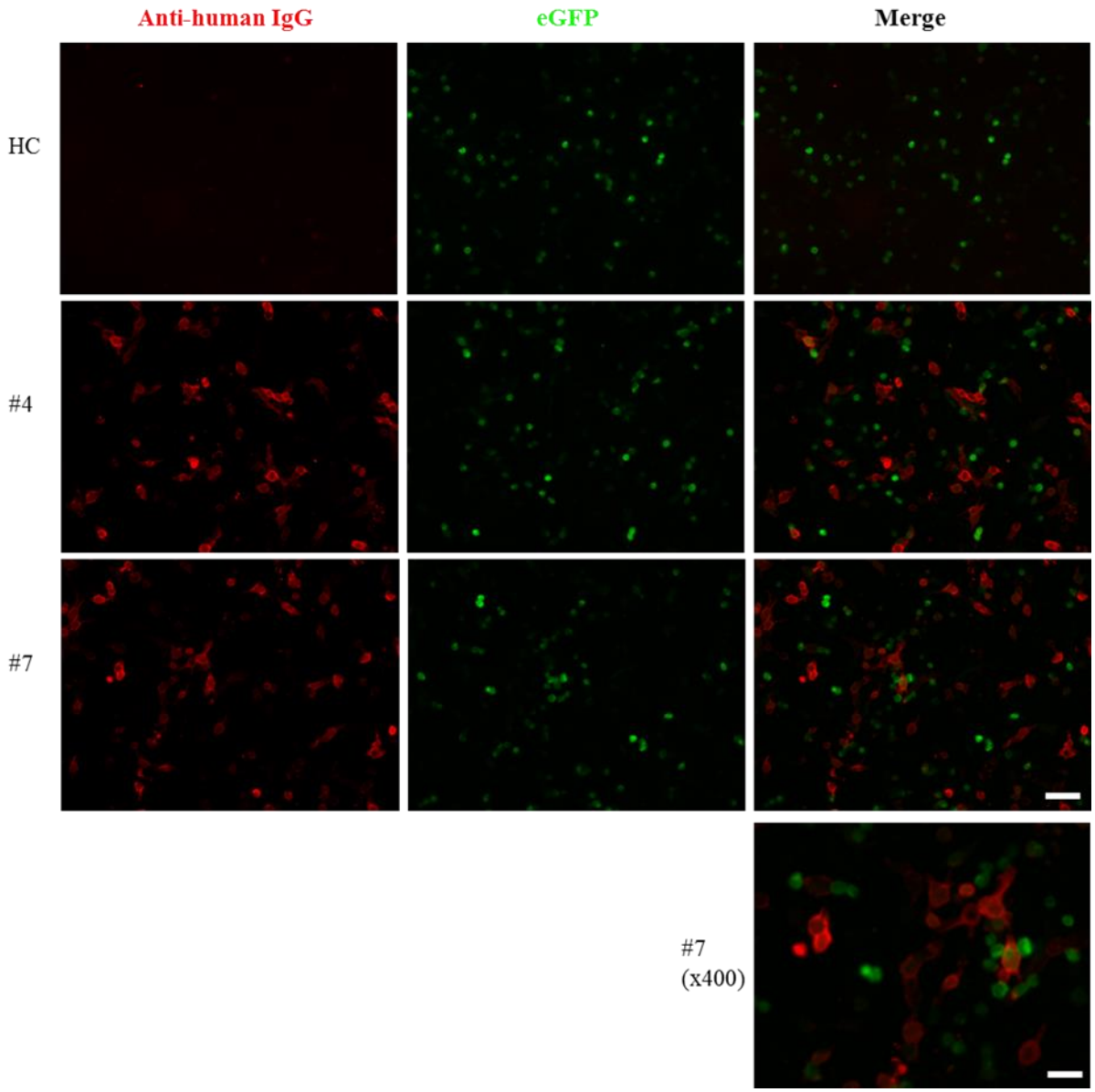

Figure 8-1 Detection of NMDAR-antibodies in transfected HEK cells.

HEK 293 cells were co-transfected with two plasmids encoding both the NR1 and NR2B subunits of the NMDA receptor as well as an additional plasmid encoding EGFP to aid visualisation (green, middle panel). Healthy control sera (top) did not bind to the surface of transfected cells. Specific binding of NMDAR-Abs in patient sera (#4 - middle and #7 –bottom panel) bind to surface of transfected cells and are detected using an anti-human secondary antibody (red, left panel). eGFP expression (middle panel) enables us to visualise that transfection was successful. Magnification x 200 and scale bar represents 100 µm. Higher magnification of NMDAR-Ab^{+} #7, x400, bottom panel, scale bar represents 50 µm.

8.1.1 Immunohistochemistry

NMDAR-antibodies were originally discovered by the novel immunoreactivity of patient CSF to rat brain sections (Ances, 2005; Dalmau, 2007). Seven NMDAR-Ab patients and two healthy control samples were screened on sagittal mouse brain sections. IgG binding of NMDAR-Abs was seen throughout the brain, including strong immunoreactivity in the hippocampal neuropil, particularly against the inner molecular layer of the dentate gyrus. Specific binding to the granule cells in the cerebellum was also seen in some NMDAR Ab samples. The two healthy control plasmas did not bind to the sections. Representative images of immunostaining of NMDAR-Ab patients and control samples to the hippocampus and cerebellum can be seen in Figure 8-2 and 8-3.

Some patient plasma showed more intense immunoreactivity to mouse tissue than others. Of the seven NMDAR-antibody positive plasmas tested, five bound to both the hippocampus and cerebellum. Two plasmas (#5 and 6) showed no immunostaining to either the hippocampus or cerebellum, despite having strong binding to the human NR1/NR2 subunits by CBA. To quantify the intensity of immunoreactivity of patient sera to the hippocampus, the cumulative probability of pixel intensity in the molecular layer of the hippocampus was analysed as described previously (Hughes, 2010). The cumulative histograms for NMDAR-Ab samples show a right-ward shift compared to control curves, indicating a stronger IgG immunoreactivity to the section, Figure 8-4a. Statistical analysis showed that NMDAR-Ab intensity binding of all patients was significantly different to control IgG intensity ($p<0.0001$, Figure 8-4b). For each sample the $\log_{EC50}$ measurements were determined, samples that bound strongly to the hippocampus had a higher $\log_{EC50}$ value than those that did not (control range: 13.62-18.43, NMDAR-Ab range: 19.00-33.83). The two NMDAR-Ab plasmas that showed no binding to tissue sections did not have a right-ward shift in their histogram and had similar $\log_{EC50}$ values to those seen with control plasma. NMDAR-Ab immunoreactivity to the hippocampus (determined by its $\log_{EC50}$ value) shows a good correlation with antibody titer (Pearson's $r=0.8681$, $p=0.0024$, Figure 8-4c).

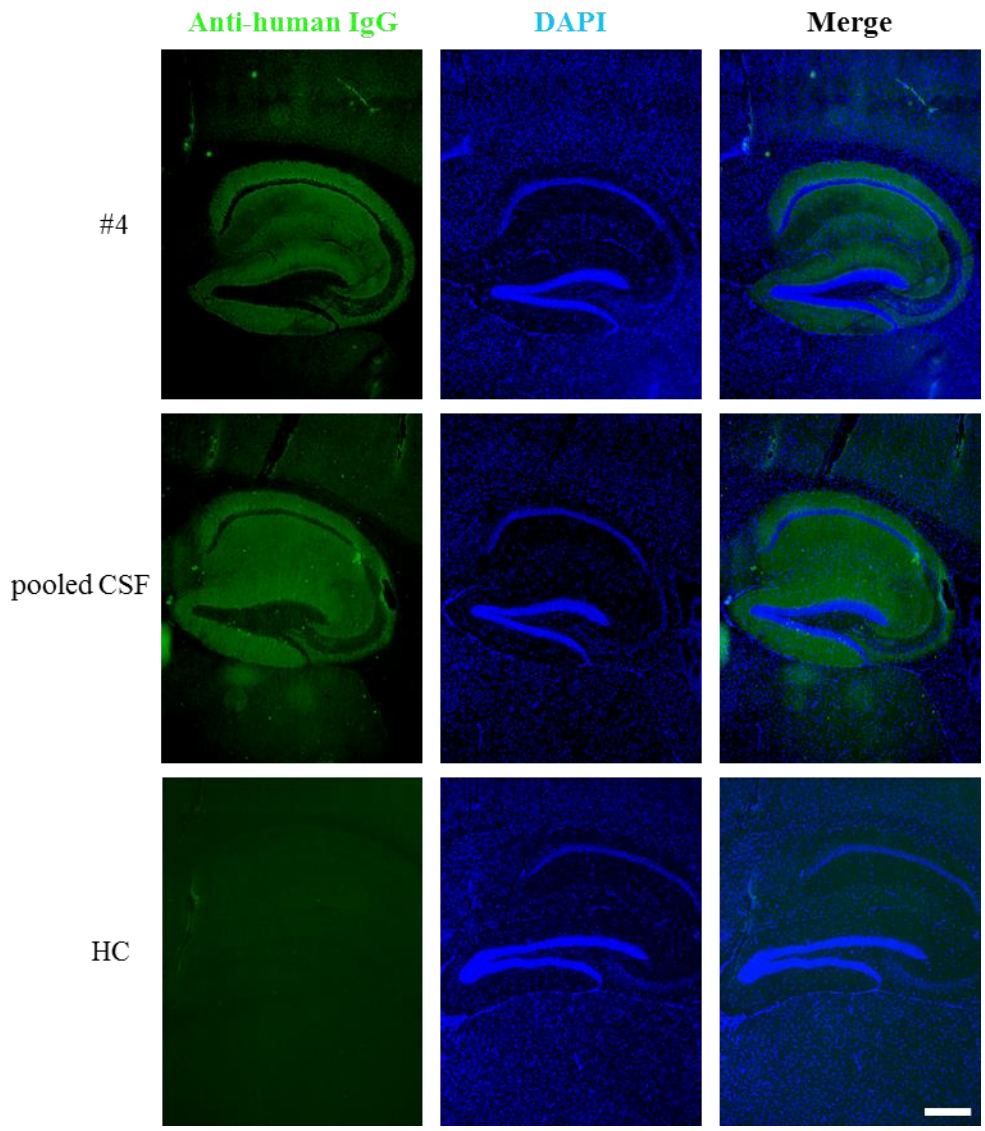

Figure 8-2 NMDAR antibodies bind to rodent hippocampus

Representative binding of NMDAR-Ab plasma #4 (1:200) and CSF (1:10) to sagittal sections shows intense binding to the hippocampus, detected using an anti-human secondary antibody (green, left panel). Healthy control serum does not specifically bind to the hippocampus. DAPI stain (blue, middle) is included to identify cell nuclei. Magnification x50 scale bar represents 400µm.

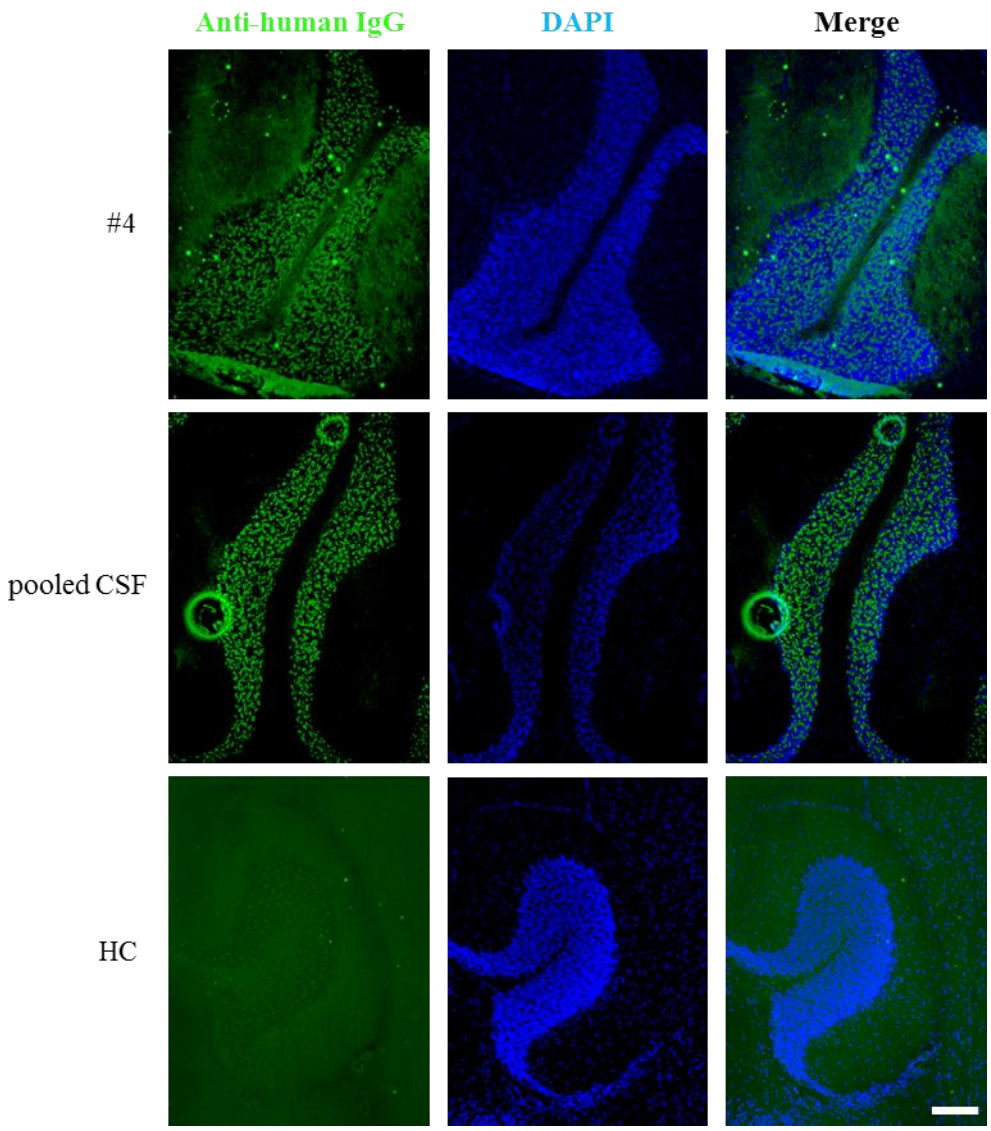

Figure 8-3 NMDAR antibodies bind to rodent cerebellum.

Representative binding of NMDAR-Ab plasma (1:200) and CSF (1:10) to sagittal sections shows intense binding to the granule cells, detected using an anti-human secondary antibody (green, left panel). Healthy control serum does not specifically bind to the cerebellum. DAPI stain (blue, middle) Magnification x50 scale bar represents 400µm.

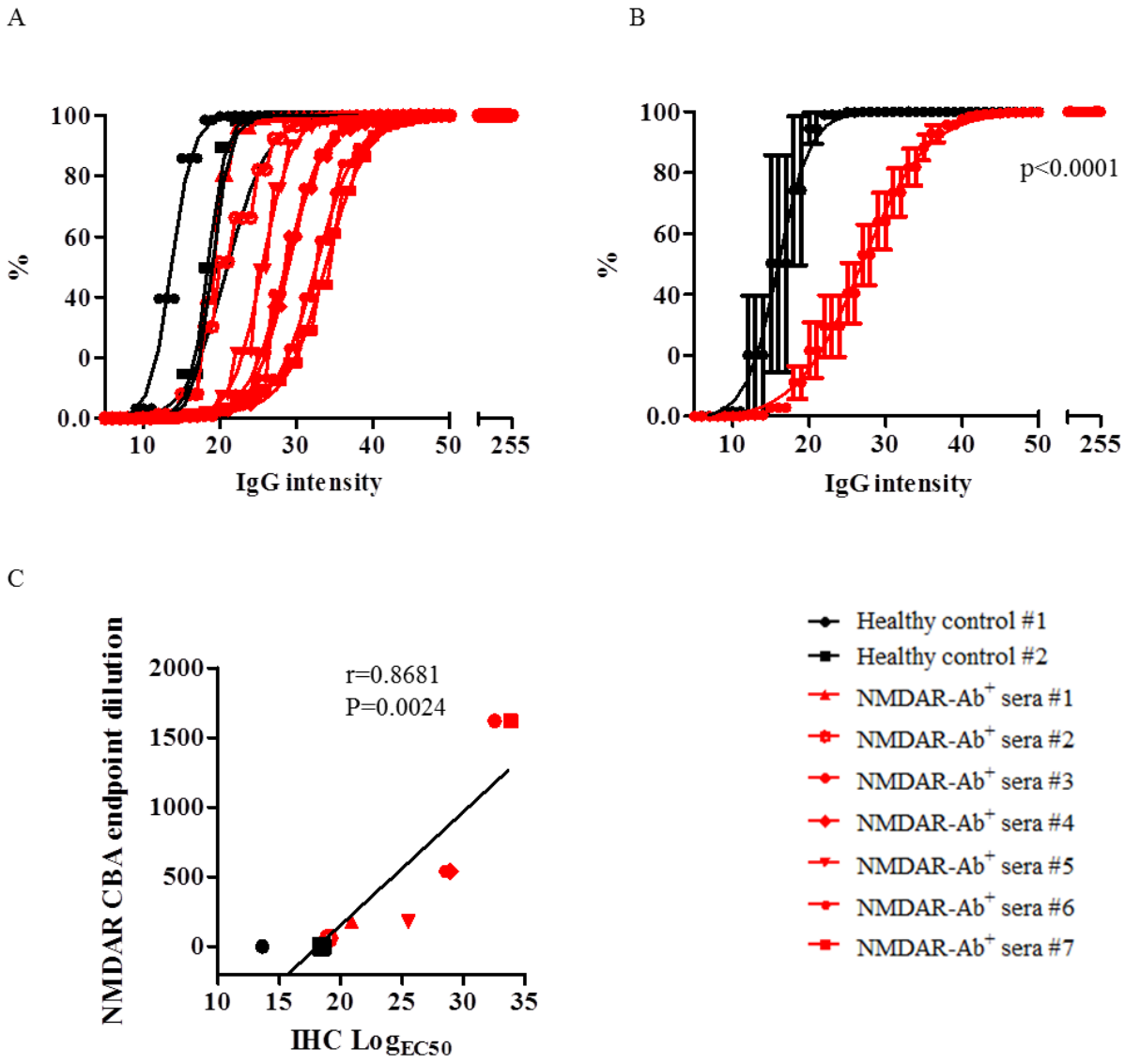

Figure 8-4 Quantification of NMDAR-antibody binding intensity to the hippocampus.

A) Individual cumulative histogram analysis of intensity of IgG binding to the hippocampus in two healthy control (black) and seven NMDAR-A$^+$ (red) plasmas (mean of two sections). B) Grouped cumulative histograms for control or patient samples; NMDAR-Abs show significantly greater binding to the hippocampus illustrated by a right-ward intensity shift ($p<0.0001$, two-sample Kolmogorov-Smirnov). C) A strong positive correlation between CBA end-titration point and IgG binding to the hippocampus was observed (Pearson's $r= 0.8601$, $p=0.0024$).

8.1.2 Hippocampal primary cultures

All seven plasma exchange samples and two healthy controls (1:100) were screened on primary cultures. Only the five of the seven NMDAR-Ab plasmas that bound to hippocampal sections also bound to the surface of primary hippocampal neurons.

IgG was purified from three NMDAR-Ab patient plasmas that had the highest antibody titers and bound strongly to rodent tissue (#3, 4 & 7), alongside the two healthy control plasmas. Two patients were female and one male. After IgG purification, all preparations were re-screened on the CBA and neuronal cultures to confirm antibody presence. IgG preparations were used in all subsequent experiments, both *in vitro* and *in vivo*.

8.1.3 Immunoadsorption of NMDAR-antibodies

To ensure that we are representing an NMDAR-Ab mediated passive transfer, we need to confirm that the patients had no other additional surface antibody reactivities. HEK cells expressing NR1/NR2B were used to investigate whether after preadsorption of patient plasma against surface epitopes of the NMDARs this would abolish binding not only of the NMDAR CBA assay, but also to primary hippocampal cultures. Three NMDAR-IgGs were screened on the NMDAR CBA before and after preadsorption against live NR1/NR2 expressing HEK 293 cells. After preadsorption, immunoreactivity of all three samples was abrogated on the CBA, indicating that all of their NMDAR-Abs had been adsorbed. Immunoreactivity of IgG's on the NMDAR CBA was unaffected by preadsorption against untransfected HEK cells (data not shown).

NMDAR- IgGs bound to the surface of live hippocampal neuron, figure 4-6. After adsorption against HEK cells expressing NR1/NR2, there was no binding of IgG to the surface of hippocampal neurons. Immunoadsorption experiments confirmed that the antibodies in these patient samples are directed against the NMDA receptor, and there are no additional antibody immunoreactivities against hippocampal surface proteins present in these samples.

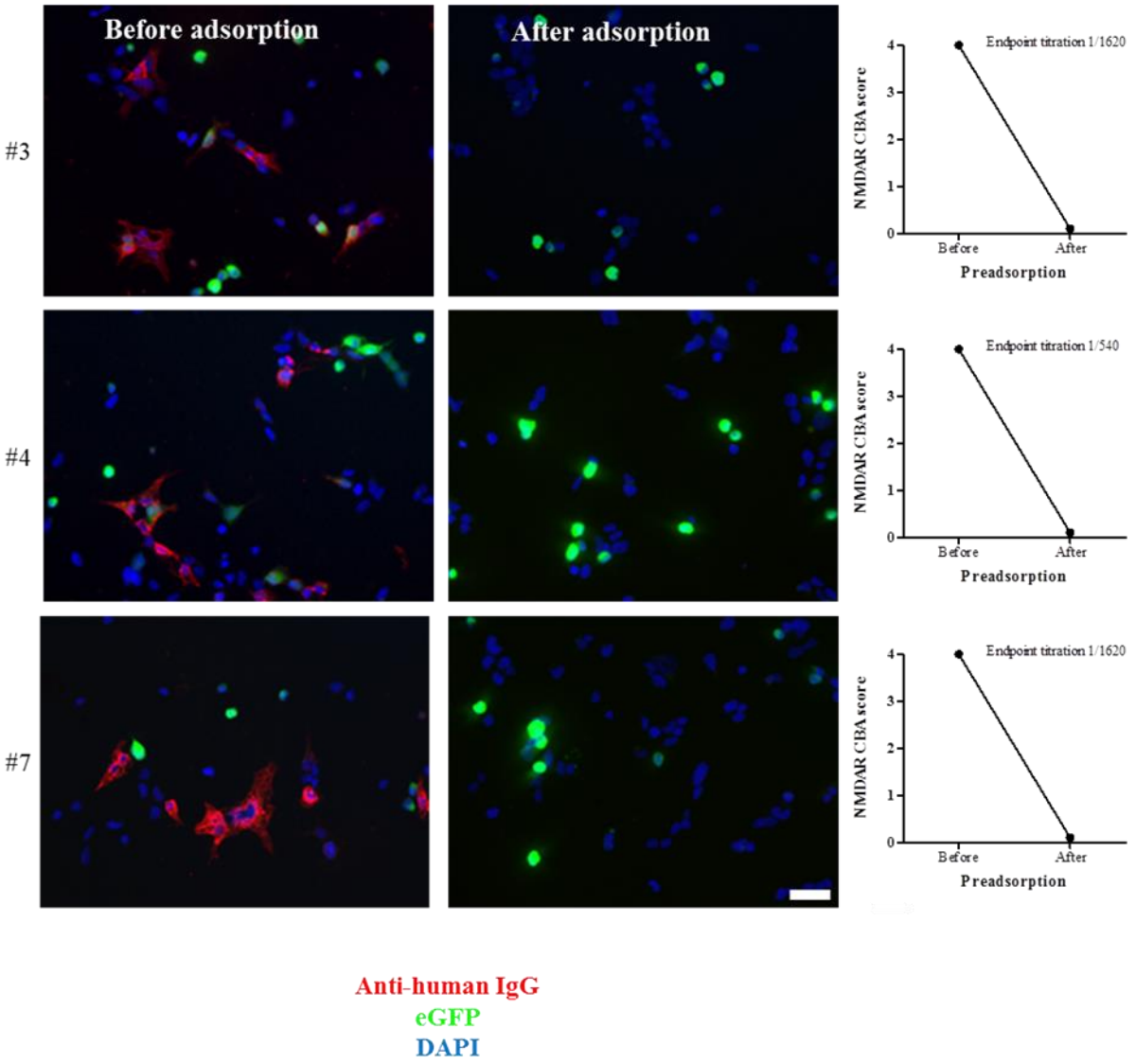

Figure 8-5 Detection of NMDAR-antibodies before and after preadsorption against NR1/NR2B transfected cells.

Binding of patient IgG to the NMDAR CBA before (left panel) and after (right panel) adsorption. CBA scores from these experiments can be seen on the right hand side. Magnification x400, scale bar represents 50µm.

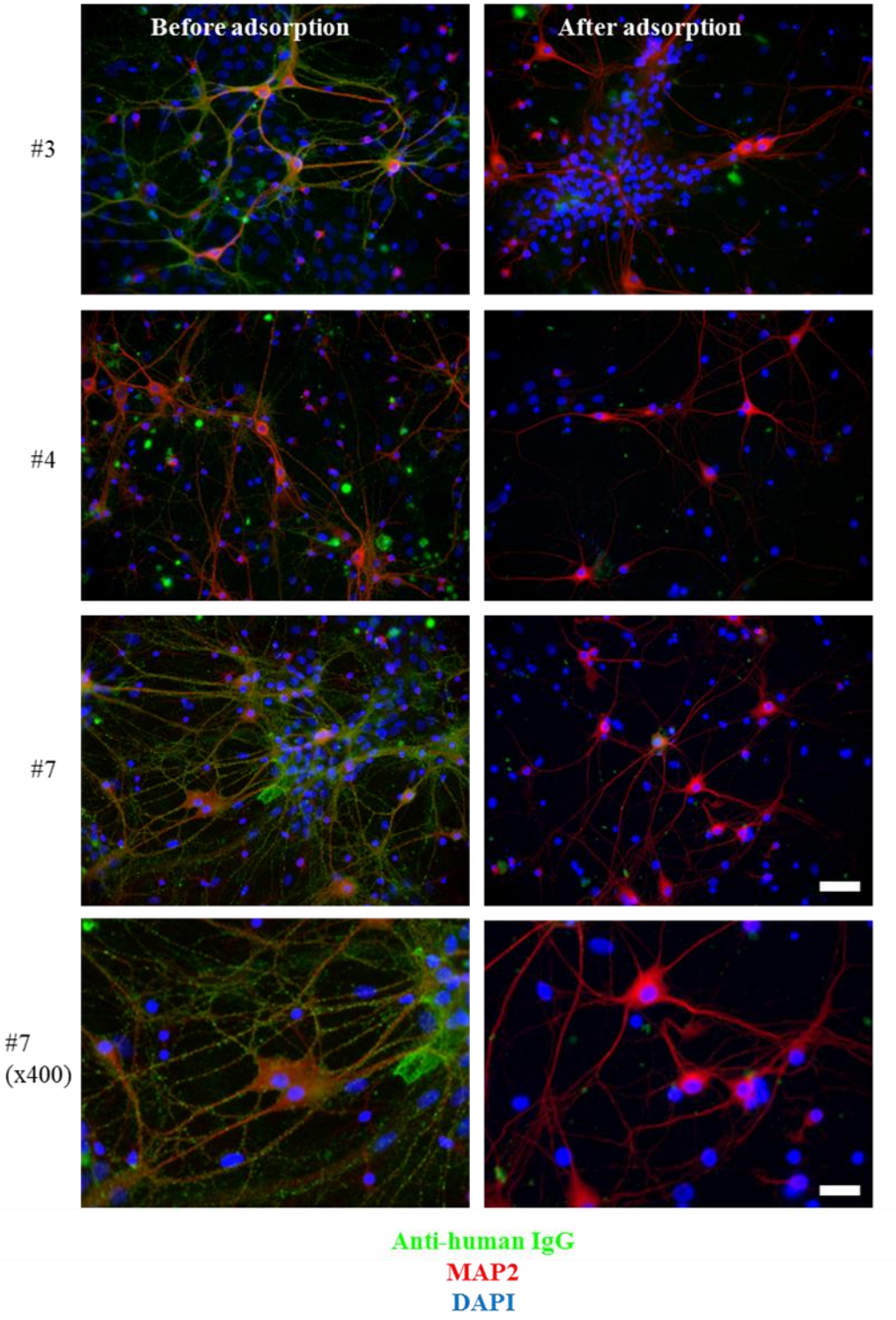

Figure 8-6 Adsorption of NMDAR-antibodies abolishes IgG binding of hippocampal neurons.

Binding of patient IgG to the surface of live primary hippocampal neurons before adsorption (left panel). After adsorption of IgG against HEK cells expressing NR1/NR2B, surface binding of IgG was abolished (right panel), indicating that patient antibodies binding to hippocampal neurons are against the NMDAR only. Magnification x200, scale bar represent 100 µm. Higher magnification of NMDAR-Ab+ #7, x400, bottom panel, scale bar represents 50 µm.

8.2 Pathogenicity of NMDAR-antibodies *in vivo*

To determine whether NMDAR-antibodies are pathogenic *in vivo*, IgG was concentrated to 25 mg/ml and then injected into mice via the intraventricular route. The lateral ventricle was chosen as our delivery site as intrathecal synthesis is seen in NMDAR-antibody patients and previous groups have had difficulties in producing a model of CNS autoimmunity without inducing EAE or breaching the blood brain barrier (Kowal, 2004; Saadoun, 2010). Total purified IgG only was chosen as the source material for injection despite antibodies being predominantly IgG1 and IgG3, as complement deposition was not observed in autopsy and biopsy material in the brains of NMDAR-antibody patients (Tüzün, 2009; Martinez-Hernandez , 2011; Bien, 2012). Each mouse received a single 10 µl injection of IgG into the lateral ventricle. Mice were assessed on a variety of tasks to identify behavioural differences after administration of NMDAR-antibodies. An overview of NMDAR-Ab and healthy control IgGs used in these experiments and a timeline of behavioural tests assessed are outlined in Figure 8-7.

Three cohorts of mice receiving treatment with either intracerebroventricular injection of healthy control or NMDAR-antibodies will be described in this chapter. An overview of the behavioural tasks each cohort was assessed on is outlined in Table 8-2.

.

Monitoring	Cohort	Number of mice (HC, NMDAR IgG-treated)
Weight	1, 2, 3	22, 28
Burrowing	1, 2 (pre-surgery)	13, 13
	1, 2, 3 (days 5 and 15)	22, 28
Open field	1, 2, 3	22, 28
Threshold	1, 2, 3	22, 28
Rotarod	1, 2, 3	22, 28
Light dark box	1, 2, 3	22, 28
Successive alleys	1, 2, 3	22, 28
Clasping	2 (first noticed day 23)	7,7
	3 (assessed days 1-40)	9, 15
Spontaneous alternation	1 (assessed between days 1-44, but not daily)	6, 6
	2 (days 1-40)	7, 7
	3 (days 1049)	5, 9*

Table 8-2 Overview of mice assessed on behavioural tasks.

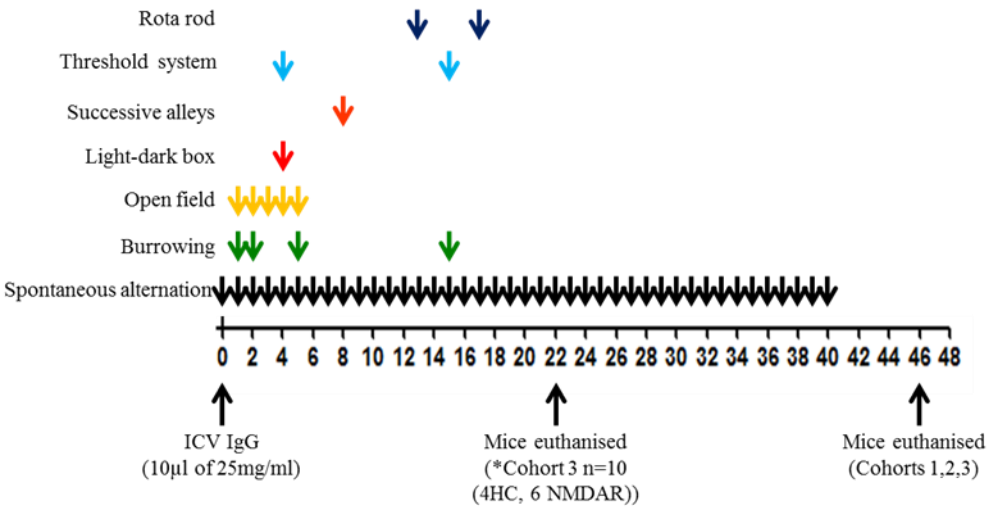

Figure 8-7 Time course of behavioural testing after intracerebroventricular injections of NMDAR-IgG and healthy control IgG into C57BL/6 female mice.

8.2.1 Test of general behaviour

After the surgical procedure, mice were monitored twice a day using a standard distress scoring system to identify early signs of ill health. Two mice were found dead from cohort two; one died 36 hours after surgery (NMDAR-IgG) and another due to an equipment error (HC-IgG); as rigour mortis had set, in the tissue from these mice were not analysed. In total data from cohorts 1, 2 and 3 (healthy control IgG n=22, NMDAR IgG n=28) were combined for all tasks except for spontaneous alternation, burrowing (day 0-2) and clasping behaviours.

Mouse body weight was assessed each day for seven days after surgery using repeated measures ANOVA. An effect of cohort ($F_{(2,44)}$=9.464 p<0.001) and IgG treatment was observed ($F_{(1,44)}$=4.220 p=0.046), although there was no cohort by treatment effect (cohort*treatment interaction $F_{(2,44)}$ =2.166 p=0.127, Figure 8-8). Within subjects analysis showed an effect of time on body weight ($F_{(7,308)}$=13.615 <0.001), and an interaction with cohort (time*cohort interaction $F_{(14, 308)}$=2.616 p=0.019). This interaction with time was independent of treatment (time*treatment interaction $F_{(7,308)}$=0.510, p=0.681) and no three way interaction was seen (time*treatment*cohort interaction $F_{(14,308)}$=0.482 p=0.826). The interaction of time which was independent on body weight most likely represents the immediate effect of surgery.

Burrowing on days one and two after surgery was only assessed the subsequent morning in mice from cohorts one and two (control IgG n=13, NMDAR-Ab n=13). No effect of cohort was observed ($F_{(1,22)}$=0.614 p=0.442). Control and NMDAR-IgG reduced burrowing in all mice between days 0 and 2 (effect of time $F_{(2,48)}$=18.993, p<0.001, effect of treatment interaction $F_{(1,24)}$=0.343, p=0.563, Figure 8-9a). This effect most likely represents the effect of surgery.

Burrowing performance on days five and fifteen was measured at two hours for all mice (control IgG n=22, NMDAR-Ab n=28). Burrowing at 2 hours showed an effect of cohort ($F_{(2,44)}$=18.817 p<0.001) but no effect of treatment ($F_{(1,44)=}$0.040 p=0.842) or cohort by treatment interaction ($F_{(2,44)}$=0.300 p=0.72, Figure 8-9b). Within subjects analysis showed an effect of time ($F_{(1,44)}$=25.070 p<0.001), where both control and patient IgG injected mice showed increased burrowing on day 15. This effect

interacted with cohort (time*cohort interaction $F_{(2,44)}$=16.491 p<0.001), but was independent of treatment (time*treatment interaction $F_{(1,44)}$=0.012 p=0.914) and no three way interaction was seen (time*treatment*cohort interaction $F_{(2,44)}$=1.066 p=0.353).

Overnight burrowing revealed no statistically significant effects as the majority of mice across all groups burrowed all of the pellets, causing a ceiling effect (data not shown).

8.2.2 Tests of locomotor activity

The open field, threshold and rotarod experiments were used to assess locomotor activity and coordination in the mouse. In the non-anxious open field the latency to rear, the number of rears and the number of squares entered was assessed on day one to day five. In all three parameters observed there was no effect of cohort (latency to rear $F_{(2,44)}$=0.016 p=0.059; number of rears $F_{(2,44)}$=0.358 p=0.681, number of rears $F_{(2,44)}$=0.552 p=0.580) so cohort was excluded from further analyses.

IgG treatment had no effect on any of the locomotor parameters measured in the open field apparatus; (latency to rear $F_{(1,48)}$=1.804 p=0.186, number of rears $F_{(1,48)}$=3.721 p=0.060 and number of squares entered $F_{(1,48)}$=1.850 p=0.180, Figure 8-10a-c). There was a progressive reduction in activity over days 1 to 5 (effect of time; latency to rear $F_{(1,48)}$=12.192 p<0.001, number of rears $F_{(1,48)}$= 8203, p< 0.001 and number of squares entered $F_{(1,48)}$=14.249, p<0.001), this effect was independent of IgG treatment group (time*treatment interaction; latency to rear $F_{(4,192)}$=0.038, p=0.977, number of rears $F_{(1,48)}$=0.067, p=0.992 and number of squares entered $F_{(1,48)}$=1.222, p=0.730). These behavioural changes seen over time are likely to reflect habituation of mice to the open field apparatus.

Mouse activity was measured on day four and fourteen on the automated threshold activity system. An effect of cohort on locomotor activity was observed for both days at both 20mV and 50mV threshold settings (day 4 20mV $F_{(2,44)}$=21.917 p<0.001; day 4 50mV $F_{(2,44)}$=29.642 p<0.001; day 14 20mV $F_{(2,44)}$=3.906 p-0.027; day 14 50mV $F_{(2,44)}$=9.012 p=0.001), so cohort was included as a between subject factor in all further analyses.

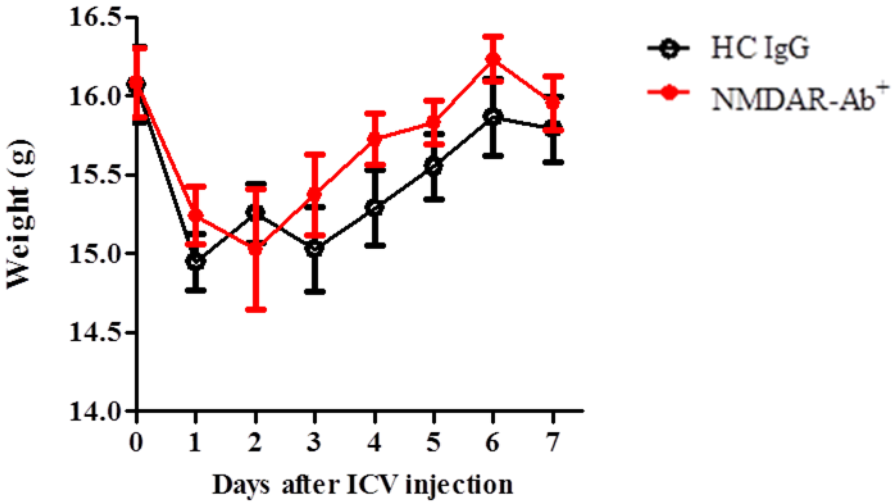

Figure 8-8 Post-operative mouse weights after intracerebroventricular injection of NMDAR-IgG or healthy control IgG.

Overall mouse weights over the seven day monitoring period did not differ between mice receiving NMDAR-IgG (n=28) or control IgG (n=22). All mice showed an initial drop in weight following surgery. Presented as mean ± SEM.

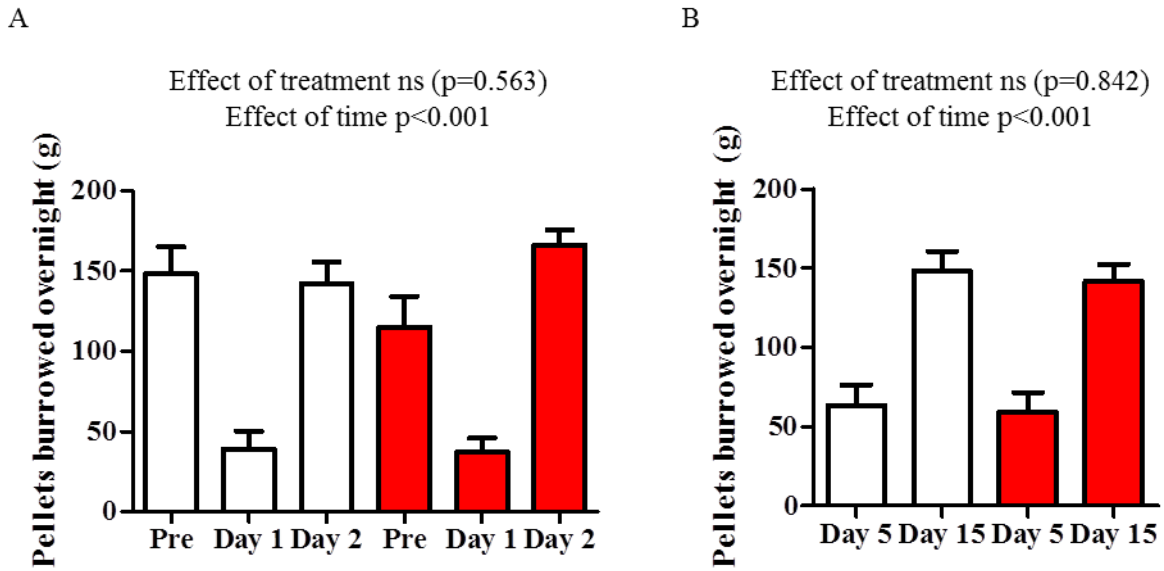

Figure 8-9 Amount of food pellets burrowed in after intracerebroventricular injection of NMDAR-IgG or healthy control IgG.

Overall there was no effect on burrowing performance between treatment mice receiving NMDAR-IgG (n=28) or control IgG (n=22) on days 0, 1 or two (A) or days 5 and 15 (B). IgG treatment reduced burrowing in all mice regardless of IgG treatment between days 0-2, which is likely to reflect the effect of surgery. Presented as mean ± SEM.

Locomotor activity changed over time on both trial days (effect of time: day 4 20mV $F_{(14,616)}$=35.228 p<0.001, day 4 50mV $F_{(14,616)}$=35.914 p<0.001; day 14 20mV $F_{(14,616)}$=38.814 p<0.001; day 4 50mV $F_{(14,616)}$=30.544 p<0.001, Figure 8-11), which was independent of IgG treatment (effect of treatment: day 4 20mV $F_{(1,44)}$=1.479 p=0.23; day 4 50mV $F_{(1,44)}$=0.134 p=0.716; day 14 20mV $F_{(1,44)}$=0.082 p=0.775; day 4 50mV $F_{(1,44)}$=0.372 p=0.545). This effect of treatment did not differ between cohorts (treatment*cohort: day 4 20mV $F_{(2,44)}$=0.638 p=0.533; day 4 50mV $F_{(2,44)}$=0.339 p=0.715; day 14 20mV $F_{(2,44)}$=0.520 p=0.598; day 14 50mV $F_{(2,44)}$=0.020 p=0.980). This likely represents the change in activity of all mice to lights on/off. The changes over time did not interact with treatment group (time*treatment interaction: day 4 20mV $F_{(14,616)}$=0.338 p=0.941; day 4 50mV $F_{(14,616)}$=1.036 p=0.399; day 14 20mV $F_{(14,616)}$=1.077 p=0.427; day 14 50mV $F_{(14,616)}$=1.363 p=0.242) but did interact with cohort (time*cohort interaction: day 4 20mV $F_{(28,616)}$=8.725 p<0.001; day 4 50mV $F_{(28,616)}$=10.352 p<0.001; day 14 20mV $F_{(28,616)}$=4.424 p<0.001; day 14 50mV $F_{(28,616)}$=4.705 p<0.001). No three way interaction was observed (time*treatment*cohort interaction: day 4 20mV $F_{(28,616)}$=1.060 p=0.393; day 4 50mV$_{(28,616)}$=0.643 p=0.785; day 14 20mV $F_{(28,616)}$=0.937 p=0.520; day 14 50mV $F_{(28,616)}$=1.306 p=0.232).

Motor performance was assessed on the rotarod on days 14 and 18. An effect of cohort was observed ($F_{(2,44)=}$7.125, p=0.002), therefore cohort was included as a between subject factor in further analyses. Rotarod performance was unaffected in NMDAR-IgG treated mice compared to mice receiving control IgG (effect of treatment: $F_{(1,44)}$=2.166 p=0.148, Figure 8-12). Cohort did not interact with treatment (treatment*cohort interaction $F_{(2,44)}$=0.260 p=0.768). There was no main effect of time ($F_{(1,44)}$=1.934 p=0.171), and time did not interact with treatment ($F_{(1,44)}$=1.130 p=0.294) or cohort ($F_{(2,44)}$=2.146 p=0.129).

Overall NMDAR-antibody injected mice showed no significant difference on locomotor activity compared to mice receiving healthy control IgG.

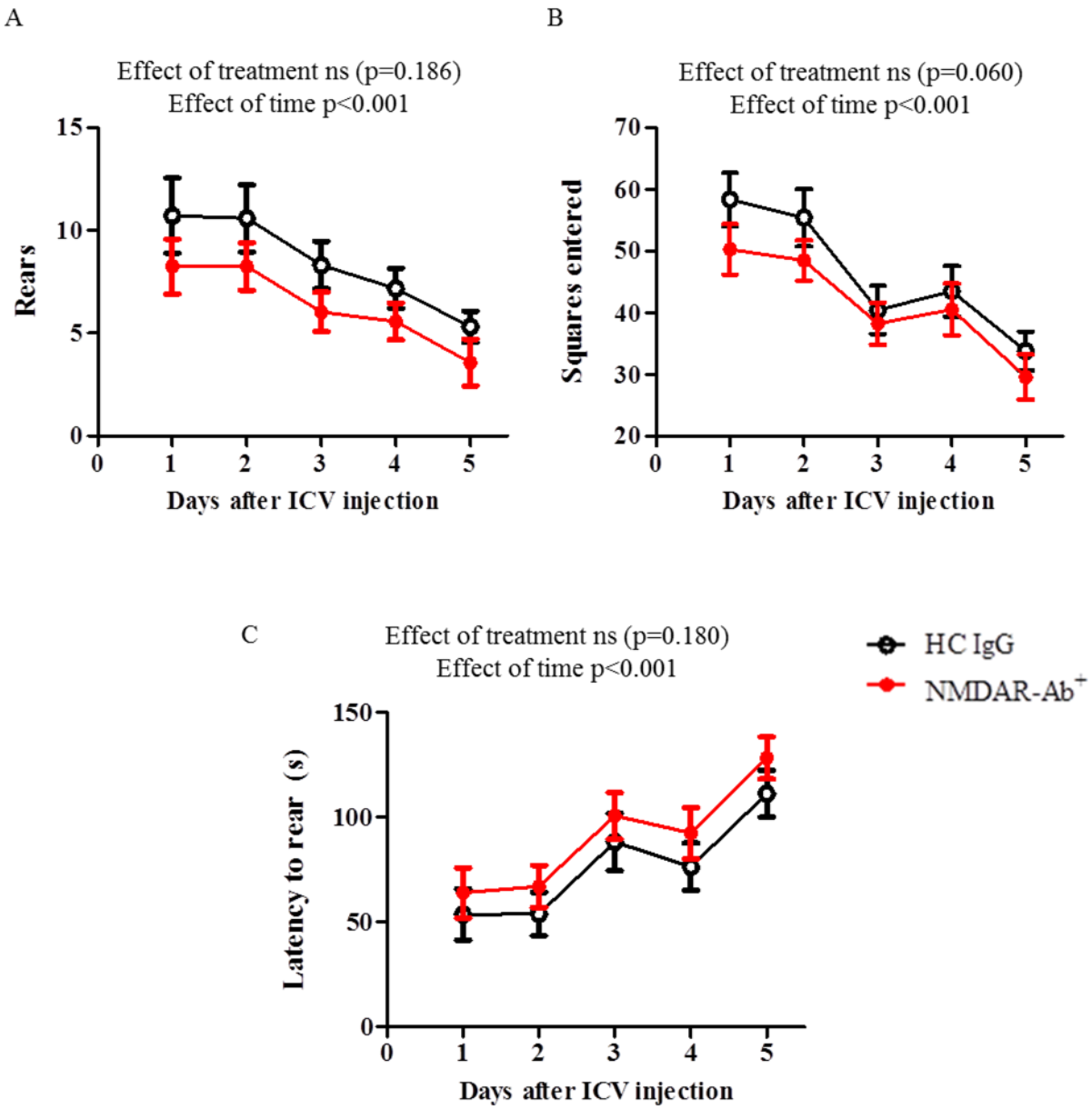

Figure 8-10 Locomotor activity of mice injected with NMDAR-IgG or healthy control IgG on the open field apparatus.

Overall there was no significant difference between mice receiving NMDAR-IgG (n=28) or healthy control IgG (n=22) at any of the five time points on either parameter; latency (A), number of rears (B) and number of squares entered (C). There was a significant effect of time on each parameter; however this did not interact with treatment (see main text). Presented as mean ± SEM.

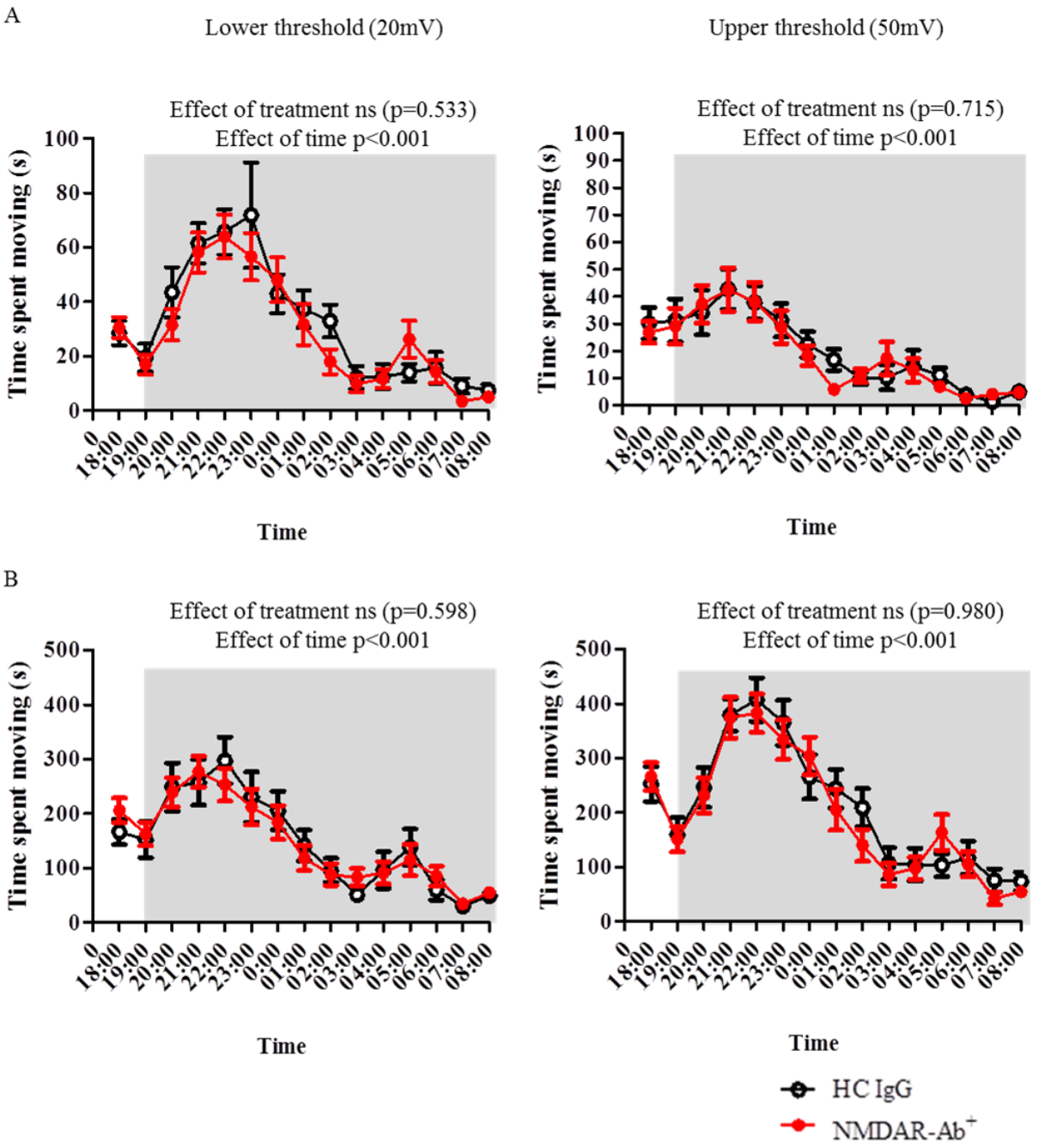

Figure 8-11 Locomotor activity of mice injected with NMDAR-IgG or healthy control IgG on the automated threshold activity system.

Overall levels of activity did not differ between mice receiving NMDAR-IgG (n=28) and HC-IgG (n=22) on day 4 (A) or day 14 (B) on either threshold (20mV and 50mV). Values represent activity in one hour blocks presented as mean ± SEM. The shaded area represents lights off between 19:00-07:00 hours.

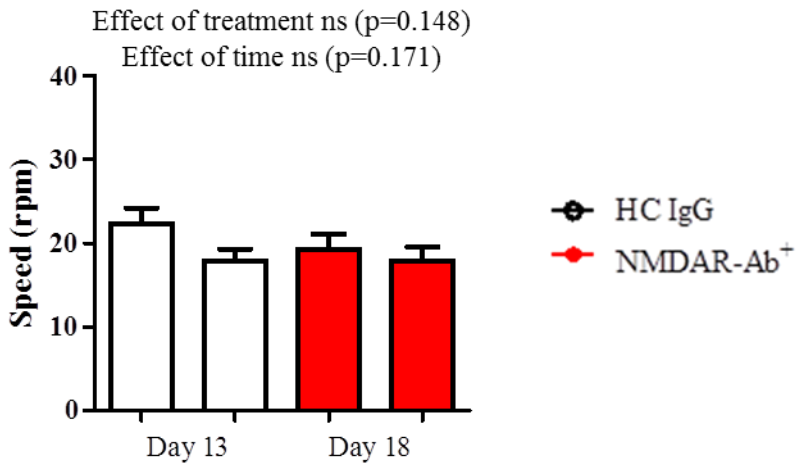

Figure 8-12 Accelerating rota rod after intracerebroventricular injection of NMDAR-IgG or healthy control IgG.

Motor coordination on the rotarod was not different between mice receiving NMDAR-IgG (n=28) or control IgG (n=22) on days 13 or day 18. Presented as mean ± SEM.

8.2.3 Tests of anxiety

Anxiety behaviours were measured on two tasks. On day 4, in the light-dark box, NMDAR-IgG mice spent similar amounts of time in the light area compared to control mice (effect of treatment $F_{(1,48)}$=0.134 p=0.716, Figure 8-13a) and no significant difference in the time it took for mice to enter the light area (latency: effect of treatment $F_{(1,48)}$=2.306 p=0.136, Figure 8-13b). Testing on the successive alleys on day 8 shows no effect of IgG on the latency for mice to enter alley two ($F_{(1,48)}$=0.009 p=0.924, Figure 8-13c) or the amounts of time spent out of alley one ($F_{(1,48)}$=2.796 p=0.101, Figure 8-13d), implying that there is no effect on anxiety levels in NMDAR-IgG treated mice.

8.2.4 General monitoring

During routine handling of cohort two, some mice were observed to transiently draw their hind limbs in towards their abdomen; we have called this observation “clasping”,

Figure 8-14a. Clasping is infrequently seen in wild-type mice (Lalonde & Strazielle, 2011), but has been observed in several models of neurodegenerative disease and motor dysfunction and can be assessed using the tail suspension test (Mangiarini et al. 1996). Briefly, mice were suspended by their tail, three times per day for 10 seconds each and their hind limbs observed for clasping behaviour. A clasping event was noted if mice withdrew one or both of their hind limbs in towards their abdomen instead of displaying the normal splaying of the limbs. Clasping behaviour was assessed each day for mice in cohort three.

Clasping was first observed in cohort two, 23 days after the initial ICV injection and was monitored until day 46. The last clasping event was observed on day 39, Figure 8-14b. Six mice receiving NMDAR-IgG displayed one or more clasping events compared to two mice injected with control IgG. Clasping behaviour over the testing period was collapsed, and mice receiving NMDAR- IgG displayed significantly more clasping events than healthy control mice ($p<0.004$, Fischer’s test). Mice receiving control IgG clasped five times in total over the testing period, compared to 96 times

clasping events in NMDAR-IgG mice, shown in Figure 8-14c. For cohort three, clasping was assessed immediately following surgery, every day until day 40. The first clasping event occurred ten days after ICV injection and the last on day 20. Six mice receiving NMDAR-IgG displayed one or more clasping events compared to one mouse injected with control IgG, Figure 8-15a. Total clasping events observed in NMDAR-IgG treated mice was fifteen compared to two in control mice over 40 days ($p=0.058$, Fisher's test). NMDAR-Ab^{+} treated mice were seen to display significantly more clasping behaviour than mice receiving control IgG when collapsing the data between days 10-20 ($p=0.039$, Fisher's test, Figure 8-15b).

Despite seizures not being systematically studied, two mice receiving NMDAR- IgG had abnormal, "seizure-like" events during the behavioural testing period. One mouse (cohort 1) fell abruptly from the cage wall, into the cage. There were no visible signs of seizures, however the mouse remained stationary and un-responsive to inquisitive cage mates and handling. After five minutes the mouse began to move once again. The second mouse (cohort 2) showed rippling/contractions of its body during routine handling. These events were only observed once in each mouse, and were observed on days 17 and 20 respectively.

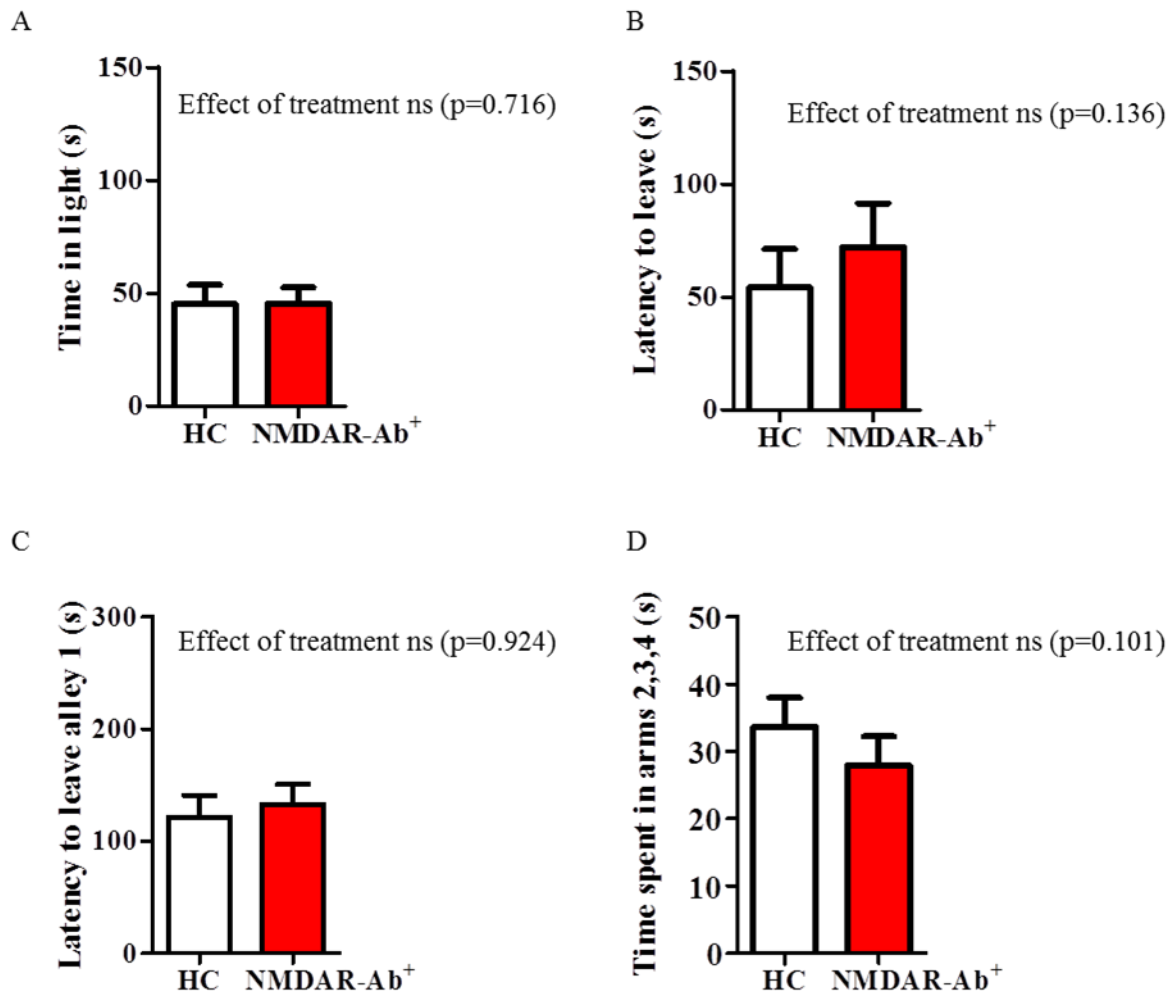

Figure 8-13 Mice receiving NMDAR-IgG show no anxiety behaviours.

Overall there was no effect on anxiety levels in mice receiving NMDAR-IgG (n=28) compared to mice receiving control IgG (n=22) in the on the time spent in the light (A) or the latency to leave the dark area (B) in the light-dark box. In the successive alleys mice showed no difference in the latency to leave alley 1 (C) and the combined time spent in alleys 2,3 and 4 (D). Presented as mean ± SEM.

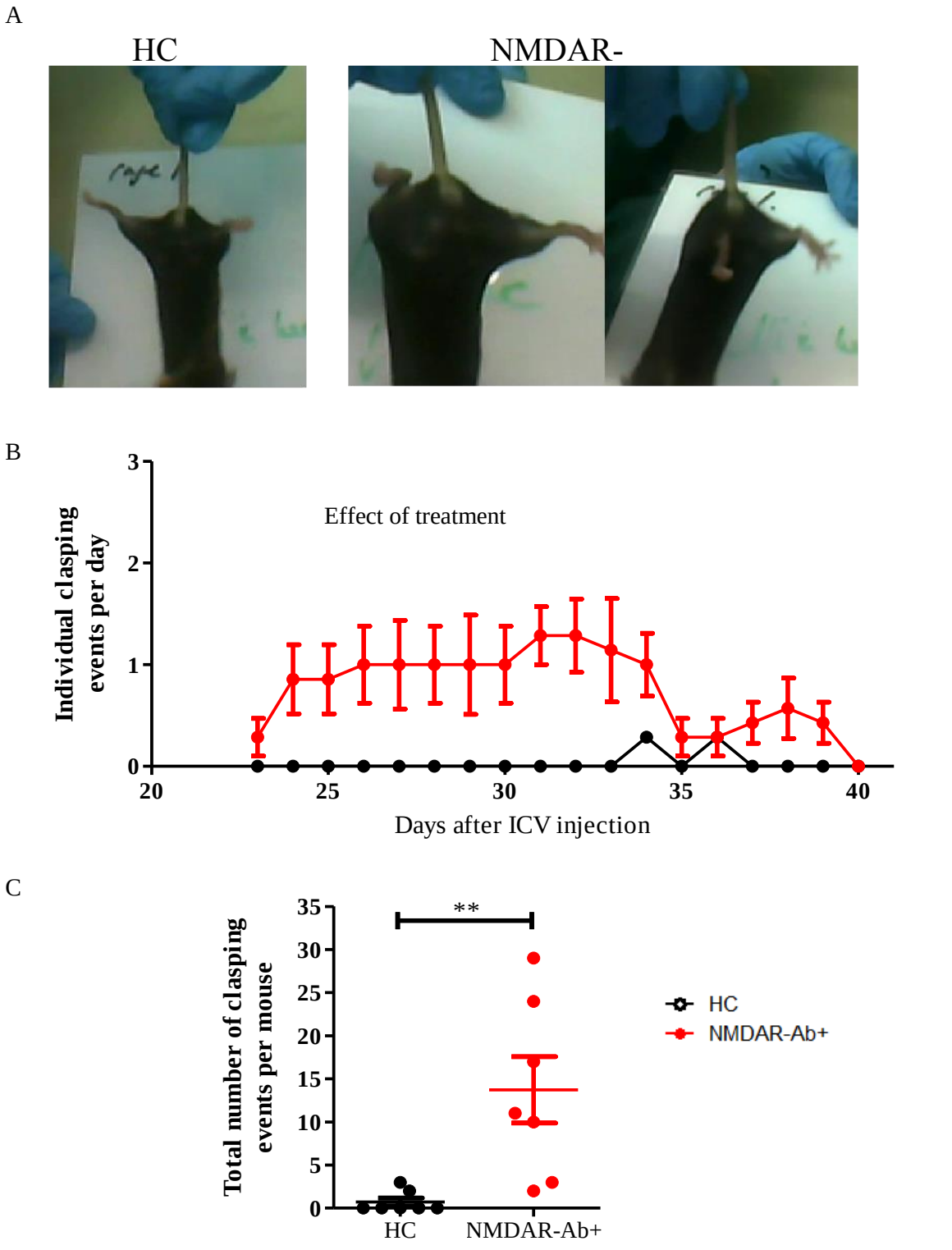

Figure 8-14 Cohort 2: Clasping behaviour of mice injected with NMDAR-IgG or healthy control IgG

A) NMDAR-Ab treated mice exhibited clasping behaviours when suspended by the tail. Clasping was defined as drawing one or both legs up to the body. B) Number of clasping evens were observed between days 23-39 and C) and clasping behaviour was seen more frequently in NMDAR-Ab treated mice (p=0.004, Mann Whitney). Data presented as total clasping events per mouse.

A

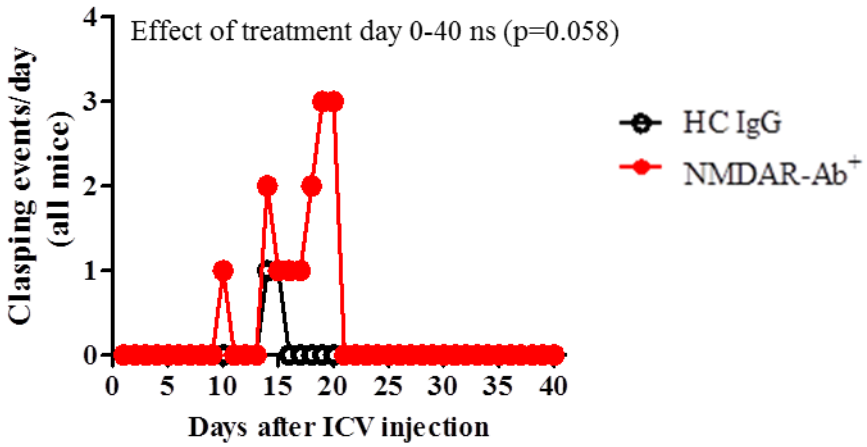

B

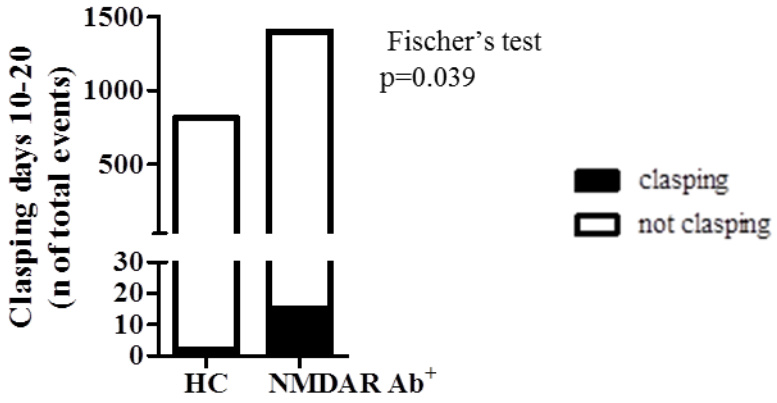

Figure 8-15 Cohort 3: Clasping behaviour of NMDAR-IgG treated mice.

A) Clasping behaviour was first observed on day 10 and last observed on day 20. B) Mice receiving NMDAR-IgG displayed significantly more clasping behaviours than mice receiving healthy control IgG when the data are collapsed across day 10-20. Data presented as total events.

8.2.5 Tests of cognition

Cognition was assessed by spontaneous alternation on a T-maze task. Cohort one was analysed separately to cohorts two and three, as performance on the T-maze task was not assessed daily.

In cohort one (healthy control IgG n=6, NMDAR-IgG n=6) performance on the spontaneous alternation task, over days 1-44 showed an effect of time ($F_{(25,250)}$=4.395 p=0.009). Mice receiving NMDAR- IgG showed reduced alternation compared to mice receiving control IgG (effect of treatment $F_{(1,10)}$=21.292, p=0.001, Figure 8-16). After correction for sphericity of the data, the alternation performance over time does not interact with treatment (time*treatment interaction $F_{(25,250)}$=2.116 p=0.081, using the Greenhouse Geisser correction) but a trend towards an interaction is observed. If not corrected however performance alternation shows a statistically significant difference across time (time*treatment interaction $F_{(25,250)}$=2.116 p=0.002).

Data for cohorts two (healthy control IgG n=7, NMDAR- IgG n=7) and three (healthy control IgG n=5, NMDAR- IgG n=9) were combined for mice tested over days 1-40 and grouped into four day blocks (total cohorts one and two; healthy control IgG n=12, NMDAR- IgG n=16). No effect of cohort was observed ($F_{(1,24)}$=0.680, p=0.418), so cohort was excluded as a between subject factor. Mice receiving NMDAR-IgG alternated significantly less than control mice (effect of treatment; $F_{(1,26)}$=16.288 p<0.001), and there was no main effect of time observed (effect of time $F_{(9,234)}$=1.541, p=0.135, Figure 8-17).

As mice in cohort two received the same patient IgG preparations as cohort one, cohorts two and three were split to look at the effects of time in each cohort. In cohort two a main effect of time ($F_{(9,108)}$=4.190, p<0.001) was observed which interacted with IgG treatment (time*treatment $F_{(9,108)}$=2.134, p=0.033, Figure 8-18a). Simple main effects analysis revealed an effect on spontaneous alternation on grouped days 4-8, 13-16 and 20-24. No effect of time was observed in cohort three ($F_{(9,108)}$=0.801, p=0.616, Figure 8-18b).

Three different NMDAR- patient IgGs were used in the third cohort of mice, however no difference in spontaneous alternation was observed for mice in cohort 3 injected with either NMDAR- IgG from patient #3, #4 or #7 (effect of treatment; $F_{(2,12)}$=0.487, p=0.626).

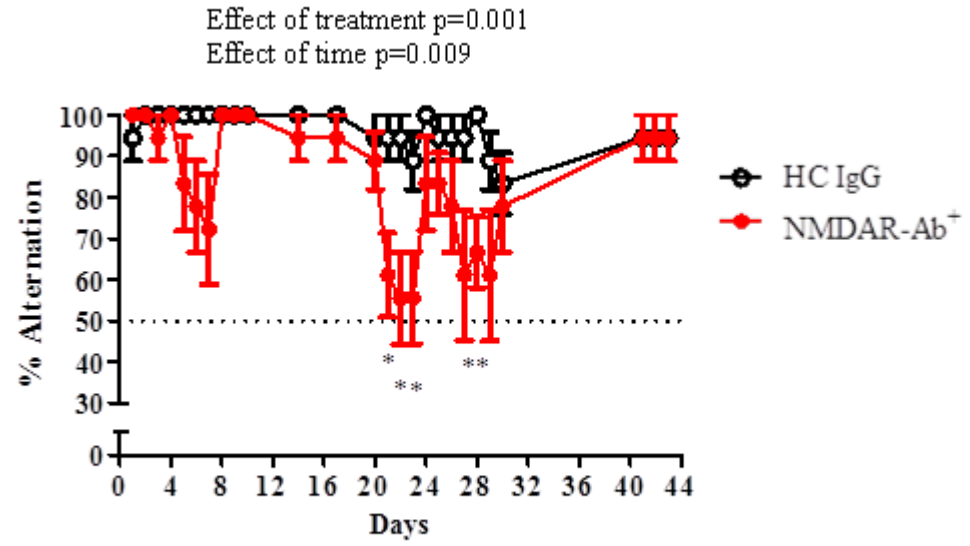

Figure 8-16 Cohort 1: Percentage of correct spontaneous alternation trials for mice injected with NMDAR-IgG or healthy control IgG.

Mice receiving NMDAR- IgG (n=6) showed reduced spontaneous alternation compared to mice receiving control IgG (n=6), p=0.001.Presented as mean ± SEM. Dotted line at 50% represents chance performance.

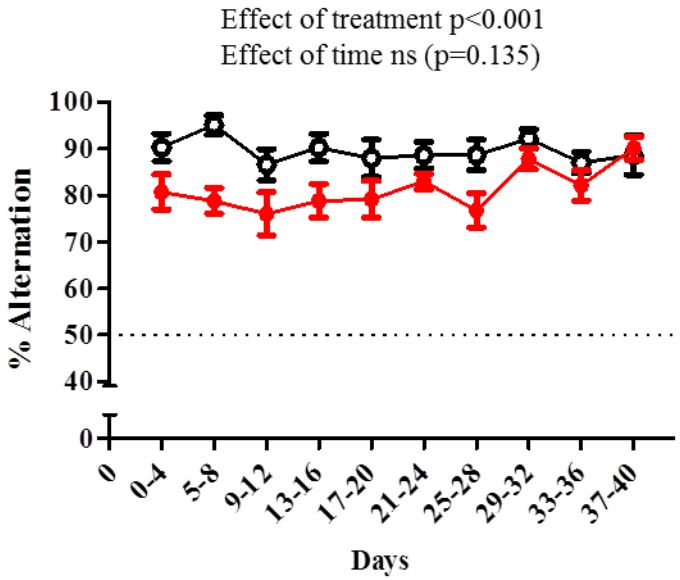

Figure 8-17 Cohort 2&3: Percentage of correct spontaneous alternation behaviour for mice injected with NMDAR-IgG or healthy control IgG.

Mice receiving NMDAR-IgG (n=16) showed reduced spontaneous alternation compared to mice receiving control IgG (n=12), p<0.001. Presented as mean ± SEM. Dotted line at 50% represents chance performance.

A

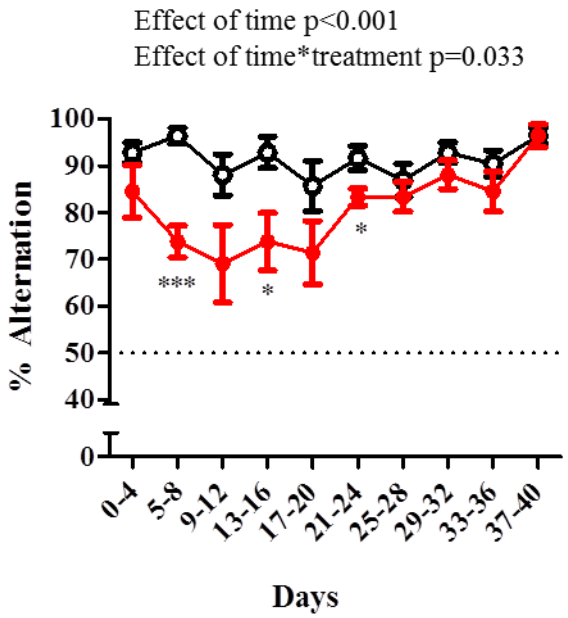

B

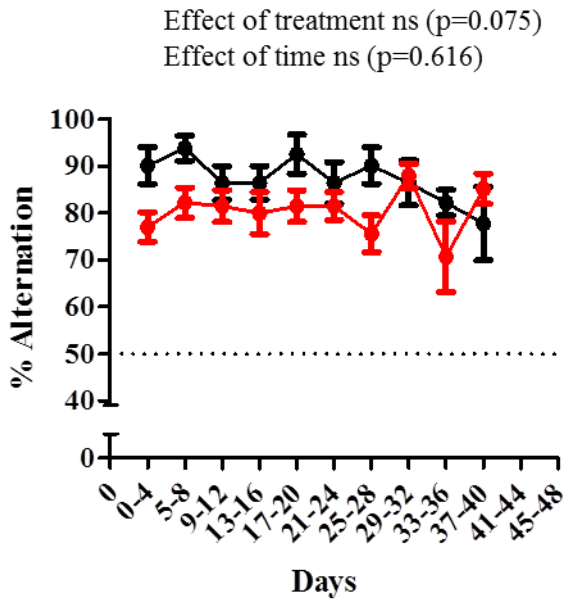

C

Simple main effects

Day	F(1,12)	p value
1-4	1.934	0.190
5-8	36.100	**<0.001**
9-12	4.129	0.065
13-16	7.385	**0.019**
17-20	2.734	0.124
21-24	7.000	**0.021**
25-28	0.562	0.230
29-32	1.600	0.468
33-36	1.364	0.266
37-40	0.000	1.00

Figure 8-18 Spontaneous alternation behaviour for mice injected with NMDAR-IgG or healthy control IgG (cohorts 2 and 3 individually).

A) Cohort 2: NMDAR-IgG (n=7) mice show a reduction in spontaneous alternation compared to mice receiving control IgG (n=7) which shows a significant interaction with time between days 5-24. B) Cohort 3: NMDAR-IgG (n=9) do not have a statistically significant reduction in spontaneous alternation compared to control-IgG mice (n=6). Dotted line at 50%, represents chance performance.

8.3 Immunohistological analysis of ICV tissue

One mouse that died during the stereotaxic procedure was injected with Evan's blue instead of IgG, to verify the injection coordinates were correct. Evan's blue was identified in the ventricular system as seen in Figure 8-19.

8.3.1 Human IgG deposition after intracerebroventricular injection

In order to assess the amount of IgG distributed in the brain immediately after injection, two mice receiving healthy control IgG were sacrificed one hour and 24 hours after injection. Mice were PBS and PFA perfused, post fixed and cryoprotected before sectioning. A brain that was not injected was used as a control. As the mice were PBS perfused, any IgG present in the blood should have been removed during the perfusion process. Subsequent PFA perfusion and post-fixation of the brain cross-links bound or unbound IgG present in the parenchyma. At one hour, human IgG staining was not found in blood vessels but was primarily observed predominantly close to the ventricles in IgG injected mice. More specifically, healthy control IgG was observed on the ventricular ependymal cells, the molecular layer of the hippocampus (directly next to the ventricle) and the corpus callosum, Figure 8-20 and 8-21. Progressively weaker detection of IgG was observed away from the ventricle, possibly representing the diffusion of IgG through the tissue. As the healthy control IgG used in this study did not bind specifically to mouse brain, as shown in Figure 8-20, this IgG immunoreactivity is unlikely to represents specific IgG binding, but merely the access of IgG in the brain parenchyma after intrathecal injection. IgG was not observed in mouse brains sacrificed 24 hours after injection. Weak human IgG staining was seen in some sections near the ependymal walls of the ventricle, indicating that most of the IgG had been removed from the CSF or had diffused into the brain parenchyma below the level of detection.

Detection of anti-human IgG was not observed in non-injected mice. Mouse IgG was not detected in the hippocampus or around the ventricle one hour after injection, illustrating that this effect is not due to cross-reactivity of mouse and human IgG, Figure 8-23.

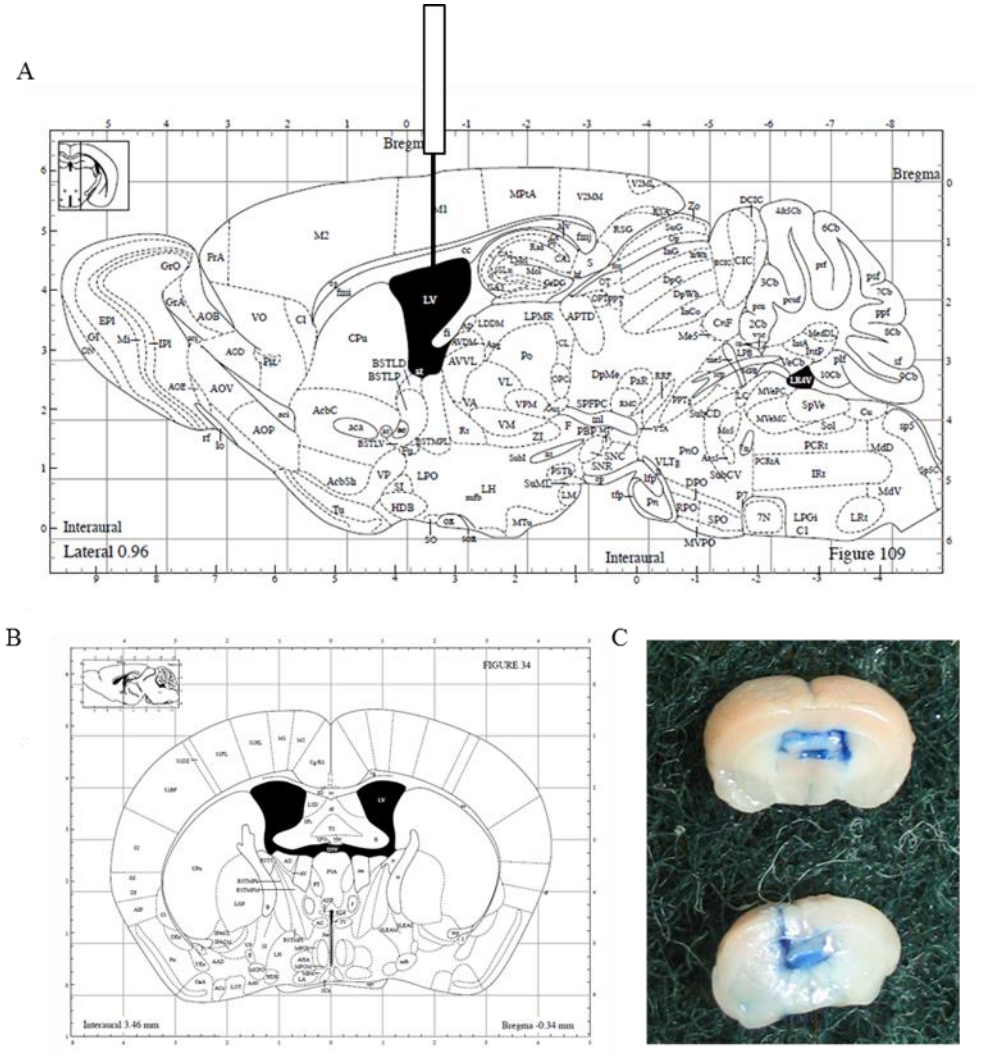

Figure 8-19 Verification of needle placement into the lateral ventricle.

A) Reconstruction of sagittal and B) coronal images of the injection site for intracerebroventricular injection. Stereotaxic coordinates from bregma are anterior-posterior -0.34mm, lateral +1.0mm, ventral -2.3mm. C) Injection of Evan's blue dye in to the lateral ventricle can be seen in the ventricular system and along the needle tract.
Figures taken from the Paxinos and Franklin 2001.

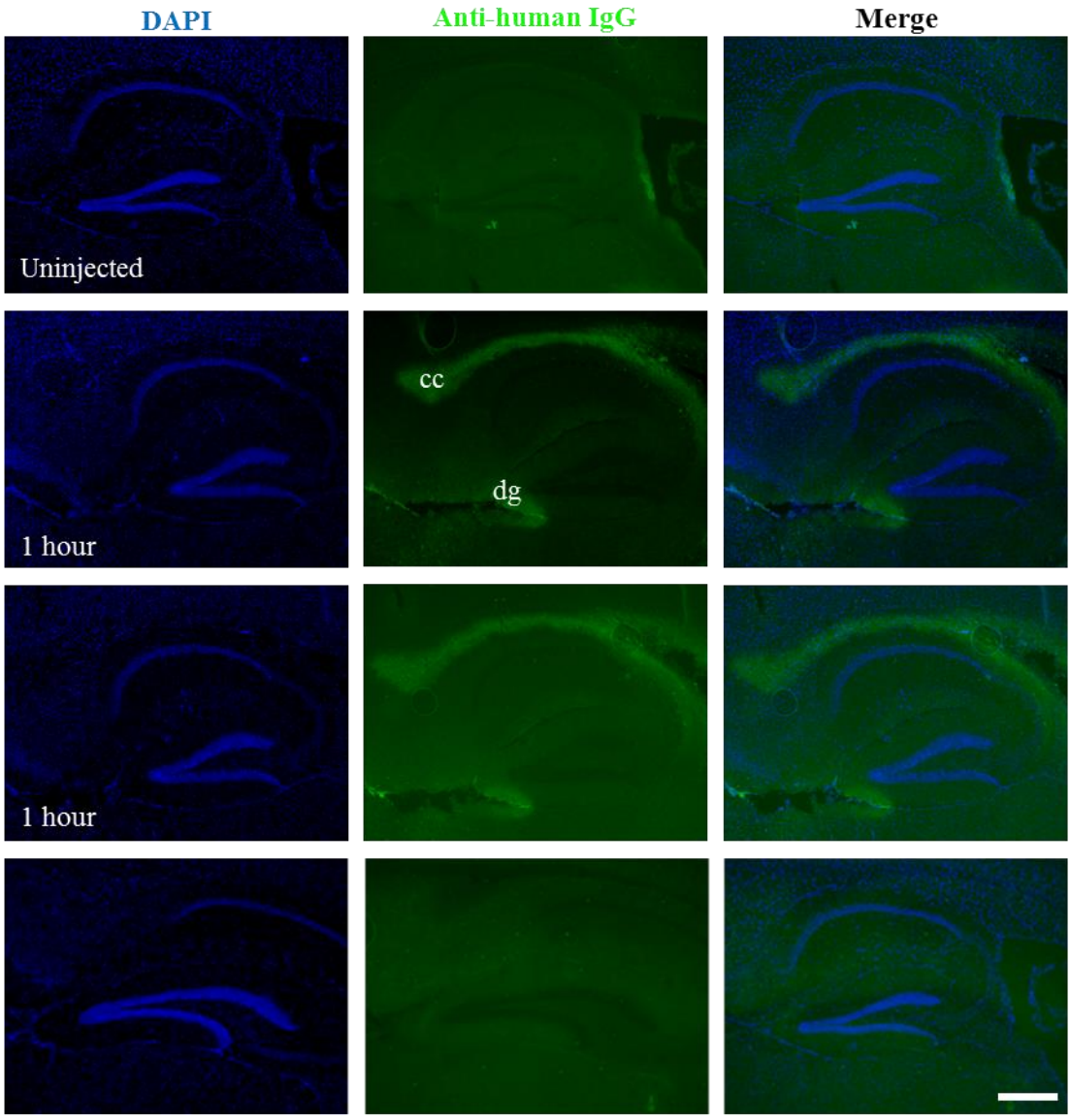

Figure 8-20 Healthy control IgG is present in the brain parenchyma one hour after intracerebroventricular injection.

No human IgG was detected in the brains of un-injected mice (top) or mice sacrificed 24 hours after injection (bottom row). IgG was detected in the brains of mice that were sacrificed one hour after injection (row two and three) in the corpus callosum and in the molecular layer of the hippocampus (adjacent to the ventricle). Magnification 50x, scale bar = 400µm cc=corpus callosum, dg= dentate gyrus.

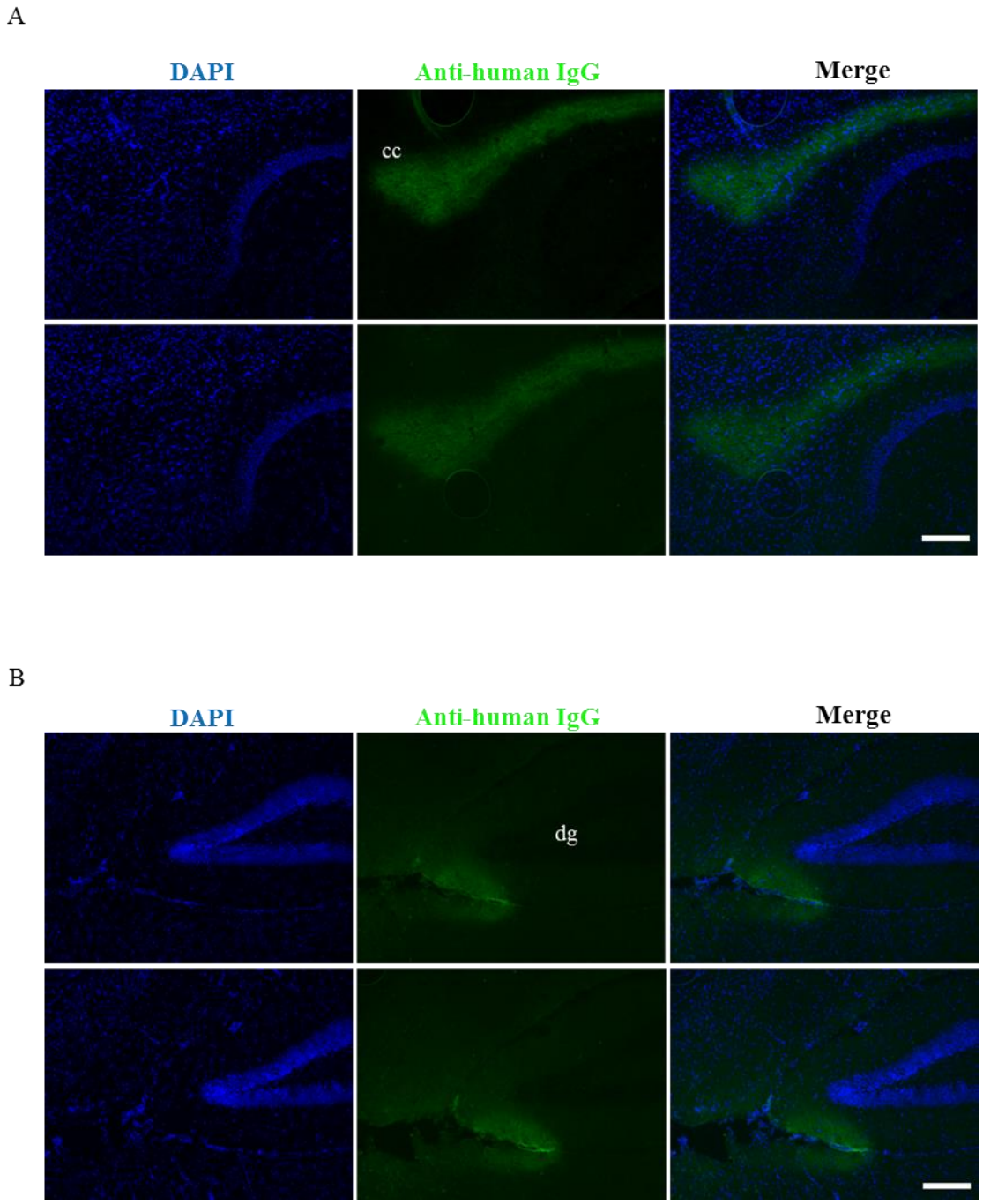

Figure 8-21 Two higher magnification images of healthy control IgG in the brain parenchyma

A) IgG was present in the corpus callosum and B) the molecular layer of the dentate gyrus one hour after intracerebroventricular injection. Magnification 100x, scale bar = 200µm. cc=corpus callosum, dg= dentate gyrus.

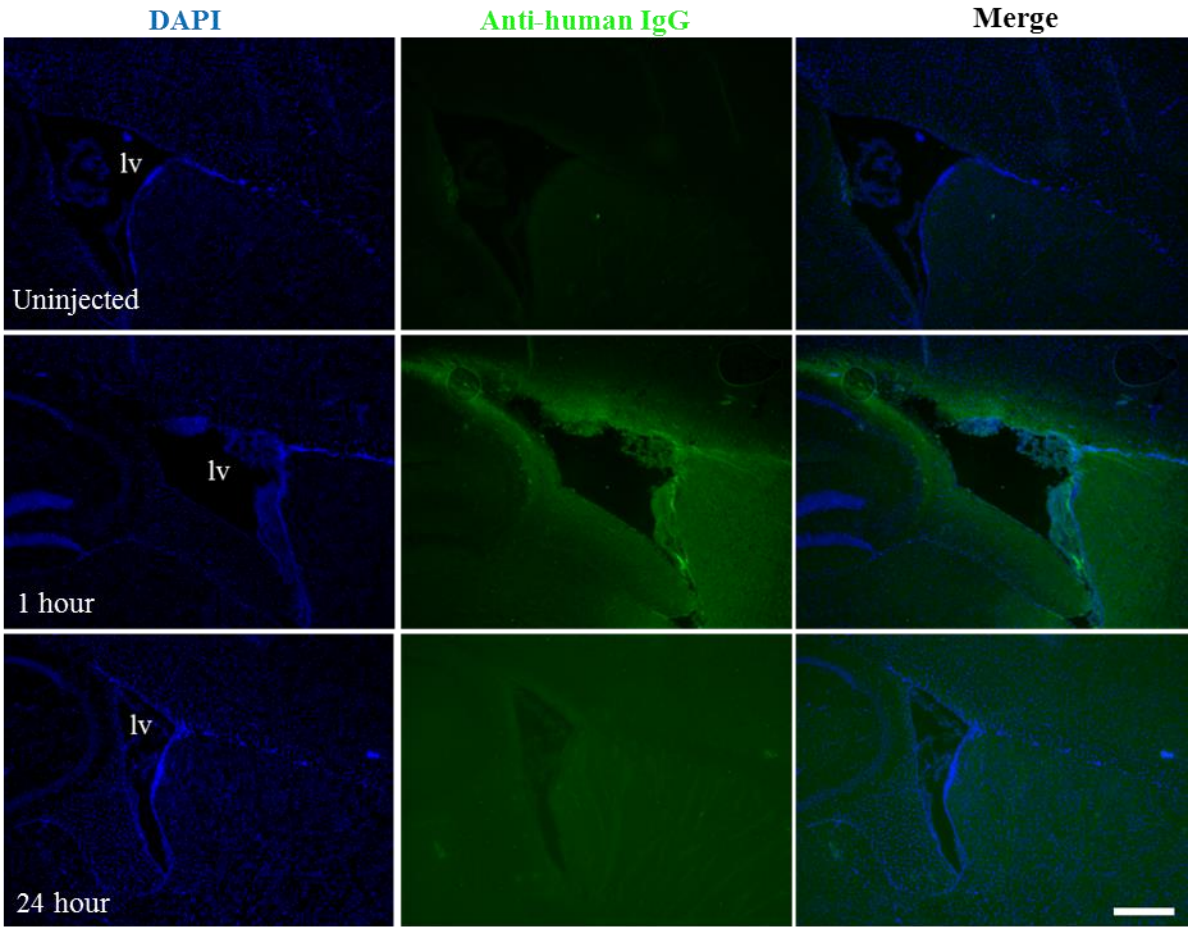

Figure 8-22 Healthy control IgG is detected around the lateral ventricle one hour after intracerebroventricular injection.

Immunostaining for human IgG is not visible around the ventricle in uninjected mice (top panel) or mice sacrificed 24 hours after injection (bottom panel). IgG can be seen around the ventricle in mice sacrificed one hour after injection (middle panel). Magnification 50x, scale bar = 400µm lv=lateral ventricle.

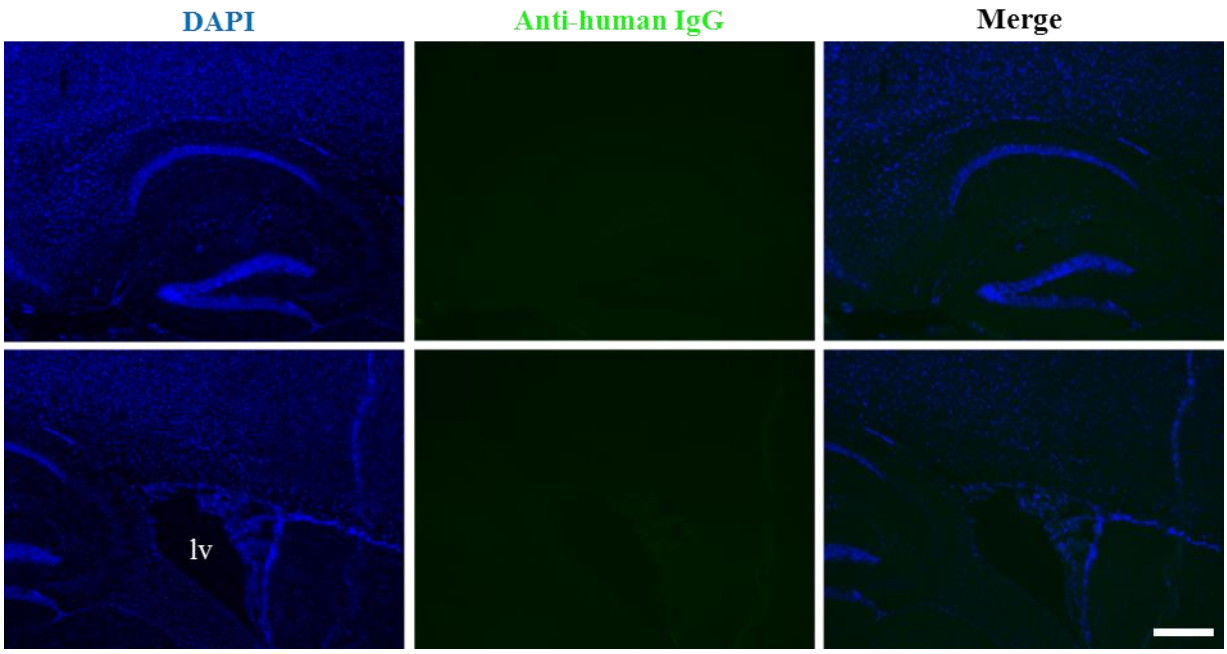

Figure 8-23 Mouse IgG was not present in the brain parenchyma one hour after intracerebroventricular injection of human IgG.

Mouse IgG was not detected in the hippocampus, corpus callosum (top panel) or the lateral ventricle (bottom panel). Magnification 50x, scale bar = 400µm cc=corpus callosum, dg=dentate gyrus, lv=lateral ventricle.

8.3.2 Quantification of NR1 expression in the hippocampus after intracerebral injection

Hippocampi were dissected from wild-type mice (n=1), NR1-hypomorph mice (n=1), and ICV injected mice (NMDAR-IgG n=20, HC-IgG n=10) culled on either day 22 or day 46; homogenised and their protein content measured. 10 μg of hippocampi protein extract were loaded on to Western blot. Probing wild type mouse brain with an NR1-commercial antibody shows a band at ~130kDa which represents the NR1 subunit of the NMDA receptor. Equal loading of NR1 hypomorph brain shows a faint band of the same molecular weight compared to wild-type tissue. The intensity of the NR1 band for 30 ICV mice was calculated using Image J software. Representative blots of wild-type mice, NR1 hypomorph, and ICV-injected mice and densitometry analysis can be seen in Figure 8-24a. No difference in densitometry analysis was seen between healthy control and NMDAR-IgG treated mice at either day 22 or day 46 after ICV injection (effect of treatment: day 22 p=0.956; day 46 p=0.393, Figure 8-24b.

8.4 Immunostaining for GFAP and CD68

As NMDARs have been reported on astrocytes and microglia, brains culled on day 22 or day 46 were stained for GFAP and CD68. No gross differences were observed for astrocyte of microglia activation in the hippocampus at day 22 or day 46. Representative images can be seen in Figures 8-25 and 8-26. Tissue was not taken immediately after ICV injection, but it may have been useful to compare possible earlier effects of NMDAR antibodies on microglia and astrocytes.

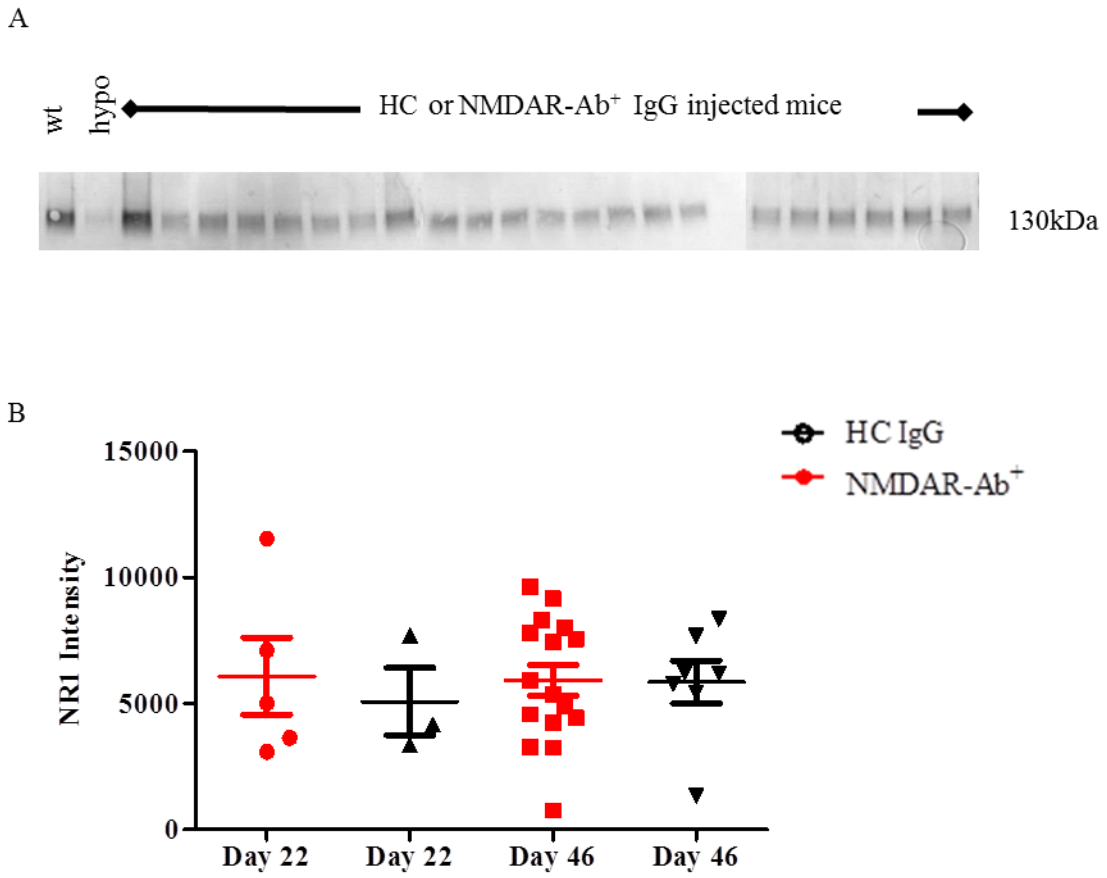

Figure 8-24 Quantification of NR1 expression in the hippocampus of mice injected with NMDAR-IgG and control IgG.

10µg of hippocampal extract from wild-type, NR1 hypomorph (10% NR1 expression) and ICV-IgG mice (control IgG n=10, NMDAR-IgG n=20) were probed for NR1 expression. A) Representative bands for NR1 on Western blot have a molecular weight above 130 kDa. B) Quantification of NR1 band intensity using Image J software shows no significant difference in mice receiving control or NMDAR-IgG on day 22 or day 46 (Mann Whitney p=0.956 and p=0.393 respectively).

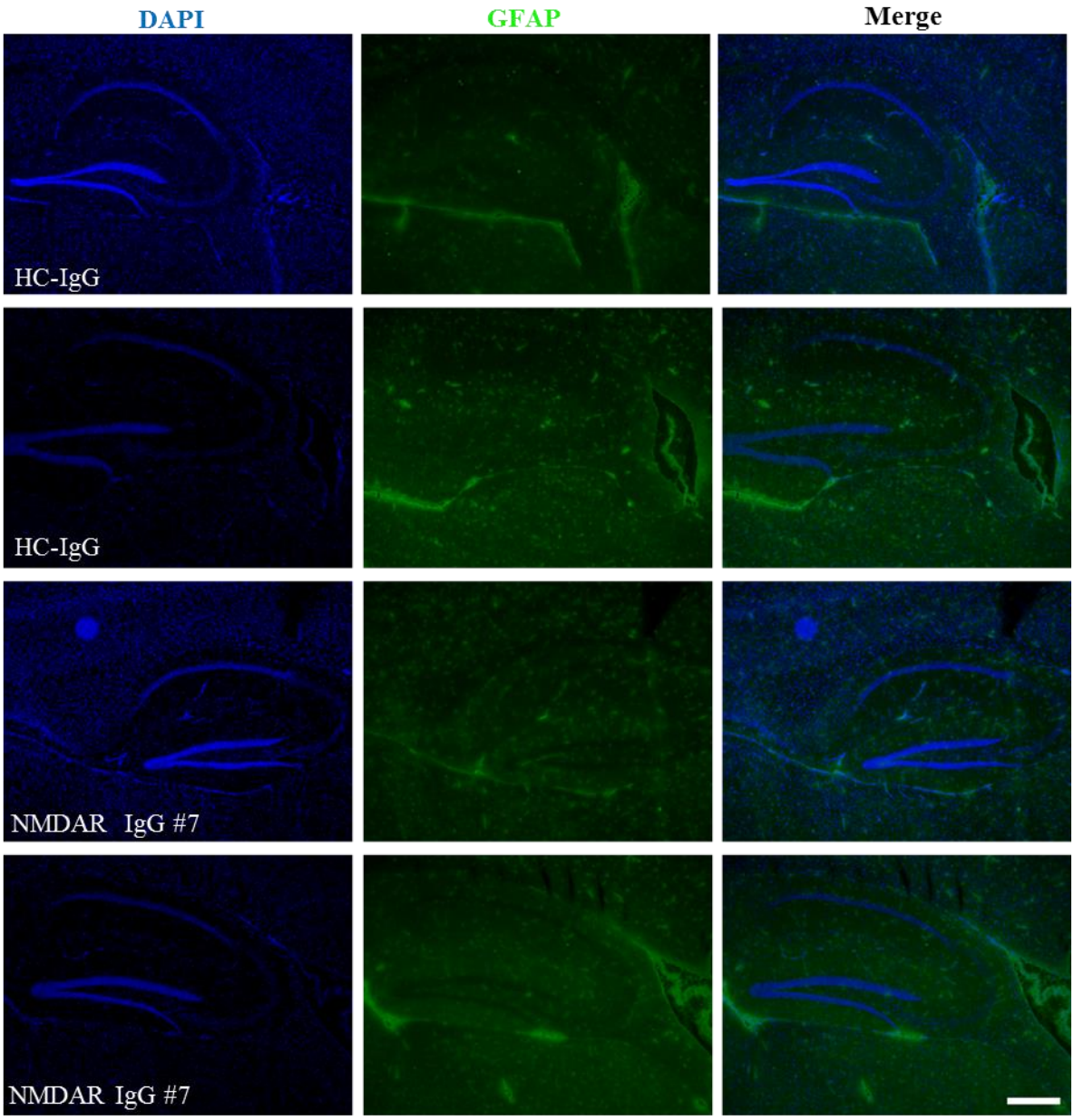

Figure 8-25 Astrocyte staining in the hippocampus.

No gross differences were observed for GFAP staining in the hippocampus of mice following intracerebroventricular injection of control IgG (top) or NMDAR-IgG (bottom). Magnification 50x, scale bar = 400µm.

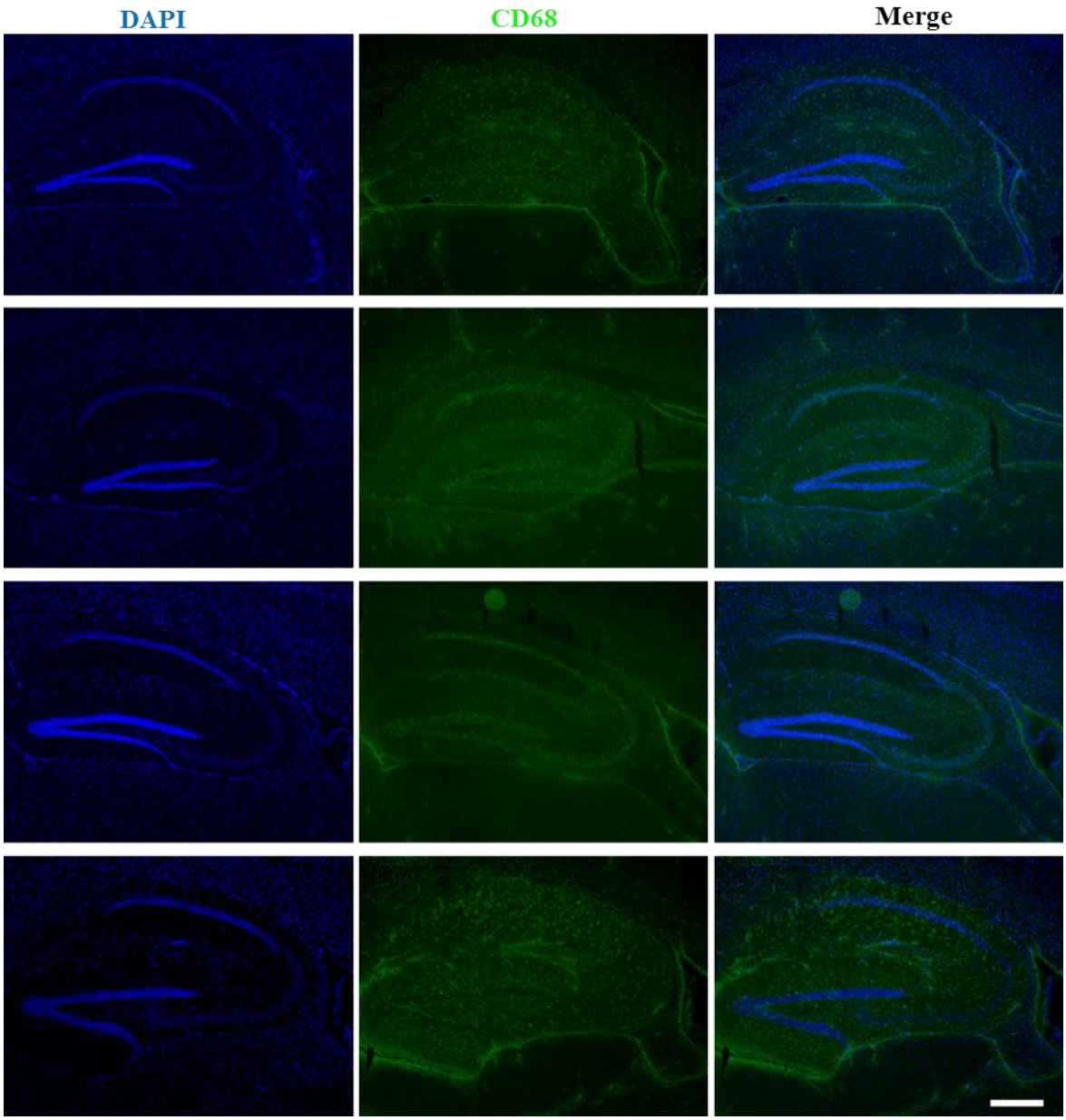

Figure 8-26 Microglia staining in the hippocampus.

No gross differences were observed for microglial activation (CD68) staining in the hippocampus of mice following intracerebroventricular injection of control IgG (top) or NMDAR-IgG (bottom). Magnification 50x, scale bar = 400µm.

8.5 Discussion

Antibodies to the NMDARs have recently been described in an immunotherapy responsive encephalopathy. Antibodies are detected against the surface of HEK cells transfected with the NR1 and NR2 subunits of the NMDAR, bind to rodent brain in a pattern consistent with NMDAR distribution and have been shown to be bind predominantly to the extracellular N-terminus of the NR1 subunit (Dalmau 2008). Initial investigations show NMDAR-antibodies reduced surface expression of by cross-linking and internalisation of the NMDARs on hippocampal primary cultures, and this process was shown to be reversible upon antibody removal (Dalmau, 2007). Autopsy findings and continuous infusion of patient antibodies into rat hippocampus showed a similar reduction in NR1 expression (Hughes, 2010). To investigate whether NMDAR-antibodies could produce features of disease *in vivo*, IgG was purified from three patients with high NMDAR-antibody titers and injected into the lateral ventricle of mice.

8.5.1 Detection of NMDAR-antibodies: binding to neuronal tissue

Immunohistochemical analysis is the first stage of screening sera for autoantibodies against CNS proteins. In the first large cohort of patients described with NMDAR-antibody encephalitis, Dalmau *et al* 2008 reported three criteria were fulfilled to confirm antibody positivity; patient IgG should bind to rodent brain sections (IHC), the surface of live hippocampal neurons and to HEK cells transfected with NR1/NR2 subunits. All seven patients used in this thesis bound to the surface of unpermeablised HEK cells transfected with either the human NR1 and NR2B subunits or the NR1 subunit alone, however only five of seven NMDAR-antibody positive patients' plasma samples bound to rodent brain sections and live primary cultures. Similar methods to those reported by Dalmau *et al* were used to study IHC reactivity, although there were a few amendments to the methods including the use of fresh unfixed tissue, the development of antibody reactivity and the use of plasma and not serum or CSF. It is probable that the IgG content in the plasma samples were lower than those found in serum, although this was not investigated, which may account for the negative immunoreactivity on brain sections in the two patients. However the authors did not specifically report whether patient CSF, sera, or both were all positive by IHC. Vitaliani *et al* reported 2/2 patients whose CSF (diluted 1:10) immunoreactivity was stronger than that of patient sera (diluted 1:250) on rat brain sections and similarly five patients with new-onset

epilepsy and NMDAR antibodies in their serum and CSF by CBA, were only positive by IHC using CSF (undiluted) and not serum (diluted 1:500) (Vitaliani, 2005; Niehusmann, 2009). It is likely that IHC screening of serum and plasma samples is not as sensitive as transfected HEK cells for detecting autoantibodies in patients with lower antibody titers. This is consistent with our IHC results where immunoreactivity against the hippocampal neuropil correlated with NMDAR-antibody titer by CBA.

Patients present initially with neuropsychiatric features and seizures and subsequently develop a movement disorder, reduced consciousness and autonomic instability. Irani *et al* hypothesised that the two phases of disease may be explained by intrathecal synthesis of IgG or alternatively antigen spreading may account for the some of the later features of disease (Irani, 2010b). As two of the three patients used in these *in vivo* experiments developed dyskinesia before undergoing plasma exchange, NMDAR-antibodies were adsorbed against HEK cells expressing NR1 and NR2B subunits. After preadsorption, patient IgG no longer bound to NMDA transfected HEK cells. More importantly, binding to the surface of live hippocampal neurons was also abolished. This result indicates the NMDAR-antibodies are the only antibodies that can be detected in these patient plasmas binding to hippocampal surface proteins. However this result does not exclude other reactive antibodies in the sera or CSF to other non-hippocampal brain regions. In contrast, others have suggested the development of dyskinesias, are similar to a dose-dependent antagonism of the NMDAR and it may be that the extended presence of antibodies is more pathologically relevant (Dalmau, 2011). Future studies investigating any changes of the serum and CSF immunoreactivity to rat brain sections may help to clarify whether there are other antibodies in these samples.

8.5.2 Overview of in vivo findings

To establish whether the NMDAR- antibody is indeed pathogenic purified IgG from patients with NMDAR-antibody encephalitis and healthy controls were passively transferred to mice. Overall we hoped the mice would manifest some of the visible features characteristic of NMDAR-encephalitis including seizures, psychiatric disturbance and a movement disorder. As mice passively transferred with patient IgG do not always manifest an overt clinical phenotype, mice were screened on a variety of behavioural tests to assess their general wellbeing, activity, anxiety and memory performance.

Gross investigation of mice showed no effect of NMDAR-antibodies on burrowing, activity levels measured on the open field task, an automated activity box or the rotarod. Anxiety was assessed using the light/dark box and successive alleys, and neither task on any operating day assessed showed a difference in mouse behaviour. NMDAR-antibody mice showed a small but significant effect on body weight ($p=0.046$), a deficit in the spontaneous alternation task in all cohorts tested ($p=0.001$ and $p<0.001$) and displayed significantly higher levels of clasping behaviour than seen in control injected animals ($p=0.004$ and $p=0.0396$). Although no formal EEG monitoring was assessed in the study, two seizure-like events were observed on days 17 and 20 in two mice that were injected with NMDAR-IgG.

NMDAR and increased body weight

Mice injected with NMDAR-IgG showed a small increase in body weight ($p=0.046$), despite no reduction in motor activity. Although the amount of food consumed was not measured in these experiments, the increase in body weight could be a result of increased food consumption. Hyperphagia has been reported in NR1 hypomorph mice (Barkus, 2012) as well as wild-type mice injected with NMDAR antagonists, MK-801 and APV-5, either into the intrathecal compartment or directly into the hindbrain (Covasa, 2004; Hung, 2006). Perhaps most relevant, hyperphagia has been reported as a feature of some patients with NMDAR-antibodies (Dalmau, 2011) and has recently been described in a 22 year old female in the absence of any neurological or psychiatric symptoms (Perogamvros, 2012). If NMDAR antibodies can access brain areas controlling feeding behaviours, it seems plausible that normal feeding can be disrupted, leading to a transient increase in body weight seen in this model.

NMDAR and spontaneous alternation

The spontaneous alternation task is popular within the pharmaceutical industry for discriminating whether or not a drug affects memory. The task is a measure of exploratory behaviour in the rodent and relies on the rodent remembering where it has been in the first trial and alternating its choice in the second trial. Cognitive impairment occurs early in the presentation of NMDAR-antibody encephalitis, and is observed in up to 80 % of patients (Titualer, 2013). Mice receiving NMDAR-antibodies showed a

significant impairment on spontaneous alternation behaviour in cohort 1 ($p=0.001$) and in combined data for cohorts 2 and 3 ($p<0.001$). Lesions of the hippocampus impair alternation performance (Deacon, 2002). Similarly intrahippocampal injection of NMDAR antagonists such as D-(-)-2-amino-5-phosphonopentanoic acid (D-AP5) reduces alternation performance in rodents (McHugh, 2008). Recently, behavioural assessment of NR1 hypomorph mice (5-10% expression) demonstrated cognitive deficits on multiple behaviour tasks including deficits on spontaneous alternation behaviour (Barkus, 2012). Despite this, spontaneous alternation is not purely hippocampal-dependent, as lesions to other brain regions including the cerebellum and basal ganglia also affect spontaneous alternation performance (Lalonde, 2002). Furthermore levels of anxiety and arousal in rodents have also been shown to have a negative effect on alternation behaviour (Bats, 2001). However mice receiving NMDAR-IgG displayed no obvious effect on anxiety behaviours, measured by successive alleys and light dark box, indicating that the deficit on the task might represent cognitive dysfunction.

NMDAR and movement disorder

NMDAR-antibody treated mice showed significantly higher levels of clasping behaviour than control mice. This effect was first seen in cohort 2 ($p=0.004$) and was also observed in cohort 3 but was only significant when analysed between days 10-21 ($p<0.036$). The pathophysiology of clasping is not completely understood. Clasping is not typically seen in wild-type mice but has been associated with mouse mutants affecting the cerebellum, brainstem and basal ganglia (reviewed in Lalonde & Strazielle, 2011). Clasping has been observed as a feature in models of neurodegenerative disease and motor dysfunction including Parkinson's and Huntington's disease, where the clasped limbs remain tightly adhered against the mouse's abdomen (Mangiarini,. 1996; Li, 2005). The motor symptoms in these two disorders have been attributed to an increase in glutamatergic activity in the corticostriatal pathways leading to a loss of dopaminergic or neostriatal neurons respectively (Mitchell & Carroll, 1997; Chen, 1999).

How does this compare to NMDAR hypofunction seen in NMDAR-encephalitis? Clasping has not been reported in mice with reduced NR1 expression nor with mice receiving NMDAR antagonists. Instead NR1-hypomorph mice or wild-type mice given sub-anaesthetic doses of NMDAR-antagonists show

stereotypic behaviours (Mohn, 1999; Barkus, 2012). In patients with NMDAR-antibody encephalitis, choreoathetoid limb and oral dyskinesias were common features in over 70 % patients (Titualer, 2013), which are thought to be due to basal ganglia dysfunction (Dalmau, 2011). Similar stereotypical behaviours, as well as tongue-dyskinesias have been induced in monkeys, cats and rodents treated with NMDAR antagonists (Haggerty, 1984; Aides, 1988).

Infusion of NMDAR-antibodies into the prefrontal cortex of rats enhanced the excitability of the motor cortex and caused a dose-dependent increase in extracellular glutamate levels in rats one hour after injection (Manto, 2011). The glutamate transporter 1 (GLT-1) is an astroglial transporter highly expressed in the hippocampus and is responsible for 90 % of glutamate transport in the brain (Danbolt, 1992; Kiryk, 2008). GLT-$1^{-/-}$ mice have reduced glutamate transport and display hind limb clasping before developing lethal spontaneous seizures at 23 weeks of age (Tanaka, 1997.; Kiryk, 2008). Similarly transgenic mouse models of Huntington's disease with polyglutamine expansions in huntingtin (Htt), display an age dependent increase in extracellular glutamate levels in the striatum and cortex which is consistent with a global down regulation of GLT-1 expression in the brain (Behrens, 2002). Treatment of these mice with ceftriaxone, an antibiotic which increases the expression of GLT1 alleviates the clasping phenotype (Miller, 2008). This evidence supports a role for NMDAR-antibody mediated clasping in the context of raised extracellular glutamate levels.

Time course of behaviour

Auto-antibodies to surface antigens in the CNS are relatively new phenomena and few behavioural models for these disorders have been described to date. A single injection of NMDAR-IgG directly in to the hippocampus caused internalisation of 20% of NMDAR at the injection site within 5-7 hours later (Mikasova, 2012). NR1 levels in other areas of the hippocampus were not assessed; however the authors reported no effect on NR1 levels in the striatum. This finding is most likely to represent the lack of IgG diffusion in to the striatum; however immunohistochemistry directly looking for human IgG deposition in the striatum after hippocampal injections is required to confirm this.

The most striking part of the data presented in this thesis is the time course of the behavioural effects. Initially mice were not assessed every day on the spontaneous alternation task. In the preliminary

study an effect of treatment group (p=0.001) but a non-significant trend of time (p=0.081) was observed, suggesting that the deficits on spontaneous alternation may be time dependent. Analysis of cohort two alone, who were injected with the same patient and control IgG preparations as cohort one showed a similar overall reduction on spontaneous alternation in NMDAR-antibody treated mice (p=0.005), an effect of time (p<0.001) and a time by treatment interaction (p=0.033). Simple main effects showed a significant time effect on days 5-8, 13-16 and 20-24. A deficit in alternation was not observed in the first block (days 1-4), p=0.190, despite the detection of control IgG in the dentate gyrus one after intracerebroventricular injection. One explanation for this is that it could take hours to days for the NMDAR-IgG to reach concentrations high enough to internalise enough NMDARs to alter mouse behaviour.

This study showed the effect of the NMDAR-antibodies on spontaneous alternation lasted approximately twenty four days, thereafter alternation levels returned to control values. In cohort three a statistically significant effect of NMDAR-IgG on spontaneous alternation was not observed, although there was a trend (p=0.075) supporting the previous two experimental cohorts. Needless to say the time effect is interesting and the recovery of behaviour in cohorts one and two may be explained by the single dose of IgG is insufficient to sustain a behavioural phenotype. Furthermore, the clinical improvement in patients in which treatment reduces their antibody titer highlights the reversible nature of disease. Indeed after a two week chronic infusion of NMDAR antibodies into the hippocampus of rats, no significant neuronal loss was observed compared to control (Hughes, 2010).

A similar time frame of antibody pathogenicity to this thesis has been demonstrated in a model of SPS associated with amphiphysin antibodies injected in to the CSF compartment. The most prominent features of SPS is motor hyperexcitability that results in muscle stiffness and spasms. Amphiphysin is an intracellular protein expressed in synaptic vesicles and it is thought to be transiently exposed, as patient antibodies have been shown to bind to amphiphysin and become subsequently internalised into GABAergic neurons amygdala (Wigge, 1998). Repeated intrathecal injection of purified amphiphysin-IgG (10 μl/day at 100 mg/ml, one injection each day for five days, followed by five injections every other day and then every three days for the next two injections) or specific-amphiphysin IgG (10mg/ml) to rats reproduced some of the clinical features of disease including

stiffness of the trunk and limb muscles (Geis, 2010a). These observations were seen six to eight days after the start of immunisation in all rats receiving patient IgG (8/8), specific amphiphysin IgG (10/10) but not in rats receiving amphiphysin-antibody depleted IgG (4/4), control IgG (9/9) or saline (7/7). Although it is interesting that the rats presented with stiffness in a similar time course to the deficit in alternation seen in mice receiving a single injection of NMDAR antibodies, it is not known whether the behavioural time course in this model represents an effect of antibody concentration in the CNS or whether it models the time course of IgG diffusion out into the parenchyma. Furthermore the authors did not demonstrate how long the phenotype was present after terminating antibody infusion. In an identical injection protocol of IgG from patients with SPS and severe anxiety with either amphiphysin antibodies (Geis, 2012) or antibodies to glutamic acid decarboxylase-65 (GAD65), the rate limiting enzyme which converts glutamate to GABA, induced anxious behaviour on the elevated plus maze on day 19 after starting the injections, but did not affect locomotor activity within the task (Geis, 2011). Unfortunately the authors did not assess anxiety behaviour before this day so the precise time course could not be determined. In all three studies, immunohistochemistry showed patient IgG, but not control IgG had entered the brain, and bound to disease appropriate regions, including the hippocampus, amygdala and the spinal cord indicating that intrathecal IgG can access the CNS parenchyma.

In contrast to this time course, injection of mGluR1 antibodies from patients with cerebellar ataxia caused severe ataxia within 30 minutes of injection in to the CSF compartment, peaking at 2-4 hours which was reversed at 24 hours (Smitt, 2000). The authors observed IgG deposition in the cerebellum at 5-12 hours after injection and demonstrated i*n vitro* that mGluR1 antibodies produce a functional block of mGluR1, similar to pharmacological antagonisms of the receptor, supporting the rapid onset and reversal of symptoms. However, the authors did not assess whether IgG was no longer detected in the brain after the ataxia phenotype had subsided.

In summary, these studies illustrate the difficulties of comparing the antibody pathogenic mechanisms *in vivo* across different CNS disorders, and the antigen location, and the specific functional properties of the antibodies may determine the time course.

8.5.3 Histological analysis of NMDAR-brains

Mice in this study received 10 µl of purified IgG (250 µg IgG). Injection of Evan's blue into a single mouse confirmed that the coordinates targeting the lateral ventricle were correct. After one hour, IgG labelling was limited to areas adjacent to the lateral ventricle including the hippocampus and the corpus callosum. It is an attractive hypothesis that the localisation of IgG may represent diffusion into the parenchyma, with the signal of IgG immunoreactivity decreasing in diameter away from the ventricle. This is supported by intense IgG binding in the molecular layer of the hippocampus and around the lateral ventricle but becoming less intense with distance. However IgG was found in the corpus callosum but was not found in the dorsal hippocampus situated directly below the ventricle suggesting that IgG may diffuse faster through white matter tracts than brain parenchyma. Alternatively IgG may have leaked back up the injection site and along the corpus callosum. Regardless, this finding indicates that IgG injected in to the lateral ventricle can access the brain parenchyma. Unfortunately mice receiving NMDAR-IgG were not culled one and 24 hours after injection. Hughes *et al* showed intense IgG deposition in the hippocampus of rats after chronic infusion (0.5 µl/ hour for 14 days) of patient CSF directly into the hippocampus, but did not show discernible binding with control CSF (Hughes, 2010). The differences of control IgG presence in the brain in the two studies may be due to different processing of the brain tissue. In this thesis brains were post fixed in 4% PFA overnight, however a shorter, 15 minute fixation, as reported in Hughes *et al* may not be sufficient to permeate the brain and fix healthy control IgG that is present in the brain but not binding to the tissue specifically. If the tissue is post fixed for a short duration, non-specific unbound IgG may be subsequently washed away during the immunohistochemical staining procedure. Future experiments, exploring patient IgG binding over time may enable the pharmacokinetics of IgG diffusion into the parenchyma and time course of internalisation to be studied.

IgG is actively removed from the brain by the neonatal Fc receptor, FcRn, that is expressed on the endothelial cells of the BBB (Zhang, 2001). Very few studies exist studying the pharmacokinetics of IgG in the brain. One study showed intracerebral injection of radiolabelled mouse IgG isotypes (1.5 µg of IgG2a or OX26 monoclonal antibody) into the rat brain had a half-life of 48 minutes compared to 10-12 hours for albumin. However IgG efflux can be competitively inhibited by mouse IgG molecules and Fc

fragments (1.5 μg), but not $F(ab')_2$ fragments suggesting that reverse transcytosis of IgG from brain to blood is mediated through binding to the Fc domain of the IgG molecule (Zhang, 2001). Mice injected in this thesis received 250 μg of patient or control IgG, 167 fold more than used by Zhang *et al*; and it is possible that the excess IgG administered into the CSF may saturate and inhibit FcRn mediated efflux of IgG, increasing the half-life of NMDAR-antibodies in the brain.

In studies of NMO passive transfer, pathogenicity was demonstrated by intraparenchymal co-injection of IgG and human complement which produced the characteristic NMO lesions with AQP-4 loss in the parenchyma. Furthermore the authors showed that intrathecal injection of patient IgG and complement also caused lesions with AQP-4 loss in the ependymal cells of the ventricle wall, confirming once again, that intrathecal IgG can enter the brain parenchyma (Saadoun, 2010). Further studies injecting 3 μg of recombinant monoclonal NMO-IgG directly into the parenchyma showed diffusion of IgG over a $5mm^2$ area in 24 hours (Ratelade, 2011). However the authors did not report what proportional of the total IgG injected this represented, not the pharmacokinetics of IgG removal.

8.5.4 Post-mortem of ICV brains

Analysis of brain histology was confined to the hippocampus for two reasons. Firstly patient IgG reacts most strongly with the hippocampal neuropil and secondly deposits of IgG and microglial activation have been reported in post mortem tissue predominantly in the hippocampus and less so in the basal forebrain, basal ganglia and the spinal cord (Tüzün et al. 2009). Hippocampal NR1 expression 22 and 46 days after the initial ICV injection was not different in mice receiving control or patient IgG at either time point. It is possible that this discrepancy may be explained by western blot measuring total NR1 protein (both intracellular and surface NR1) which might have masked a modest reduction in NR1 surface levels on day 22. In hindsight, a membrane preparation from dissected hippocampi could have addressed this question. Furthermore, mice sacrificed on day 22 were from cohort 3 which overall did not have a significant effect of treatment on spontaneous alternation ($p=0.075$). The lack of difference in NR1 expression at day 46 may not be surprising as behavioural changes were no longer observed at this time point, which could be a reflection of NMDAR turnover.

There was no obvious difference in astrocyte and microglial activation between mice receiving control and patient IgG despite activation seen in post-mortem tissue. As immunopathology studies support a role for microglia activation in disease pathology, we cannot rule out the possibility that NMDAR-antibodies affect microglia function at an earlier time point in our passive transfer model.

As NR1 expression levels were not reduced on day 22 or day 46, the mechanism by which the behaviour is altered in these mice cannot be specifically stated. Mikasova *et al* injected 0.4 μl of patient IgG (1mg/ml) into the dorsal hippocampus of mice and demonstrated a reduction NMDAR 5-7 hours late, however the authors did not determine if a greater reduction in NMDARs would occur with a bigger dose of patient IgG, or with a longer time course until analysis. The recovery of NMDARs after antibody-mediated internalisation has been reported *in vitro* four days after the wash-out of patient antibodies and earlier time points of NR1 recovery were not assessed (Hughes, 2010). Future studies of brains sacrificed earlier after injection are crucial in confirming that these changes in spontaneous alternation and clasping are attributed to NMDAR internalisation.

Multiple studies have characterised the turnover of NMDAR *in vitro* (Huh, 1999). Huh *et al* were the first to identify biphasic degradation of the NR1 subunit in cerebellar neuronal cultures. Firstly a surface pool of NR1 which associates with NR2 was shown to have a half-life of 34 hours and a second pool of NR1 subunits had a shorter half-life of 2 hours. This short lived pool is thought to function as a reserve population waiting to assemble into the membrane and in early stages of the disease may be sufficient to compensate for the loss of NMDARs. Shimizu *et al* produced a doxycycline inducible conditional mouse knockout of NR1 subunits in the CA1 (iCA1-KO) region of the hippocampus and reported regional suppression of the NR1 subunit 3-5 days after doxycycline induction, which began to reappear within 5-days after doxycycline withdraw (Shimizu, 2012). However the authors did not report the time course for complete recovery of NMDAR expression. Further conditional NR1 knockouts in the forebrain (iFB-KO) showed a complete reduction of NR1 expression after 5 days of doxycycline treatment and a complete recovery of NR1 two months later (Cui, 2004). The lack of complete recovery at 5-days post drug withdrawal in the first study and the complete recovery of NR1 expression at two months emphasises how little is known about the time course for NR1 recovery *in vivo*, but that it occurs somewhere within 5-60 days of being knocked out. Of course one must be cautious of extrapolating this work directly as

secondary changes after prolonged NR1 suppression may be responsible for the delay in NR1 recovery in these models. The majority of patients with NMDAR-antibodies respond well to early immunotherapy intervention, regardless of gender or age, although the reversal of symptoms is not immediate (Titualer, 2013). However, approximately 20% of cases patients do not improve, which is usually due to a delay in time to tumour removal or the initiation of immunotherapies (Dalmau, 2008). After immunosuppression or plasma exchange, serum NMDAR-antibodies fall and it is conceivable that NR1 surface expression may recover quickly as demonstrated after removal of patient antibodies *in vitro*. However the time course of antibody mediated NR1 internalisation has not been investigated *in vivo*. As this disease has only recently been described in 2007, detailed long term follow up studies on cognitive function have not been reported.

Finke *et al* detailed neuropsychological assessment of nine adult patients 23-69 months after a diagnosis of NMDAR-antibody encephalitis. Eight out of nine patients showed sustained cognitive deficits, with larger deficits correlating with time to treatment (Finke, 2012). MRI findings showed white matter lesions in the patient with the worst performance, similar to those seen in patients with schizophrenia, or rodents following chronic ketamine exposure (Pomarol-Clotet, 2010; Liao, 2010) . Due to the recent identification of NMDAR-antibodies, the patients in this cohort had a median delay of 43 months between presentation and treatments. Given the growing recognition of the disorder and the recognition of early immunotherapy intervention the residual cognitive deficits seen in future studies may decrease. Pharmacological studies in humans have shown that NMDAR antagonism with PCP or ketamine can have long lasting effects, despite the short plasma half-life of these drugs (Rainey, 1975; White, 1985). Furthermore the long-term effects of ketamine as an antidepressant has recently been reported in humans (Zarate, 2006). Zarate *et al* showed that depressed subjects previously unresponsive to standard anti-depressant therapies showed a significant clinical improvement lasting at least one week after an intravenous infusion of ketamine. Furthermore a case study showed a long lasting effect on mood after a 5 day infusion of ketamine to two patients with drug-resistant depression (Correll, 2006). In rodents chronic administration of sub-anaesthetic doses of NMDAR-antagonists have been reported to have persistent deficits on social interaction, cognition and emotional deficits which persisted after drug withdrawal (Mouri, 2007; Enomoto, 2005). However the majority of studies did not report

cellular changes in NMDAR expression or receptor signalling molecules. Chatterjee *et al* characterised the neurochemical and molecular effects of 10 day chronic ketamine model of psychosis in mice and found tissue alterations in acetylcholine, dopamine, serotonin, and noradrenaline levels as well as changes in the mRNA of the neurotransmitter receptors in the brain (Chatterjee, 2012).

Hence it is likely that the behavioural effects from a single dose of NMDAR antibodies *in vivo* could persist longer than the presence of the antibody in the brain, which may explain the 20 day deficit seen on the spontaneous alternation task.

8.5.5 Witebsky's postulates: demonstration of pathogenicity

The aim of this work was to investigate the pathogenicity of NMDAR-antibodies. Whilst passive transfer models have shown NMDAR-antibodies reduce NR1 expression *in vivo* the behavioural phenotypes of these mice have not been studied. Furthermore, these studies were not available at the time of thesis commencement. Mice received a single IgG injection into the lateral ventricle and behavioural experiments demonstrated abnormalities in spontaneous alternation and hind-limb clasping that may be analogous to certain phenotypes associated with NMDAR-antibody encephalitis. These behavioural data do not reproduce all features of disease so as to satisfy Witebsky's postulates, but provide further evidence of NMDAR-antibody pathogenicity in the CNS. Perhaps this model mimics the human disease with the early cognitive features on the spontaneous alternation task occurring from around day 5, and the later presenting dyskinesias observed around day 10.

8.6 Limitations and future directions

Animal models based on passive transfer of IgG molecules into the brain are an over-simplification of the pathogenesis process in disease. A passive transfer experiment considers only the humoral component of disease and does not address the factors inducing NMDAR-antibodies, in particular the presence of a tumour driving the immune response in a large proportion of these patients. The passive transfer experiment in this thesis relies on the NMDAR-antibodies cross reacting with the mouse NR1 subunit. 99% homology in the amino acid sequence is found between the two species, with only six amino acids different in the amino-terminus of the extracellular domain. Furthermore patients with

high NMDAR-antibody titers can bind to rodent neuronal tissue supporting the suitability of the mouse as a vector for modelling human disease.

NMDAR-antibody mediated encephalitis has a complex clinical presentation and it is difficult to attribute mouse behaviours directly to the clinical presentation. Patients initially present with seizures and neuropsychiatric features and later with the onset of a movement disorder, a fall in consciousness and autonomic disturbances. In this thesis we observed deficits in spontaneous alternation and hind-limb clasping that may represent cognitive dysfunction and the movement disorder in NMDAR-antibody encephalitis. Further EEG and video-monitoring studies addressing the seizure-like events observed in two mice are required to characterise if mice injected with NMDAR-antibodies are indeed having seizures. In fact, C57BL/6 mice used in this study are reportedly seizure resistant (Engstrom, 1988). As seizures are observed in 70% of patients with NMDAR-encephalitis (Titulaer, 2013), ideally a mouse strain which is more prone to seizures, such as the DBA/2, may be preferred in future studies.

NMDAR-IgA antibodies have recently been described in 7/24 patients with progressive cognitive decline and an unclear aetiology. Similarly to IgG NMDAR-antibodies they reduce surface NMDAR expression and NMDAR-synaptic currents. In addition to this they also affect other synaptic components, including the pre-synaptic marker synapsin and vesicular glutamate transport (VGLUT). The authors found IgA antibodies were also present in 31% of patient sera with NMDAR-IgG antibodies, although no comparison of titers or CSF levels were shown (Prüss, 2012). Whether passive transfer of NMDAR-IgA antibodies would affect spontaneous alternation and clasping behaviour is not known.

Perhaps most importantly, this model of a single intracerebroventricular injection does not represent the presence of antibodies in patient sera for days, weeks or months before or during the clinical presentation, despite the profound effects observed on performance on spontaneous alternation. A more representative model could be achieved with continuous delivery of NMDAR-antibodies over several days to weeks into CSF compartment or the periphery. Ideally continuous infusion of NMDAR-antibodies should aim to sustain serum or CSF antibody levels comparable to those seen in

disease and to reproduce IgG deposition in areas of the brain, including the hippocampus, that have been found in post-mortem studies.

Chapter 9: Conclusions

The evidence for an autoimmune aetiology for these disorders comes from the association of conserved clinical features with the presence of a specific autoantibody to an extracellular epitope, the association with other autoimmune disorders, and a significant clinical improvement correlating with a fall in antibody titer after immunosuppressive intervention. The work in this thesis focused on the pathogenic effect of CASPR2 and LGI1 antibodies *in vitro* and the pathogenicity of NMDAR-antibodies *in vivo*.

The immune basis for NMDAR-antibody encephalitis is well described. NMDAR-antibodies bind to the surface of the NR1 subunit and cross react with brain tissue. *In vitro* studies have shown antibodies reversibly reduce synaptic expression of NMDAR in hippocampal neurons and co-incidentally decrease NMDAR-mediated currents. Furthermore antibodies may also have an acute effect of receptor function. Patients respond to immunotherapy and their clinical outcome improves as antibody levels decrease. The gold standard for proving antibody pathogenicity is passive transfer of patient IgG to mice, two studies have shown that injection of antibodies directly in to the hippocampus reduces NR1-expression in that region. The pathogenesis of NMDAR-antibodies was studied in this thesis looking the effects on NMDAR-antibodies on mouse behaviour.

These results show further evidence to that provided in the literature that NMDAR-antibodies could be pathogenic. This has been established on the basis of differences on specific behavioural tasks between mice injected with healthy control or NMDAR-antibody positive IgG. Although these changes were modest in comparison to pharmacological and genetic manipulations of the NMDAR, the behavioural phenotypes observed in spontaneous alternation, clasping and seizures show similarities to the clinical presentation in these patients. The behavioural changes seen in this thesis were transient which may support the idea that the disease is reversible when treated early. Whilst internalisation of the NMDA receptor has not been demonstrated in these studies, many studies have shown NMDA receptor internalisation both *in vitro* and *in vivo.* Future investigations of the effects of sustained delivery of NMDAR-antibodies on NR1 expression and mouse behaviour are required.

To validate the result of the passive transfer, it will be necessary to demonstrate whether the NMDAR antibodies in this thesis caused internalisation at an earlier time points in the experiment, as shown by others. However more global issues are unresolved. After injection where does the IgG diffuse to? Do patient antibodies in this thesis cause receptor internalisation? Is this effect hippocampal specific? Can these symptoms be maintained with longer injection protocols? Further insight into the model will be gained by assessing the degree of patient IgG penetration in the parenchyma after intrathecal injection and subsequent immunoblots analysis of IgG diffusion and the effect on NMDAR expression in different brain regions over the course of the immunisation protocol. Future studies focussing on continuous delivery of IgG in to the CNS, particularly into the intrathecal compartment may be more representative of the disease process.

Antibody access to the brain

As NMDAR antibodies are commonly observed in the CSF, it is probable these antibodies access the brain parenchyma. In patients with VGKC-complex antibodies, CSF antibodies are less commonly reported (Tan, 2008). It is possible that VGKC-complex serum antibodies enter the brain via the circumventricular organs or through a leaky blood brain barrier. Prodromal infections have been reported in some patients and may compromise the integrity of the barrier (Vincent, 2004; Jarius. 2008). Recent *in vivo* studies in lupus, demonstrated that lipopolysaccharide (LPS) and epinephrine could cause a regional specific disruption in the blood brain barrier allowing the extravasation of SLE-IgG into the hippocampus and amygdala respectively (Kowal, 2004; Kowal, 2006). The anatomical location of the leaky barrier determined whether cognitive or emotional features of disease were observed. At a gross level, these observations demonstrate that serum antibodies can gain access to the CNS under inflammatory conditions, and that the regional disruption of the blood brain barrier may help to explain the multiple clinical phenotypes associated with the same antibody.

CASPR2 antibodies have been described in limbic encephalitis, cerebellar ataxia and Morvan's syndrome as well in patients with only neuromyotonia. It may be that selected sites of barrier permeability dichotomises with the patients subgroups; for example the thalamus may be compromised in Morvan's syndrome explaining the sleep disturbances commonly seen in these

patients, whereas in patients with gait dysfunction, the cerebellum may be compromised. In neuromyotonia, it seems probable that an intact blood brain barrier prevents the serum antibodies access to the brain. This hypothesis could be investigated by monitoring the blood brain barrier integrity at specific anatomical sites in humans or *in vivo* passive transfer models in the presence of regional-specific blood-brain barrier modulators, such as demonstrated in SLE.

Bibliography

Aalberse R., Schuurman J, Ree R (1999). The Apparent Monovalency of Human IgG4 Is Due to Bispecificity. Int Arch Allergy Immunol, 1118(2-4):187-9.

Abou-Zeid E, Boursoulian LJ, Metzer WS, Gundogdu B (2012). Morvan Syndrome: a case report and review of the literature. J Clin Neuromuscul Dis, 13(4):214-27.

Agius M, Twaddle G, Fairclough R (1998). Epitope Spreading in Experimental Autoimmune Myasthenia Gravis. Ann N Y Acad Sci, 3(841):365-7.

Aldes LD, Prater SR, Chronister RB, Marco LA (1988). Ketamine as a pharmacological model for tongue dyskinesia. Biol Psychiatry, 23(2):159-68.

Ances BM, Vitaliani R, Taylor RA, Liebeskind DS, Voloschin A, Houghton DJ, Galetta SL, Dichter M, Alavi A, Rosenfeld MR, Dalmau J (2005). Treatment-responsive limbic encephalitis identified by neuropil antibodies: MRI and PET correlates. Brain, 128(8):1764-1777.

Arking DE, Cutler DJ, Brune CW, Teslovich TM, West K, Ikeda M, Rea A, Guy M, Lin S, Cook EH, Chakravarti A (2008). A Common Genetic Variant in the Neurexin Superfamily Member CNTNAP2 Increases Familial Risk of Autism. Am J Hum Genet, 82(1):160-4.

Barber P.A, Anderson NE, Vincent A (2000). Morvan's syndrome associated with voltage-gated K+ channel antibodies. Neurology, 54(3):771-2.

Barkus C, Dawson LA, Sharp T, Bannerman DM (2012). GluN1 hypomorph mice exhibit wide-ranging behavioral alterations. Genes, Brain and Behav, 11(3):342-351.

Bats S, Thoumas JL, Lordi B, Tonon MC, Lalonde R, Caston J (2001). The effects of a mild stressor on spontaneous alternation in mice. Behav Brain Res,118(1):11-5.

Baulac S, Ishida S, Mashimo T, Boillot M, Fumoto N, Kuwamura M, Ohno Y, Takizawa A, Aoto T, Ueda M, Ikeda A, LeGuern E, Takahashi R, Serikawa T (2012). A rat model for LGI1-related epilepsies. Hum Mol Genet, 21(16):3546-57

Becker EB, Zuliani L, Pettingill R, Lang B, Waters P, Dulneva A, Sobott F, Wardle M, Graus F, Bataller L, Robertson NP, Vincent A (2012). Contactin-associated protein-2 antibodies in non-paraneoplastic cerebellar ataxia. J Neurol Neurosurg Psychiatry, 83(4):437-40.

Behrens PF, Franz P, Woodman B, Lindenberg KS, Landwehrmeyer GB (2002). Impaired glutamate transport and glutamate-glutamine cycling: downstream effects of the Huntington mutation. Brain, 125(8);1908-1922.

Belforte JE, Zsiros V, Sklar ER, Jiang Z, Yu G, Li Y, Quinlan EM, Nakazawa K (2009). Postnatal NMDA receptor ablation in corticolimbic interneurons confers schizophrenia-like phenotypes. Nat Neurosci, 13(1);76-83.

Bella J, Hindle KL, McEwan PA, Lovell SC (2008). The leucine-rich repeat structure. Cell Mol Life Sci,65(15);2307-33

Bien CG, Vincent A, Barnett MH, Becker AJ, Blümcke I, Graus F, Jellinger KA, Reuss DE, Ribalta T, Schlegel J, Sutton I, Lassmann H, Bauer J (2012). Immunopathology of autoantibody-associated encephalitides: clues for pathogenesis. Brain, 135(5);1622-1638.

Brew HM, Gittelman JX, Silverstein RS, Hanks TD, Demas VP, Robinson LC, Robbins CA, McKee-Johnson J, Chiu SY, Messing A, Tempel BL (2007). Seizures and reduced life span in mice lacking the potassium channel subunit Kv1.2, but hypoexcitability and enlarged Kv1 currents in auditory neurons. J Neurophysiol,98(3):1501-25.

Browne DL, Gancher ST, Nutt JG, Brunt ER, Smith EA, Kramer P, Litt M (1994). Episodic ataxia/myokymia syndrome is associated with point mutations in the human potassium channel gene, KCNA1. Nat Genet, 8(2);136-40.

Buckley C, Oger J, Clover L, Tüzün E, Carpenter K, Jackson M, Vincent A (2001). Potassium channel antibodies in two patients with reversible limbic encephalitis. Ann Neurol, 50(1);73-8.

Burges J, Vincent A, Molenaar PC, Newsom-Davis J, Peers C, Wray D (1994). Passive transfer of seronegative myasthenia gravis to mice. Muscle Nerve,17(12);1393-400.

Butler A, Wei AG, Baker K, Salkoff L (1989). A family of putative potassium channel genes in Drosophila. Science, 243(4893);943-47.

Camdessanché JP, Streichenberger N, Cavillon G, Rogemond V, Jousserand G, Honnorat J, Convers P, Antoine JC (2011). Brain immunohistopathological study in a patient with anti-NMDAR encephalitis. Eur J Neurol, 18(6);929-31

Chabrol E, Navarro V, Provenzano G, Cohen I, Dinocourt C, Rivaud-Péchoux S, Fricker D, Baulac M, Miles R, Leguern E, Baulac S (2010). Electroclinical characterization of epileptic seizures in leucine-rich, glioma-inactivated 1-deficient mice. Brain, 133(9);2749-62

Chatterjee M, Verma R, Ganguly S, Palit G (2012). Neurochemical and molecular characterization of ketamine induced experimental psychosis model in mice. Neuropharmacology, 63(6);1161-71.

Chen N, Luo T, Wellington C, Metzler M, McCutcheon K, Hayden MR, Raymond LA (1999). Subtype-Specific Enhancement of NMDA Receptor Currents by Mutant Huntingtin. J Neurochem, 72(5):1890-98.

Chernova OB, Somerville RP, Cowell JK (1998). A novel gene, LGI1, from 10q24 is rearranged and downregulated in malignant brain tumors. Oncogene, 17(22):2873-81.

Cirelli C, Bushey D, Hill S, Huber R, Kreber R, Ganetzky B, Tononi G (2005). Reduced sleep in Drosophila Shaker mutants. Nature, 434(7037):1087-92.

Coesmans M, Smitt PA, Linden DJ, Shigemoto R, Hirano T, Yamakawa Y, van Alphen AM, Luo C, van der Geest JN, Kros JM, Gaillard CA, Frens MA, de Zeeuw CI (2003). Mechanisms underlying cerebellar motor deficits due to mGluR1-autoantibodies. Ann Neurol, 53(3):325-36.

Collingridge GL, Olsen RW, Peters J, Spedding M (2009). A nomenclature for ligand-gated ion channels. Neuropharmacology,56(1):2-5

Contet, C., Rawlins, N, Deacon R (2001). A comparison of 129S2/SvHsd and C57BL/6JOlaHsd mice on a test battery assessing sensorimotor, affective and cognitive behaviours: implications for the study of genetically modified mice. Behav Brain Res, 124(1):33-46.

Correll, G.E. & Futter, G.E (2006). Two Case Studies of Patients with Major Depressive Disorder Given Low-Dose (Subanesthetic) Ketamine Infusions. Pain Med, 7(1):92-5

Covasa M, Hung CY, Ritter RC, Burns GA (2004). Intracerebroventricular administration of MK-801 increases food intake through mechanisms independent of gastric emptying. Am J Physiol Regul Integr Comp Physiol, 287(6):R1462-7

Crawley J, Goodwin FK (1980). Preliminary report of a simple animal behavior model for the anxiolytic effects of benzodiazepines. Pharmacol Biochem Behav, 13(2):167-70.

Cui Z, Wang H, Tan Y, Zaia KA, Zhang S, Tsien JZ (2004). Inducible and Reversible NR1 Knockout Reveals Crucial Role of the NMDA Receptor in Preserving Remote Memories in the Brain. Neuron, 41(5):781-93.

Drachman DB, Angus CW, Adams RN, Michelson JD, Hoffman GJ (1978). Myasthenic antibodies cross-link acetylcholine receptors to accelerate degradation. N Engl J Med, 298(20):1116-22.

Dale RC, Irani SR, Brilot F, Pillai S, Webster R, Gill D, Lang B, Vincent A (2009). N-methyl-D-aspartate receptor antibodies in pediatric dyskinetic encephalitis lethargica. Ann Neurol, 66(5):704-9.

Dalmau J, Tüzün E, Wu HY, Masjuan J, Rossi JE, Voloschin A, Baehring JM, Shimazaki H, Koide R, King D, Mason W, Sansing LH, Dichter MA, Rosenfeld MR, Lynch DR (2007). Paraneoplastic anti–N-methyl-D-aspartate receptor encephalitis associated with ovarian teratoma. Ann Neurol, 61(1):25-36.

Dalmau J, Furneaux HM, Rosenblum MK, Graus F, Posner JB (1991). Detection of the anti-Hu antibody in specific regions of the nervous system and tumor from patients with paraneoplastic encephalomyelitis/sensory neuronopathy. Neurology, 41(11):1757-64.

Duncan GE, Moy SS, Lieberman JA, Koller BH (2006). Typical and atypical antipsychotic drug effects on locomotor hyperactivity and deficits in sensorimotor gating in a genetic model of NMDA receptor hypofunction. Pharmacol Biochem Behav, 85(3):481-91.

Dalmau J, Rosenfeld MR (2008). Paraneoplastic syndromes of the CNS. Lancet Neurol, 7(4):327-40.

Dalmau J, Gleichman AJ, Hughes EG, Rossi JE, Peng X, Lai M, Dessain SK, Rosenfeld MR, Balice-Gordon R, Lynch DR (2008). Anti-NMDA-receptor encephalitis: case series and analysis of the effects of antibodies. Lancet Neurol, 7(12):1091-8.

Danbolt NC, Storm-Mathisen J, Kanner BI (1992). An [Na+ + K+]coupled L-glutamate transporter purified from rat brain is located in glial cell processes. Neuroscience, 51(2):295-310.

DeGiorgio LA, Konstantinov KN, Lee SC, Hardin JA, Volpe BT, Diamond B (2001). A subset of lupus anti-DNA antibodies cross-reacts with the NR2 glutamate receptor in systemic lupus erythematosus. Nat Med, 7(11):1189-93.

Deacon RM, Bannerman DM, Kirby BP, Croucher A, Rawlins JN (2002). Effects of cytotoxic hippocampal lesions in mice on a cognitive test battery. Behav Brain Res, 133(1):57-68.

Deacon MR, Rawlins JN (2006). T-maze alternation in the rodent. Nat Protoc, 1(1):7-12.

Douglas CL, Vyazovskiy V, Southard T, Chiu SY, Messing A, Tononi G, Cirelli C (2007). Sleep in Kcna2 knockout mice. BMC Biol, 9(5):42-46

Duncan GE, Moy SS, Perez A, Eddy DM, Zinzow WM, Lieberman JA, Snouwaert JN, Koller BH (2004). Deficits in sensorimotor gating and tests of social behavior in a genetic model of reduced NMDA receptor function. Behav Brain Res, ;153(2):507-19.

Duncan GE, Inada K, Koller BH, Moy SS (2010). Increased sensitivity to kainic acid in a genetic model of reduced NMDA receptor function. Brain Res, 11;1307:166-76.

Dunstan EJ, Winer JB (2006). Autoimmune limbic encephalitis causing fits, rapidly progressive confusion and hyponatraemia. Age Ageing, 35(5):536-7.

Engel A, Lambert E, Howard F (1977). Immune complexes (IgG and C3) at the motor end-plate in myasthenia gravis: ultrastructural and light microscopic localization and electrophysiologic correlations. Mayo Clin Proc, 52(5):267-80.

Enomoto T, Noda Y, Mouri A, Shin EJ, Wang D, Murai R, Hotta K, Furukawa H, Nitta A, Kim HC, Nabeshima T (2005). Long-lasting impairment of associative learning is correlated with a dysfunction of NMDA-ERK signaling in mice following withdrawal from repeated administration of phencyclidine. Mol Pharmacol, 68(6):1765-74.

Finke C, Kopp UA, Prüss H, Dalmau J, Wandinger KP, Ploner CJ (2012). Cognitive deficits following anti-NMDA receptor encephalitis. J Neurol Neurosurg Psychiatry, 83(2):195-8.

Fuchs S, Nevo D, Tarrab-Hazdai R, Yaar I, (1976). Strain differences in the autoimmune response of mice to acetylcholine receptors. Nature, 263(5575):329-30.

Fambrough, D.M., Drachman, D.B. & Satyamurti, S (1973). Neuromuscular Junction in Myasthenia Gravis: Decreased Acetylcholine Receptors. Science, 182(4109):293-295.

Flanagan EP, McKeon A, Lennon VA, Boeve BF, Trenerry MR, Tan KM, Drubach DA, Josephs KA, Britton JW, Mandrekar JN, Lowe V, Parisi JE, Pittock SJ (2010). Autoimmune Dementia: Clinical Course and Predictors of Immunotherapy Response. Mayo Clin Proc, 85(10):881-97.

Florance NR, Davis RL, Lam C, Szperka C, Zhou L, Ahmad S, Campen CJ, Moss H, Peter N, Gleichman AJ, Glaser CA, Lynch DR, Rosenfeld MR, Dalmau J (2009). Anti-N-methyl-D-aspartate receptor (NMDAR) encephalitis in children and adolescents. Ann Neurol, 66(1):11-8

Forrest D, Yuzaki M, Soares HD, Ng L, Luk DC, Sheng M, Stewart CL, Morgan JI, Connor JA, Curran T (1994). Targeted disruption of NMDA receptor 1 gene abolishes NMDA response and results in neonatal death. Neuron, 13(2):325-38.

Fradley RL, O'Meara GF, Newman RJ, Andrieux A, Job D, Reynolds DS (2005). STOP knockout and NMDA NR1 hypomorphic mice exhibit deficits in sensorimotor gating. Behav Brain Res, 163(2):257-64.

Frassoni C, Spreafico R, Franceschetti S, Aurisano N, Bernasconi P, Garbelli R, Antozzi C, Taverna S, Granata T, Mantegazza R (2001). Labeling of rat neurons by anti-GluR3 IgG from patients with Rasmussen encephalitis. Neurology, 57(2):324-7.

Friedman JI, Vrijenhoek T, Markx S, Janssen IM, van der Vliet WA, Faas BH, Knoers NV, Cahn W, Kahn RS, Edelmann L, Davis KL, Silverman JM, Brunner HG, van Kessel AG, Wijmenga C, Ophoff RA, Veltman JA (2007). CNTNAP2 gene dosage variation is associated with schizophrenia and epilepsy. Mol Psychiatry, 13(3):261-66

Fukamauchi F, Aihara O, Wang YJ, Akasaka K, Takeda Y, Horie M, Kawano H, Sudo K, Asano M, Watanabe K, Iwakura Y (2001). TAG-1-Deficient Mice Have Marked Elevation of Adenosine A1 Receptors in the Hippocampus. Biochem Biophys Res Commun, 281(1):220-26.

Fukata Y, Adesnik H, Iwanaga T, Bredt DS, Nicoll RA, Fukata M (2006). Epilepsy-Related Ligand/Receptor Complex LGI1 and ADAM22 Regulate Synaptic Transmission. Science, 313(5794):1792-5.

Fukata Y, Lovero KL, Iwanaga T, Watanabe A, Yokoi N, Tabuchi K, Shigemoto R, Nicoll RA, Fukata M (2010). Disruption of LGI1-linked synaptic complex causes abnormal synaptic transmission and epilepsy. Proc Natl Acad Sci U S A, 107(8):3799-804

Furlan S, Roncaroli F, Forner F, Vitiello L, Calabria E, Piquer-Sirerol S, Valle G, Perez-Tur J, Michelucci R, Nobile C (2006). The LGI1/Epitempin gene encodes two protein isoforms differentially expressed in human brain. J Neurochem, 98(3):985-91.

Furley AJ, Morton SB, Manalo D, Karagogeos D, Dodd J, Jessell TM (1990). The axonal glycoprotein TAG-1 is an immunoglobulin superfamily member with neurite outgrowth-promoting activity. Cell, 61(1):157-70.

Gasque P, Dean YD, McGreal EP, VanBeek J, Morgan BP (2000). Complement components of the innate immune system in health and disease in the CNS. Immunopharmacology, 49(1-2):171-86.

Geis C, Weishaupt A, Hallermann S, Grünewald B, Wessig C, Wultsch T, Reif A, Byts N, Beck M, Jablonka S, Boettger MK, Üçeyler N, Fouquet W, Gerlach M, Meinck HM, Sirén AL, Sigrist SJ, Toyka KV, Heckmann M, Sommer C (2010). Stiff person syndrome-associated autoantibodies to amphiphysin mediate reduced GABAergic inhibition. Brain, 133(11):3166-80.

Geis C, Grünewald B, Weishaupt A, Wultsch T, Toyka KV, Reif A, Sommer C (2012). Human IgG directed against amphiphysin induces anxiety behavior in a rat model after intrathecal passive transfer. J Neural Transm, 119(8):981-5.

Geis C, Weishaupt A, Grünewald B, Wultsch T, Reif A, Gerlach M, Dirkx R, Solimena M, Perani D, Heckmann M, Toyka KV, Folli F, Sommer C (2011). Human Stiff-Person Syndrome IgG Induces Anxious Behavior in Rats. PLoS One, 6(2):e16775

Giometto B, Marchiori GC, Nicolao P, Scaravilli T, Lion A, Bardin PG, Tavolato B., 1997. Sub-acute cerebellar degeneration with anti-Yo autoantibodies: immunohistochemical analysis of the immune reaction in the central nervous system (1997). Neuropathol Appl Neurobiol, 23(6):468-74.

Gleichman AJ, Spruce LA, Dalmau J, Seeholzer SH, Lynch DR (2012). Anti-NMDA Receptor Encephalitis Antibody Binding Is Dependent on Amino Acid Identity of a Small Region within the GluN1 Amino Terminal Domain. J Neurosci, 32(32):11082-94

Toro-Goyco E, Cora EM, Kessler MJ, Martinez-Carrion M (1986). Induction of experimental myasthenia gravis in rhesus monkeys: a model for the study of the human disease. P R Health Sci J, 5(1):13-8.

Graus F, Boronat A, Xifró X, Boix M, Svigelj V, García A, Palomino A, Sabater L, Alberch J, Saiz A (2010). The expanding clinical profile of anti-AMPA receptor encephalitis. Neurology, 74(10):857-9

Graus F, Illa I, Agusti M, Ribalta T, Cruz-Sanchez F, Juarez C (1991). Effect of intraventricular injection of an anti-Purkinje cell antibody (anti-Yo) in a guinea pig model. J Neurol Sci, 106(1):82-7.

Greenlee JE, Burns JB, Rose JW, Jaeckle KA, Clawson S (1995). Uptake of systemically administered human anticerebellar antibody by rat Purkinje cells following blood-brain barrier disruption. Acta Neuropathol, 89(4):341-5.

Gu W, Brodtkorb E, Steinlein OK (2002a). LGI1 is mutated in familial temporal lobe epilepsy characterized by aphasic seizures. Ann Neurol, 52(3):364-7.

Gu W, Wevers A, Schröder H, Grzeschik KH, Derst C, Brodtkorb E, de Vos R, Steinlein OK (2002b). The LGI1 gene involved in lateral temporal lobe epilepsy belongs to a new subfamily of leucine-rich repeat proteins. FEBS Lett, 519(1-3):71-6.

Haggerty GC, Forney RB, Johnson JM. J (1984). The effect of a single administration of phencyclidine on behavior in the rat over a 21-day period. Toxicol Appl Pharmacol, 75(3):444-53.

Hart IK, Maddison P, Newsom-Davis J, Vincent A, Mills KR (2002). Phenotypic variants of autoimmune peripheral nerve hyperexcitability. Brain, 125(8):1887-95.

Hart IK, Waters C, Vincent A, Newland C, Beeson D, Pongs O, Morris C, Newsom-Davis J (1997). Autoantibodies detected to expressed K+ channels are implicated in neuromyotonia. Ann Neurol, 41(2):238-46.

Hinson SR, Pittock SJ, Lucchinetti CF, Roemer SF, Fryer JP, Kryzer TJ, Lennon VA (2007). Pathogenic potential of IgG binding to water channel extracellular domain in neuromyelitis optica. Neurology, 69(24):2221-31.

Hinson SR, Roemer SF, Lucchinetti CF, Fryer JP, Kryzer TJ, Chamberlain JL, Howe CL, Pittock SJ, Lennon VA (2008). Aquaporin-4-binding autoantibodies in patients with neuromyelitis optica impair glutamate transport by down-regulating EAAT2. J Exp Med, 205(11):2473-81.

Ho YY, Ionita-Laza I, Ottman R (2012). Domain-dependent clustering and genotype-phenotype analysis of LGI1 mutations in ADPEAF. Neurology, 78(8):563-68.

Hoch W, McConville J, Helms S, Newsom-Davis J, Melms A, Vincent A (2001). Auto-antibodies to the receptor tyrosine kinase MuSK in patients with myasthenia gravis without acetylcholine receptor antibodies. Nat Med, 7(3):365-68.

Huerta PT, Kowal C, DeGiorgio LA, Volpe BT, Diamond B (2006). Immunity and behavior: Antibodies alter emotion. Proc Natl Acad Sci U S A, 103(3):678-83.

Hughes EG, Peng X, Gleichman AJ, Lai M, Zhou L, Tsou R, Parsons TD, Lynch DR, Dalmau J, Balice-Gordon RJ (2010). Cellular and Synaptic Mechanisms of Anti-NMDA Receptor Encephalitis. J Neurosci, 30(17):5866-75.

Huh KH, Wenthold RJ (1999). Turnover Analysis of Glutamate Receptors Identifies a Rapidly Degraded Pool of the N-Methyl-D-aspartate Receptor Subunit, NR1, in Cultured Cerebellar Granule Cells. J Biol Chem, 274(1):151-57.

Hung CY, Covasa M, Ritter RC, Burns GA (2006). Hindbrain administration of NMDA receptor antagonist AP-5 increases food intake in the rat. Am J Physiol Regul Integr Comp Physiol, 290(3):R642-51.

Hutchinson M, Waters P, McHugh J, Gorman G, O'Riordan S, Connolly S, Hager H, Yu P, Becker CM, Vincent A (2008). Progressive encephalomyelitis, rigidity, and myoclonus: a novel glycine receptor antibody. Neurology, 71(16):1291-2.

Irani SR, Alexander S, Waters P, Kleopa KA, Pettingill P, Zuliani L, Peles E, Buckley C, Lang B, Vincent A (2010a). Antibodies to Kv1 potassium channel-complex proteins leucine-rich, glioma inactivated 1 protein and contactin-associated protein-2 in limbic encephalitis, Morvan's syndrome and acquired neuromyotonia. Brain, 133(9):2734-48.

Irani SR, Bera K, Waters P, Zuliani L, Maxwell S, Zandi MS, Friese MA, Galea I, Kullmann DM, Beeson D, Lang B, Bien CG, Vincent A (2010b). N-methyl-D-aspartate antibody encephalitis: temporal progression of clinical and paraclinical observations in a predominantly non-paraneoplastic disorder of both sexes. Brain, 133(6):1655-67.

Irani SR, Michell AW, Lang B, Pettingill P, Waters P, Johnson MR, Schott JM, Armstrong RJ, S Zagami A, Bleasel A, Somerville ER, Smith SM, Vincent A (2011). Faciobrachial dystonic seizures precede Lgi1 antibody limbic encephalitis. Ann Neurol, 69(5):892-900.

Isaacs H (1961). A syndrome of continuous muscle-fibre activity. J Neurol Neurosurg Psychiatry, 24(4):319-25.

Jacob S, Viegas S, Leite MI, Webster R, Cossins J, Kennett R, Hilton-Jones D, Morgan BP, Vincent A (2012). Presence and Pathogenic Relevance of Antibodies to Clustered Acetylcholine Receptor in Ocular and Generalized Myasthenia Gravis Clustered AChR Antibodies in Myasthenia Gravis. Arch Neurol, 69(8):994-1001.

Jarius S, Hoffmann L, Clover L, Vincent A, Voltz R (2008). CSF findings in patients with voltage gated potassium channel antibody associated limbic encephalitis. J Neurol Sci, 268(1-2):74-7.

Javitt DC, Zukin Sr (1991). Recent advances in the phencyclidine model of schizophrenia. Am J Psychiatry, 148(10):1301-8.

Toyka KV, Drachman DB, Griffin DE, Pestronk A, Winkelstein JA, Fishbeck KH, Kao I (1977). Myasthenia gravis. Study of humoral immune mechanisms by passive transfer to mice. N Engl J Med, 296(3):125-31.

Kalachikov S, Evgrafov O, Ross B, Winawer M, Barker-Cummings C, Martinelli Boneschi F, Choi C, Morozov P, Das K, Teplitskaya E, Yu A, Cayanis E, Penchaszadeh G, Kottmann AH, Pedley TA, Hauser WA, Ottman R, Gilliam TC (2002). Mutations in LGI1 cause autosomal-dominant partial epilepsy with auditory features. Nat Genet, 30(3):335-41.

Khan NL, Jeffree MA, Good C, Macleod W, Al-Sarraj S (2009). Histopathology of VGKC antibody-associated limbic encephalitis. Neurology, 72(19):1703-5.

Kinoshita M, Nakatsuji Y, Kimura T, Moriya M, Takata K, Okuno T, Kumanogoh A, Kajiyama K, Yoshikawa H, Sakoda S (2009). Neuromyelitis optica: Passive transfer to rats by human immunoglobulin. Biochem Biophys Res Commun, 386(4):623-7.

Kiryk A, Aida T, Tanaka K, Banerjee P, Wilczynski GM, Meyza K, Knapska E, Filipkowski RK, Kaczmarek L, Danysz W (2008). Behavioral characterization of GLT1 (+/-) mice as a model of mild glutamatergic hyperfunction. Neurotox Res, 13(1):19-30.

Kleopa KA, Elman LB, Lang B, Vincent A, Scherer SS (2006). Neuromyotonia and limbic encephalitis sera target mature Shaker-type K+ channels: subunit specificity correlates with clinical manifestations. Brain, 129(6):1570-84.

Kowal C, Degiorgio LA, Lee JY, Edgar MA, Huerta PT, Volpe BT, Diamond B (2006). Human lupus autoantibodies against NMDA receptors mediate cognitive impairment. Proc Natl Acad Sci U S A, 103(52):19854-9.

Kowal C, DeGiorgio LA, Nakaoka T, Hetherington H, Huerta PT, Diamond B, Volpe BT (2004). Cognition and Immunity; antibody impairs memory. Immunity, 21(2):179-88.

Krystal JH, Karper LP, Seibyl JP, Freeman GK, Delaney R, Bremner JD, Heninger GR, Bowers MB Jr, Charney DS (1994). Subanesthetic effects of the noncompetitive NMDA antagonist, ketamine, in humans: psychotomimetic, perceptual, cognitive, and neuroendocrine responses. Arch Gen Psychiatry, 51(3):199-214.

Lennon VA, Lambert EH (1989). Autoantibodies Bind Solubilized Calcium Channel-ω-Conotoxin Complexes From Small Cell Lung Carcinoma: A Diagnostic Aid for Lambert-Eaton Myasthenic Syndrome. Mayo Clin Proc, 64(12):1498-504.

Lai M, Hughes EG, Peng X, Zhou L, Gleichman AJ, Shu H, Matà S, Kremens D, Vitaliani R, Geschwind MD, Bataller L, Kalb RG, Davis R, Graus F, Lynch DR, Balice-Gordon R, Dalmau J (2009). AMPA receptor antibodies in limbic encephalitis alter synaptic receptor location. Ann Neurol, 65(4):424-34.

Lai M, Huijbers MG, Lancaster E, Graus F, Bataller L, Balice-Gordon R, Cowell JK, Dalmau J (2010). Investigation of LGI1 as the antigen in limbic encephalitis previously attributed to potassium channels: a case series. Lancet Neurol, 9(8):776-85.

Lalic T, Pettingill P, Vincent A, Capogna M (2011). Human limbic encephalitis serum enhances hippocampal mossy fiber-CA3 pyramidal cell synaptic transmission. Epilepsia, 52(1):121-31.

Lalonde R, Strazielle C (2011). Brain regions and genes affecting limb-clasping responses. Brain Res Rev, 67(1-2):252-9.

Lalonde R (2002). The neurobiological basis of spontaneous alternation. Neurosci Biobehav Rev, 26(1):91-104.

Lancaster E, Huijbers MG, Bar V, Boronat A, Wong A, Martinez-Hernandez E, Wilson C, Jacobs D, Lai M, Walker RW, Graus F, Bataller L, Illa I, Markx S, Strauss KA, Peles E, Scherer SS, Dalmau J

(2011a). Investigations of caspr2, an autoantigen of encephalitis and neuromyotonia. Ann Neurol, 69(2):303-11.

Lancaster E, Lai M, Peng X, Hughes E, Constantinescu R, Raizer J, Friedman D, Skeen MB, Grisold W, Kimura A, Ohta K, Iizuka T, Guzman M, Graus F, Moss SJ, Balice-Gordon R, Dalmau J (2010b). Antibodies to the GABAB receptor in limbic encephalitis with seizures: case series and characterisation of the antigen. Lancet Neurol, 9(1):67-76

Lancaster E, Martinez-Hernandez E, Titulaer MJ, Boulos M, Weaver S, Antoine JC, Liebers E, Kornblum C, Bien CG, Honnorat J, Wong S, Xu J, Contractor A, Balice-Gordon R, Dalmau J (2011c). Antibodies to metabotropic glutamate receptor 5 in the Ophelia syndrome. Neurology, 77(18):1698-701.

Lancaster E, Dalmau J (2012d). Neuronal autoantigens—pathogenesis, associated disorders and antibody testing. Nat Rev Neurol, 8(7):380-90.

Lee EK, Maselli RA, Ellis WG, Agius MA (1998). Morvan's fibrillary chorea: a paraneoplastic manifestation of thymoma. J Neurol Neurosurg Psychiatry, 65(6):857-62.

Leite MI, Jacob S, Viegas S, Cossins J, Clover L, Morgan BP, Beeson D, Willcox N, Vincent A (2008). IgG1 antibodies to acetylcholine receptors in 'seronegative' myasthenia gravis. Brain, 131(7):1940-52.

Lennon VA, Kryzer TJ, Pittock SJ, Verkman AS, Hinson SR (2005). IgG marker of optic-spinal multiple sclerosis binds to the aquaporin-4 water channel. J Exp Med, 202(4):473-7.

Lennon VA, Lindstrom JM, Seybold ME (1975). Experimental autoimmune myasthenia: A model of myasthenia gravis in rats and guinea pigs. J Exp Med, 141(6):1365-75.

Lennon VA, Lambert EH, Leiby KR, Okarma TB, Talib S (1991). Recombinant human acetylcholine receptor alpha-subunit induces chronic experimental autoimmune myasthenia gravis. J Immunol, 146(7):2245-8.

Lennon VA, Lindstrom JM, Seybold ME (1976). Experimental autoimmune myasthenia gravis: cellular and humoral immune responses. Ann N Y Acad Sci, 274:283-99.

Leonardi E, Andreazza S, Vanin S, Busolin G, Nobile C, Tosatto SC (2011). A computational model of the LGI1 protein suggests a common binding site for ADAM proteins. PLoS One, 6(3):e18142.

Levite M, Fleidervish IA, Schwarz A, Pelled D, Futerman AH (1999). Autoantibodies to the Glutamate Receptor Kill Neurons via Activation of the Receptor Ion Channel. J Autoimmun, 3(1):61-72.

Li JY, Popovic N, Brundin P (2005). The use of the R6 transgenic mouse models of Huntington's disease in attempts to develop novel therapeutic strategies. NeuroRx, 2(3):447-64.

Liao Y, Tang J, Ma M, Wu Z, Yang M, Wang X, Liu T, Chen X, Fletcher PC, Hao W (2010). Frontal white matter abnormalities following chronic ketamine use: a diffusion tensor imaging study. Brain, 133(7):2115-22.

Liguori R, Vincent A, Clover L, Avoni P, Plazzi G, Cortelli P, Baruzzi A, Carey T, Gambetti P, Lugaresi E, Montagna P (2001). Morvan's syndrome: peripheral and central nervous system and cardiac involvement with antibodies to voltage-gated potassium channels. Brain, 124(12):2417-26.

Lindstrom JM, Lennon VA, Seybold ME, Whittingham S (1976). Experimental autoimmune myasthenia gravis and myasthenia gravis: biochemical and immunochemical aspects. Ann N Y Acad Sci, 274:254-74.

Lucchinetti CF, Mandler RN, McGavern D, Bruck W, Gleich G, Ransohoff RM, Trebst C, Weinshenker B, Wingerchuk D, Parisi JE, Lassmann H (2002). A role for humoral mechanisms in the pathogenesis of Devic's neuromyelitis optica. Brain, 125(7):1450-61.

Lévi-Strauss M, Mallat M (1987). Primary cultures of murine astrocytes produce C3 and factor B, two components of the alternative pathway of complement activation. J Immunol, 139(7):2361-6.

Löscher WN, Wanschitz J, Reiners K, Quasthoff S (2004). Morvan's syndrome: clinical, laboratory, and in vitro electrophysiological studies. Muscle Nerve, 30(2):157-63.

Luby ED, Cohen BD, Rosenbaum G, Gottlieb JS, Kelley R (1959). Study of a New Schizophrenomimetic Drug—Sernyl. AMA Arch Neurol Psychiatry, 81(3):363-9.

Dalmau J, Lancaster E, Martinez-Hernandez E, Rosenfeld MR, Balice-Gordon R (2011). Clinical experience and laboratory investigations in patients with anti-NMDAR encephalitis. Lancet Neurol, 10(1):63-74.

Maddison P (2006). Neuromyotonia. Clin Neurophysiol, 117(10):2118-27.

Madrid A, Gil-Peralta A, Gil-Néciga E, González JR, Jarrín S (1996). Morvan's fibrillary chorea: remission after plasmapheresis. J Neurol. 1996, 243(4):350-3.

Mangiarini L, Sathasivam K, Seller M, Cozens B, Harper A, Hetherington C, Lawton M, Trottier Y, Lehrach H, Davies SW, Bates GP (1996). Exon 1 of the HD gene with an expanded CAG repeat is sufficient to cause a progressive neurological phenotype in transgenic mice. Cell, 87(3):493-506.

Manto M, Dalmau J, Didelot A, Rogemond V, Honnorat J (2011). Afferent facilitation of corticomotor responses is increased by IgGs of patients with NMDA-receptor antibodies. J Neurol, 258(1):27-33.

Manto M, Dalmau J, Didelot A, Rogemond V, Honnorat J (2010). In vivo effects of antibodies from patients with anti-NMDA receptor encephalitis: further evidence of synaptic glutamatergic dysfunction. Orphanet J Rare Dis, 26(5):31.

Marignier R, Chenevier F, Rogemond V, Sillevis Smitt P, Renoux C, Cavillon G, Androdias G, Vukusic S, Graus F, Honnorat J, Confavreux C (2010). Metabotropic glutamate receptor type 1 autoantibody-associated cerebellitis: a primary autoimmune disease? Arch Neurol, 67(5):627-30.

Martinez-Hernandez E, Horvath J, Shiloh-Malawsky Y, Sangha N, Martinez-Lage M, Dalmau J (2011). Analysis of complement and plasma cells in the brain of patients with anti-NMDAR encephalitis. Neurology, 77(6):589-93.

Moriyoshi K, Masu M, Ishii T, Shigemoto R, Mizuno N, Nakanishi S (1991). Molecular cloning and characterization of the rat NMDA receptor. Nature, 354(6348):31-7.

McConville J, Farrugia ME, Beeson D, Kishore U, Metcalfe R, Newsom-Davis J, Vincent A (2004). Detection and characterization of MuSK antibodies in seronegative myasthenia gravis. Ann Neurol, 55(4):580-4.

McHugh SB, Niewoehner B, Rawlins JN, Bannerman DM (2008). Dorsal hippocampal N-methyl-d-aspartate receptors underlie spatial working memory performance during non-matching to place testing on the T-maze. Behav Brain Res, 186(1):41-7.

McIlhinney RA, Molnár E, Atack JR, Whiting PJ (1996). Cell surface expression of the human N-methyl-d-aspartate receptor subunit 1a requires the co-expression of the NR2A subunit in transfected cells. Neuroscience, 70(4):989-97.

McKnight K, Jiang Y, Hart Y, Cavey A, Wroe S, Blank M, Shoenfeld Y, Vincent A, Palace J, Lang B (2005). Serum antibodies in epilepsy and seizure-associated disorders. Neurology, 65(11):1730-6.

Mikasova L, De Rossi P, Bouchet D, Georges F, Rogemond V, Didelot A, Meissirel C, Honnorat J, Groc L (2012). Disrupted surface cross-talk between NMDA and Ephrin-B2 receptors in anti-NMDA encephalitis. Brain, 135(5):1606-21.

Miller BR, Dorner JL, Shou M, Sari Y, Barton SJ, Sengelaub DR, Kennedy RT, Rebec GV (2008). Up-regulation of GLT1 expression increases glutamate uptake and attenuates the Huntington's disease phenotype in the R6/2 mouse. Neuroscience, 153(1):329-37.

Mitchell IJ, Carroll CB (1997). Reversal of Parkinsonian symptoms in primates by antagonism of excitatory amino acid transmission: Potential mechanisms of action. Neurosci Biobehav Rev, 21(4):469-75.

Mohn AR, Gainetdinov RR, Caron MG, Koller BH (1999). Mice with Reduced NMDA Receptor Expression Display Behaviors Related to Schizophrenia. Cell, 98(4):1-10.

Monyer H. (1992). Heteromeric NMDA Receptors: Molecular and Functional Distinction of Subtypes. Cell, 98(4):427-36.

Monyer H, Burnashev N, Laurie DJ, Sakmann B, Seeburg PH (1994). Developmental and regional expression in the rat brain and functional properties of four NMDA receptors. Neuron, 12(3):529-40.

Morante-Redolat JM, Gorostidi-Pagola A, Piquer-Sirerol S, Sáenz A, Poza JJ, Galán J, Gesk S, Sarafidou T, Mautner VF, Binelli S, Staub E, Hinzmann B, French L, Prud'homme JF, Passarelli D, Scannapieco P, Tassinari CA, Avanzini G, Martí-Massó JF, Kluwe L, Deloukas P, Moschonas NK, Michelucci R, Siebert R, Nobile C, Pérez-Tur J, López de Munain A (2002). Mutations in the LGI1/Epitempin gene on 10q24 cause autosomal dominant lateral temporal epilepsy. Hum Mol Genet, 11(9):1119-28.

Morgan BP (1989). Complement membrane attack on nucleated cells: resistance, recovery and non-lethal effects. Biochem J, 264(1):1-14.

Moscato EH, Jain A, Peng X, Hughes EG, Dalmau J, Balice-Gordon RJ (2010). Mechanisms underlying autoimmune synaptic encephalitis leading to disorders of memory, behavior and cognition: insights from molecular, cellular and synaptic studies. Eur J Neurosci, 32(2):298-309.

Mouri A, Noda Y, Noda A, Nakamura T, Tokura T, Yura Y, Nitta A, Furukawa H, Nabeshima T (2007). Involvement of a Dysfunctional Dopamine-D1/N-Methyl-D-aspartate-NR1 and

Ca2+/Calmodulin-Dependent Protein Kinase II Pathway in the Impairment of Latent Learning in a Model of Schizophrenia Induced by Phencyclidine. Mol Pharmacol, 71(6):1598-609.

Newsom-Davis J, Pinching AJ, Vincent A, Wilson SG (1978). Function of circulating antibody to acetylcholine receptor in myasthenia gravis: Investigation by plasma exchange. Neurology, 28(3):266-72.

Nagado T, Arimura K, Sonoda Y, Kurono A, Horikiri Y, Kameyama A, Kameyama M, Pongs O, Osame M (1999). Potassium current suppression in patients with peripheral nerve hyperexcitability. Brain, 122(11):2057-66.

Niehusmann P, Dalmau J, Rudlowski C, Vincent A, Elger CE, Rossi JE, Bien CG (2009). Diagnostic value of N-methyl-D-aspartate receptor antibodies in women with new onset epilepsy. Arch Neurol, 66(4):458-64.

Natsuk WL, Plescia OJ, Osserman KE (1960). Changes in serum complement activity in patients with myasthenia gravis. Proc Soc Exp Biol Med, 105:177-184.

Newsom-Davis J, Mills KR (1993). Immunological associations of acquired neuromyotonia (Isaacs' syndrome). Report of five cases and literature review. Brain, 116 (2):453-69.

Nobile C, Michelucci R, Andreazza S, Pasini E, Tosatto SC, Striano P (2009). LGI1 mutations in autosomal dominant and sporadic lateral temporal epilepsy. Hum Mutat, 30(4):530-6.

Ogawa Y, Oses-Prieto J, Kim MY, Horresh I, Peles E, Burlingame AL, Trimmer JS, Meijer D, Rasband MN (2010). ADAM22, a Kv1 channel-interacting protein, recruits membrane-associated guanylate kinases to juxtaparanodes of myelinated axons. J Neurosci, 30(3):1038-48.

Ottman R, Rosenberger L, Bagic A, Kamberakis K, Ritzl EK, Wohlschlager AM, Shamim S, Sato S, Liew C, Gaillard WD, Wiggs E, Berl MM, Reeves-Tyer P, Baker EH, Butman JA, Theodore WH (2008). Altered language processing in autosomal dominant partial epilepsy with auditory features. Mol Cell Neurosci, 42(4):448-57.

Owuor K, Harel NY, Englot DJ, Hisama F, Blumenfeld H, Strittmatter SM (2009). LGI1-associated epilepsy through altered ADAM23-dependent neuronal morphology. Mol Cell Neurosci, 42(4):448-57.

Pinching AJ, Peters DK (1976). Remission of myasthenia gravis following plasma-exchange. Lancet, 2(8000):1373-6.

Pangburn MK, Pangburn KL, Koistinen V, Meri S, Sharma AK (2000). Molecular mechanisms of target recognition in an innate immune system: interactions among factor H, C3b, and target in the alternative pathway of human complement. J Immunol, 164(9):4742-51.

Paoli, M (2001). An elusive propeller-like fold. Nat Struct Biol, 8(9):744-5.

Pardridge WM (1998). CNS Drug Design Based on Principles of Blood-Brain Barrier Transport.

J Neurochem, 70(5):1781-92.

Park DC, Murman DL, Perry KD, Bruch LA (2007). An autopsy case of limbic encephalitis with voltage-gated potassium channel antibodies. Eur J Neurol, 14(10):e5-6.

Patrick J, Lindstrom J, Culp B, McMillan J (1973). Studies on Purified Eel Acetylcholine Receptor and Anti-Acetylcholine Receptor Antibody. Proc Natl Acad Sci U S A, 70(12):3334-8.

Paxinos G, Franklin KBJ (2001). The Mouse brain in stereotaxic coordinates, 2nd edition. Academic Press. ISBN-13: 978-0125476362.

Pettingill P, Irani SR, Kleopa KA, Schiza N, Waters P, Mazia C, Zuliani L, Watanabe O, Lang B, Buckley C, Vincent A (2012). Morvan syndrome: Clinical and serological observations in 29 cases. Ann Neurol, 72(2):241-55.

Perogamvros L, Schnider A, Leemann B (2012). The Role of NMDA Receptors in Human Eating Behavior. Cogn Behav Neurol, 25(2):93-7.

Petersen JG, Dorrington KJ (1974). An in Vitro System for Studying the Kinetics of Interchain Disulfide Bond Formation in Immunoglobulin G. J Biol Chem, 249(17):5633-41.

Peñagarikano O, Abrahams BS, Herman EI, Winden KD, Gdalyahu A, Dong H, Sonnenblick LI, Gruver R, Almajano J, Bragin A, Golshani P, Trachtenberg JT, Peles E, Geschwind DH (2011). Absence of CNTNAP2 leads to epilepsy, neuronal migration abnormalities, and core autism-related deficits. Cell, 147(1):235-46.

Poliak S, Salomon D, Elhanany H, Sabanay H, Kiernan B, Pevny L, Stewart CL, Xu X, Chiu SY, Shrager P, Furley AJ, Peles E (2003). Juxtaparanodal clustering of Shaker-like K+ channels in myelinated axons depends on Caspr2 and TAG-1. J Cell Biol, 162(6):1149-60.

Poliak S, Gollan L, Martinez R, Custer A, Einheber S, Salzer JL, Trimmer JS, Shrager P, Peles E (1999). Caspr2, a New Member of the Neurexin Superfamily, Is Localized at the Juxtaparanodes of Myelinated Axons and Associates with K+ Channels. Neuron, 24(4):1037-47.

Pomarol-Clotet E, Canales-Rodríguez EJ, Salvador R, Sarró S, Gomar JJ, Vila F, Ortiz-Gil J, Iturria-Medina Y, Capdevila A, McKenna PJ (2010). Medial prefrontal cortex pathology in schizophrenia as revealed by convergent findings from multimodal imaging. Mol Psychiatry, 15(8):823-30.

Pozo-Roisch P, Clover L, Saiz A, Vincent A, Graus F (2003). Voltage gated-potassium channels in limbic encephalitis. Ann Neurol. 2003 Oct;54(4):530-3

Prüss H, Höltje M, Maier N, Gomez A, Buchert R, Harms L, Ahnert-Hilger G, Schmitz D, Terborg C, Kopp U, Klingbeil C, Probst C, Kohler S, Schwab JM, Stoecker W, Dalmau J, Wandinger KP (2012). IgA NMDA receptor antibodies are markers of synaptic immunity in slow cognitive impairment. Neurology, 78(22):1743-53.

Perez-Otano I, Schulteis CT, Contractor A, Lipton SA, Trimmer JS, Sucher NJ, Heinemann SF (2001). Assembly with the NR1 Subunit Is Required for Surface Expression of NR3A-Containing NMDA Receptors. J Neurosci, 21(4):1228-37.

Ratelade J, Bennett JL, Verkman AS (2011). Evidence against Cellular Internalization in Vivo of NMO-IgG, Aquaporin-4, and Excitatory Amino Acid Transporter 2 in Neuromyelitis Optica. J Biol Chem, 286(52):45156-64.

Rainey JM Jr, Crowder MK (1975). Prolonged psychosis attributed to phencyclidine: Report of three cases. Am J Psychiatry, 132(10):1076-8.

Rasband M, Trimmer JS, Schwarz TL, Levinson SR, Ellisman MH, Schachner M, Shrager (1998).

Rasband M, Trimmer JS, Scwarz TL, Levinson SR, Ellisman MH, Schachner M, Sharager C. (1998). Potassium channel distribution, clustering, and function in remyelinating rat axons, J Neurosci. 18(1):36-47.

Riemersma S, Vincent A, Beeson D, Newland C, Hawke S, Vernet-der Garabedian B, Eymard B, Newsom-Davis J (1996). Association of arthrogryposis multiplex congenita with maternal antibodies inhibiting fetal acetylcholine receptor function. Journal of Clinical Investigation, 98(10);2358-2363.

Rhodes KJ, Strassle BW, Monaghan MM, Bekele-Arcuri Z, Matos MF, Trimmer JS (1997). Association and Colocalization of the Kvβ1 and Kvβ2 β-Subunits with Kv1 α-Subunits in Mammalian Brain K+Channel Complexes. J Neurosci, 17(21):8246-58.

Rogers SW, Andrews PI, Gahring LC, Whisenand T, Cauley K, Crain B, Hughes TE, Heinemann SF, McNamara JO (1994). Autoantibodies to glutamate receptor GluR3 in Rasmussen's encephalitis. Science, 265(5172):648-51.

Rose NR, Bona C (1993). Defining criteria for autoimmune diseases (Witebsky's postulates revisited). Immunol Today, 14(9):426-30.

Rubio-Agustí I, Dalmau J, Sevilla T, Burgal M, Beltrán E, Bataller L (2011). Isolated hemidystonia associated with NMDA receptor antibodies. Mov Disord, 26(2):351-2.

Saadoun S, Waters P, Bell BA, Vincent A, Verkman AS, Papadopoulos MC (2010). Intra-cerebral injection of neuromyelitis optica immunoglobulin G and human complement produces neuromyelitis optica lesions in mice. Brain, 133(2):349-61.

Sagane K, Hayakawa K, Kai J, Hirohashi T, Takahashi E, Miyamoto N, Ino M, Oki T, Yamazaki K, Nagasu T (2005). Ataxia and peripheral nerve hypomyelination in ADAM22-deficient mice. BMC Neurosci, 6(6):33.

Sagane K, Ishihama Y, Sugimoto H (2008). LGI1 and LGI4 bind to ADAM22, ADAM23 and ADAM11. Int J Biol Sci, 4(6):387-96.

Savvaki M, Panagiotaropoulos T, Stamatakis A, Sargiannidou I, Karatzioula P, Watanabe K, Stylianopoulou F, Karagogeos D, Kleopa KA (2008). Impairment of learning and memory in TAG-1 deficient mice associated with shorter CNS internodes and disrupted juxtaparanodes. Mol Cell Neurosci, 39(3):478-90.

Scheel H, Tomiuk S, Hofmann K (2002). A common protein interaction domain links two recently identified epilepsy genes. Hum Mol Genet, 11(15):1757-62.

Schulte U, Thumfart JO, Klöcker N, Sailer CA, Bildl W, Biniossek M, Dehn D, Deller T, Eble S, Abbass K, Wangler T, Knaus HG, Fakler B (2006). The Epilepsy-Linked Lgi1 Protein Assembles into Presynaptic Kv1 Channels and Inhibits Inactivation by Kvβ1. Neuron, 49(5):697-706.

Scott VE, Muniz ZM, Sewing S, Lichtinghagen R, Parcej DN, Pongs O, Dolly JO (2002). Antibodies specific for distinct Kv subunits unveil a heterooligomeric basis for subtypes of .alpha.-dendrotoxin-sensitive potassium channels in bovine brain. Biochemistry, 33(7):1617-23.

Senechal KR, Thaller C, Noebels JL (2005). ADPEAF mutations reduce levels of secreted LGI1, a putative tumor suppressor protein linked to epilepsy. Hum Mol Genet, 14(12):1613-20.

Shillito P, Molenaar PC, Vincent A, Leys K, Zheng W, van den Berg RJ, Plomp JJ, van Kempen GT, Chauplannaz G, Wintzen AR (1995). Acquired neuromyotonia: Evidence for autoantibodies directed against K+ channels of peripheral nerves. Ann Neurol, 38(5):714-22.

Shimizu E, Tang YP, Rampon C, Tsien JZ (2012). NMDA Receptor-Dependent Synaptic Reinforcement as a Crucial Process for Memory Consolidation. Science, 290(5494):1170-4.

Shiraishi H, Motomura M, Yoshimura T, Fukudome T, Fukuda T, Nakao Y, Tsujihata M, Vincent A, Eguchi K (2005). Acetylcholine receptors loss and postsynaptic damage in MuSK antibody-positive myasthenia gravis. Ann Neurol, 57(2):289-93.

Silva J, Sharma S, Hughes B, Yu YE, Cowell JK (2010). Homozygous inactivation of the LGI1 gene results in hypomyelination in the peripheral and central nervous systems. J Neurosci Res, 88(15):3328-36.

Singhrao SK, Neal JW, Rushmere NK, Morgan BP, Gasque P (2000). Spontaneous Classical Pathway Activation and Deficiency of Membrane Regulators Render Human Neurons Susceptible to Complement Lysis. Am J Pathol, 157(3):905-18.

Sinha S, Newsom-Davis J, Mills K, Byrne N, Lang B, Vincent A (1991). Autoimmune aetiology for acquired neuromyotonia (Isaacs' syndrome). Lancet, 338(8759):75-7.

Sirerol-Piquer MS, Ayerdi-Izquierdo A, Morante-Redolat JM, Herranz-Pérez V, Favell K, Barker PA, Pérez-Tur J (2006). The epilepsy gene LGI1 encodes a secreted glycoprotein that binds to the cell surface. Hum Mol Genet, 15(23):3436-45.

Smart SL, Lopantsev V, Zhang CL, Robbins CA, Wang H, Chiu SY, Schwartzkroin PA, Messing A, Tempel BL (1998). Deletion of the KV1.1 Potassium Channel Causes Epilepsy in Mice. Neuron, 20(4):809-19.

Sillevis Smitt P, Kinoshita A, De Leeuw B, Moll W, Coesmans M, Jaarsma D, Henzen-Logmans S, Vecht C, De Zeeuw C, Sekiyama N, Nakanishi S, Shigemoto R., Kinoshita, A., de Leeuw, B (2000). Paraneoplastic cerebellar ataxia due to autoantibodies against a glutamate receptor. N Engl J Med, 342(1):21-7.

Sommer C, Weishaupt A, Brinkhoff J, Biko L, Wessig C, Gold R, Toyka KV (2005). Paraneoplastic stiff-person syndrome: passive transfer to rats by means of IgG antibodies to amphiphysin. Lancet, 365(9468):1406-11.

Sonoda Y, Arimura K, Kurono A, Suehara M, Kameyama M, Minato S, Hayashi A, Osame M (1996). Serum of Isaacs' syndrome suppresses potassium channels in PC-12 cell lines. Muscle Nerve, 19(11):1439-46.

Staub E, Pérez-Tur J, Siebert R, Nobile C, Moschonas NK, Deloukas P, Hinzmann B (2002). The novel EPTP repeat defines a superfamily of proteins implicated in epileptic disorders. Trends Biochem Sci, 27(9):441-4.

Strauss KA, Puffenberger EG, Huentelman MJ, Gottlieb S, Dobrin SE, Parod JM, Stephan DA, Morton DH (2006). Recessive symptomatic focal epilepsy and mutant contactin-associated protein-like 2. N Engl J Med, 354(13):1370-7.

Striano P, Busolin G, Santulli L, Leonardi E, Coppola A, Vitiello L, Rigon L, Michelucci R, Tosatto SC, Striano S, Nobile C (2011). Familial temporal lobe epilepsy with psychic auras associated with a novel LGI1 mutation. Neurology, 76(13):1173-6.

Tan KM, Lennon VA, Klein CJ, Boeve BF, Pittock SJ (2008). Clinical spectrum of voltage-gated potassium channel autoimmunity. Neurology, 70(20):1883-90.

Tanaka K, Watase K, Manabe T, Yamada K, Watanabe M, Takahashi K, Iwama H, Nishikawa T, Ichihara N, Kikuchi T, Okuyama S, Kawashima N, Hori S, Takimoto M, Wada K (1997). Epilepsy and Exacerbation of Brain Injury in Mice Lacking the Glutamate Transporter GLT-1. Science, 276(5319):1699-702.

Tao MH, Smith RI, Morrison SL (1993). Structural features of human immunoglobulin G that determine isotype- specific differences in complement activation. J Exp Med, 178(2):661-7.

Thieben MJ, Lennon VA, Boeve BF, Aksamit AJ, Keegan M, Vernino S (2004). Potentially reversible autoimmune limbic encephalitis with neuronal potassium channel antibody. Neurology, 62(7):1177-82.

Thomas R, Favell K, Morante-Redolat J, Pool M, Kent C, Wright M, Daignault K, Ferraro GB, Montcalm S, Durocher Y, Fournier A, Perez-Tur J, Barker PA (2010). LGI1 Is a Nogo Receptor 1 Ligand that Antagonizes Myelin-Based Growth Inhibition. J Neurosci, 30(19):6607-12.

Thouin A, Bera K, Vincent A, Cunningham M (2012). 094 Anti-NMDA receptor antibodies disrupt cortical network activity in vitro. Journal of Neurology, Neurosurgery & Psychiatry, 83(3):1-2.

Titulaer MJ, McCracken L, Gabilondo I, Armangué T, Glaser C, Iizuka T, Honig LS, Benseler SM, Kawachi I, Martinez-Hernandez E, Aguilar E, Gresa-Arribas N, Ryan-Florance N, Torrents A, Saiz A, Rosenfeld MR, Balice-Gordon R, Graus F, Dalmau J (2013). Treatment and prognostic factors for long-term outcome in patients with anti-NMDA receptor encephalitis: an observational cohort study. Lancet Neurol, 12(2):157-65.

Tomimitsu H, Arimura K, Nagado T, Watanabe O, Otsuka R, Kurono A, Sonoda Y, Osame M, Kameyama M (2004). Mechanism of action of voltage gated K+ channel antibodies in acquired neuromyotonia. Ann Neurol, 56(3):440-4.

Toyka KV, Brachman DB, Pestronk A, Kao I (1975). Myasthenia gravis: passive transfer from man to mouse. Science, 190(4212):397-9.

Traka M, Goutebroze L, Denisenko N, Bessa M, Nifli A, Havaki S, Iwakura Y, Fukamauchi F, Watanabe K, Soliven B, Girault JA, Karagogeos D (2003). Association of TAG-1 with Caspr2 is essential for the molecular organization of juxtaparanodal regions of myelinated fibers. J Cell Biol, 162(6):1161-72.

Trimmer JS, Rhodes KJ. Localization of voltage-gated ion channels in mammalian brain (2004). Annu Rev Physiol, 66:477-519.

Twyman RE, Gahring LC, Spiess J, Rogers SW (1995). Glutamate receptor antibodies activate a subset of receptors and reveal an agonist binding site. Neuron, 14(4):755-62.

Tüzün E, Zhou L, Baehring JM, Bannykh S, Rosenfeld MR, Dalmau J (2009). Evidence for antibody-mediated pathogenesis in anti-NMDAR encephalitis associated with ovarian teratoma. Acta Neuropathol, 118(6):737-43

Ulbrich MH, Isacoff EY (2008). Rules of engagement for NMDA receptor subunits. Proc Natl Acad Sci U S A, 105(37):14163-8.

van Swieten J, Koudstaal P, Visser M, Schouten H (1988). Interobserver agreement for the assessment of handicap in stroke patients. Stroke, 19 (5):604-607.

Vincent A, Buckley C, Schott JM, Baker I, Dewar BK, Detert N, Clover L, Parkinson A, Bien CG, Omer S, Lang B, Rossor MN, Palace J (2004). Potassium channel antibody-associated encephalopathy: a potentially immunotherapy-responsive form of limbic encephalitis. Brain, 127(3):701-12.

Vincent A (2009). Autoimmune channelopathies: new antibody-mediated disorders of the central nervous system. F1000 Biol Rep, 17(1):61.

Vincent A, Irani SR (2010). Caspr2 Antibodies in Patients with Thymomas. J Thorac Oncol, ;5(10 Suppl 4):S277-80.

Vincent A, Bien CG, Irani SR, Waters P (2011). Autoantibodies associated with diseases of the CNS: new developments and future challenges. Lancet Neurol, 10(8):759-72.

Vincent A, Newsom-Davis J (1982). Acetylcholine receptor antibody characteristics in myasthenia gravis. I. Patients with generalized myasthenia or disease restricted to ocular muscles. Clin Exp Immunol, 49(2):257-65.

Vincent A. Clinical Neuroimmunology, 2nd edition. Oxford University Press. ISBN-13: 978-0198510680.

Vitaliani R, Mason W, Ances B, Zwerdling T, Jiang Z, Dalmau J (2005). Paraneoplastic encephalitis, psychiatric symptoms, and hypoventilation in ovarian teratoma. Ann Neurol, 58(4):594-604.

Wang H, Kunkel DD, Martin TM, Schwartkroin PA, Tempel BL (1993). Heteromultimeric K^+ channels in terminal and juxtaparanodal regions of neurons. Nature, 365(6441):75–79

White PF, Schüttler J, Shafer A, Stanski DR, Horai Y, Trevor AJ (1985). Comparative pharmacology of the ketamine isomers. Studies in volunteers. Br J Anaesth, 57(2):197-203.

Waters PJ, McKeon A, Leite MI, Rajasekharan S, Lennon VA, Villalobos A, Palace J, Mandrekar JN, Vincent A, Bar-Or A, Pittock SJ (2012). Serologic diagnosis of NMO: a multicenter comparison of aquaporin-4-IgG assays. Neurology, 78(9):665-71.

Watson R, Jiang Y, Bermudez I, Houlihan L, Clover L, McKnight K, Cross JH, Hart IK, Roubertie A, Valmier J, Hart Y, Palace J, Beeson D, Vincent A, Lang B (2004). Absence of antibodies to glutamate receptor type 3 (GluR3) in Rasmussen encephalitis. Neurology, 63(1):43-50.

Waxman EA, Lynch DR (2005). N-methyl-D-aspartate Receptor Subtypes: Multiple Roles in Excitotoxicity and Neurological Disease. Neuroscientist, 11(1):37-49.

Weens JH, Schwartz RS (1974). Etiological factors in autoimmune hemolytic anemia. Ser Haematol, 7(3):303-27.

Weigert C (1901). Pathologisch-anatomischer Beitäg zur Erb'schen Krankheit. Neurologisches Zentrablatt, 20:597-601.

Wiendl H, Bien CG, Bernasconi P, Fleckenstein B, Elger CE, Dichgans J, Mantegazza R, Melms A (2001). GluR3 antibodies: Prevalence in focal epilepsy but no specificity for Rasmussen's encephalitis. Neurology, 57(8):1511-4.

Wigge P, McMahon HT (1998). The amphiphysin family of proteins and their role in endocytosis at the synapse. Trends Neurosci, 21(8):339-44.

Witebsky E, Rose NR, Terplan K, Paine JR, Egan RW (1957). Chronic thyroiditis and autoimmunization. J Am Med Assoc, 164(13):1439-47.

Watanabe M, Inoue Y, Sakimura K, Mishina M (1992). Developmental changes in distribution of NMDA receptor channel subunit mRNAs. Neuroreport, 3(12):1138-40.

Yu YE, Wen L, Silva J, Li Z, Head K, Sossey-Alaoui K, Pao A, Mei L, Cowell JK (2010). Lgi1 null mutant mice exhibit myoclonic seizures and CA1 neuronal hyperexcitability. Hum Mol Genet, 19(9):1702-11.

Zandi MS, Irani SR, Lang B, Waters P, Jones PB, McKenna P, Coles AJ, Vincent A, Lennox BR (2011). Disease-relevant autoantibodies in first episode schizophrenia. J Neurol, 258(4):686-8.

Zarate CA, Singh JB, Carlson PJ, Brutsche NE, Ameli R, Luckenbaugh DA, Charney DS, Manji HK (2006). A randomized trial of an N-methyl-D-aspartate antagonist in treatment-resistant major depression. Arch Gen Psychiatry, 63(8):856-64.

van der Zee JS, van Swieten P, Aalberse RC (1986). Serologic aspects of IgG4 antibodies. II. IgG4 antibodies form small, nonprecipitating immune complexes due to functional monovalency. J Immunol, 137(11):3566-71.

Zhang Q, Tanaka K, Sun P, Nakata M, Yamamoto R, Sakimura K, Matsui M, Kato N (2012). Suppression of synaptic plasticity by cerebrospinal fluid from anti-NMDA receptor encephalitis patients. Neurobiol Dis, 45(1):610-5.

Zhang Y, Pardridge WM (2001). Mediated efflux of IgG molecules from brain to blood across the blood–brain barrier. J Neuroimmunol, 114(1-2):168-72.

Zhang Y, Pardridge WM., 2001. Rapid transferrin efflux from brain to blood across the blood-brain barrier. J Neurochem, 76(5):1597-600.

Zhou YD, Lee S, Jin Z, Wright M, Smith SE, Anderson MP (2009). Arrested maturation of excitatory synapses in autosomal dominant lateral temporal lobe epilepsy. Nat Med, 15(10):1208-14

Zipfel PF, Skerka C (2009). Complement regulators and inhibitory proteins. Nat Rev Immunol, 9(10):729-40.

Zuberi SM, Eunson LH, Spauschus A, De Silva R, Tolmie J, Wood NW, McWilliam RC, Stephenson JB, Kullmann DM, Hanna MG (1999). A novel mutation in the human voltage-gated potassium channel gene (Kv1.1) associates with episodic ataxia type 1 and sometimes with partial epilepsy. Brain, 122(5):817-825.

Zweier C, de Jong EK, Zweier M, Orrico A, Ousager LB, Collins AL, Bijlsma EK, Oortveld MA, Ekici AB, Reis A, Schenck A, Rauch A (2009). CNTNAP2 and NRXN1 are mutated in autosomal-recessive Pitt-Hopkins-like mental retardation and determine the level of a common synaptic protein in Drosophila. Am J Hum Genet, 85(5):655-66.

Appendix

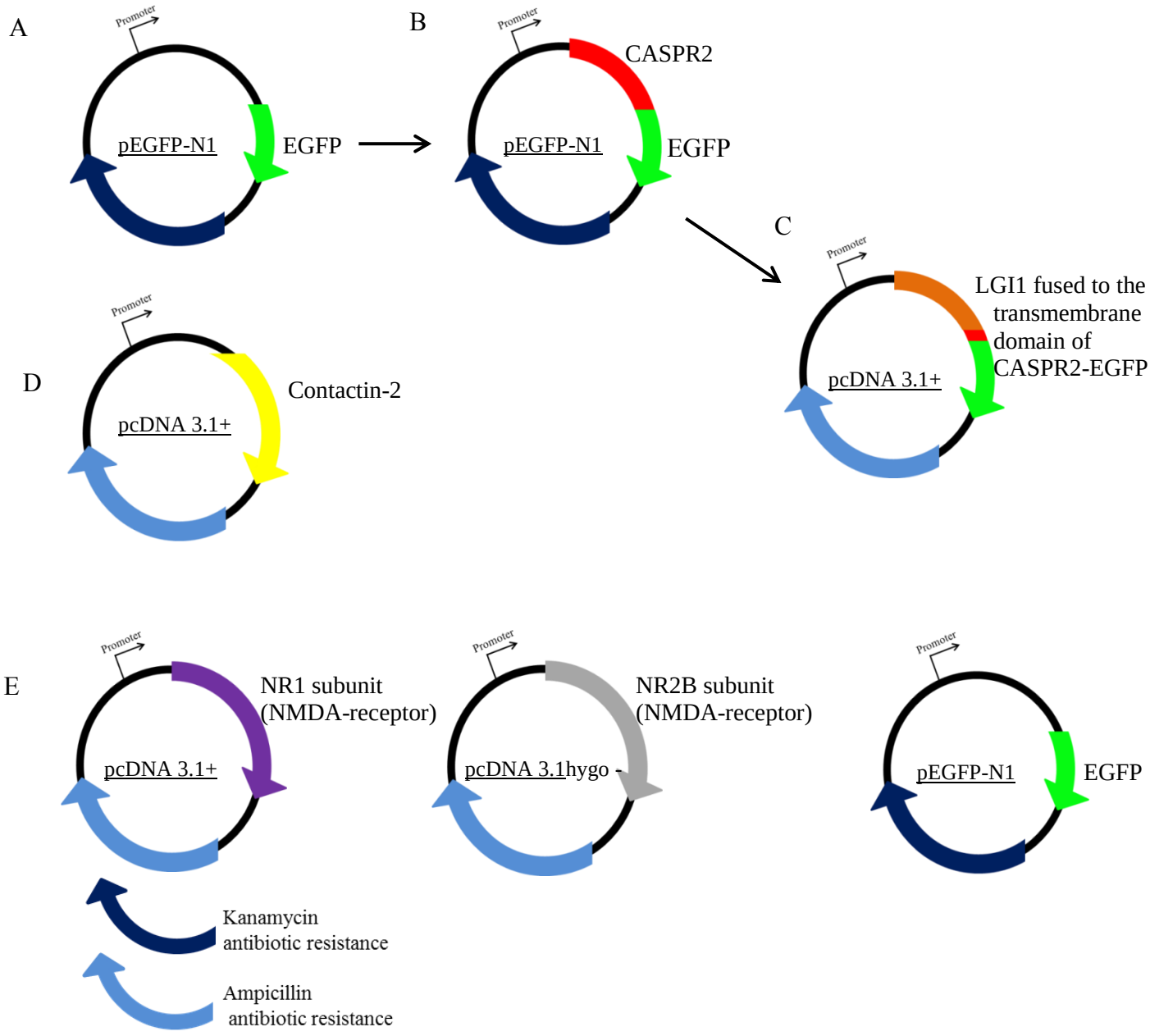

Figure 1. Schematic of plasmids used in this thesis.

Six plasmid constructs were used in this thesis. EGFP was expressed alone in pEGFP-N1 (A). For detection of VGKC-complex antibodies, cDNA encoding CASPR2 was sub-cloned into pEGFP-N1, enabling visualisation of CASPR2-EGFP expressing cells (B). The CASPR2-C terminus (including the transmembrane domain and 13 extracellular amino acids) was ligated from pEGFP-N1 was fused to LGI1 and cloned into pcDNA3.1, producing a membrane-tethered LGI1 molecule that also expressed EGFP (C). Contactin-2 was expressed alone in pCDNA3.1+ and was not tagged with EGFP (D). For NMDA receptor antibody assays, HEK cells were transfected with plasmids encoding the NR1 and NR2 subunits alongside the pEGFP-N1 plasmid, which enabled transfection to be visualised (E).

Plasmid	Antigen cloned into plasmid	EGFP-incorporated	Reason for Construct
pEGFP-N1 (Clontech Laboratories)	None	Yes	- Transfection marker
pEGFP-N1 (Clontech Laboratories)	CASPR2	Yes (C-terminal)	- Transfect into HEK cells to screen for antibodies against CASPR2 - Tagged to enable antigen-expression to be visualised
pCDNA 3.1+ (Invitrogen)	LGI1 (fused to the transmembrane domain of CASPR2-EGFP)	Yes (C-terminal)	- Transfect into HEK cells to screen for antibodies against LGI1 - Tagged to enable antigen-expression to be visualised
pCDNA 3.1+ (Invitrogen)	Contactin-2	No	- Transfect into HEK cells to screen for antibodies against Contactin-2
pCDNA 3.1+ (Invitrogen)	NMDAR, NR1 subunit	No	- Co-transfect into HEK cells with NR2B to screen for antibodies against the NMDA receptor - Co-transfect with pEGFP-N1 plasmid to visualise transfection
pCDNA 3.1hygro- (Invitrogen)	NMDAR, NR2 subunit	No	- Co-transfect into HEK cells with NR1 to screen for antibodies against the NMDA receptor - Co-transfect with pEGFP-N1 plasmid to visualise transfection

Figure 2. Overview of plasmids used in this thesis, the location of their EGFP tag and the reason for use

Publications generated from this thesis

Data from this thesis (Chapters 3 and 4) went into two publications, see attached.

1) Irani SR, Alexander S, Waters P, Kleopa KA, Pettingill P, Zuliani L, Peles E, Buckley C, Lang B, Vincent A (2010a). Antibodies to Kv1 potassium channel-complex proteins leucine-rich, glioma inactivated 1 protein and contactin-associated protein-2 in limbic encephalitis, Morvan's syndrome and acquired neuromyotonia. Brain, 133(9):2734-48.

2) Pettingill P, Irani SR, Kleopa KA, Schiza N, Waters P, Mazia C, Zuliani L, Watanabe O, Lang B, Buckley C, Vincent A (2012). Morvan syndrome: Clinical and serological observations in 29 cases. Ann Neurol, 72(2):241-55.